Role of Cysteine in MtrC-Flavin Interactions of *Shewanella oneidensis*

Michael Peter Norman

PhD Thesis

University of East Anglia
School of Biological Sciences
Norwich

September 2017

Acknowledgements

First and foremost, I would like to thank my supervisor Dr Tom Clarke for giving me the opportunity to carry out this PhD. Under his supervision I have learned and developed many skills. I will always be grateful for these four years that have been filled with, what can only be described as, perfect moments. Of course, none of this would be possible without funding from the BBSRC DTP. I would also like to thank my secondary supervisor Dr Gary Rowley for his advice and input in meetings over the years. Thanks must also be given to Professor David Richardson as my associate supervisor for giving his time and insight. I would also like to thank him for hosting extended group meetings at Wood Hall. These allowed me to benefit from discussions and sharing of ideas with the 'Heme Team' with special thanks given to Professor Julea Butt and her group.

Thanks must be given to a number of collaborators of the group for directly contributing to this project. Dr Liang Shi for kindly providing many of the bacterial strains used in this study, as well as, Dr Ricardo Louro and Dr Catarina Paquete for carrying out NMR analysis.

Importantly I would like to thank Dr Marcus Edwards and Dr Gaye White for being my 'on the ground' supervisors. Their brilliant guidance and help over the years has been greatly appreciated and crucial for the progression of my PhD. Both were patient teachers throughout my studies and I cannot emphasise enough how invaluable this was to me.

I would like to acknowledge all members of Lab 2.30, past and present. Many of whom taught me vital skills and generally made UEA a great place to work. This of course extends to everyone who has partaken in the long held tradition of coffee time. Discussion with you all has helped me develop as a scientist, not just in terms of my project, but also from your collective insight into academic science. I especially want

to thank Jon Davies who battled through the PhD alongside me and was a great conference / travel buddy on many occasions. Our discussions, with and without beer, have been invaluable in countering the madness of science or lab life! I also want to thank Amy Easey without whom TeaTime Science would not exist. This has been a great distraction during tough times in the lab and a fantastic jumping off point into the fantastic world of science engagement.

Special thanks needs to be given to Sam Rowe. Having been flatmates for the majority of our PhDs I can safely say he's not bad for a chemist. He has been a great support throughout my PhD and played a large part in making the last few years as good as they've been. Escaping on a few big trips together also helped keep the PhD batteries charged!

Finally, I would like to thank my parents for supporting me throughout my life, even if they still barely know what I actually do! They have always been there for me and keep me grounded. In the same vine, I want to thank my friends from the Fens for reminding me that life away from science does exist. I also want to thank the Norwich gang for looking after me and often keeping me very well fed!

There are of course many others who have helped me in numerous ways over the duration of my PhD and I thank you all.

Publications Including Work Appearing in Thesis

Edwards, M. J., White, G. F., Norman, M., Tome-Fernandez, A., Ainsworth, E., Shi, L., Fredrickson, J. K., Zachara, J. M., Butt, J. N., Richardson, D. J. and Clarke, T. a. (2015) 'Redox Linked Flavin Sites in Extracellular Decaheme Proteins Involved in Microbe-Mineral Electron Transfer.', *Scientific Reports*. Nature Publishing Group, 5(July), p. 11677.

Abstract

Many microorganisms can utilise a wide range of terminal electron acceptors, including solid minerals in the environment. *Shewanella oneidensis* is a well studied model for extracellular electron transfer with many of its biochemical pathways the subject of investigation. *S. oneidensis* utilises c-type cytochromes embedded in its outer membrane to link the oxidation of carbon sources to the reduction of extracellular terminal electron acceptors. Although the MtrCAB complex is known to be the primary pathway by which electrons, originating in the reduced menaquinol pool, can be conducted across the bacterial outer membrane and to extracellular terminal electron acceptors, the exact mechanism by which electrons are transferred from MtrC to electron acceptors remains unclear. MtrA and MtrC are decaheme cytochromes that form wire-like molecular pathway for electrons to be conducted across the bacterial membrane. MtrB is a porin that allows close contact between the periplasmic MtrA and the extracellular facing MtrC. Flavin molecules, secreted by *S. oneidensis*, have been shown to interact with MtrC either forming cofactor like associations with the protein (forming a flavocytochrome) or functioning as soluble electron shuttles transiently interacting with the protein. The evidence for each mechanism may be dependant on the redox state of a conserved disulphide bond in domain III of MtrC. Chemical reduction of this bond allows formation of a MtrC-flavin bound flavocytochrome form of MtrC. This form could react better with minerals to dictate the mechanism of electron transfer.

Mutations made to *mtrC* resulted in the substitution of the cysteine disulphide residues to alanine residues in the MtrC amino acid sequence. Growth studies showed *S. oneidensis* expressing these MtrC variants experienced extended lag phases when growing under aerobic conditions. This was shown to be caused by cytotoxic levels of hydrogen peroxide, generated from reduction of molecular oxygen, accumulating around the bacterial cells. Protein studies

implicated stronger interactions between FMN and MtrC, in disulphide disrupted variants, as the cause of increased reactive oxygen species generation. We hypothesise the disulphide bond in domain III of MtrC functions as a redox switch imparting protein level control over reactivity of MtrC in oxygen variable environments with FMN bound MtrC being the

Abbreviations

ATP	Adenosine Triphosphate
ETC	Electron Transport Chain
NAD	Nicotinamide Adenine Dinucleotide
TCA	Tricarboxylic Acid
DNA	Deoxyribonucleic Acid
bp	Base Pairs
OD	Optical Density
OMC	Outer Membrane Cytochrome
Mtr	Metal Reductase
FMN	Flavin Mononucleotide
SDS	Sodium Dodecyl Sulfate
PAGE	Polyacrylamide Gel Electrophoresis
HEPES	(4-(2-hydroxyethyl)-1-piperazineethanesulfonic acid)
NaCl	Sodium Chloride
LDAO	N,N-Dimethyldodecylamine N-oxide
PEG	Polyethylene Glycol
DMSO	Dimethyl Sulfoxide
LB	Luria Broth
ROS	Reactive Oxygen Species
H_2O_2	Hydrogen Peroxide
e^-	Electron
H^+	Proton
ΔmtrC	Knockout *mtrC* Gene
pMtrC	Plasmid Containing Native *mtrC* Gene
pC444A	Plasmid Containing *mtrC* with C444A Substitution
pC453A	Plasmid Containing *mtrC* with C453A Substitution
pC444A,C453	Plasmid Containing *mtrC* with Double Cysteine Substitution

Contents

Chapter 1

Introduction

Life has evolved to flourish in every ecological niche on planet Earth. Biodiversity may vary across environments, but even those historically thought inhospitable are now known to provide everything needed for life (McKay and Young, 1997). It is not macroscopic life that prevails on this planet however; rather the majority of life is comprised of microscopic organisms belonging to the bacterial and archaeal prokaryotic domains of life (Woese and Fox, 1977). This is not surprising when the number of bacterial species is estimated to be between 10^7 and 10^9 worldwide (Schloss and Handelsman, 2004).

The high level of species richness in prokaryotic organisms is in no small part due to the relatively high DNA mutation rate within cells and the short generation times. This has allowed prokaryotic cells to adapt to a vast range of environments each with its own stresses and limits on bioavailable elements (Brooks *et al.*, 2011). These adaptions vary depending on the environment with prokaryotes displaying a multitude of different survival strategies. Cellular morphology as well as reproductive and replicative strategies are often the most readily observed differences. The rod shaped *Escherichia coli* bacteria divide via binary fission, with daughter cells identical to the parent. In contrast species of *Streptomyces* grow via the formation of filamentous mycelium with many species undergoing sporulation to reproduce (Madigan *et al.*, 2008). Less visible differences also occur within prokaryotic cells at the molecular protein level.

The evolution of different proteins allows for numerous biochemical pathways to exist. Some of the most varied pathways are those relating to metabolism. This is widely encompassing of anabolic and catabolic pathways designed to balance the synthesis and breakdown of complex molecules. This variability allows bacteria to adapt to utilise a wide range of elements in the environment, many of which would not be bioavailable to higher order organisms, in cellular processes such as respiration (Richardson, 2000).

1.1 Metabolism

1.1.1 The Coupling of Oxidation and Reduction

Cellular respiration is ultimately the production of energy (in the form of ATP) from coupling oxidation of a low redox potential electron donor to the reduction of a high redox potential electron acceptor. The free energy difference between the starting donor and the end acceptor is used to maintain a proton gradient across a membrane that in turn provides the energy to drive the enzymatic conversion of ADP to ATP. This generation of ATP occurs via the electron transfer chain (ETC) where electrons are passed through protein pumps that drive the translocation of protons across a membrane to generate the gradient needed for ATPase to function. The type of respiration undertaken often depends on the availability of terminal electron acceptors in the natural environment of the organism. Aerobic respiration is often preferred due to the large free energy difference between electron donor and oxygen however many microorganisms have evolved to utilise a number of different terminal electron acceptors in the absence of oxygen during anaerobic respiration. For these processes to function optimally, electron donors, such as NADH, first must be generated through metabolic pathways to drive ATP generation (Nelson, Lehninger and Cox, 2008).

Many eukaryotic organisms exhibit similar metabolic and respiratory pathways based on glucose functioning as the initial electron donor (Groen *et al.*, 1982). In these organisms, glycolysis occurs to convert glucose to pyruvate and in the process generate small amounts of NADH and ATP (Figure 1.1). Pyruvate next undergoes pyruvate decarboxylation via the pyruvate dehydrogenase complex. This is a complex of three proteins consisting of pyruvate dehydrogenase, dihydrolipoyl transacetylase and dihydrolipoyl dehydrogenase (Patel and Roche, 1990). The result of this reaction is the production of acetyl CoA which can then feed into the citric acid (TCA) cycle and generate further NADH and FADH (Figure 1.2). Both of these can function as electron donors in the electron transport chain in oxidative phosphorylation.

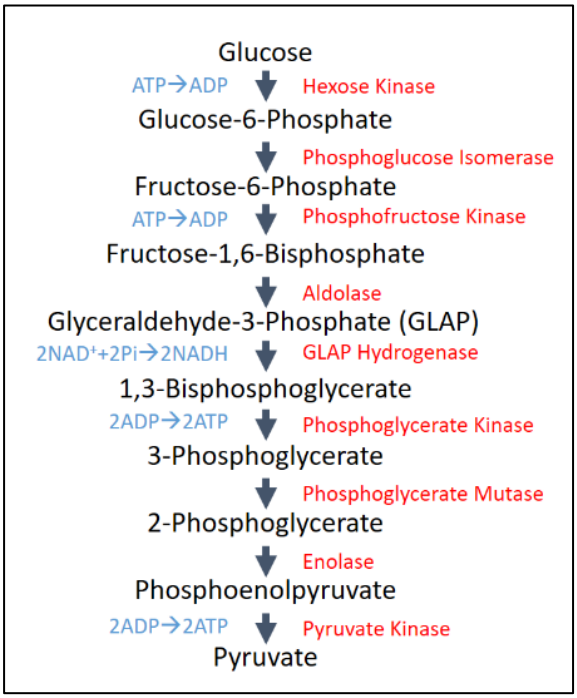

Figure 1.1 – Overview of conversion of glucose to pyruvate in glycolysis. Enzymes highlighted in red and significant respiratory molecules used in reactions highlighted in blue.

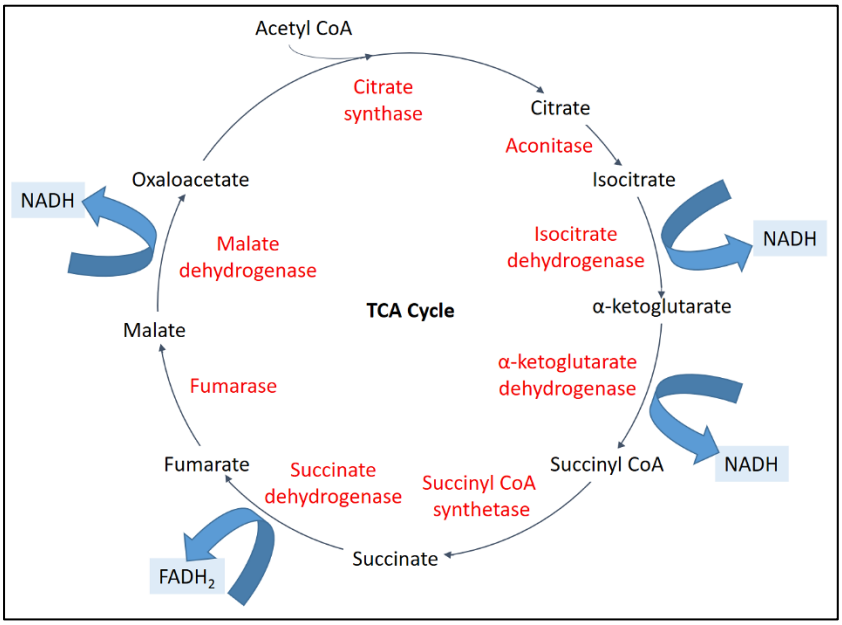

Figure 1.2 – Schematic of TCA cycle. Enzymes highlighted in red and generated electron donors used in downstream respiratory processes highlighted in blue.

Oxidative phosphorylation found in mammalian cells is generally the best known form of aerobic respiration owing to its prevalence across many species and domains of life. Our own species is included within this and this has led to an understanding of the process being vital in treatment of many metabolic diseases we face (Shoffner, 2001). NADH generated from the TCA cycle localises to the ETC in the inner membrane of gram negative bacteria where it comes into contact with NADH dehydrogenase (complex I). Here NADH is oxidised to NAD^+ in a two electron transfer that ultimately results in the reduction of ubiquione to ubiquinol within the lipid membrane. This electron transfer also results in the translocation of four protons across the membrane building a gradient between the cytoplasm and the periplasm. Succinate dehydrogenase (complex II), as previously mentioned, also reduces the quinone pool as a result of the conversion of succinate to fumarate. Cytochrome bc_1 complex (complex III) becomes reduced by the quinol pool that passes the resultant electrons to the soluble electron carrier cytochrome *c*. The energy from the electrons are again used to pump further protons across the membrane increasing the proton gradient more. Electrons carried by cytochrome *c* are used to reduce cytochrome *c* oxidase (complex IV) before this terminal oxidase reduces molecular oxygen to H_2O (Groen *et al.*, 1982). This removes electrons from the chain allowing for the process to continue (Figure 1.3). The proton motive force generated across the membrane form the proton gradient is then used to drive ATPase which catalyses the formation of ATP from ADP and inorganic phosphate (Mitchell, 1961).

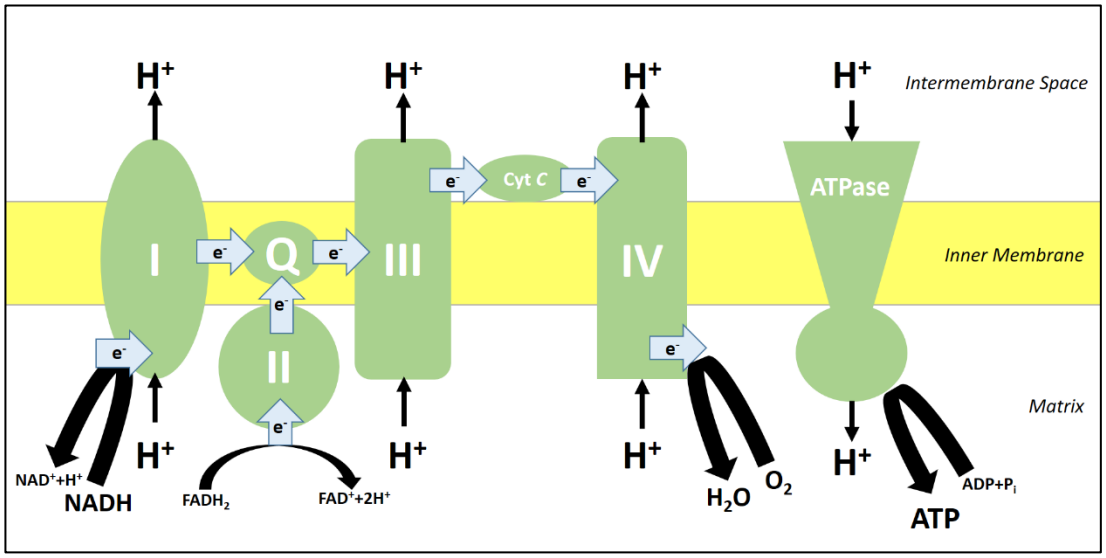

Figure 1.3 – Diagrammatical representation of mammalian mitochondrial electron transport chain (ETC) under aerobic conditions. Proteins involved in the ETC labelled with their complex numbering. Electron flow through the system indicated via blue arrows. Substrate oxidation and reduction highlighted along with ATP formation.

1.1.2 Metabolic Diversity in Eukaryotes

This outline of respiratory metabolism applies to only a narrow spectrum of species. Eukaryotic organisms typically exhibit this pathway with little variation when considering the domain as a whole. Part of the reason for this is the compartmentalisation of much of the pathway into mitochondria. Mitochondria themselves are thought to have originated as free living bacteria that, at some point in evolutionary history, were engulfed by another cell. This lead to the endosymbiosis seen between mitochondria and eukaryotic cells (Yang *et al.*, 1985). Because of this, many of the same pathways have been conserved within the mitochondrial genome leading to less respiratory diversity.

There are of course a number of differential adaptions within the eukaryotes. Some organisms have adapted to low oxygen environments, utilising alternative terminal electron acceptors. Some of the more differentiated transfer electrons to protons instead of oxygen whilst many others follow fermentative pathways and substrate level phosphorylation to survive the lack of bioavailable exogenous acceptors

(Embley and Martin, 2006). Many yeasts continue to utilise fermentative pathways even in the presence of oxygen, instead coupling the oxidation of sugars with the reduction of pyruvate formed during the breakdown of said sugars. This allows ATP to be generated whilst ensuring a sufficient pool of oxidised NAD^+ to facilitate the breakdown of the carbon source (Trevelyan and Harrison, 1952). Plants demonstrate another adaption that sets them apart from other eukaryotes. They utilise photosynthesis to generate their carbon source from the energy in light rather than relying on uptake of exogenous carbon sources to fuel their metabolism (Nelson, Lehninger and Cox, 2008).

1.1.3 Metabolic Diversity in Prokaryotes

The level of variability in eukaryotic metabolic pathways may seem vast but it is dwarfed by that seen in prokaryotes. There are some microorganisms that follow similar respiratory pathways to those seen in mammalian mitochondria. *Rickettsia prowazekii* have been found to contain a full set of genes required for the TCA and electron transport chain previously described (Andersson *et al.*, 1998). This allows the bacteria to utilise the same carbon sources and undergo respiration identical to that seen in mitochondria. This also implicates the species, among others, as highly related to that of the mitochondrial free living ancestor.

Other bacteria use more adaptive pathways encompassing all those found in eukaryotes. *Cyanobacteria* species are autotrophs that, much like plants, utilise the energy of sunlight to drive photosynthesis to generate NADH. Oxygenic bacteria are thought to be the precursors of chloroplasts and as such photosynthesis in these organisms functions very similarly (Mulkidjanian *et al.*, 2006). Light is used to split water molecules into molecular oxygen and protons. The resultant electrons are passed through a series of proteins that pump more protons across the bacterial membrane. This leads to a gradient that can drive the formation of ATP from ADP. NADPH is also formed through this process, which can be used to fix carbon dioxide into glucose. This glucose can then be broken down to produce NADH which can be used in the ETC to generate larger amounts of ATP (Alberts *et al.*, 2002).

Fermentation is also widespread throughout prokaryotic species. This heterotrophic process is perhaps even more diverse in bacteria than it is in yeasts. Louis Pasteur demonstrated in the 1860s how bacteria were capable of fermenting the ethanol produced from yeast fermentation to acetyl acid (Pasteur, 1860; Berche, 2012). Since then many species have been studied showing great variation in the sugars each is capable of fermenting even within genera. For example, *Neisseria meningitidis* has been shown to ferment glucose and maltose, but not sucrose and lactose. *Neisseria gonorrhoea*, however, ferments glucose, but not maltose, sucrose or lactose (Brown, 1974; Madigan *et al.*, 2008). This diversity is often exploited in medical testing as well as in the food and chemical industry. In all cases of fermentation the fundamental process remains the same. A carbon source is oxidised leading to the generation of ATP and NADH. An endogenous downstream product from this reaction is then reduced by the NADH to replenish the NAD^+ pool so fermentation can continue. *Escherichia coli* utilise this method of energy metabolism in the form of mixed acid fermentation. This process allows two stages of ATP and NADH production. The first is the glycolysis reaction, which, as previously stated generates two molecules of ATP and two molecules of NADH. The pyruvate produced from this can then be converted into a variety of end products, often requiring NADH to reduce the pyruvate. The resultant products help to balance the requirements of other metabolic pathways with excess (or unwanted) products excreted from the cell. It is important to note that the end products, although produced from the reduction of pyruvate, must provide a degree of free energy when balanced against the starting glucose to allow for a cellular energy net gain (Hogg, 2013). Other pathways such as the entner-doudoroff (ED) pathway and the pentose phosphate pathway (PPP) are also employed to utilise carbon sources through alternative pathways.

Heterotrophs utilising exogenous organic substrates through pathways such as the Embden Meyerhof Parnas (EMP) pathway, are also incredibly varied across prokaryotes. The well studied *E. coli* species has been seen to metabolise over 30 different carbon sources in the form of amino sugars, sugar alcohols, sugar acids, as well as pentose and hexose sugars. Although different enzymes are used to

catabolise these carbon sources, the end product is often pyruvate which can then feed into downstream respiratory pathways (Cooper, 1986). This is also how lactate is often metabolised, with lactate dehydrogenase catalysing the interconversion of lactate to pyruvate (Garvie, 1980). As well as catabolising common sugars such as glucose, fructose and maltose, many bacteria are capable of using other carbon sources in their metabolism. Some bacteria like *Clostridium stercorarium* can use enzymes that allow the breakdown of polysaccharides such as cellulose (Zverlov and Schwarz, 2008). Others, such as *Citrobacter*, have evolved to utilise acetate and formate with both being converted to acetyl-CoA via acetyl-CoA synthetases and formate dehydrogenases, respectively. This acetyl-CoA can then feed into the TCA cycle of these bacteria to generate NADH (Kim *et al.*, 2012). Sometimes described as distinct from heterotrophy, methylotrophy is the utilisation of C_1 compounds such as methane (De Marco, 2004). *Methylococcus capsulatus* is an example of these bacteria that oxidise methane via the ribulose monophosphate pathway to formaldehyde. This can then be assimilated into biomass or further oxidised to formate, generating cellular energy (Chistoserdova, Kalyuzhnaya and Lidstrom, 2009).

Chemolithotrophs derive their energy from oxidation of inorganic compounds. Hydrogen can be metabolised via either soluble or membrane bound hydrogenases. The soluble enzyme is less common than the membrane forms. In *Nocardia opaca* it oxidises hydrogen and reduces NAD^+ to increase the electron donor pool to the electron transport chain in the cell (Schink and Schlegel, 1978). Both Fe-Fe and Ni-Fe hydrogenase membrane associated enzymes have been seen to facilitate the oxidation of hydrogen to protons (usually quickly reacting to form water) with the electrons transferred into the quinone pool (Shafaat *et al.*, 2013). Notably this process is seen able to function in the reverse allowing electrons to be removed from the quinone pool in the form of hydrogen. Even examples of bacteria utilising minerals as electron donors are numerous. Iron oxidising bacteria such as the gram negative *Acidithiobacillus ferrooxidans* can oxidise ferrous iron in the environment to form solid ferric compounds. This occurs at the surface of the cell with resultant electrons being used to produce NADH which can then act as an electron donor in the bacteria's ETC

(Johnson, Kanao and Hedrich, 2012). These lithotrophic organisms emphasise how bacteria are able to utilise many electron donors that are not bioavailable to many other organisms. These processes often, rather ironically, alters the redox state of the minerals making the elements more bioavailable in the environment (Bond, Druschel and Banfield, 2000).

1.1.3 Metabolic Diversity in *Shewanella*

It is important to remember all the diversity mentioned up until this point is focused on catabolism of carbon sources and electron donor utilisation. The species spoken of this far are often not limited to the metabolism they exemplify here. This is made possible by the huge variations within metabolic pathways between bacterial species (Richardson, 2000). This metabolic flexibility can be seen in *Shewanella oneidensis* where high respiratory diversity and versatility is beneficial for survival owing to the generally low amounts of any one terminal electron acceptor in the environment. This bacteria can catabolise a range of carbon sources including lactate, formate, acetate, pyruvate and a variety of amino acids. *S. oneidensis* is however unable to use glucose as a carbon source due to the absence of 6-phosphofructokinase with a preference for three-carbon sugars (Serres and Riley, 2006). *S. oneidensis* is also not considered a fermentative organism even though a fermentative lactate dehydrogenase has been identified within the genome (Serres and Riley, 2006). The ability of *S. oneidensis* to utilise such a variety of carbon sources appears linked to the terminal electron acceptor available. Under anaerobic conditions with lactate and TMAO used as the sole carbon source and electron acceptor respectively, a complete TCA cycle can be observed (Tang *et al.*, 2007). This allows many of the aforementioned carbon sources to undergo conversion through the pentose pathway and enter the TCA cycle as acetyl-CoA. Other studies, under different conditions, have shown an incomplete TCA cycle (lacking 2-oxoglutarate dehydrogenase), with many other carbon sources undergoing conversion through the serine-isocitrate lyase pathway (which itself is incomplete) to serine which is then able to enter the TCA cycle as oxaloacetate via an oxidising degradation pathway (Scott and Nealson, 1994).

The resulting NADH is oxidised by NADH dehydrogenases which pumps protons across the inner membrane generating a proton motive force (Qiu *et al.*, 2013). *Shewanella* species express a number of NADH dehydrogenases, with only *S. denitrificans* expressing a single NADH dehydrogenase. This species is also known to use denitrification pathways and the reduced menaquinone pool to translocate protons across its membrane generating proton motive force (Bertero *et al.*, 2003). *Shewanella* species are also known to use formate to generate a proton motive force. Formate can be generated via the pyruvate formate lyase pathway during anaerobic growth. It known to be oxidised by formate dehydrogenase enzymes transferring the resulting electrons into the menaquinone pool and utilising the resulting protons to generate a protein motive force (Kane *et al.*, 2016). Succinate dehydrogenase, Ni-Fe hydrogenase and sulphite dehydrogenase are also known to be present in the genome of *S. oneidensis* MR-1 and all help to generate a proton motive force whilst reducing the ubiquinone and menaquinone pools (Qiu *et al.*, 2013). This proton gradient is then used to drive ATPase generating ATP for the cell (Figure 1.4). It is worth noting that the level of complexity in carbon metabolism, highlighted here in *Shewanella* species, is not unusual for bacteria (Richardson, 2000). In fact, in many cases the real complexity arises when considering the respiratory pathways associated with re-oxidising the ubiquinone and menaquinone pools.

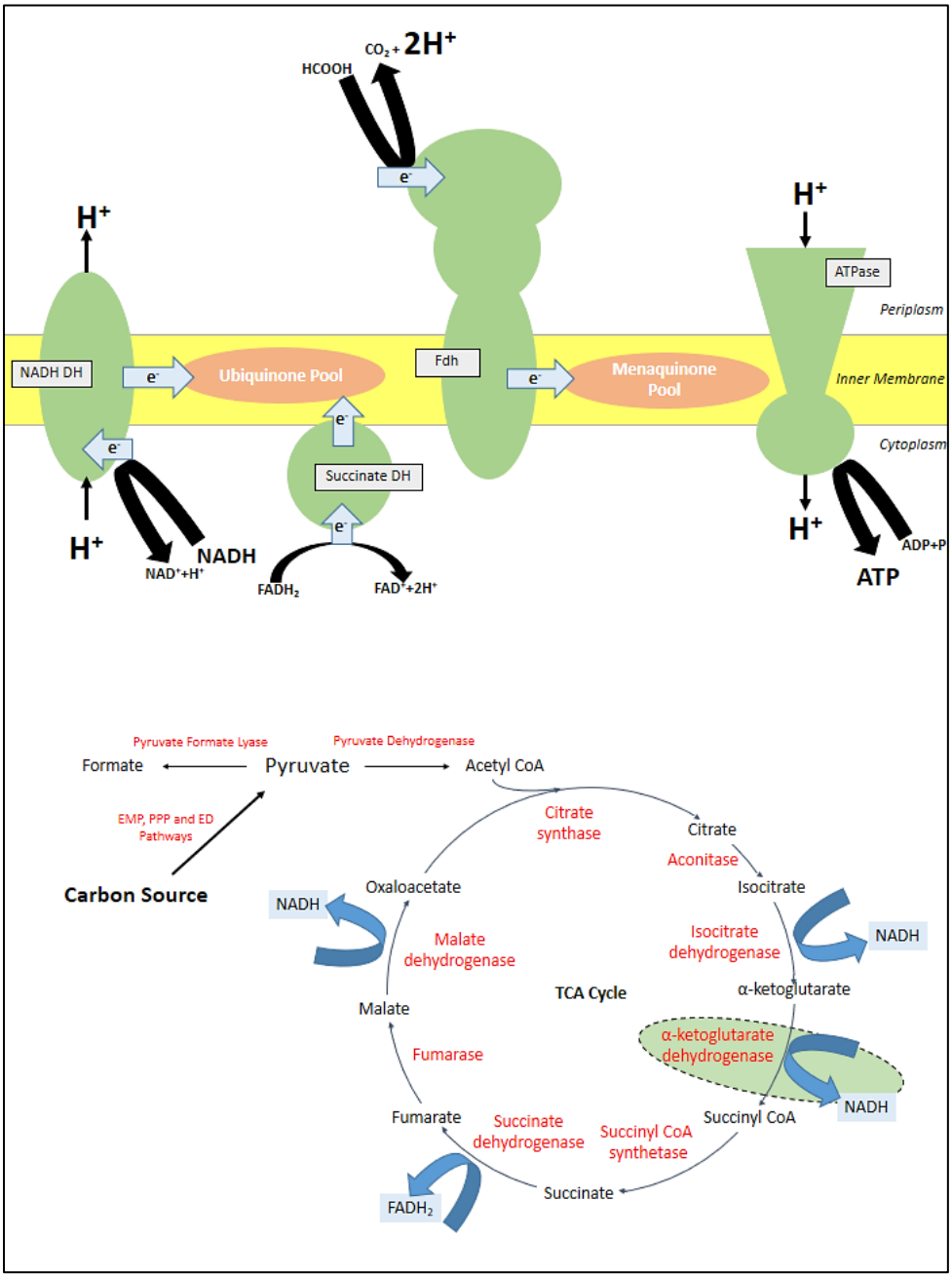

Figure 1.4 – Overview of carbon catabolism in *S. oneidensis* and main dehydrogenases (DH) involved with proton motive force generation coupled with ubiquinone and menaquinone pool reduction. Missing step of TCA cycle under certain conditions highlighted.

1.2 Terminal Respiratory Enzymes

1.2.1 Aerobic Oxidases

Although there is huge variation in the organisation of the ETC across the domains of life, the fundamentals behind all ETC systems are largely the same. Protons are pumped across a membrane to generate a proton motive force which is used to drive the generation of ATP. These proton pumps require electrons to function and so all require the oxidation of an electron donor (often NADH) and in many cases the quinone pool in the inner membrane is reduced to facilitate this process (Bueno *et al.*, 2012). In the case of aerobic respiration there is a terminal oxidase present to reduce oxygen to H_2O. This oxidises the quinone and allows the metabolic pathways to continue (Crane, 2007). This category of enzyme is broad with the main types defined as cytochrome oxidases or quinol oxidases. The electron donor each type use utilise allows classification of these heme-copper oxidases into distinct types. All exhibit low spin heme and high spin copper binuclear centres at which the reduction of oxygen takes place (Pereira *et al.*, 2008). However, while each oxidase has a similar heme centre, they can be differentiated into three main categories the a, b and c type cytochrome oxidases. These differ in their affinity for oxygen and proton channels with their expression appears linked to this, with multiple oxidase genes often present in the same bacterial species (Sousa *et al.*, 2012). *Rhodobacter sphaeroides* express three oxidases, one bb_3 type quinol oxidase and two cytochrome c oxidases (aa_3 and cbb_3). The aa_3 and quinol oxidase was found more highly expressed under aerobic growth conditions whilst cbb_3 expression is upregulated under micro aerobic conditions (Toledo-Cuevas *et al.*, 1998). This oxidase has shown high affinity for oxygen in the order of 7 nM allowing for aerobic respiration to continue even in environments where oxygen levels are often considered too low for this form of respiration (Preisig *et al.*, 1996).

1.2.2 Anaerobic Reductases

Although many organisms have evolved to utilise oxygen as a terminal electron acceptor, microorganisms have often evolved to use other pathways and abundant electron acceptors in their environmental niche. Some are able to use oxygen when it is present but are also able to switch their respiration when oxygen becomes in short supply. These organisms are termed facultative anaerobes. Others have evolved to exclusively use substitutes for oxygen and are termed obligate anaerobes. These organisms are unable to use oxygen in their respiration and its presence is often toxic to the cells (Madigan *et al.*, 2008).

Nitrate respiration is a well studied example of anaerobic respiration. This respiratory pathway consists of four main reactions that provide the cell with less free energy (and so less ATP) than aerobic respiration does although this is still enough for many bacteria to survive and divide (Simon, van Spanning and Richardson, 2008). This dissimilatory reduction of nitrate, termed denitrification, leads to the conversion of nitrate to gaseous nitrogen (Figure 1.5). The reactions involved are catalysed by the Nar proteins. NarGHI are a membrane associated complex and couples quinol oxidation with protein translocation across the membrane. This again generates a proton motive force capable of driving ATP synthesis (Berks *et al.*, 1995). To further emphasise the diversity in prokaryotic respiratory pathways, it is worth noting that many bacterial species use nitrate respiration but reduce the nitrate to different products. Others utilise the reduction of nitrite to ammonium via the Nrf pathway (Cole and Richardson, 2008).

Reaction 1	$2NO_3^- + 4e^- + 4H^+ \rightarrow 2NO_2^- + 2H_2O$
Reaction 2	$2NO_2^- + 2e^- + 4H^+ \rightarrow 2NO + 2H_2O$
Reaction 3	$2NO + 2e^- + 2H^+ \rightarrow N_2O + H_2O$
Reaction 4	$N_2O + 2e^- + 2H^+ \rightarrow N_2 + H_2O$

Figure 1.5 – Reaction equations for the four steps of the denitrification pathway. This anaerobic respiratory pathway allows generation of ATP to continue in the absence of oxygen as a terminal electron acceptor.

Other species have adapted to different environments, with pathways specific for the reduction of other acceptors. Sulphur and thiosulphate are reduced by *Salmonella enterica* via the PhsABC complex (Burns and DiChristina, 2009). Trimethylamine oxide (TMAO), found in high concentrations in dead fish, can be reduced to hydrogen sulphide by *Shewanella putrefaciens*, a large cause of fish spoilage (Gram, Trolle and Huss, 1987). Dimethyl sulfoxide (DMSO) is reduced by many marine microbes (Griebler and Slezak, 2001). This forms dimethyl sulphide and provides the distinct smell of the sea. Carbon compounds such as fumarate are also utilised by bacteria. Fumarate reductase is a flavocytochrome that facilitates this reduction. It is one of the most widespread systems allow a broad spectrum of microorganisms to undergo this form of anaerobic respiration (Leys *et al.*, 1999).

Even compounds usually considered highly toxic can be utilised by prokaryotic respiration. *E. coli* has been seen to utilise hydrogen peroxide (H_2O_2) as a terminal electron acceptor via a non-detoxifying peroxidase only expressed in the absence of oxygen (Khademian and Imlay, 2017). This compound was, until recently, considered universally toxic to bacteria with reduction of H_2O_2 being carried out as a defence mechanism to reactive oxygen species (ROS). Another toxic substance, arsenate is known to uncouple the glycolysis pathway resulting in a reduction of ATP generation. This often results in arsenate containing compounds being toxic to organisms (Hughes, 2002). However even this has been seen to be utilised as a terminal electron acceptor in respiration. *Chrysiogenes arsenatis* and *Bacillus selenitireducens* both express characterised arsenate reductases with genes for the enzyme also being identified in *Shewanella* species (Saltikov and Newman, 2003). The cellular localisation of these enzymes appears to vary between soluble in the periplasm and membrane associated depending on the species of bacteria the protein is isolated from (Stolz *et al.*, 2006). In all cases the quinol pool is linked to the arsenate reductases to allow for reduction of the terminal electron acceptor and for the electron transport chain to continue to produce a proton gradient and thus generate ATP.

1.2.3 Dissimilatory Metal Reduction

It was long thought electron donors and acceptors had to first be taken into bacterial cells before they could be used in respiratory processes. This assumption was proven incorrect when dissimilatory metal reduction was observed. Mineral respiring organisms are able to make use of solid minerals in the extracellular environment to provide a source of electrons in respiration or indeed use them as terminal electron acceptors. Throughout both these processes the minerals remain outside the cell and instead electrons are transferred into or out of the cell across the bacterial membrane. The diversity among microorganisms able to carry out this extracellular electron transfer is vast with species from relatively unrelated phyla now known to utilise this form of respiration. Over the last 20 years, dissimilatory metal reducing bacteria have become the subject of much research with the aim of better understanding the biochemical processes involved with this respiration to potentially exploit systems for biotechnological applications (White et al., 2016).

Geobacter is a genus of gram-negative delta proteobacteria isolated in river sediment (Coates *et al.*, 1996). Species of *Geobacter* are strict anaerobes which makes their study much more difficult, however this has not stopped them becoming a model organism for extracellular electron transport. There are 111 c-type cytochromes predicted from the genome of *Geobacter sulfurreducens* (Methé *et al.*, 2003) many of which are predicted contain multiple heme groups. Currently the exact process of transporting electrons, shuttled across the periplasm from the electron transport chain by the triheme protein PpcA, across the outer membrane is still unknown (Lloyd *et al.*, 2003). However, the deletion of a number of outer membrane cytochromes (including OmcB, OmcS, OmcT, OmcE and OmcZ) has been seen to impact the ability of *G. sulfurreducens* to reduce extracellular ferric iron (Richter, Schicklberger and Gescher, 2012). This again suggests the importance of conductive molecular wires linking respiration to the environmental electron acceptors.

Extracellular electron transfer is not unique to gram-negative bacteria. *Thermincola potens* is a gram-positive bacterium shown to be capable of reducing solid ferric

minerals. Although the cell architecture of *T. potens* is vastly different to that of gram-negative dissimilatory metal reducing bacteria, there is increasing evidence that c-type cytochromes again play a large role in transporting electrons out of the cells. When the genome of the species was sequenced there was an abundance of multi-heme cytochromes predicted. A number of such cytochromes were found localised to the extracellular surface and when the proteins were degraded the ability of *T. potens* to reduce environmental ferric iron was reduced (Carlson *et al.*, 2012). Characterisation of these cytochromes is now underway to investigate their potential to form molecular wires able to conduct electrons from the electron transport chain directly out of the cell (Costa *et al.*, 2015).

Perhaps the most best understood example of dissimilatory metal reduction is that of *Shewanella*. *Shewanella* is a genus of gram-negative facultative anaerobes belonging to the gamma proteobacteria. Many species are found at the oxic / anoxic interface in river and lake sediment layers where they are able to grow planktonic or within biofilms including *S. oneidensis* first isolated in lake Oneida, New York (Myers and Nealson, 1988). As well as having the ability to catabolise the wide range of carbon sources mentioned previously, *Shewanella* species have also evolved to respire using a wide range of terminal electron acceptors. The bacteria has been seen able to switch between these respiratory pathways rapidly with evidence that many of the pathways are constitutively expressed even when not in use (Jeffrey S. McLean *et al.*, 2008). This suggests a greater level of protein level regulation rather than genomic level.

Three terminal oxidases are coded for in the genome of *Shewanella oneidensis*; a bd type quinol oxidase, a cbb_3 type cytochrome c oxidase and an A type oxidase (Heidelberg *et al.*, 2002). The expression of each of these oxidases varies dependant on the nutrient composition of the environment the bacteria are growing in (Le Laz *et al.*, 2016). Anaerobic respiratory pathways also exist in *Shewanella* allowing the bacteria to grow without the presence of oxygen by utilising many inorganic soluble chemical acceptors. Nitrate, nitrite, tetrathionate and TMAO can all be reduced as electron acceptors by NapAB, NrfAB, Trt and TorCA respectively (Beliaev *et al.*,

2001; El-Sharoud, 2008). Sulphur can be reduced by the PsrABC complex, homologous to the PhsABC of Salmonella(Burns and DiChristina, 2009). Organic compounds such as fumarate can also enter the cell and be used as electron acceptors via fumarate reductase (Fredrickson et al., 2008). In *Shewanella* species this linking of quinol pool to reductase appears to be carried out by the membrane associated CymA that directs electron transduction to various reductases, dependant on the available terminal electron acceptor (Zargar and Saltikov, 2009).

Perhaps the most remarkable group of electron acceptors *Shewanella* can utilise are the solid metal compounds in the extracellular environment. Often in the form of minerals, ferric iron and manganese are both capable of sustaining bacterial growth (White et al., 2016). The coupling of carbon source oxidation with these insoluble terminal electron acceptors requires electrons to be transported from the electron transport chain, through the membranes and out of the cell. This is accomplished through systems of electron conductive proteins, namely the MtrCAB pathway in *Shewanella*. In fact extracellular electron transport in *Shewanella* species is not only limit to extracellular minerals. The DmsEFAB complex allows reduction of the organosulphur compound DMSO via outer membrane proteins (Gralnick et al., 2006). This again highlights the versatility of *Shewanella* as a model organism in the field.

As previously stated, *Shewanella* species are not the only bacteria to have evolved systems to utilise solid minerals in the extracellular environment. There are many examples of species across numerous phyla with the term dissimilatory metal reducing bacteria used to describe them collectively. In fact, certain archaea have also been found to respire via mineral reduction. This suggests coupling of the oxidation of organic substrates to the reduction of metals is an incredibly old and successful form of respiration (Vargas *et al.*, 1998).

Although many of the extracellular electron transfer process mentioned here have been widely studied, there are still many questions left unanswered especially with respect to how electrons initially (or terminally) pass from the bacterial cell to the mineral in the environment. In many cases studies have highlighted outer membrane

cytochromes (OMCs) to play a crucial role. These are membrane associated proteins facing out into the extracellular environment. Dissimilatory metal reducing bacteria often have numerous OMCs coded for in their DNA highlighting their importance. Knock out studies have shown that in many cases minerals can not be reduced without these OMCs. A distinct feature of these proteins is their ability to conduct electrons through their structure via heme ligands. Other filamentous proteins have been highlighted as potentially allowing the transduction of electrons over large distances again using conductive ligands to link the cellular surface to the terminal electron acceptor. Whether all these OMCs interact directly with extracellular minerals or rather utilise intermediate electron carries around the cells is a topic of much debate (White *et al.*, 2016).

1.3 Application of Extracellular Electron Transfer

1.3.1 Microbial Fuel Cells

Extracellular electron transport is not simply researched for its novelty in microbial metabolism. There are many biotechnological applications for the system that have been suggested as far back as 1911 when the idea of microbial fuel cells was first discussed (Potter, 1911). Microbial fuel cells work on the theory that if terminal electron acceptors are replaced by an electrode, dissimilatory metal reducing bacteria will reduce this anode just as they would naturally occurring iron minerals. There is then a flow of electrons into a circuit that can be used to power devices. At the end of the circuit, a cathode is oxidised by oxygen (or another suitable oxidiser) to complete the circuit.

This technology has proven to have high potential in many industries where large amounts of waste carbon are accessibly to use a feedstock for bacterial cultures. Prototype microbial fuel cells have been trialled in the brewing industry and sewage treatment plants where wastewater was cleaned through the breakdown of high

concentrations of organic contaminants whilst electricity is generated. These systems are especially attractive as anaerobic digesters can easily be converted to microbial fuel cells without large scale remodelling of the sites (Pant *et al.*, 2010).

1.3.2 Application in Microbial Electrosynthesis

There is huge potential for microbial fuel cell technology to be incorporated into a number of industries. However, more recently research into microbial electrosynthesis – utilising extracellular electron transport systems – has been receiving increased attention. Reversing the respiratory systems in dissimilatory metal reducing bacteria can allow for electrons to be fed into the cells. These electrons can then be used to drive bacterial metabolism, with the aim to convert a low value substrate into a high value product. This process has been heavily investigated in *S. oneidensis*. A biofilm of *S. oneidensis* can be established on the surface of a graphite electrode by first poising the voltage at an oxidising potential of +0.24 V. This enables the bacteria to utilise the electrode as a terminal electron acceptor and promotes biofilm establishment. Once the biofilm has been established the potential of the electrode can be made reducing (-0.36 V), to act as an electron donor, and fumarate can be added as an electron acceptor. The electrons from the electrode pass into the cell via the MtrCAB pathway and are then transferred to fumarate reductase (FccA) where they are used to reduce fumarate to succinate (Ross *et al.*, 2011). Succinate is a higher value product than the fumarate substrate and this shows the principle for microbial electrosynthesis.

1.3.3 Application in Bioremediation

Dissimilatory metal reducing bacteria are hugely important in the cycling of trace metals in the environment. Often the levels of iron and other trace metals are limiting factors restricting growth of all clades of life. One main reason for this is the bioavailability of such elements, with soluble forms of metals being the easiest to utilise. Mineral reducing bacteria, respiring on solid minerals, cause changes in the redox state of metals. This often affects the metals solubility - for example the

reduction of insoluble ferric iron to soluble ferrous iron – and as such the availability in ecosystems (Borch *et al.*, 2009).

This ability to affect solubility of metal compounds has led to the use of *S. oneidensis* and other mineral reducing bacteria in bioremediation projects. Often metal contamination is hard to remove from the environment and leakage into water systems is a major problem. The ability to immobilise such contamination by altering the redox state of the metals has the potential to reduce environmental damage often caused by human activity. There is even potential to utilise mineral reducing bacteria in bioremediation of radioactive waste. Studies have observed uranium VI reduction at the cell surface of *S. putrefaciens* driven by electron transfer through outer membrane cytochromes (Wildung *et al.*, 2000). Other dissimilatory metal reducing species such as *Geobacter sulfurreducens* have also been seen able to reduce radioactive metals with cytochrome components of the extracellular electron transport pathway again being implicated in this process (Lloyd *et al.*, 2003).

1.4 Extracellular Electron Transfer

1.4.1 Extracellular Electron Transport in *Shewanella*

As previously stated, the best understood system for extracellular electron transfer is perhaps still that of *S. oneidensis* MR-1. The genome of this microbe encodes for around 40 putative c-type cytochromes (Meyer *et al.*, 2004). Many of these have been characterised allowing for electron transit systems to be described; from the reduced menaquinone pool at the inner membrane, through membrane associated proteins, and away from the cell to terminal electron acceptors.

During respiration, electrons are used to pump protons across the inner membrane generating a proton gradient. The resultant proton motive force is then used to power ATPase and thus generates ATP. At the end of this process, during anaerobic

respiration, electrons are passed into the menaquinone pool where they reduce the periplasmic facing, inner membrane associated, quinol oxidase CymA. This tetraheme cytochrome is then capable of reducing periplasmic proteins, such as the small tetraheme cytochrome (STC) and fumarate reductase. The periplasmic cytochrome pool can then become oxidised by the passing of electrons to the MtrCAB complex (Ross *et al.*, 2007). The first protein in the complex reduced is MtrA. This 32 kDa decaheme cytochrome has been shown to insert into and form a tight association with the 28 strand membrane porin MtrB (Hartshorne *et al.*, 2009). Electrons reduce the heme residues of MtrA before passing to MtrC. MtrC (another decaheme cytochrome) faces the extracellular environment anchored to the membrane by a lipid anchor and also associates with MtrB (Beliaev and Saffarini, 1998). The β-barrel MtrB protein allows MtrA and MtrC to come within very close proximity to one another (Figure 1.6). This close proximity, and crossover of the heme reduction windows of the two proteins, allows electrons to pass from the heme residues of MtrA to the nearby heme of MtrC (Pitts *et al.*, 2003). The heme residues of this OMC have been shown to oxidise and reduce over a wide potential window, spanning from +100 to -500 mV. This allows for rapid conduction of electrons through the protein and ultimately reduction of terminal electron acceptors (Hartshorne *et al.*, 2007).

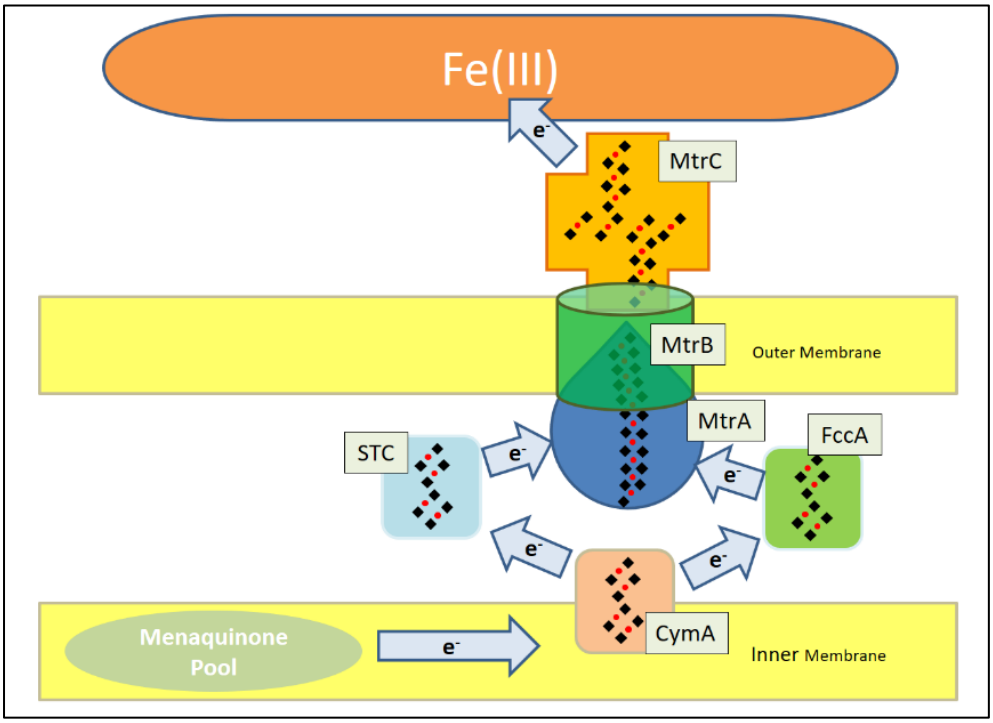

Figure 1.6 – Diagrammatical representation of mineral respiration and extracellular electron transfer pathway in *S. oneidensis*. Carbon catabolism results in the reduction of the menaquinone pool. Electrons from this reduced menaquinone pool are passed to CymA before passing across the periplasm to the MtrCAB complex via electron carrier proteins (such as STC and FccA). MtrA is the first cytochrome in the complex to become reduced, with electrons transducting through the heme residues of the protein. Electrons are able to hop to the heme residues of MtrC due to the close proximity the porin protein MtrB allows for. The hemes of MtrC become reduced before electrons are pass to the terminal electron acceptor in the extracellular environment (here shown as ferric iron). Electron flow highlighted be blue arrows throughout diagram.

1.4.2 Mechanisms of Electron Transfer

Although many OMCs have been biochemically characterised, and their role in mineral respiration is generally known, there are few examples where the exact mechanism of interaction with extracellular terminal acceptors is considered clear. There are generally three main categories of electron transfer mechanism thought to apply to this final step of mineral reduction. All three of these mechanisms have

evidence supporting them and apply to most examples of dissimilatory metal reducing bacteria discussed. *S. oneidensis* is considered one of the most studied model organisms in the field and so the following descriptions will focus on this organism and its associated OMCs. However, it should be noted that none are exclusive to *S. oneidensis.*

First is the model of direct electron transfer (Figure 1.7, Panel A) which states terminal electron acceptors become reduced when they come into direct contact with OMC proteins (and so the bacterial cell). Specific binding affinity allows for a tight interaction to occur between the mineral surface and the outer membrane cytochrome (Lower *et al.*, 2007). The close proximity allows for electrons to transfer the short distance from the outermost heme residue of the OMC to the terminal electron acceptor. It is worth noting a number of studies have demonstrated limitations to this model. Kinetic characterisation of the outer membrane cytochromes showed direct electron transfer to insoluble electron acceptors (such as goethite) did occur, however, rates were not viable to support cell growth (Ross, Brantley and Tien, 2009). This investigation also took the accessory outer membrane cytochromes, such as OmcA in *S.* oneidensis, into account and still surmised that another element was needed in the system to enhance transfer rates. More recent studies suggest that this discrepancy between electron transfer rates between OMCs and mineral terminal acceptors may have in part been due to the non-physiologically relevant nature of isolated OMC studies. In these studies proteoliposome were developed to allow a controlled model of the bacterial cell. Chemical reductants could be encapsulated in lipid membranes with MtrCAB complexes embedded in the lipid bilayer. This provided a conductive link between the reductant and the terminal acceptor, akin to that in whole cell models (White *et al.*, 2012). Here, when solid phase ferric iron compounds were used as terminal electron acceptors, electron transfer rates were recorded to be 10^3 times faster through the MtrCAB complex. This experiment suggests direct electron transfer through the MtrCAB complex would be rapid enough to sustain bacterial cell growth, contrary to past protein studies (White *et al.*, 2013).

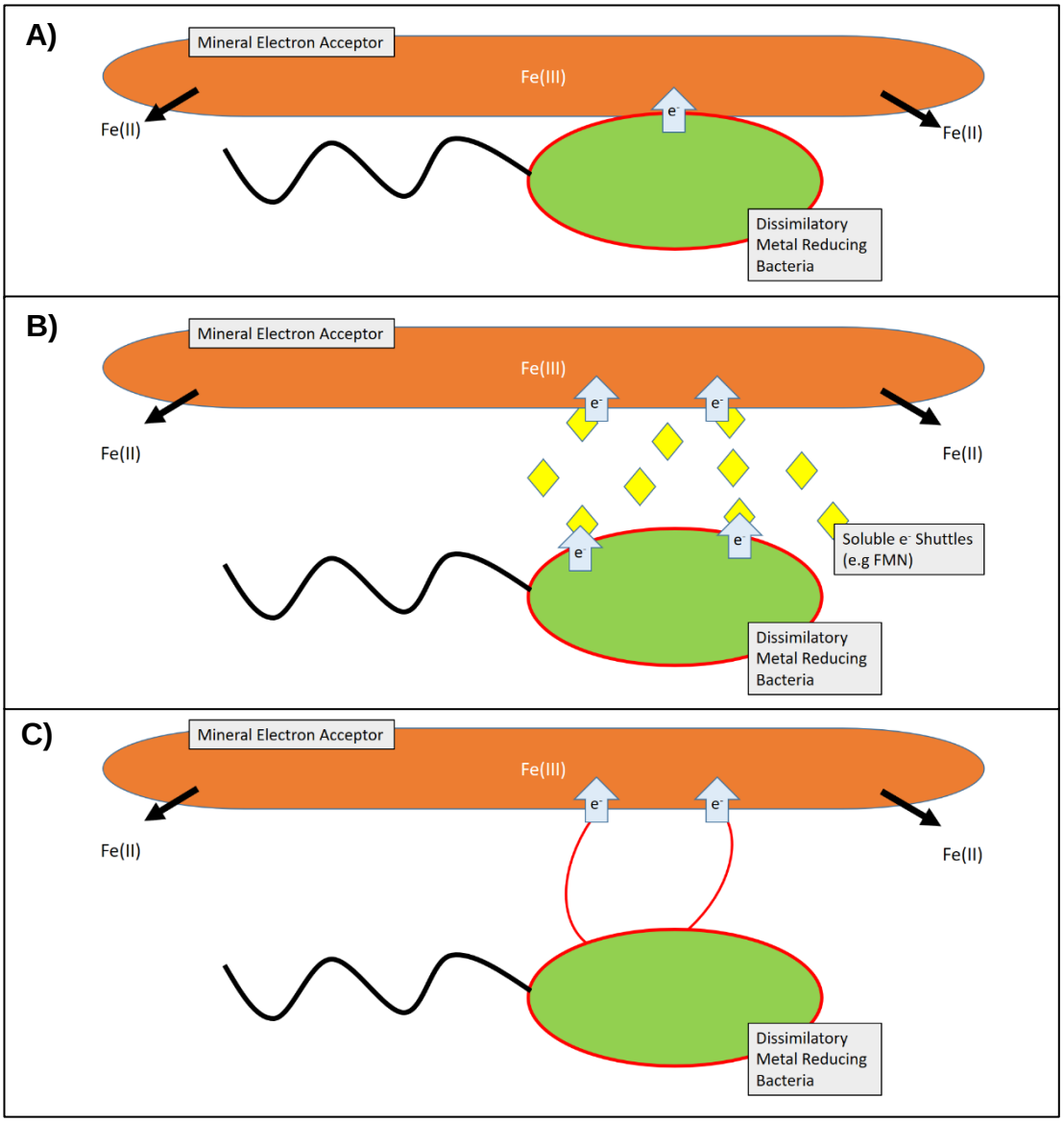

Figure 1.7 – Overview of models of electron transfer from dissimilatory metal reducing bacteria to terminal electron acceptor (shown in the form of ferric mineral). A) Direct electron transfer from OMC (represented by red membrane colouring) to electron acceptor. B) Flavin mediated electron transfer with flavin molecules acting as electron shuttles oxidising OMC before diffusing into environment. These shuttles then reduce the terminal electron acceptor. C) Electron transfer from dissimilatory metal reducing bacteria to terminal electron acceptor via nanowires. Conductive pili structures extend from bacterial cells and make contact with terminal electron acceptor allowing electrons to flow away from the cell. Electron flow highlighted as blue arrows.

Many studies utilise electrochemical techniques to probe the reduction potentials of the OMCs and the reduction windows over which electron transfer can occur. In many of these studies, bacterial biofilm or protein is fixed to an electrode before an applied potential is cycled between oxidising and reducing potentials. Electron flow elicits a signal which can be attributed to reduction or oxidation of OMCs and thus extracellular electron transfer (Kissinger and Heineman, 1996). There has also long been issues with reported potential ranges when direct electron transfer can occur. The potential window in which the onset of direct electron transfer from MtrC to electrodes has been reported as ranging from 0 and +0.4 V (Okamoto, Nakamura and Hashimoto, 2011). However the heme potential range for MtrC is reported to be between -0.4 and 0 V (Breuer *et al.*, 2015). As the direct electron transfer model holds this outer membrane cytochrome as the final protein in contact with the terminal electron acceptor, a more favourable potential window would be expected. The difference has previously been attributed to the differences in the environment where the bacteria are in contact with the electrode (Carmona-Martinez *et al.*, 2011). However, a more recent study has suggested that many of the reported high potential signals, attributed to direct electron transfer, are the result of iron in solution interacting with the electrode. This iron is thought to be released from cell lysis, a possibility not previously considered. A hypothesis supported when the addition of deferoxamine, an iron chelator only able to remove non-complexed iron, depletes the high potential signals recorded (Jeuken, 2016). This issue is likely not restricted to studies involving MtrC but other OMCs also.

The second model is that of flavin mediated electron shuttling (Figure 1.7, Panel B). *S. oneidensis* are known to secrete small flavin molecules such as flavin mononucleotide (FMN) into the extracellular environment. The exact function of these molecules secreted into growth medium has not been clearly defined even though it requires a relatively large investment of cellular energy to produce the molecules and is a conserved characteristic across the genus (von Canstein *et al.*, 2008). It is thought that this flavin can oxidise MtrC and so take electrons out of the cell. These reduced molecules then diffuse through the environment until they come into contact with terminal electron acceptors which are in turn reduced by the flavin molecules. Many studies have shown that flavin molecules must play a role in the process as

genetically engineered strains, unable to secrete flavin, are less able to reduce extracellular electron acceptors (Nicholas J. Kotloski and Gralnick, 2013). There are also investigations highlighting the ability of culture supernatant to enhance electron transfer from a biofilm to an electrode. *S. oneidensis* biofilms were generated on electrodes and their reducing potential was recorded. The electrode and biofilm were then transferred to an electrochemical cell containing fresh media where the rate of electron transfer to the electrode was seen to drop by more than 70 %. When the growth medium was replaced with that from the original electrochemical cell, the reduction potential of the cells was restored. This highlighted soluble mediators (later determined to be riboflavin and flavin mononucleotide) in the medium as crucial for high levels of electron transfer between the bacterial cells and the electrode (Marsili *et al.*, 2008).

The final model of extracellular electron transfer is via nanowires (Figure 1.7, Panel C). Large filamentous appendages have been observed extending away from the cells of metal reducing bacteria under electron acceptor limited conditions (Gorby *et al.*, 2006). In some instances, these structures have been shown unable to conduct electrons away from the bacterial cell and to terminal electron acceptors (Reguera *et al.*, 2005). Originally, these appendages were thought to be pili structures however, the conductive element of the pili remained undescribed and no corresponding structural gene has been identified - unlike in *Geobacter* where PilA protein units make up conductive pili (Pirbadian *et al.*, 2014). Knocking out *pilA* in *Geobacter* reduced the rate of electron transfer from cells to electrodes by preventing nanowire formation (Reguera *et al.*, 2006). Whereas genetic knockout studies in *Shewanella* have shown that nanowire conductivity can be reduced by deleting the OMCs (*mtrC* and *omcA*) genes (Pirbadian *et al.*, 2014). This suggestion that the nanowire structures themselves did not conduct electrons was further confirmed when fluorescence studies showed *Shewanella* nanowires are in fact extensions of the outer membrane rather than pili. In this study FM 4-64FX dye was used to selectively stain for bacterial membrane. The nanowires themselves stained showing that they consisted of membrane components rather than protein units. The investigation then went on to fluorescently labelled MtrC and OmcA expressed in the cell. The results

here showed the nanowire was studded with the outer membrane cytochromes implicating the Mtr pathway as the element capable of electron transfer (Pirbadian *et al.*, 2014). In light of these findings, it seems increasingly likely that a greater understanding of extracellular electron transfer in *S. oneidensis* will only come from better understanding of the MtrCAB system.

1.4.3 Outer Membrane Cytochromes

The MtrCAB complex is found across many species of *Shewanella* with a notable exception being *S. denitrificans*. This species is found in environments with a limited variety of terminal electron acceptors and its respiratory versatility reflects this, with it only able to grow anaerobically through the reduction of nitrate to nitrogen (Hau and Gralnick, 2007). Between other *Shewanella* species there is high sequence homology between the *mtrCAB* genes indicating a highly conserved mechanism of extracellular electron transfer.

The genomes of many species show a homologous system coded for by the *mtrDEF* genes (Figure 1.8). Although similar in sequence and structure, their function is of yet relatively uncharacterised. There have been some studies suggesting they function as a redundancy mechanism for the MtrCAB complex. MtrE has been shown able of replacing MtrB as the porin allowing for functional electron transport across the membrane and under some conditions, when MtrCAB is removed, MtrDEF is seen capable of iron reduction, albeit much slower rates (Coursolle and J. A. Gralnick, 2012). These homologues operate under separate promoters from *mtrCAB* suggesting highly specific inducing conditions (Fredrickson *et al.*, 2008) with biofilm formation and type of available respiratory electron acceptor being most closely linked to expression (J. S. McLean *et al.*, 2008). MtrF was the first outer membrane cytochrome from *Shewanella* to have its crystal structure solved. The heme groups were seen to be arranged in a staggered cross motif with eight hemes spanning the 65 Å length of the protein. The other remaining two hemes transect perpendicular to this chain aligning with heme 1 and 6. All hemes were found to be within 7 Å of each

other, allowing for rapid electron exchange between them (Clarke *et al.*, 2011). This crystal structure was used to model the structure of MtrC which showed the heme groups of MtrC were also arranged in this staggered cross arrangement (Edwards *et al.*, 2012), later proven through the crystal structure of MtrC (Edwards *et al.*, 2015).

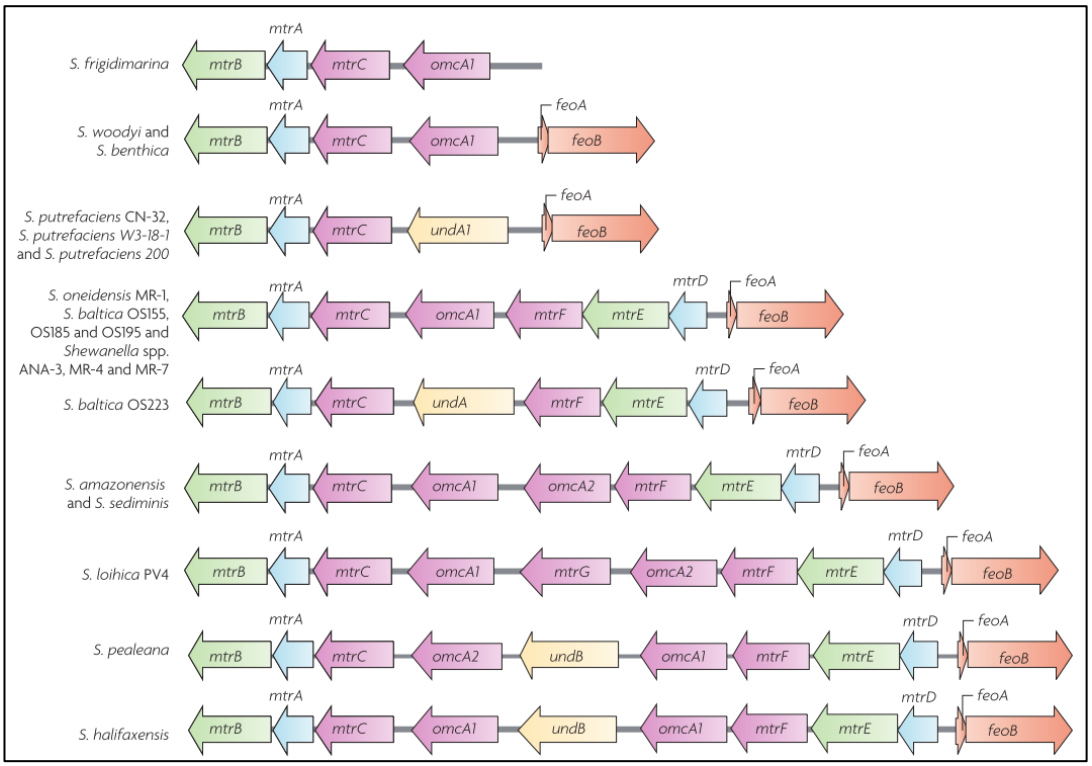

Figure 1.8 – Summary of cytochromes implicated in extracellular electron transfer encoded by the genome of *Shewanella* species. Note presence of *mtrCAB* in all species along with a copy of either the *omcA* or *undA* gene. Membrane porin proteins highlighted in green, periplasmic decaheme proteins highlighted in blue, outer membrane decaheme proteins highlighted in purple. Taken from (Fredrickson *et al.*, 2008).

There are also accessory outer membrane cytochromes expressed in many species (Figure 1.8). These are the OmcA and UndA proteins. OmcA is another decaheme cytochrome that has also been shown capable of mineral reduction. There is some evidence that OmcA forms a complex with MtrC to assist in mineral reduction (Shi *et al.*, 2006). MtrC has been seen to localise to regions of the cell membrane in close

proximity to mineral electron acceptors. OmcA however, has also been observed localised more diffusely throughout the membrane of *S. oneidensis*, with no correlation to MtrCAB localisation or mineral proximity (Reardon *et al.*, 2010). This difference in localisation has suggested a difference in function between MtrC and OmcA. This has been supported by studies highlighting MtrC as the dominant reducer of ferric minerals. OmcA knockout mutants in biofilms display deficiencies in forming tight associations with mineral electron acceptors rather than inhibition of cell growth – as seen in MtrC depleted mutants (Mitchell *et al.*, 2012). UndA is markedly different from other outer membrane cytochromes as it has 11 heme groups. The purpose of this additional heme is unknown, although UndA is known to be a functional homologue to OmcA (Edwards *et al.*, 2012). These clades of OMC are more closely related than they are to the MtrC and MtrF clades. Notably though, the structure of both OmcA and UndA share a number of similarities to that of MtrC and its MtrF homologue. All are composed of four domains with domain I and III containing Greek key split β-barrels. Domain I and IV act as the central core housing the heme groups of the proteins (Shi *et al.*, 2016). Although these cytochromes share little DNA sequence homology (with *mtrF*, *omcA* and *undA* showing 51, 49.9 and 49.7 % respectively) and even less amino acid sequence homology (with *mtrF*, *omcA* and *undA* showing 31.7, 24.9 and 24.8 % respectively), the heme groups themselves are arranged in a staggered cross motif spanning the proteins (Figure 1.9). This highlights the potential for a conserved mechanism of electron transfer across all main clades of outer membrane cytochrome (Edwards *et al.*, 2014).

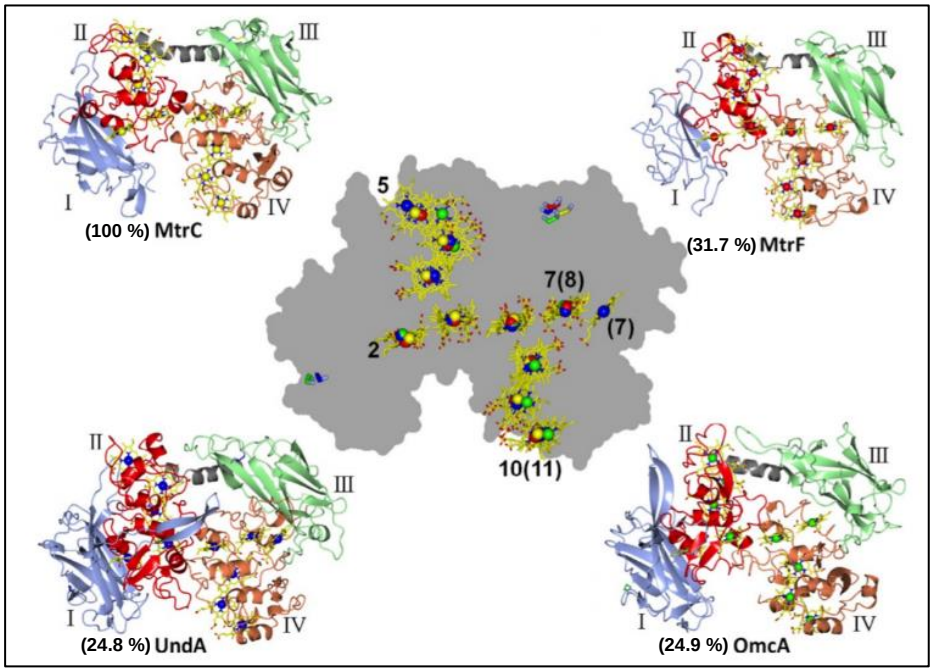

Figure 1.9 – Crystal structures for the outer membrane cytochromes of *S. oneidensis*. Domains of MtrC (PDB ID 4LM8), MtrF (PDB ID 3PMQ), OmcA (PDB ID 4LMH) and UndA (PDB ID 3UCP) indicated with distinctive 'staggered cross' arrangement of heme also highlighted. Amino acid sequence homology to MtrC shown for each OMC. Heme number referring to MtrC, MtrF and OmcA with parenthesis referring to UndA. Conserved disulphide bonds in domain I and III represented as sticks. All proteins purified from *Shewanella* species prior to crystallisation and subsequent structural solving. Modified from (White *et al.*, 2016).

1.4.4 Recent Advances Uniting Flavin Mediated and Direct Transfer

The dominant system of extracellular electron transfer in *S. oneidensis* is via the MtrCAB pathway. Notably there is disparity between measured electron transfer rates through the complex and physiologically viable rates to support bacterial growth (Okamoto, Nakamura and Hashimoto, 2011). This disparity is often resolved in studies where flavin molecules are present suggesting a crucial role in the system (N J Kotloski and Gralnick, 2013; Okamoto *et al.*, 2013). Ascertaining the exact function of flavin in this system now appears to be the prevalent question in the field with a focus on uniting the model of flavin mediated and direct electron transfer.

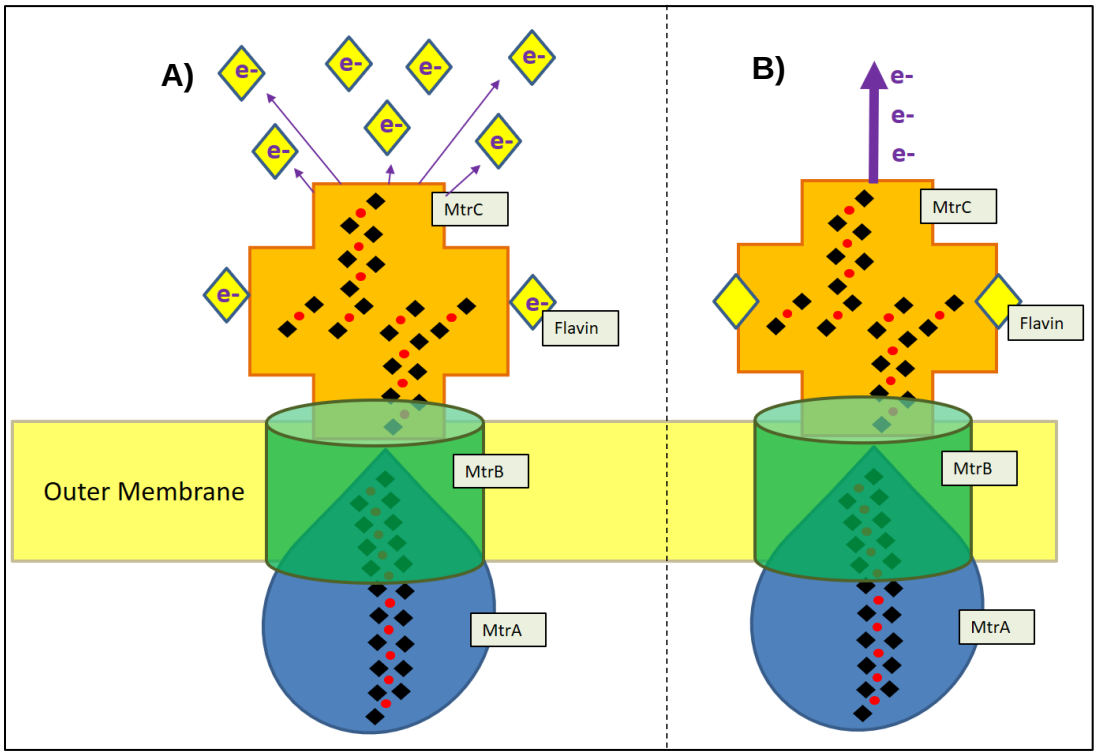

Figure 1.10 – Proposed mechanisms of flavin enhanced electron transfer away from MtrC. A) Flavin molecules acting as shuttles, oxidising MtrC before diffusing to terminal electron acceptor that is in turn reduced by the flavin molecules. B) Flavin molecules associating tightly with MtrC, affecting electrochemical potentials of the system and enhancing direct electron transfer rate.

With regard to flavin molecules mediating electron transfer as shuttles (Figure 1.10 Panel A), favourable redox potentials between the outer membrane cytochromes and the flavin molecules themselves could be expected to allow for fast, two-electron transfer rates. However, when the redox potentials of the components in the system are measured there is a 270 mV endogenic gap between that of FMN / reduced FMN and that of MtrCAB / reduced MtrCAB (Okamoto, Nakamura and Hashimoto, 2011).This energy gap implies far slower electron transfer rates via this mechanism than previous expected. When considering flavin molecules as cofactors, binding to the outer membrane cytochromes and enhancing electron via a one-electron pathway instead of functioning as shuttles, a shift in the electrochemical potential can be observed. Flavin mononucleotide binding to MtrC (Figure 1.10 Panel B) was seen to

shift the electrochemical potential of the FMN from -260 mV to -145 mV, allowing for faster electron transfer rates in line with levels proposed for sustaining bacterial growth (Okamoto *et al.*, 2013). Further studies suggested specific binding between different flavin molecule types and different outer membrane cytochromes. FMN was seen to specifically bind to MtrC and increase electron transfer rates 15 fold, whereas riboflavin was seen to bind to OmcA and only increased electron transfer rates 6 fold (Okamoto *et al.*, 2014). This result not only emphasises the potential model of a flavocytochrome complex allowing for fast direct electron transfer to mineral terminal electron acceptors, but also highlights MtrC-FMN as the dominant reducing cytochrome in *S. oneidensis*.

MtrC protein purified from *S. oneidensis* does not contain bound flavin whilst relatively strong FMN-MtrC binding has been shown in experiments involving purified protein samples. (Edwards *et al.*, 2015). This suggests controlled binding only occurs under specific conditions. The resolution of the MtrC crystal structure allowed for further investigation into flavin binding sites. Molecular dynamic studies have highlighted a potential binding pocket for flavin molecules near heme 7 of MtrC (Hong and Pachter, 2016). When this is put into context of the crystal structure, the binding pocket must be within domain III of the protein to be in close enough proximity to affect the potential of the heme. An interesting feature seen in domain III of MtrC (Figure 1.11) is a conserved disulphide bond between cysteine residues at amino acid positions 444 and 453 (Edwards *et al.*, 2015). To investigate if this structural feature was implicated in flavin binding, glutathione was used to selectively reduce the disulphide bond in purified MtrC samples. These samples were then incubated with flavin mononucleotide before elution through a size exclusion column. This separated FMN free in solution from the protein. Upon observation it was noted that FMN had become tightly associated with MtrC when the disulphide bond was chemically reduced (Edwards *et al.*, 2015). These findings again suggest a tight, cofactor like binding of FMN to MtrC during mineral reduction. This also highlights the potential for protein structure level control in that formation of the disulphide bond in domain III prevents flavin binding and perhaps on extracellular electron transfer.

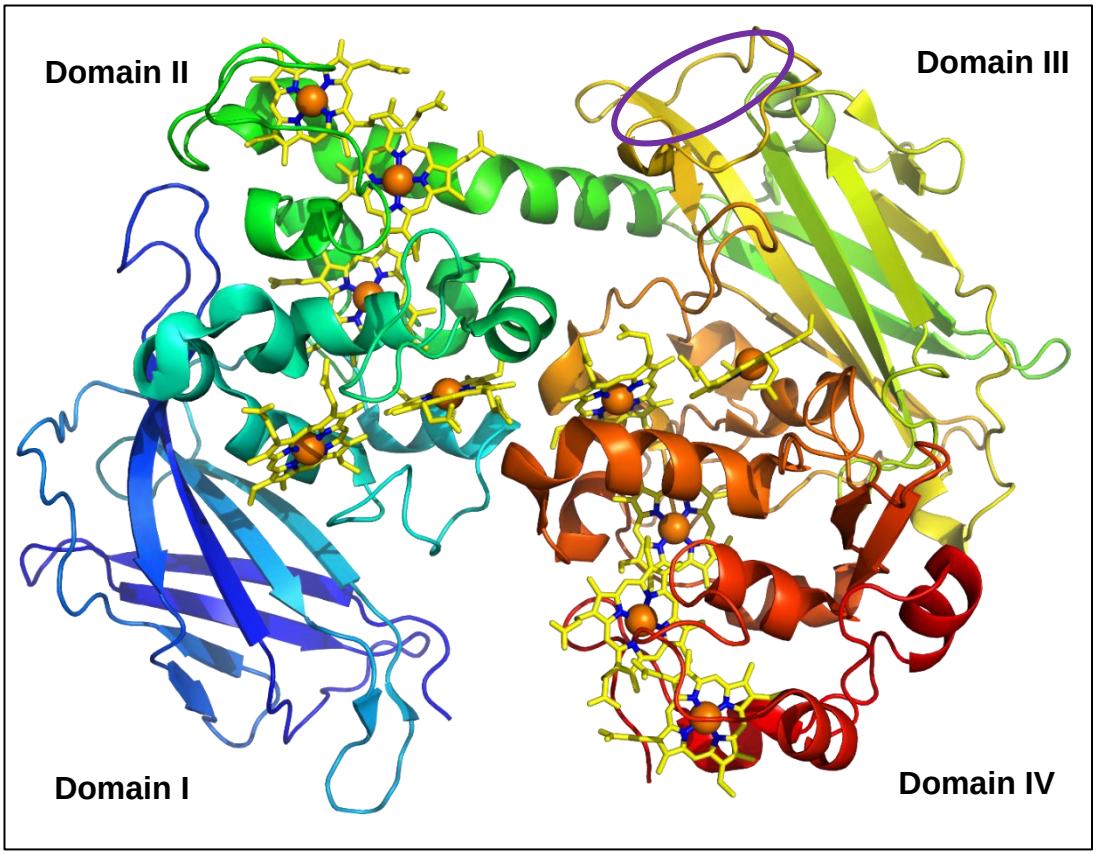

Figure 1.11 – Crystal structure of MtrC at 1.8 Å resolution (PDB ID 4LM8). Cartoon representation of MtrC structure with domains highlighted. Staggered cross motif of heme groups shown as yellow sticks with Fe cofactors as orange spheres. Disulphide bond region highlighted in purple.

1.5 Thesis Aims

This thesis aims to build on recent research to add clarity to the model of electron transfer, in *S. oneidensis,* through the MtrCAB complex and to the extracellular terminal electron acceptor. Conditions induced through the use of reducing agents have been shown to allow binding of FMN to MtrC, however the biological relevance of these experiments is still in question. Molecular genetic techniques such, as site directed mutagenesis, were here use to specifically investigate the purpose of the conserved disulphide bond present in domain III of MtrC. This allowed for further biochemical analysis of the function of flavin molecules in the system. As well as

giving insight into the physiological relevance of a proposed control mechanism to the bacterial cell itself.

Chapter 3 documents the generation of MtrC where the cysteine residues at amino acid positions 444 and 453 have been substituted for alanine residues. It then goes on to look at conditions under which the protein is expressed and the effect of expressing this form of MtrC on the cell via bacterial growth studies. Doing so allowed further probing of the system to begin investigating the implications of this structural change on how MtrC functions in the MtrCAB complex, both as an electron condute and as a potential binder of flavin. This was achieved through comparison of growth of bacterial cultures under aerobic and anaerobic conditions. Commonly used terminal electron acceptors were also used to assess the functionality of the MtrCAB pathway.

Chapter 4 investigates the cause of a notable extended lag phase phenotype seen in *S. oneidensis* expressing the mutant form of MtrC to ascertain if the observed phenotype had physiological relevance. This growth defect was only seen under aerobic growth conditions and so much of the work focuses on the cause of this oxygen toxicity. Investigation first looked at quantifying the amount of reactive oxygen species (a likely candidate for the toxic effect of oxygen on the cells) present in the samples. Once evidence was obtained relating to the cause of the extended lag phase, these findings were confirmed by supplementing growth medium with enzymes capable of breaking down excess reactive oxygen species, testing for growth restoration.

Chapter 5 studies purified MtrC where the cysteine residues forming the disulphide bond in domain 3 of the protein have been substituted (thus breaking the disulphide bridge). Studies focus on ascertaining the effect of removing this disulphide bridge in regards to flavin binding to MtrC under a variety of conditions to ascertain if this structural change alone is enough to allow formation of the previously reported FMN-MtrC complex. These experiments were accomplished via fluorescence spectroscopy and crystallography on MtrC variants to compare conditions where

flavin binding could be seen in each form of the protein. Attempting to separate the FMN-MtrC complex through gel filtration columns gave insight into the strength of binding in each of the forms and how well this was maintained upon exposure to different conditions. Fluorescence spectroscopy allowed assaying in these experiments whilst crystallography was employed to identify specific structural changes that allowed binding to occur.

Chapter 6 discusses the findings of this thesis in detail. Results from all chapters are used together to provide a broader prospective of what they mean in regards to models of extracellular electron transfer in *S. oneidensis*. Focus is also turned towards the physiological relevance of findings here to *S. oneidensis* in their natural environment and how they may impact biotechnological application of dissimilatory metal reducing bacteria.

1.6 References

Alberts, B., Johnson, A., Lewis, J., Raff, M., Roberts, K. and Walter, P. (2002) 'Molecular biology of the cell. new york: Garland science; 2002', *Classic textbook now in its 5th Edition*.

Andersson, S. G. E., Zomorodipour, A., Andersson, J. O., Sicheritz-Ponten, T., Alsmark, U. C., Podowski, R. M., Naslund, A. K., Eriksson, A.-S. S., Winkler, H. H., Kurland, C. G., Sicheritz-Pontén, T., Alsmark, U. C., Podowski, R. M., Näslund, A. K., Eriksson, A.-S. S., Winkler, H. H. and Kurland, C. G. (1998) 'The genome sequence of *Rickettsia prowazekii* and the origin of mitochondria', *Nature*, 396(6707), pp. 133–140. doi: 10.1038/24094 [doi].

Beliaev, A. S. and Saffarini, D. A. (1998) 'Fe(III) and Mn(IV) Reduction Outer Membrane Protein Required for Encodes an Shewanella putrefaciens mtrB', *J. Bacteriol*, 180(23), pp. 6292–6297. Available at: http://jb.asm.org/content/180/23/6292%5Cnhttp://jb.asm.org/content/180/23/6292#ref-list-1.

Beliaev, A. S., Saffarini, D. A., McLaughlin, J. L. and Hunnicutt, D. (2001) 'MtrC, an outer membrane decahaem c cytochrome required for metal reduction in Shewanella putrefaciens MR-1', *Mol Microbiol*, 39. doi: 10.1046/j.1365-2958.2001.02257.x.

Berche, P. (2012) 'Louis Pasteur, from crystals of life to vaccination', *Clinical Microbiology and Infection*. Elsevier, 18, pp. 1–6.

Berks, B. C., Page, M. D., Richardson, D. J., Reilly, A., Cavill, A., Outen, F. and Ferguson, S. J. (1995) 'Sequence analysis of subunits of the membrane-bound nitrate reductase from a denitrifying bacterium: the integral membrane subunit provides a prototype for the dihaem electron-carrying arm of a redox loop.', *Molecular microbiology*. England, 15(2), pp. 319–331.

Bertero, M. G., Rothery, R. A., Palak, M., Hou, C., Lim, D., Blasco, F., Weiner, J. H. and Strynadka, N. C. J. (2003) 'Insights into the respiratory electron transfer pathway from the structure of nitrate reductase A', *Nature Structural & Molecular Biology*. Nature Publishing Group, 10(9), p. 681.

Bond, P. L., Druschel, G. K. and Banfield, J. F. (2000) 'Comparison of Acid Mine Drainage Microbial Communities in Physically and Geochemically Distinct Ecosystems', *Applied and Environmental Microbiology*. American Society for Microbiology, 66(11), pp. 4962–4971. Available at: http://www.ncbi.nlm.nih.gov/pmc/articles/PMC92406/.

Borch, T., Kretzschmar, R., Kappler, A., Cappellen, P. Van, Ginder-Vogel, M., Voegelin, A. and Campbell, K. (2009) 'Biogeochemical redox processes and their impact on contaminant dynamics', *Environmental Science & Technology*. ACS Publications, 44(1), pp. 15–23.

Breuer, M., Rosso, K. M., Blumberger, J. and Butt, J. N. (2015) 'Multi-haem cytochromes in Shewanella oneidensis MR-1: structures, functions and opportunities', *Journal of The Royal Society Interface*, 12(102), pp. 20141117–20141117. doi: 10.1098/rsif.2014.1117.

Brooks, A. N., Turkarslan, S., Beer, K. D., Lo, F. Y. and Baliga, N. S. (2011) 'Adaptation of cells to new environments', *Wiley interdisciplinary reviews. Systems biology and medicine*, 3(5), pp. 544–561. doi: 10.1002/wsbm.136.

Brown, W. J. (1974) 'Modification of the Rapid Fermentation Test for Neisseria gonorrhoeae', 27(6), pp. 1027–1030. Available at: http://aem.asm.org/content/27/6/1027.full.pdf.

Bueno, E., Mesa, S., Bedmar, E. J., Richardson, D. J. and Delgado, M. J. (2012) 'Bacterial adaptation of respiration from oxic to microoxic and anoxic conditions: redox control.', *Antioxidants & redox signaling*, 16(8), pp. 819–52. doi: 10.1089/ars.2011.4051.

Burns, J. L. and DiChristina, T. J. (2009) 'Anaerobic respiration of elemental sulfur and thiosulfate by Shewanella oneidensis MR-1 requires psrA, a homolog of the phsA gene of Salmonella enterica serovar typhimurium LT2', *Applied and Environmental Microbiology*, 75(16), pp. 5209–5217. doi: 10.1128/AEM.00888-09.

von Canstein, H., Ogawa, J., Shimizu, S. and Lloyd, J. R. (2008) 'Secretion of flavins by Shewanella species and their role in extracellular electron transfer.', *Applied and environmental microbiology*, 74(3), pp. 615–23. doi: 10.1128/AEM.01387-07.

Carlson, H. K., Iavarone, A. T., Gorur, A., Yeo, B. S., Tran, R., Melnyk, R. A., Mathies, R. A., Auer, M. and Coates, J. D. (2012) 'Surface multiheme c-type cytochromes from Thermincola potens and implications for respiratory metal reduction by Gram-positive bacteria', *Proceedings of the National Academy of Sciences*, 109(5), pp. 1702–1707. doi: 10.1073/pnas.1112905109.

Carmona-Martinez, A. A., Harnisch, F., Fitzgerald, L. A., Biffinger, J. C., Ringeisen, B. R. and Schröder, U. (2011) 'Cyclic voltammetric analysis of the electron transfer of Shewanella oneidensis MR-1 and nanofilament and cytochrome knock-out mutants', *Bioelectrochemistry*, 81(2), pp. 74–80. doi: 10.1016/j.bioelechem.2011.02.006.

Chistoserdova, L., Kalyuzhnaya, M. G. and Lidstrom, M. E. (2009) 'The expanding world of methylotrophic metabolism', *Annual review of microbiology*. Annual Reviews, 63, pp. 477–499.

Clarke, T. A., Edwards, M. J., Gates, A. J., Hall, A., White, G. F., Bradley, J., Reardon, C. L., Shi, L., Beliaev, A. S., Marshall, M. J., Wang, Z., Watmough, N. J., Fredrickson, J. K., Zachara, J. M., Butt, J. N. and Richardson, D. J. (2011) 'Structure of a bacterial cell surface decaheme electron conduit'. doi: 10.1073/pnas.1017200108/-/DCSupplemental.www.pnas.org/cgi/doi/10.1073/pnas.1017200108.

Coates, J. D., Phillips, E. J., Lonergan, D. J., Jenter, H. and Lovley, D. R. (1996) 'Isolation of Geobacter species from diverse sedimentary environments.', *Applied and Environmental Microbiology*. Am Soc Microbiol, 62(5), pp. 1531–1536.

Cole, J. A. and Richardson, D. J. (2008) 'Respiration of Nitrate and Nitrite.', *EcoSal Plus*, 3(1).

Cooper, R. A. (1986) 'Convergent Pathways of Sugar', *Carbohydrate Metabolism in Cultured Cells*. Plenum Publishing Corporation, p. 461.

Costa, N. L., Carlson, H. K., Coates, J. D., Louro, R. O. and Paquete, C. M. (2015) 'Heterologous expression and purification of a multiheme cytochrome from a Gram-positive bacterium capable of performing extracellular respiration', *Protein Expression and Purification*, 111, pp. 48–52. doi: 10.1016/j.pep.2015.03.007.

Crane, F. L. (2007) 'Discovery of ubiquinone (coenzyme Q) and an overview of function', *Mitochondrion*. Elsevier, 7, pp. S2–S7.

Edwards, M. J., Baiden, N., Johs, A., Tomanicek, S. J., Liang, L., Shi, L., Fredrickson, J. K., Zachara, J. M., Gates, A. J., Butt, J. N., Richardson, D. J. and Clarke, T. A. (2014) 'The X-ray crystal structure of Shewanella oneidensis OmcA reveals new insight at the microbe-mineral interface.', *FEBS letters*. Available at: http://www.sciencedirect.com/science/article/pii/S0014579314002993 (Accessed: 23 April 2014).

Edwards, M. J., Fredrickson, J. K., Zachara, J. M., Richardson, D. J. and Clarke, T. a (2012) 'Analysis of structural MtrC models based on homology with the crystal structure of MtrF.', *Biochemical Society transactions*, 40(6), pp. 1181–5. doi: 10.1042/BST20120132.

Edwards, M. J., Hall, A., Shi, L., Fredrickson, J. K., Zachara, J. M., Butt, J. N., Richardson, D. J. and Clarke, T. A. (2012) 'The crystal structure of the extracellular 11-heme Cytochrome UndA reveals a conserved 10-heme motif and defined binding site for Soluble Iron Chelates', *Structure*, 20. doi: 10.1016/j.str.2012.04.016.

Edwards, M. J., White, G. F., Norman, M., Tome-Fernandez, A., Ainsworth, E., Shi, L., Fredrickson, J. K., Zachara, J. M., Butt, J. N., Richardson, D. J. and Clarke, T. a. (2015) 'Redox Linked Flavin Sites in Extracellular Decaheme Proteins Involved in Microbe-Mineral Electron Transfer.', *Scientific Reports*. Nature Publishing Group, 5(July), p. 11677. doi: 10.1038/srep11677.

El-Sharoud, W. (2008) *Bacterial physiology*. Springer.

Embley, T. M. and Martin, W. (2006) 'Eukaryotic evolution, changes and challenges', *Nature*, 440(7084), pp. 623–630. doi: 10.1038/nature04546.

Fredrickson, J. K., Romine, M. F., Beliaev, A. S., Auchtung, J. M., Driscoll, M. E., Gardner, T. S., Nealson, K. H., Osterman, A. L., Pinchuk, G., Reed, J. L., Rodionov, D. a, Rodrigues, J. L. M., Saffarini, D. a, Serres, M. H., Spormann, A. M., Zhulin, I. B. and Tiedje, J. M. (2008) 'Towards environmental systems biology of Shewanella.', *Nature reviews. Microbiology*, 6(8), pp. 592–603. doi: 10.1038/nrmicro1947.

Garvie, E. I. (1980) 'Bacterial lactate dehydrogenases', *Microbiological Reviews*, 44(1), pp. 106–139. Available at: https://www.ncbi.nlm.nih.gov/pmc/articles/PMC373236/pdf/microrev00062-0116.pdf.

Gorby, Y. A., Yanina, S., McLean, J. S., Rosso, K. M., Moyles, D., Dohnalkova, A., Beveridge, T. J., Chang, I. S., Kim, B. H., Kim, K. S., Culley, D. E., Reed, S. B., Romine, M. F., Saffarini, D. A., Hill, E. A., Shi, L., Elias, D. A., Kennedy, D. W., Pinchuk, G., Watanabe, K., Ishii, S., Logan, B., Nealson, K. H. and Fredrickson, J. K. (2006) 'Electrically conductive bacterial nanowires produced by Shewanella oneidensis strain MR-1 and other microorganisms', *Proceedings of the National Academy of Sciences* , 103(30), pp. 11358–11363. doi: 10.1073/pnas.0604517103.

Gralnick, J. A., Vali, H., Lies, D. P. and Newman, D. K. (2006) 'Extracellular respiration of dimethyl sulfoxide by Shewanella oneidensis strain MR-1', *Proceedings of the National Academy of Sciences of the United States of America*. National Acad Sciences, 103(12), pp. 4669–4674.

Gram, L., Trolle, G. and Huss, H. (1987) 'Detection of specific spoilage bacteria from fish stored at low (0 C) and high (20 C) temperatures', *International Journal of Food Microbiology*, 4, pp. 65–72. Available at: http://www.sciencedirect.com/science/article/pii/0168160587900602.

Griebler, C. and Slezak, D. (2001) 'Microbial Activity in Aquatic Environments Measured by Dimethyl Sulfoxide Reduction and Intercomparison with Commonly Used Methods Microbial Activity in Aquatic Environments Measured by Dimethyl Sulfoxide Reduction and Intercomparison with Commonly Used M', 67(1), pp. 100–109. doi: 10.1128/AEM.67.1.100.

Groen, A. K., Wanders, R. J., Westerhoff, H. V, Van der Meer, R. and Tager, J. M. (1982) 'Quantification of the contribution of various steps to the control of mitochondrial respiration.', *Journal of Biological Chemistry*. ASBMB, 257(6), pp. 2754–2757.

Hartshorne, R. S., Jepson, B. N., Clarke, T. A., Field, S. J., Fredrickson, J., Zachara, J., Shi, L., Butt, J. N. and Richardson, D. J. (2007) 'Characterization of Shewanella oneidensis MtrC: A cell-surface decaheme cytochrome involved in respiratory electron transport to extracellular electron acceptors', *Journal of Biological Inorganic Chemistry*, 12(7), pp. 1083–1094. doi: 10.1007/s00775-007-0278-y.

Hartshorne, R. S., Reardon, C. L., Ross, D., Nuester, J., Clarke, T. a, Gates, A. J., Mills, P. C., Fredrickson, J. K., Zachara, J. M., Shi, L., Beliaev, A. S., Marshall, M. J., Tien, M., Brantley, S., Butt, J. N. and Richardson, D. J. (2009) 'Characterization of an electron conduit between bacteria and the extracellular environment.', *Proceedings of the National Academy of Sciences of the United States of America*, 106(52), pp. 22169–74. doi: 10.1073/pnas.0900086106.

Hau, H. H. and Gralnick, J. A. (2007) 'Ecology and biotechnology of the genus Shewanella.', *Annual review of microbiology*. United States, 61, pp. 237–258. doi: 10.1146/annurev.micro.61.080706.093257.

Heidelberg, J. F., Paulsen, I. T., Nelson, K. E., Gaidos, E. J., Nelson, W. C., Read, T. D., Eisen, J. A., Seshadri, R., Ward, N., Methe, B., Clayton, R. A., Meyer, T., Tsapin, A., Scott, J., Beanan, M., Brinkac, L., Daugherty, S., DeBoy, R. T., Dodson, R. J., Durkin, A. S., Haft, D. H., Kolonay, J. F., Madupu, R., Peterson, J. D., Umayam, L. A., White, O., Wolf, A. M., Vamathevan, J., Weidman, J., Impraim, M., Lee, K., Berry, K., Lee, C., Mueller, J., Khouri, H., Gill, J., Utterback, T. R., McDonald, L. A., Feldblyum, T. V, Smith, H. O., Venter, J. C., Nealson, K. H. and Fraser, C. M. (2002) 'Genome sequence of the dissimilatory metal ion-reducing bacterium Shewanella oneidensis', *Nat Biotechnol*, 20(11), pp. 1118–1123. doi: 10.1038/nbt749.

Hogg, S. (2013) *Essential microbiology*. John Wiley & Sons.

Hong, G. and Pachter, R. (2016) 'Bound Flavin–Cytochrome Model of Extracellular Electron Transfer in Shewanella oneidensis: Analysis by Free Energy Molecular Dynamics Simulations', *The Journal of Physical Chemistry B*. American Chemical Society, 120(25), pp. 5617–5624. doi: 10.1021/acs.jpcb.6b03851.

Hughes, M. F. (2002) 'Arsenic toxicity and potential mechanisms of action.', *Toxicology letters*. Netherlands, 133(1), pp. 1–16.

Jeuken, L. (2016) 'A re-evaluation of electron transfer mechanisms in microbial electrochemistry : Shewanella releases iron that mediates extracellular electron transfer', (1), pp. 829–835. doi: 10.1002/celc.201500505.

Johnson, D. B., Kanao, T. and Hedrich, S. (2012) 'Redox Transformations of Iron at Extremely Low pH: Fundamental and Applied Aspects', *Frontiers in Microbiology*. Frontiers Research Foundation, 3, p. 96. doi: 10.3389/fmicb.2012.00096.

Kane, A. L., Brutinel, E. D., Joo, H., Maysonet, R., VanDrisse, C. M., Kotloski, N. J. and Gralnick, J. A. (2016) 'Formate metabolism in Shewanella oneidensis generates proton motive force and prevents growth without an electron acceptor', *Journal of bacteriology*. Am Soc Microbiol, 198(8), pp. 1337–1346.

Khademian, M. and Imlay, J. A. (2017) 'Escherichia coli cytochrome c peroxidase is a respiratory oxidase that enables the use of hydrogen peroxide as a terminal electron acceptor', *Proceedings of the National Academy of Sciences*. National Acad Sciences, 114(33), pp. E6922–E6931.

Kim, Y.-M., Lee, S.-E., Park, B.-S., Son, M.-K., Jung, Y.-M., Yang, S.-O., Choi, H.-K., Hur, S.-H. and Yum, J. H. (2012) 'Proteomic analysis on acetate metabolism in Citrobacter sp. BL-4', *International journal of biological sciences*. Ivyspring International Publisher, 8(1), p. 66.

Kissinger, P. and Heineman, W. R. (1996) *Laboratory Techniques in Electroanalytical Chemistry, revised and expanded*. CRC press.

Kotloski, N. J. and Gralnick, J. a. (2013) 'Flavin electron shuttles dominate extracellular electron transfer by Shewanella oneidensis', *mBio*, 4(1), pp. 10–13. doi: 10.1128/mBio.00553-12.

Kotloski, N. J. and Gralnick, J. A. (2013) 'Flavin electron shuttles dominate extracellular electron transfer by Shewanella oneidensis', *MBio*, 4(1). doi: 10.1128/mBio.00553-12.

Le Laz, S., kpebe, A., Bauzan, M., Lignon, S., Rousset, M. and Brugna, M. (2016) 'Expression of terminal oxidases under nutrient-starved conditions in Shewanella oneidensis: detection of the A-type cytochrome c oxidase'. The Author(s), 6, p. 19726. Available at: http://dx.doi.org/10.1038/srep19726.

Leys, D., Tsapin, A. S., Nealson, K. H., Meyer, T. E., Cusanovich, M. A. and Van Beeumen, J. J. (1999) 'Structure and mechanism of the flavocytochrome c fumarate reductase of Shewanella putrefaciens MR-1', *Nature Structural & Molecular Biology*. Nature Publishing Group, 6(12), pp. 1113–1117.

Lloyd, J. R., Leang, C., Myerson, A. L. H., Coppi, M. V., Cuifo, S., Methe, B., Sandler, S. J. and Lovely, D. R. (2003) 'Biochemical and genetic characterization of PpcA, a periplasmic c-type cytochrome in Geobacter sulfurreducens', *Biochemical Journal*, 369(1), pp. 153–161. doi: 10.1042/bj20020597.

Lower, B. H., Shi, L., Yongsunthon, R., Droubay, T. C., McCready, D. E. and Lower, S. K. (2007) 'Specific bonds between an iron oxide surface and outer membrane cytochromes MtrC and OmcA from Shewanella oneidensis MR-1', *Journal of Bacteriology*, 189(13), pp. 4944–4952. doi: 10.1128/JB.01518-06.

Madigan, M. T., Martinko, J. M., Dunlap, P. V and Clark, D. P. (2008) 'Brock biology of microorganisms 12th edn', *Int. Microbiol*, 11, pp. 65–73.

De Marco, P. (2004) 'Methylotrophy versus heterotrophy: a misconception', *Microbiology*. Microbiology Society, 150(6), pp. 1606–1607.

Marsili, E., Baron, D. B., Shikhare, I. D., Coursolle, D., Gralnick, J. a and Bond, D. R. (2008) 'Shewanella secretes flavins that mediate extracellular electron transfer.', *Proceedings of the National Academy of Sciences of the United States of America*, 105(10), pp. 3968–3973. doi: 10.1073/pnas.0710525105.

McKay, C. P. and Young, R. E. (1997) 'Life in Extreme Environments'.

McLean, J. S., Majors, P. D., Reardon, C. L., Bilskis, C. L., Reed, S. B., Romine, M. F. and Fredrickson, J. K. (2008) 'Investigations of structure and metabolism within Shewanella oneidensis MR-1 biofilms', *Journal of Microbiological Methods*, 74(1), pp. 47–56. doi: 10.1016/j.mimet.2008.02.015.

McLean, J. S., Pinchuk, G. E., Geydebrekht, O. V., Bilskis, C. L., Zakrajsek, B. A., Hill, E. A., Saffarini, D. A., Romine, M. F., Gorby, Y. A., Fredrickson, J. K. and Beliaev, A. S. (2008) 'Oxygen-dependent autoaggregation in Shewanella oneidensis MR-1', *Environmental Microbiology*. Blackwell Publishing Ltd, 10(7), pp. 1861–1876. doi: 10.1111/j.1462-2920.2008.01608.x.

Methé, B. A., Nelson, K. E., Eisen, J. A., Paulsen, I. T., Nelson, W., Heidelberg, J. F., Wu, D., Wu, M., Ward, N., Beanan, M. J., Dodson, R. J., Madupu, R., Brinkac, L. M., Daugherty, S. C., DeBoy, R. T., Durkin, A. S., Gwinn, M., Kolonay, J. F., Sullivan, S. A., Haft, D. H., Selengut, J., Davidsen, T. M., Zafar, N., White, O., Tran, B., Romero, C., Forberger, H. A., Weidman, J., Khouri, H., Feldblyum, T. V, Utterback, T. R., Van Aken, S. E., Lovley, D. R. and Fraser, C. M. (2003) 'Genome of *Geobacter sulfurreducens*: Metal reduction in subsurface environments.', *Science (New York, N.Y.)*, 302(5652), pp. 1967–1969. doi: 10.1126/science.1088727.

Meyer, T. E., Tsapin, A. I., Vandenberghe, I., de Smet, L., Frishman, D., Nealson, K. H., Cusanovich, M. A. and van Beeumen, J. J. (2004) 'Identification of 42 possible cytochrome C genes in the Shewanella oneidensis genome and characterization of six soluble cytochromes.', *Omics : a journal of integrative biology*. United States, 8(1), pp. 57–77. doi: 10.1089/153623104773547499.

Mitchell, A. C., Peterson, L., Reardon, C. L., Reed, S. B., Culley, D. E., Romine, M. R. and Geesey, G. G. (2012) 'Role of outer membrane c-type cytochromes MtrC and OmcA in Shewanella oneidensis MR-1 cell production, accumulation, and detachment during respiration on hematite', *Geobiology*, 10(4), pp. 355–370. doi: 10.1111/j.1472-4669.2012.00321.x.

Mitchell, P. (1961) 'Coupling of phosphorylation to electron and hydrogen transfer by a chemi-osmotic type of mechanism', *Nature*. Springer, 191(4784), pp. 144–148.

Mulkidjanian, A. Y., Koonin, E. V, Makarova, K. S., Mekhedov, S. L., Sorokin, A., Wolf, Y. I., Dufresne, A., Partensky, F., Burd, H., Kaznadzey, D., Haselkorn, R. and Galperin, M. Y. (2006) 'The cyanobacterial genome core and the origin of photosynthesis', *Proceedings of the National Academy of Sciences*, 103(35), pp. 13126–13131. doi: 10.1073/pnas.0605709103.

Myers, C. and Nealson, K. H. (1988) 'Bacterial manganese reduction and growth with manganese oxide as the sole electron acceptor', *Science*, 240. doi: 10.1126/science.240.4857.1319.

Nelson, D. L., Lehninger, A. L. and Cox, M. M. (2008) *Lehninger principles of biochemistry*. Macmillan.

Okamoto, A., Hashimoto, K., Nealson, K. H. and Nakamura, R. (2013) 'Rate enhancement of bacterial extracellular electron transport involves bound flavin semiquinones', *Proceedings of the National Academy of Sciences*, 110(19), pp. 7856–7861.

Okamoto, A., Kalathil, S., Deng, X., Hashimoto, K., Nakamura, R. and Nealson, K. H. (2014) 'Cell-secreted Flavins Bound to Membrane Cytochromes Dictate Electron Transfer Reactions to Surfaces with Diverse Charge and pH.', *Scientific reports*, 4, p. 5628. doi: 10.1038/srep05628.

Okamoto, A., Nakamura, R. and Hashimoto, K. (2011) 'In-vivo identification of direct electron transfer from Shewanella oneidensis MR-1 to electrodes via outer-membrane OmcA-MtrCAB protein complexes', *Electrochimica Acta*. Elsevier Ltd, 56(16), pp. 5526–5531. doi: 10.1016/j.electacta.2011.03.076.

Pant, D., Van Bogaert, G., Diels, L. and Vanbroekhoven, K. (2010) 'A review of the substrates used in microbial fuel cells (MFCs) for sustainable energy production', *Bioresource Technology*, 101(6), pp. 1533–1543. doi: 10.1016/j.biortech.2009.10.017.

Pasteur, L. (1860) 'Mémoire sur la fermentation alcoolique.', *Ann Chimie Physique*, 58, p. 359–360.

Patel, M. S. and Roche, T. E. (1990) 'Molecular biology and biochemistry of pyruvate dehydrogenase complexes.', *The FASEB Journal*. FASEB, 4(14), pp. 3224–3233.

Pereira, M. M., Sousa, F. L., Veríssimo, A. F. and Teixeira, M. (2008) 'Looking for the minimum common denominator in haem–copper oxygen reductases: Towards a unified catalytic mechanism', *Biochimica et Biophysica Acta (BBA)-Bioenergetics*. Elsevier, 1777(7), pp. 929–934.

Pirbadian, S., Barchinger, S. E., Leung, K. M., Byun, H. S., Jangir, Y., Bouhenni, R. a., Reed, S. B., Romine, M. F., Saffarini, D. a., Shi, L., Gorby, Y. a., Golbeck, J. H. and El-Naggar, M. Y. (2014) 'Shewanella oneidensis MR-1 nanowires are outer membrane and periplasmic extensions of the extracellular electron transport components', *Proceedings of the National Academy of Sciences*, 111(35), pp. 1–6. doi: 10.1073/pnas.1410551111.

Pitts, K. E., Dobbin, P. S., Reyes-Ramirez, F., Thomson, A. J., Richardson, D. J. and Seward, H. E. (2003) 'Characterization of the Shewanella oneidensis MR-1 decaheme cytochrome MtrA: Expression in Escherichia coli confers the ability to reduce soluble FE(III) chelates', *Journal of Biological Chemistry*, 278(30), pp. 27758–27765. doi: 10.1074/jbc.M302582200.

Potter, M. C. (1911) 'Electrical Effects Accompanying the Decomposition of Organic Compounds', *Proceedings of the Royal Society of London. Series B, Containing Papers of a Biological Character*, 84(571), p. 260 LP-276. Available at: http://rspb.royalsocietypublishing.org/content/84/571/260.abstract.

Preisig, O., Zufferey, R., Thöny-Meyer, L., Appleby, C. A. and Hennecke, H. (1996) 'A high-affinity cbb3-type cytochrome oxidase terminates the symbiosis-specific respiratory chain of Bradyrhizobium japonicum.', *Journal of bacteriology*. Am Soc Microbiol, 178(6), pp. 1532–1538.

Qiu, D., Wei, H., Tu, Q., Yang, Y., Xie, M., Chen, J., Pinkerton, M. H., Liang, Y., He, Z. and Zhou, J. (2013) 'Combined genomics and experimental analyses of respiratory characteristics of Shewanella putrefaciens W3-18-1', *Applied and environmental microbiology*. Am Soc Microbiol, 79(17), pp. 5250–5257.

Reardon, C. L., Dohnalkova, A. C., Nachimuthu, P., Kennedy, D. W., Saffarini, D. A., Arey, B. W., Shi, L., Wang, Z., Moore, D., McLean, J. S., Moyles, D., Marshall, M. J., Zachara, J. M., Fredrickson, J. K. and Beliaev, A. S. (2010) 'Role of outer-membrane cytochromes MtrC and OmcA in the biomineralization of ferrihydrite by Shewanella oneidensis MR-1', *Geobiology*, 8(1), pp. 56–68. doi: 10.1111/j.1472-4669.2009.00226.x.

Reguera, G., McCarthy, K. D., Mehta, T., Nicoll, J. S., Tuominen, M. T. and Lovley, D. R. (2005) 'Extracellular electron transfer via microbial nanowires', *Nature*, 435(7045), pp. 1098–1101. doi: 10.1038/nature03661.

Reguera, G., Nevin, K. P., Nicoll, J. S., Covalla, S. F., Woodard, T. L. and Lovley, D. R. (2006) 'Biofilm and nanowire production leads to increased current in Geobacter sulfurreducens fuel cells', *Applied and Environmental Microbiology*, 72(11), pp. 7345–7348. doi: 10.1128/AEM.01444-06.

Richardson, D. J. (2000) 'Bacterial respiration: a flexible process for a changing environment', *Microbiology*. Microbiology Society, 146(3), pp. 551–571.

Richter, K., Schicklberger, M. and Gescher, J. (2012) 'Dissimilatory reduction of extracellular electron acceptors in anaerobic respiration', *Applied and Environmental Microbiology*, 78(4), pp. 913–921. doi: 10.1128/AEM.06803-11.

Ross, D. E., Brantley, S. L. and Tien, M. (2009) 'Kinetic characterization of OmcA and MtrC, terminal reductases involved in respiratory electron transfer for dissimilatory iron reduction in Shewanella oneidensis MR-1', *Applied and Environmental Microbiology*, 75(16), pp. 5218–5226. doi: 10.1128/AEM.00544-09.

Ross, D. E., Flynn, J. M., Baron, D. B., Gralnick, J. A. and Bond, D. R. (2011) 'Towards electrosynthesis in Shewanella: Energetics of reversing the Mtr pathway for reductive metabolism', *PLoS ONE*, 6(2). doi: 10.1371/journal.pone.0016649.

Ross, D. E., Ruebush, S. S., Brantley, S. L., Hartshorne, R. S., Clarke, T. a, Richardson, D. J. and Tien, M. (2007) 'Characterization of protein-protein interactions involved in iron reduction by Shewanella oneidensis MR-1.', *Applied and environmental microbiology*, 73(18), pp. 5797–808. doi: 10.1128/AEM.00146-07.

Saltikov, C. W. and Newman, D. K. (2003) 'Genetic identification of a respiratory arsenate reductase', *Proc Natl Acad Sci USA*, 100. doi: 10.1073/pnas.1834303100.
Schink, B. and Schlegel, H. G. (1978) 'Hydrogen metabolism in aerobic hydrogen-oxidizing bacteria.', *Biochimie*. France, 60(3), pp. 297–305.

Schloss, P. D. and Handelsman, J. (2004) 'Status of the microbial census', *Microbiol Mol Biol Rev*, 68(4), pp. 686–691. doi: 68/4/686 [pii]\r10.1128/MMBR.68.4.686-691.2004.

Scott, J. H. and Nealson, K. H. (1994) 'A biochemical study of the intermediary carbon metabolism of Shewanella putrefaciens.', *Journal of Bacteriology*. Am Soc Microbiol, 176(11), pp. 3408–3411.

Serres, M. H. and Riley, M. (2006) 'Genomic analysis of carbon source metabolism of Shewanella oneidensis MR-1: predictions versus experiments', *Journal of bacteriology*. Am Soc Microbiol, 188(13), pp. 4601–4609.

Shafaat, H. S., Rüdiger, O., Ogata, H. and Lubitz, W. (2013) '[NiFe] hydrogenases: a common active site for hydrogen metabolism under diverse conditions', *Biochimica et Biophysica Acta (BBA)-Bioenergetics*. Elsevier, 1827(8), pp. 986–1002.

Shi, L., Chen, B., Wang, Z., Elias, D. A., Mayer, M. U., Gorby, Y. A., Ni, S., Lower, B. H., Kennedy, D. W. and Wunschel, D. S. (2006) 'Isolation of a high-affinity functional protein complex between OmcA and MtrC: two outer membrane decaheme c-type cytochromes of Shewanella oneidensis MR-1', *J Bacteriol*, 188. doi: 10.1128/JB.01966-05.

Shi, L., Dong, H., Reguera, G., Beyenal, H., Lu, A., Liu, J., Yu, H.-Q. and Fredrickson, J. K. (2016) 'Extracellular electron transfer mechanisms between microorganisms and minerals', *Nature Reviews Microbiology*. Nature Publishing Group, 14(10), pp. 651–662. doi: 10.1038/nrmicro.2016.93.

Shoffner, J. M. (2001) 'An introduction: oxidative phosphorylation diseases', in *Seminars in neurology*. Copyright© 2001 by Thieme Medical Publishers, Inc., 333 Seventh Avenue, New York, NY 10001, USA. Tel.:+ 1 (212) 584-4662, pp. 237–250.
Simon, J., van Spanning, R. J. M. and Richardson, D. J. (2008) 'The organisation of proton motive and non-proton motive redox loops in prokaryotic respiratory systems.', *Biochimica et biophysica acta*. Netherlands, 1777(12), pp. 1480–1490. doi: 10.1016/j.bbabio.2008.09.008.

Sousa, F. L., Alves, R. J., Ribeiro, M. A., Pereira-Leal, J. B., Teixeira, M. and Pereira, M. M. (2012) 'The superfamily of heme–copper oxygen reductases: types and evolutionary considerations', *Biochimica et Biophysica Acta (BBA)-Bioenergetics*. Elsevier, 1817(4), pp. 629–637.

Stolz, J. F., Basu, P., Santini, J. M. and Oremland, R. S. (2006) 'Arsenic and selenium in microbial metabolism', *Annu. Rev. Microbiol.* Annual Reviews, 60, pp. 107–130.

Tang, Y. J., Meadows, A. L., Kirby, J. and Keasling, J. D. (2007) 'Anaerobic central metabolic pathways in Shewanella oneidensis MR-1 reinterpreted in the light of isotopic metabolite labeling', *Journal of Bacteriology*, 189(3), pp. 894–901. doi: 10.1128/JB.00926-06.

Toledo-Cuevas, M., Barquera, B., Gennis, R. B., Wikström, M. and García-Horsman, J. A. (1998) 'The cbb 3-type cytochrome c oxidase from Rhodobacter sphaeroides, a proton-pumping heme-copper oxidase', *Biochimica et Biophysica Acta (BBA)-Bioenergetics*. Elsevier, 1365(3), pp. 421–434.

Trevelyan, W. E. and Harrison, J. S. (1952) 'Studies on yeast metabolism. 1. Fractionation and microdetermination of cell carbohydrates', *Biochemical Journal*, 50(3), pp. 298–303. Available at: https://www.ncbi.nlm.nih.gov/pmc/articles/PMC1197652/pdf/biochemj00910-0022.pdf.

Vargas, M., Kashefi, K., Blunt-Harris, E. L. and Lovley, D. R. (1998) 'Microbiological evidence for Fe(III) reduction on early Earth', *Nature*, 395(6697), pp. 65–67. Available at: http://dx.doi.org/10.1038/25720.

White, G. F., Edwards, M. J., Gomez-Perez, L., Richardson, D. J., Butt, J. N. and Clarke, T. A. (2016) *Mechanisms of Bacterial Extracellular Electron Exchange*. 1st edn, *Advances in Bacterial Electron Transport Systems and Their Regulation*. 1st edn. Elsevier Ltd. doi: 10.1016/bs.ampbs.2016.02.002.

White, G. F., Shi, Z., Shi, L., Dohnalkova, A. C., Fredrickson, J. K., Zachara, J. M., Butt, J. N., Richardson, D. J. and Clarke, T. a (2012) 'Development of a proteoliposome model to probe transmembrane electron-transfer reactions.', *Biochemical Society transactions*, 40(6), pp. 1257–60. doi: 10.1042/BST20120116.

White, G. F., Shi, Z., Shi, L., Wang, Z., Dohnalkova, A. C., Marshall, M. J., Fredrickson, J. K., Zachara, J. M., Butt, J. N., Richardson, D. J. and Clarke, T. a (2013) 'Rapid electron exchange between surface-exposed bacterial cytochromes and Fe(III) minerals.', *Proceedings of the National Academy of Sciences of the United States of America*, 110(16), pp. 6346–51. doi: 10.1073/pnas.1220074110.

Wildung, R. E., Gorby, Y. A., Krupka, K. M., Hess, N. J., Li, S. W., Plymale, A. E., McKinley, J. P. and Fredrickson, J. K. (2000) 'Effect of electron donor and solution chemistry on products of dissimilatory reduction of technetion by Shewanella putrefaciens', *Appl. Environ. Microbiol.*, 66(6), pp. 2451–2460. doi: 10.1128/AEM.66.6.2451-2460.2000.

Woese, C. R. and Fox, G. E. (1977) 'Phylogenetic structure of the prokaryotic domain: the primary kingdoms', *Proceedings of the National Academy of Sciences*. National Acad Sciences, 74(11), pp. 5088–5090.

Yang, D., Oyaizu, Y., Oyaizu, H., Olsen, G. J. and Woese, C. R. (1985) 'Mitochondrial origins.', *Proc Natl Acad Sci U S A*, 82(13), pp. 4443–4447. doi: 10.1073/pnas.82.13.4443.

Zargar, K. and Saltikov, C. W. (2009) 'Lysine-91 of the tetraheme c-type cytochrome CymA is essential for quinone interaction and arsenate respiration in Shewanella sp. strain ANA-3', *Archives of Microbiology*, 191(11), pp. 797–806. doi: 10.1007/s00203-009-0511-x.

Zverlov, V. V and Schwarz, W. H. (2008) 'Bacterial Cellulose Hydrolysis in Anaerobic Environmental Subsystems—Clostridium thermocellumandClostridium stercorarium, Thermophilic Plant- fiber Degraders', *Annals of the New York Academy of Sciences*. Wiley Online Library, 1125(1), pp. 298–307.

Chapter 2

Materials and Methods

2.1 General Methods*

2.1.1 Media Preparation

Luria broth (LB) media was prepared with 25 g of Miller pre-mix. This contained: 10 g tryptone, 5 g yeast extract and 10 g NaCl per litre of media prepared. To make solid LB media 1.5 % (weight/volume) agar was added.

2.1.2 Agarose Gel Electrophoresis

Gels containing 1 % agarose were made by adding 1 g of agarose to 100 ml of Tris-acetate-EDTA (TAE) buffer. This was then heated in a microwave until the agarose had dissolved. The agarose solution was then cooled to approximately 60 ^{O}C prior to addition of 5 µl of 10 mg/ml ethidium bromide solution. After mixing, the solution was poured into a casting tray to set.

Samples to be run on agarose gels were prepared by mixing a ratio of 5:1 (sample : loading dye) using 6X orange gel loading dye (NEB). Samples were then loaded onto gels prior to electrophoresis. This was carried out at a constant potential of 100 V current at 40 mA for 90 min. Resulting gels were visualised and imaged using a ChemiDoc^{TM} UV transilluminator (Bio-Rad).

2.1.3 SDS Polyacrylamide Gel Electrophoresis (SDS-PAGE)

Polyacrylamide gels for SDS PAGE were made to have a final concentration of polyacrylamide of 10 %, with a 4 % polyacrylamide stacking gel component (Table 2.1). Gels and running buffers were prepared using standard method (Laemmli, 1970).

* Unless otherwise stated, reagents were sourced from Thermo-Fisher.

2X SDS PAGE loading buffer was made containing 0.125 M Tris pH 6.8, 4 % (weight/volume) SDS, 20 % (volume/volume) glycerol, 5 M urea, and 0.005% (weight/volume) bromophenol blue. Gels were run using a Hoefer SE260 Mighty Small gel system at a potential of 150 V current set to 60 mA. Running time varied between 60-90 min or until the loading dye leading band was seen to reach the end of the gel.

Table 2.1 – Polyacrylamide gel recipe to give gels with 10 % acrylamide content for SDS PAGE. Volumes of ingredients yields total volume of 30 ml running gel component and 10 ml stacking gel component (enough for 2X polyacrylamide gels).

Gel Component	Volume Required for 10 % Running Gel / ml	Volume Required for 4 % Stacking Gel / ml
30 % Acrylamide Solution	10	1.33
1.5 M Tris, pH 8.8	7.5	-
0.5 M Tris, pH 6.8	-	2.5
10 % SDS	0.3	0.1
Distilled Water	12.09	6.1
10 % APS	0.1	0.05
TEMED	0.01	0.005

2.1.4 Heme-Linked Peroxidase Staining of SDS Polyacrylamide Gels

Gels to be stained for general protein were washed with analytical grade water (Fisher) prior to incubating at room temperature for 15 min in Coomassie protein stain (InstantBlue™, Expedeon). After this time stain had developed allowing for visualisation of protein.

Gels to be stained specifically for heme containing proteins were washed with analytical grade water (Fisher) prior to being incubated at room temperature for 10 min in 50 ml of 0.25 M sodium acetate pH 5.0. After this incubation, 20 ml of 1 mg/ml

3,3',5,5'-tetramethylbenzidine dihydrochloride hydrate (TMBD) solution was prepared in methanol and added to the sodium acetate gel incubation solution. Further incubation for 10 min was performed in the dark before addition of 200 µL 30 % hydrogen peroxide to solution. Gels were again incubated in the dark for a further 5 min until stain had developed.

This staining method highlights the presence of proteins that can reduce O_2 when TMBD is present to function as an electron donor. Generally only heme containing proteins are able to catalyse this reaction, although instances of non-heme cytochrome oxidase/nitrite reductases have also been seen capable of this reaction (Miller and Nicholas, 1984).

2.1.5 Western Blotting

Immediately after SDS PAGE, gels were briefly washed in analytical grade water (Fisher) prior to submerging in transfer buffer (20 mM Tris.HCl pH 8.3 and 192 mM glycine in 20 % Methanol) for 15 min. PVDF membrane was activated by washing with 100 % methanol before rinsing with analytical grade water. The membrane was then washed in transfer buffer for 5 min. 10 sheets of blotting paper were incubated in transfer buffer until saturated. 5 sheets of saturated blotting paper were then layered onto the anodic surface followed by the PVDF membrane onto which the gel was placed. The remaining 5 sheets of saturated blotting paper were layered on top of this allowing connection with the cathodic surface. Air bubbles were gently pressed out of the stack prior to transfer using a semi-dry transfer system (Scie-Plas) running at a constant current of 95 mA (~10 V) for 60 min.

PVDF membrane was removed from blotter and incubated overnight in blocking solution of TBS consisting of: 140 mM NaCl and 20 mM Tris, pH 7.5 with 5 % (weight/volume) skimmed milk power added. This was then washed for 3 times in 20 ml of TBST made up of: TBS with 0.1% (volume/volume) TWEEN20 added. After the last wash 1 % skimmed milk powder was dissolved in 15 ml TBST and MtrC antibody (targeted to amino acid residues 399-410) was added. The blot was then incubated

for 1 h with this solution containing the primary antibody. After this incubation, the blot was washed in 20 ml TBST containing 1 % skimmed milk powder followed by 3 further washes in 20 ml pure TBST. The blot was then incubated for 1 h in 15 ml TBST containing 1 % skimmed milk powder and anti-rabbit secondary antibody. After this, the blot was washed in 20 ml TBST containing 1 % skimmed milk powder before being washed 3 times in 20 ml pure TBST, followed by 3 further washes in 20 ml TBS to remove background noise (Burnette, 1981). Premixed BCIP/NBT solution (Sigma-Aldrich) was used to cover the blot for 15-30 min allowing alkaline phosphatase conjugated antibodies to be visualised.

Primary antibodies used in this protocol were raised against amino acid residues 399-410. These were tested prior to use in this experiment on whole cell and pure MtrC protein samples to ensure specificity.

2.3.6.2 Intact MALDI-MS analysis of $MtrC_{C453A}$

Purity of $MtrC_{C453}$ sample was confirmed by performing SDS PAGE with samples prepared and loaded for electrophoresis as previously described. The gel was stained with InstantBlue™ (Expedeon) to check the purity of the sample. 20 µl of 1 µg/ml $MtrC_{C453A}$ in 20 mM HEPES pH 7.6 was transferred to a 1.5 mL microcentrifuge tube, intact MALDI-MS and analysis was performed by the John Innes Centre Proteomics Facility using a SYNAPT G2Si mass spectrometer (Waters). In this process the peptide chain was ionised and mass calculated via time of flight. Digestion was not undertaken prior to analysis allowing for full length peptide to be compared to predicted amino acid mass of MtrC.

2.2 Site Directed Mutagenesis

2.2.1 Plasmid Extraction

Plasmids were purified using plasmid miniprep kits (Qiagen), as per manufacturer's instructions. A Thermo^{TM} nano-drop spectrophotometer was used to assess the quality of the purified plasmids.

2.2.2 Polymerase Chain Reaction

Polymerase chain reaction (PCR) was performed on samples prepped as per Table 2.2 using a Techne TC-512 PCR machine. Primers used listed in Table 2.3 with separate reactions being carried out to generate *mtrC:C444A* and *mtrC:C453A* using relevant primer sets.

These primers contain altered DNA bases (highlighted in red on table) that code for alanine instead of the wild type cysteine. As the PCR reaction occurs, the double stranded plasmid DNA is split upon heating before the temperature is reduced to allow annealing of primers to the plasmid DNA. The primers will bind specifically to their complimentary sequences in the plasmid sequence before temperatures optimal for DNA extension is reached. At this temperature, free nucleotides are added to the primer regions, leading to replication of the plasmid DNA. Importantly the altered DNA sequence coded in the primers are now incorporated into the resultant copies of the plasmid, fixing the mutation into the DNA. During the reaction, the reaction mixture was heated to 95 ^{O}C for 300 sec before 35 cycles of denaturing, annealing and polymerase extension steps (95 ^{O}C for 30 sec, 60 ^{O}C for 60 sec, and 72 ^{O}C for 90 sec, respectively). A final extension step was carried out at 72 ^{O}C for 300 sec.

For generation of cysteine mutants in the membrane bound form of MtrC, template of pBAD202/D-TOPO cloning vector containing *mtrC* gene was used. This was kindly provided by Dr Liang Shi (PNNL) and were constructed as per documented in

literature (Shi *et al.*, 2005). For generation of cysteine mutants in the soluble form of MtrC, modified plasmid template was used. This plasmid was constructed by Dr Jessica Van Wonderen (UEA) with removal of the protein's lipid anchor as well as removal of all c-terminal tags. A strep II tag was instead inserted at the c-terminus of the protein sequence to allow easier purification in a two-fold way. The removal of the lipid anchor causes the MtrC protein to be effectively excreted out into the surrounding medium allowing for cells to be removed and growth medium to be concentrated to harvest the protein without having to go through the cell lysis process. The strep II tag also allowed for easier purification as it allowed a two-step rapid purification process of the target MtrC specifically, without the need for ion exchange and gel filtration steps to separate total cell protein.

Products checked for amplification via agarose gel electrophoresis prior to addition of 5 µl Dpn1 buffer and 1 µl Dpn1 (Thermo). This was incubated for 1 hour at 4 ^{O}C to digest methylated template DNA before inactivation of Dpn1 by heating to 80 ^{O}C for 10 min. This left mutant plasmid amplification product as confirmed via sequencing described in section 2.2.4.

Table 2.2 - PCR reaction components. All reagents purchased from ThermoFisher unless source otherwise described.

Component	Amount (µl)
High-Fidelity Buffer	10
dNTP (10 mM)	1
Forward Primer (25 mM)	1
Reverse Primer (25 mM)	1
Template DNA (60 ng/µl)	1
DMSO	2.5
Molecular Grade H_2O (Fisher)	33
Phusion Polymerase	0.5

Table 2.3 - Primers used to induce C444A and C453A mutations with deviation from wild type *mtrC* highlighted. Designed and synthesised using Eurofins MWG.

Primer Name	Primer Sequence
MtrC_C444A_F	gtaggttggtcaatggcttctagcgaaggtaag
MtrC_C444A_R	cttaccttcgctagaagccattgaccaacctac
MtrC_C453A_F	taagtttgtagacgctgcagaccctgca
MtrC_C453A_R	tgcagggtctgcagcgtctacaaactta

Single cysteine mutant plasmids used as template in further PCR reactions to generate mutant *mtrC* where both cysteine residues were substituted to alanine. From this point plasmids containing *mtrC* and mutant genes will be donated pMtrC (native MtrC expressing), pC444A (single cysteine substitution at amino acid position 444), pC453A (single cysteine substitution at amino acid position 453) or pC444A,C453A (double cysteine substitution). Plasmids generated summarised in Table 2.4.

Table 2.4 – Summary table of plasmids generated through site directed mutagenesis. Plasmid name, expression vector, purification tag and if membrane anchor is present shown.

Plasmid Name	Vector	Tag	Membrane Anchor
pMtrC membrane bound	pBAD202/D-TOPO	His	+
pC444A membrane bound	pBAD202/D-TOPO	His	+
pC453A membrane bound	pBAD202/D-TOPO	His	+
pC444A,C453A membrane bound	pBAD202/D-TOPO	His	+
pMtrC soluble form	pBAD202/D-TOPO	Strep-II	-
pC444A soluble form	pBAD202/D-TOPO	Strep-II	-
pC453A soluble form	pBAD202/D-TOPO	Strep-II	-
pC444A,C453A soluble form	pBAD202/D-TOPO	Strep-II	-

2.2.3 Preparation of Chemically Competent *E. coli*

E. coli 803 cells were streaked from glycerol stocks onto an LB agar plate and incubated at 37 ^{O}C overnight. Single colonies were picked after 24 h and used to inoculate sterile 10 ml LB media prior to overnight incubation at 37 ^{O}C, shaking at 220 rpm. 1 ml aliquots were taken from overnight cultures and used to inoculate 100 ml LB. This culture was then incubated at 37 ^{O}C shaking at 220 rpm until an OD_{600} of 0.45-0.6 was achieved. The culture was then incubated for 10 min on ice before harvesting cells via centrifugation at 3500 x g for 10 min using Allegra 64R centrifuge chilled to 4 ^{O}C. Pelleted *E. coli* 803 were resuspended in 20 ml sterile, ice-cold $CaCl_2$ prior to incubation on ice for 20 min. The cells were again harvested by centrifugation at 3500 x g for 10 min then resuspended in 2.4 ml of 100 mM $CaCl_2$ (Dagert and Ehrlich, 1979). The *E. coli* 803 cells were divided into 100 µl aliquots and incubated at 4 ^{O}C for a further 4 h after which time they were deemed competent and used in transformation protocol or stored in 20 % glycerol at -80 ^{O}C for future use.

2.2.4 Transformation of Competent *E. coli* 803 Cells

For each different mutant *mtrC* variant generated, 5 µl of amplified PCR reaction product was added to 100 µl aliquot of chemically competent *E. coli* 803 cells. This mixture was mixed gently before incubation for 15 min on ice. Heat shock transformation was performed on cells by incubating sample at 42 ^{O}C for 30 sec before immediately being transferred back to ice. 250 µl of sterile LB medium was added to the sample prior to incubation for 60 min at 37 ^{O}C, shaking at 220 rpm. Cells were pelleted via centrifugation in Eppendorf 5424 benchtop centrifuge at 5000 rpm. Supernatant was poured off with residual used to resuspend cells prior to plating cell solution onto LB agar plates containing 50 µg/ml kanamycin. After overnight incubation at 37 ^{O}C, individual colonies were picked and used to inoculate individual 10 ml LB media. These were again incubated overnight at 37 ^{O}C, this time shaking at 220 rpm. Samples of resulting cultures were spread onto LB agar plates containing 50 µg/ml kanamycin to generate stocks before the remaining overnight cultures underwent plasmid extraction. Extracted plasmids were sent for sequencing performed by Eurofins MWG to confirm substitution of alanine to cysteine residues

had occurred. Sequencing of the mutated region was carried out a minimum of three times with full plasmid sequencing carried out at least once to confirm no non-specific mutations had occurred in other loci. This stage was important to ensure all results shown in later experiments could be attributed to the specific substitution of cysteine residues to alanine.

2.2.5 Conjugation of pMtrC and mutant *mtrC* into *S. oneidensis ΔmtrC*

Stocks of *E. coli* 803 (containing either pMtrC, pC444A, pC453A or pC444A,C453A), *E. coli* DH5α (pRK2013) and *S. oneidensis ΔmtrC* (LS661) were used to inoculate separate 10 ml LB cultures. The cultures containing *E. coli* 803 and *E. coli* DH5α were supplemented with 50 µg/ml kanamycin and the *S. oneidensis* cultures were supplemented with 100 µg/ml carbenicillin. All cultures were grown overnight shaking at 220 rpm with the *E. coli* cultures being incubated at 37 ^{O}C and the *S. oneidensis* culture incubated at 30 ^{O}C. 1.5 ml of each of these cultures was transferred to separate Eppendorf tubes prior to pelleting of cells by centrifuging at 5000 rpm in Eppendorf 5424 benchtop centrifuge. The supernatant was discarded and cell pellets were resuspended in 1 ml sterile LB to wash remaining antibiotics from samples. Samples were centrifuged as before to pellet cells with supernatant again being discarded. All three cell pellets were then resuspended in the same 1 ml aliquot of LB and mixed in one tube. This combined sample was again pelleted prior to supernatant being discarded and pellet being resuspended in 50 µl sterile LB. All 50 µl cell suspension was transferred to the centre of a LB agar plate and incubated at 30 ^{C}C overnight.

The bacterial conjugation was removed from the surface of the LB agar and resuspended in 10 ml LB prior to a six fold serial dilution in more sterile LB. 100 µl of each dilution was spread onto separate LB agar plates and incubated overnight at 30 ^{O}C. Individual colonies were picked and used to inoculate separate 10 ml LB cultures supplemented with 50 µg/ml kanamycin and 100 µg/ml carbenicillin. These were incubated overnight at 30 ^{O}C shaking at 220 rpm. Aliquots of each culture were spread onto LG agar plates supplemented with required antibiotics with the remaining

cultures undergoing plasmid extraction with resulting samples being sent for sequencing by Eurofins MWG to confirm plasmid had transferred without unwanted modifications. From this point *S. oneidensis ΔmtrC* (LS661) cell lines containing plasmids will be referred to as *S. oneidensis ΔmtrC* pMtrC (native MtrC expressing), *S. oneidensis ΔmtrC* pC444A (single cysteine substitution at amino acid position 444), *S. oneidensis ΔmtrC* pC453A (single cysteine substitution at amino acid position 453) or *S. oneidensis ΔmtrC* C444A,C453A (double cysteine substitution).

S. oneidensis ΔmtrC (LS661) used in this experiment was provided by Dr Liang Shi (PNNL). This strain of *S. oneidensis* was produced via a double-crossover recombination process using a suicide vector to result in the deletion of the *mtrC* gene. This was done by first constructing a suicide plasmid containing sequences complimentary to the flanking regions of *mtrC* and the *sacB* gene. This plasmid was transformed into *S. oneidensis* where it underwent homologous recombination becoming inserted into the chromosome. The cells were then plated onto a sucrose containing medium to select for cells that had undergone a second homologous recombination event resulting in the removal of the suicide plasmid DNA (including *sacB* the gene causing sensitivity to sucrose) and the *mtrC* target gene (Reyrat *et al.*, 1998).

2.3 Growth Studies

2.3.1 Growth Curves of *Shewanella oneidensis*

Nutrient agar plated colonies, grown from glycerol stocks of *S. oneidensis ΔmtrC* pMtrC, *S. oneidensis ΔmtrC* pC444A, *S. oneidensis ΔmtrC* pC453A and *S. oneidensis ΔmtrC* pC444A,C453A were used to inoculate individual 10 ml LB cultures supplemented with 50 µg/ml of kanamycin . These were incubated overnight at 30 ^{O}C shaking at 220 rpm. 100 µl aliquots from these cultures were used to inoculate a further 3 X 10 ml LB cultures supplemented with 50 µg/ml kanamycin for each *S. oneidensis* cell line. To each triplet of cultures, one was supplemented with 0 mM

arabinose, one was supplemented with 5 mM arabinose and the other was supplemented with 10 mM arabinose. This gave 12 cultures: three different conditions (varying arabinose concentration) for each of the four cell lines. Supplementation of media with arabinose allowed expression of genes previously inserted into the pBAD plasmid. This was due to the presence of arabinose allowing polymerase to access and bind to the arabinose operon (Figure 2.1).

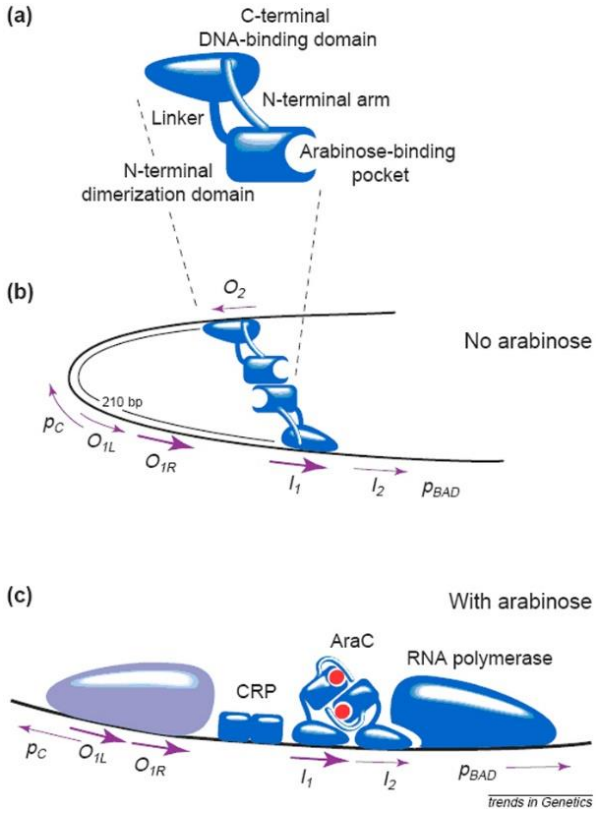

Figure 2.1 – Arabinose operon explained. (a) Highlights the proteins involved in the expression control mechanism of the arabinose operon. (b) Indicates the conformation of the proteins in the absence of arabinose. This arrangement makes a loop of DNA preventing polymerase binding and translating the genes inserted into the pBAD plasmid. (c) Highlights the changes to the protein conformation that resolves the DNA loop and allows polymerase binding to the operon and translating the inserted genes. This results in the expression of the MtrC protein forms in the experiments described here. Figure taken from Brown, W., Ralston, A. & Shaw, K. (2008).

300 µl aliquots of each condition were transferred to a 96 well PCR plate. This was then incubated for 25 h at 30 ^{O}C in a BMG FLUROstar Omega plate reader with aerobic conditions achieved by shaking at 400 rpm for 1700 sec before each OD_{600} read was taken (1800 sec interval between each read, 20 individual scans averaged for each read).

The same experiment was repeated under anaerobic conditions. LB media was supplemented with 50 mM sodium fumarate to act as an electron acceptor in the place of O_2. 1 ml aliquots of cultures were transferred into a 48 well PCR plate before being transferred into a MBraun Unilab glovebox with O_2 maintained below 2 ppm and leaving for 30 min for O_2 to dissipate out of the wells and culture solution. A transparent cover slip was then adhered over the wells before the plate lid was glued into place using an airtight adhesive. The plate was then removed from the glove box and incubated in the plate reader under conditions stated previously but without agitation before each read to help maintain anaerobic conditions. A control of inoculated LB lacking sodium fumarate was included on the plate to confirm anaerobic conditions.

All of these experiments were repeated at larger volumes to ensure results were not artefacts of growth at small volumes in the plate reader or the result of chemical leakage from the plastic plates used. For these experiments, aerobic growth cultures were scaled up to 100 ml LB media (same supplements as listed above were added) and incubated in 250 ml conical flasks at 30 ^{O}C shaking at 220 rpm. For anaerobic growths, 50 ml falcon tubes were filled with media before being sealed and sparged with N_2 prior to inoculation. Samples were manually obtained using syringes through suberseals and OD_{600} recorded using a Hitachi U-3310 benchtop spectrometer.

2.3.2 Restoration of Growth using ROS Scavenger Enzymes

Growth curve experiments (Section 2.3.1) were repeated with *S. oneidensis ΔmtrC* pMtrC, *S. oneidensis ΔmtrC* pC444A, *S. oneidensis ΔmtrC* pC453A and *S. oneidensis ΔmtrC* pC444A,C453A cell lines grown in 100 ml LB supplemented with

50 µg/ml of kanamycin and 5 mM arabinose. However, in this experiment culture medium was also supplemented with either 0.3 U/ml of catalase, 0.3 U/ml of superoxide dismutase or 0.3 U/ml of catalase and 0.3 U/ml of superoxide dismutase. 1 ml samples were taken from cultures regularly over 25 h and OD_{600} was recorded at each time point using a Hitachi U-3310 benchtop spectrometer.

2.3.3 Restoration of growth using Glucose to Repress Expression

Glycerol stocks of *S. oneidensis ΔmtrC* pMtrC and *S. oneidensis ΔmtrC* pC453A were used to inoculate 10 ml LB cultures supplemented with 50 µg/ml of kanamycin and incubated overnight at 30 ^{O}C shaking at 220 rpm. 100 µl inoculum was taken from these cultures and used to inoculate separate 100 ml LB cultures supplemented with 50 µg/ml of kanamycin before the cultures were incubated at 30 ^{O}C shaking at 220 rpm. Growth was monitored by measure OD_{600} of 1 ml samples from cultures until OD_{600} of ~0.4 was achieved. At this time 5 mM arabinose and 2 % (weight/volume) of glucose was added to cultures (Guzman *et al.*, 1995). Incubation continued at 30 ^{O}C shaking at 220 rpm with regular OD_{600} measurements over a total duration of 25 h.

2.3.4 Viable Cell Counts

To measure viable cell counts relative to OD_{600} values recorded for cell suspensions, serial dilutions (down to $1:10^9$) of inoculated media were performed and 100 µl of each dilution was spread onto LB agar plates (containing antibiotics and / or arabinose where appropriate). These plates were then incubated at 30 ^{o}C for 48 h to allow colonies to grow large enough to distinguish contaminants and false positives. Colonies were then counted and recorded using ‘OpenCFU’ software.

Minimum of three dilutions were averaged and used to calculate CFU per ml of original cell suspension. Repeats of these were carried out and further averages were taken to give a more statistically relevant CFU per ml.

2.3.5 Hydrogen Peroxide Kill Curve

To replicate the phenotype seen when cells were grown expressing mutant MtrC protein, overnight growths of *S. oneidensis ΔmtrC* and *S. oneidensis* Mr1 were pelleted and resuspended in media containing varying amounts of hydrogen peroxide (0, 0.1 and 2.5 mM). These were incubated for 15 min with 1 ml aliquot samples taken at 5 min intervals to be pelleted and resuspended in fresh media. Serial dilutions were then set up of each sample and plated to ascertain viable cell counts.

2.3.6 Zones of Inhibition

Further investigations into the physiological relevance of the amounts of H_2O_2 detected in cell samples were carried out using zones of inhibition as a measure. Cultures of *S. oneidensis* Mr1 and *E. coli* were grown overnight before being spread onto separate LB agar plates (containing antibiotics where appropriate). To these plates, 13 mm disks of filter paper previously soaked in 0-5 mM concentrations of H_2O_2 (0, 0.25, 0.5, 1, 2.5 and 5 mM) were placed onto the plates prior to incubation overnight at 30 ^{o}C. After incubation lawns of bacteria could be seen on the plate and zones around the filter paper disks where the bacteria could not grow. The diameter of these zone of inhibition were measured at multiple angles around the centre point and averaged to give a quantitative value for the effect of the H_2O_2 on cell growth.

2.4 Protein Expression

2.4.1 Anaerobic Protein Expression

Glycerol stocks of *S. oneidensis ΔmtrC* pMtrC, *S. oneidensis ΔmtrC* pC444A, *S. oneidensis ΔmtrC* pC453A and *S. oneidensis ΔmtrC* pC444A,C453A were used to inoculate individual 10 ml LB cultures supplemented with 50 µg/ml of kanamycin . These were incubated overnight at 30 ^{O}C shaking at 220 rpm. 0.5 ml aliquots were taken from these to inoculate separate 50 ml LB media supplemented with 50 µg/ml of kanamycin and 50 mM sodium fumarate. These cultures were sparged with

nitrogen to remove dissolved oxygen prior to being sealed in 50 ml Falcon tube using airtight suberseals. Cultures were incubated at 30 ^{O}C with cell growth monitored by measuring OD_{600} of 1 ml samples extracted through the suberseals, using syringes, on a Hitachi U-3310 spectrometer. When OD_{600} had reached ~0.2, 5 mM arabinose was added to cultures (again through the suberseals using syringes). Cultures again incubated at 30 ^{O}C overnight at which time the cells were pelted via centrifugation at 3500 x g for 10 min using an Allegra 64R centrifuge before being resuspended in 20 mM HEPES pH 7.8. At this point, whole cell samples were prepared for SDS PAGE analysis and western blotting (as previously described).

For samples used in cell fractionation and protein localisation experiments, resuspended cell pellet samples were taken and cell lysis Complete^{TM} protease inhibitor was added (as per manufactures instructions). Each sample then underwent 6X 10 sec bursts of sonication with 50 sec incubation on ice occurring between each round of sonication. Lysed cell samples were then centrifuged at 6000 rpm for 10 min in Eppendorf 5424 benchtop centrifuge to remove large cell debris. Supernatant was then transferred to clean tubes prior to ultracentrifugation at 40,000 rpm in a Beckman Optima XL100K Ti45 rotor for 30 min to pellet the cell membranes. Supernatant was removed and stored as soluble fraction, pelleted membranes were resuspended in 20 mM HEPES pH 7.8 with 2 % (volume/volume) triton X-100 and incubated at 4 ^{O}C overnight to allow solubilisation of membranes. Samples were then prepared for SDS PAGE (as previously described) with resultant gels undergoing western blot analysis.

2.4.2 Aerobic Protein Expression

Glycerol stocks of *S. oneidensis ΔmtrC* pMtrC, *S. oneidensis ΔmtrC* pC444A, *S. oneidensis ΔmtrC* pC453A and *S. oneidensis ΔmtrC* pC444A,C453A were used to inoculate individual 10 ml LB cultures supplemented with 50 µg/ml of kanamycin. These were incubated overnight at 30 ^{O}C shaking at 220 rpm. 1 ml aliquots were taken from these to inoculate separate 50 ml LB media supplemented with 50 µg/ml of kanamycin and 20 mM sodium fumarate (previously sparged with nitrogen to remove dissolved oxygen). Cultures were incubated under anaerobic conditions, at

30 ^{O}C with cell growth monitored by measuring OD_{600} of 1 ml samples on a Hitachi U-3310 spectrometer. When OD_{600} had reached ~0.2, 5 mM arabinose was added to cultures and oxygen was introduced to cultures (by removing air tight suberseal and replacing with sterile foam bung) before again being incubated at 30 ^{O}C shaking at 220 rpm for a further 1-5 h as indicated for each experiment. After this time cells were pelleted by centrifugation at 3500 x g for 10 min using an Allegra 64R centrifuge. Cell pellets were resuspended in 20 mM HEPES pH 7.8 and normalised via samples being diluted to an OD_{600} value of 0.5. Samples were then prepared for SDS PAGE analysis (as previously described) and resulting gels were heme stained or western blotted to assess MtrC (native or mutant forms) cytochrome expression levels.

Expression levels were quantitatively compared using ImageJ software to compare pixel density of the MtrC and MtrC variant protein bands in heme strained gel images. These were first normalised to background staining in each respective lane of the gel prior to comparison between the samples.

2.5 Iron Reduction Assays

2.5.1 Whole Cell Ferric Iron Reduction

Glycerol stocks of *S. oneidensis* Mr1, *S. oneidensis ΔmtrC, S. oneidensis ΔmtrC* pMtrC, *S. oneidensis ΔmtrC* pC444A, *S. oneidensis ΔmtrC* pC453A and *S. oneidensis ΔmtrC* pC444A,C453A were used to inoculate individual 10 ml LB cultures supplemented with 50 µg/ml of kanamycin. These were incubated overnight at 30 ^{O}C shaking at 220 rpm. 0.5 ml aliquots were taken from these to inoculate separate 50 ml LB media supplemented with 50 µg/ml of kanamycin and 50 mM sodium fumarate. These cultures were sparged with nitrogen to remove dissolved oxygen prior to being sealed in 50 ml Falcon tube using airtight suberseals. Cultures were incubated at 30 ^{O}C with cell growth monitored by measuring OD_{600} of 1 ml samples extracted through the suberseals, using syringes, on a Hitachi U-3310 spectrometer. When OD_{600} had reached ~0.2 5 mM arabinose was added to cultures (again through the suberseals

using syringes). Cultures again incubated at 30 ^{O}C overnight at which time the cells were pelted via centrifugation at 3500 x g for 10 min using an Allegra 64R centrifuge before being resuspended in 20 mM HEPES pH 7.8 to an OD_{600} of 1. 5 ml aliquots of normalised cell samples was then added to 20 ml LB supplemented with 5 mM arabinose and 20 mM ferric iron (either soluble iron(III) citrate or insoluble goethite (FeO(OH)) depending on experiment). Cultures were then sparged with nitrogen to remove dissolved oxygen before incubating at 30 ^{O}C shaking at 220 rpm for 4 h with 1 ml samples taken hourly. These 1 ml samples underwent ferrozine assay to asses ferric iron reduction to ferrous iron.

A stock of ferrozine reagent was prepared by mixing 10 mM ferrozine with 100 mM ammonium acetate. 30 µl aliquots of this stock was added to 1 ml culture samples and absorbance at 562 nm was recorded using a Hitachi U-3310 spectrometer. Using a standard curve generated from known iron(II) chloride concentration, concentration of reduced iron in the samples could be determined (Viollier *et al.*, 2000). Standard curve gave y=0.101x (data not shown). In these experiments the complexation of ferrous iron to ferrozine (3-(2-Pyridyl)-5,6-diphenyl-1,2,4-triazine-p,p′-disulfonic acid monosodium salt hydrate) gives rise to the absorbance at 562 nm. This allowed for reduction of ferric iron to be monitored as concentration of ferrous iron is equivalent to concentration of Fe(II)-ferrozine complex.

2.5.2 Ferrozine Assay to Monitor Culture Growth on Goethite

Glycerol stocks of *S. oneidensis* Mr1, *S. oneidensis ΔmtrC, S. oneidensis ΔmtrC* pMtrC, *S. oneidensis ΔmtrC* pC444A, *S. oneidensis ΔmtrC* pC453A and *S. oneidensis ΔmtrC* pC444A,C453A were used to inoculate individual 10 ml LB cultures supplemented with 50 µg/ml of kanamycin. These were incubated overnight at 30 ^{O}C shaking at 220 rpm. 0.5 ml aliquots were taken from these to inoculate separate 50 ml LB media supplemented with 50 µg/ml of kanamycin and 20 mM goethite. These cultures were sparged with nitrogen to remove dissolved oxygen before being incubated at 30 ^{O}C shaking at 220 rpm with 1 ml samples taken every hour to undergo ferrozine assay (carried out as previously described).

2.6 Hydrogen Peroxide Detection

2.6.1 Indigo Carmine Assay

To investigate potential hydrogen peroxide in cell cultures, an indigo carmine assay was used. *S. oneidensis ΔmtrC* pMtrC and *S. oneidensis ΔmtrC* pC453A were grown anaerobically in 50 ml LB media (supplemented with 50 mM sodium fumarate and 5 mM arabinose). Samples were then taken from each culture and assayed in a glove box (with oxygen maintained under 0.2 ppm) using Oxygen Vacu-vials® kit K-7503 from CHEMetrics using Hitachi U-3310 spectrometer. The cultures were then grown aerobically for 2 h after being supplemented with 50 ml fresh LB media before further samples were taken and assayed. The cultures were then sparged with argon gas for 5 min to remove any oxygen where upon another sample was taken and assayed. Final samples were assayed after incubation with 0.3 U catalase for 15 min and further sparging with argon for 5 min to remove oxygen formed from the process.

The resulting reactions were analysed by recording wavelength scan readings between 450 – 700 nm. The height of peak at 610 nm (optimum absorbance for reacted indigo carmine) was calculated removing scatter. The difference between 610 nm peak height for sparged samples prior to catalase incubation and after was taken to be representative of hydrogen peroxide removal and thus amount present (Gilbert, Behymer and Castaneda, 1982). The indigo carmine itself is a redox sensitive dye that is readily reduced by hydrogen peroxide and oxygen. This change in the oxidation state leads to the dye appearing visibly blue with a sharp absorbance peak at 610 nm.

A standard curve was generated by assaying solutions of known hydrogen peroxide concentrations and plotting concentration against resultant absorbance peak height at 610 nm. y=mx+c for this was used to calculate estimates for the amount of hydrogen peroxide present in cell suspension samples.

2.6.2 Fluorimetric Hydrogen Peroxide Assay

Samples of 0.5 µM MtrC and $MtrC_{C453A}$ were reduced via addition of sodium dithionite under anaerobic conditions. Reduction of proteins was monitored through the use of a Jenway 7310 spectrometer by monitoring the distinctive heme reduction peak shift from 410 nm (oxidised) to 420 nm (reduced). Samples were then exposed to oxygen prior to undergoing hydrogen peroxide assay, carried out as per manufacturer's instructions (Sigma-Aldrich product code: MAK165). Experiment was repeated with addition of 0.1 µM of oxidised FMN to protein samples prior to exposure to oxygen. Hydrogen peroxide was again assayed for following manufacturers instructions.

A standard curve was generated by assaying solutions of known hydrogen peroxide concentrations and plotting concentration against resultant absorbance peak height at 610 nm. y=mx+c for this was used to calculate estimates for the amount of hydrogen peroxide present in cell suspension samples.

2.7 Protein Purification

2.7.1 Membrane Bound $MtrC_{C453A}$

S. oneidensis ΔmtrC pC453A (membrane bound form) glycerol stocks were used to inoculate 10X 10 ml LB media (supplemented with 50 µg/ml kanamycin) prior to being incubated overnight at 30 ^{O}C shaking at 220 rpm. These cultures were used as inoculum for 10X 1 l LB media (supplemented with 50 µg/ml kanamycin and 0.3 U/ml catalase). Cultures were incubated at 30 ^{O}C shaking at 150 rpm until cell growth had reached OD_{600} of ~0.5. At this point 5 mM arabinose was used to induce expression of pC453A. Cultures were again incubated at 30 ^{O}C shaking at 150 rpm for 10 h after which time cells were pelleted via centrifugation at 6000 rpm using Avanti J-26 floor standing centrifuge (Beckman, 8.1000 rotor). After cells were resuspended in 20 mM HEPES pH 7.5 cell lysis Complete^{TM} protease inhibitor were added (as per manufactures instructions) to samples to preserve protein. Resuspended cells were

French pressed at 1000 psi three time to lyse the cells. The membranes were pelleted by ultracentrifugation at 40,000 rpm in a Beckman Optima XL100K Ti45 rotor for 2 h prior to resuspension in 100 mM HEPES pH 7.2 with 0.5 % (weight to volume) sarkosyl and incubated at 4 ^{O}C for 1 h. The membranes were again pelleted via ultracentrifugation at 40,000 rpm in a Beckman Optima XL100K Ti45 rotor for 2 h before being resuspended in 20 mM HEPES pH 7.8 with 2 % (volume/volume) triton X-100 detergent and incubated overnight at 4 ^{O}C.

A 26/45 fast flow DEAE sepharose ion exchange column (GE Healthcare Life Sciences) was first equilibrated with 20 mM HEPES pH 7.8 with 2 % (volume/volume) triton X-100, using AKTA prime system. Solubilised membrane samples were loaded onto the column prior to washing with 1 l of 20 mM HEPES pH 7.8 with 2 % triton X-100 before being eluted over a salt gradient from 0 – 1 M over 900 ml with 11 ml fractions collected. Eluted fractions were check for MtrCAB protein through the use of SDS PAGE and heme staining. The fractions containing the desired protein were pooled and diluted 3 fold prior to being loaded onto a 5 ml Q-sepharose column, equilibrated using 20 mM HEPES pH 7.5 with 5 mM LDAO detergent. Bound protein washed with 20 ml 20 mM HEPES pH 7.5 with 5 mM LDAO prior to elution with 20 mM HEPES pH 7.5 with 5 mM LDAO and 250 mM NaCl, collecting 2 ml fractions. Fractions concentrated in 50 kDa cut off VivaSpin® spin column (Satorius) to a volume of 1 ml. Sample loaded onto S200 gel filtration column equilibrated with 20 mM HEPES pH 7.5, 150 mM NaCl with 5 mM LDAO prior to elution with same buffer, 2 ml fractions collected. Fractions analysed via SDS PAGE using Coomassie staining to identify pure samples of MtrCAB complex.

2.7.2 Soluble MtrC

S. oneidensis ΔmtrC pC453A (soluble form) glycerol stocks were used to inoculate 10X 10 ml LB media (supplemented with 50 µg/ml kanamycin) prior to being incubated overnight at 30 ^{O}C shaking at 220 rpm. These cultures were used as inoculum for 10X 1 l LB media (supplemented with 50 µg/ml kanamycin and 0.3 U/ml catalase). Cultures were incubated at 30 ^{O}C shaking at 150 rpm until cell growth had

reached OD_{600} of ~0.5. At this point 5 mM arabinose was used to induce expression of pC453A. Cultures were again incubated at 30 ^{O}C shaking at 150 rpm for 10 h after which time cells were pelleted via centrifugation at 6000 rpm using Avanti J-26 floor standing centrifuge (Beckman, 8.1000 rotor) and supernatant media recovered.
Media was loaded directly onto a StrepTactin™ column (GE Healthcare Life Sciences) equilibrated with 100 mM Tris/HCl pH 8, 150 mM NaCl and 1 mM EDTA. When saturated 10 ml elution buffer consisting of 100 mM Tris/HCl pH 8, 150 mM NaCl, 1 mM EDTA and 25 mM biotin was used to eluted bound protein, collecting 1 ml fractions. After this elution the column was regenerated using 10 mM NaOH prior to repeating the equilibration, loading and elution process. This cycle was repeated until all 10 l media had been run through the column. Collected fractions were analysed via SDS PAGE and Coomassie protein staining to assess purity of $MtrC_{C453A}$ protein. Pure fractions were then pooled and concentrated using a 50 kDa cut off VivaSpin® spin column (Satorius) until desired concentration had been reached, dependant on the experiment (concentration was determined using a Hitachi U-3310 benchtop spectrometer to measure absorbance at 410 nm which was then used to calculate concentration using an ε_{410} of 1260 $mM^{-1}cm^{-1}$).

2.8 Protein Crystallography

2.8.1 Crystallisation of $MtrC_{C453A}$

All experiments and analysis in this section were carried out under the supervision and guidance of Dr Marcus Edwards, UEA. Mtr_{C453A} samples were concentrated to 10 $mg.ml^{-1}$ (final concentration) using a 50 kDa cut off VivaSpin® spin column (Satorius) and quantified via spectroscopy. Sitting drop vapour diffusion crystallisation was then carried out using a range of conditions with two drops per condition at 1:1 and 2:1 ratios of mother liquor : protein. Crystallisation experiments were set up using Douglas Instruments Oryx robotics to dispense 1 µl drops After approximately 72 h incubation at 16 ^{o}C crystal formation was observed with crystals then harvested using 0.1-0.2 mm LithoLoops from conditions containing 30 % PEG 6000, 0.2 M sodium

acetate pH 5 and 0.1 M calcium chloride. These were then cryoprotected in solution containing 12 % glycerol as a cryoprotectant prior to vitrifying in liquid nitrogen.

2.8.2 X-Ray Diffraction of $MtrC_{C453A}$ Crystals

X-ray diffraction of $MtrC_{C453A}$ crystals was carried out using beamline i04 (Diamond Light Source). Wavelength of 0.97 Å was used to collect 360^{o} of data using 0.2^{o} Ω oscillations with 0.1 s exposures to the unattenuated 20 x 20 µm beam. This produced 900 images of data that were integrated using Mosflm (Leslie and Powell, 2007) and scaled using Aimless from the CCP4 suite, which allowed a maximum resolution to be determined from the Bragg spots reported by the detector. A space group, average cell dimensions and statistical checks were determined using POINTLESS form the CCP4 suite (Evans, 2011).

Collected datasets were used to solve the structure of $MtrC_{C453A}$ via molecular replacement using Phaser from the CCP4 suite. This was then refined using Phenix.refine from the Phenix suite with final model building and refinement manually performed using COOT (McCoy, 2007). Whole protein structure figures generated using PyMOL software.

2.9 Protein-FMN Interaction Studies

2.9.1 UV-Visible Spectroscopy

UV-Visible spectra of oxidised cytochrome protein samples was collected across a 350 to 700 nm wavelength range using a Hitachi U-3310 benchtop spectrometer. Spectra of buffer without protein addition was obtained and used to baseline all protein measurements. Where mentioned, protein concentration of cytochromes calculated from 410 nm soret peak using an ε_{410} of 1260 $mM^{-1}cm^{-1}$.

To obtain reduced protein samples, 0.5 µM additions of sodium dithionite were added to protein samples under anaerobic conditions within a MBraun Unilab glove box with O_2 maintained below 2 ppm. After each addition UV-vis spectra was recorded using a Jenway 7315 spectrometer, within the glovebox, prior to further addition until full reduction of heme peak (410 nm) was observed).

2.9.2 Quenching of Fluorescence Signal Upon Addition of FMN

Samples of 0.5 µM MtrC and $MtrC_{C453A}$-MtrAB were transferred to a reduced volume fluorescence cuvette prior to their fluorescence spectra being recorded with excitation held at 365 nm and emission spectra being recorded over 400-700 nm (Varian Carry Eclipse Florescence spectrometer). Fluorescence spectrometer was first blanked against darkness and resultant spectra for protein samples were normalised against spectra of protein buffers (20 mM HEPES pH 7.5 for MtrC sample, 20 mM HEPES pH 7.5 with 5 mM LDAO for $MtrC_{C453A}$-MtrAB sample). FMN was added to protein samples to give a final concentration of 0.5 µM with fluorescence spectra then immediately recorded again. Sample mixtures were incubated for 10 min at room temperature before a further fluorescence spectra was recorded allowing for observation of quenching (via comparison of distinct FMN fluorescence peak at ~510 nm).

For investigation of FMN binding to $MtrC_{C453A}$ (soluble form protein), buffer consisting of 20 mM HEPES pH 7.5 was prepared in a reduced volume fluorescence cuvette. Spectrometer blanked as before with excitation set to 365 nm with emission this time being recorded only at 510 nm. Fluorescence of buffer recorded before addition of FMN to give final concentration of 0.2 µM at which time a further recording was taken. FMN continued to be added in 0.2 µM increments with fluorescence readings taken after each addition until a FMN concentration of 1.8 µM had been reached. This process was repeated with fresh buffer with the addition of 0.5 µM MtrC before again repeating with 0.5 µM $MtrC_{C453A}$ added to the buffer. Intensity of fluorescence was plotted against FMN concentration to instigate any quenching of FMN fluorescence, upon addition, due to interactions with the protein samples.

2.9.3 Size Exclusion Column Separation of FMN and Protein

Aerobic FMN-protein interaction studies were carried out by incubating samples of 0.5 μM MtrC or $MtrC_{C453A}$-MtrAB (buffered in 20 mM HEPES pH 7.5 or 20 mM HEPES pH 7.5 with 5 mM LDAO respectively) with 0.5 μM FMN for 30 min at room temperature with samples kept in the dark. Sample mixtures were then eluted through PD10 size exclusion columns equilibrated with 20 mM HEPES pH 7.5, collecting 1 ml fractions. Fractions containing protein sample were identified and quantified through UV-vis spectroscopy to highlight indicative heme soret peak at 410 nm and using an ε_{410} of 1260 $mM^{-1}cm^{-1}$. These fractions then underwent fluorescence spectroscopy with excitation held at 365 nm and emission spectra being recorded over 400-700 nm (Varian Carry Eclipse Florescence spectrometer). Spectrometer was blanked against darkness and resultant spectra were normalised to protein concentration and buffer background. Resultant fluorescence spectra were analysed for indicative FMN fluorescence signal at 510 nm as seen in FMN positive control.

Anaerobic FMN-protein interaction studies were carried out within a MBraun Unilab glovebox, with O_2 maintained below 2 ppm, by incubating samples of 0.5 μM MtrC or $MtrC_{C453A}$ (buffered in 20 mM HEPES pH 7.5) with 0.5 μM FMN for 30 min at room temperature with samples kept in the dark. Sample mixtures were then eluted through PD10 size exclusion columns equilibrated with 20 mM HEPES pH 7.5, collecting 1 ml fractions. Fractions were removed from glovebox with those containing protein sample were identified and quantified through UV-vis spectroscopy to highlight indicative heme soret peak at 410 nm and using an ε_{410} of 1260 $mM^{-1}cm^{-1}$. These fractions then underwent fluorescence spectroscopy with excitation held at 365 nm and emission spectra being recorded over 400-700 nm (Varian Carry Eclipse Florescence spectrometer). Spectrometer was blanked against darkness and resultant spectra were normalised to protein concentration. This process was repeated for protein samples with the addition of either 1 mM DTT or 50 μM sodium dithionite (dependant on experiment). Resultant fluorescence spectra were analysed for indicative FMN fluorescence signal at 510 nm (Edwards *et al.*, 2015).

To qualitatively assess strength of FMN-protein interaction, samples showing evidence of interaction after anaerobic PD10 size exclusion column elution were again eluted through a PD10 size exclusion column, this time under aerobic conditions. 1 ml fractions were collected with protein containing fractions being identified through UV-vis spectroscopy prior to undergoing fluorescence spectroscopy with excitation held at 365 nm and emission spectra being recorded over 400-700 nm (Varian Carry Eclipse Florescence spectrometer). Resultant fluorescence spectra were again analysed for indicative FMN fluorescence signal at 510 nm after normalising to protein concentration.

2.10 References

Burnette, W. N. (1981) '"Western blotting": electrophoretic transfer of proteins from sodium dodecyl sulfate-polyacrylamide gels to unmodified nitrocellulose and radiographic detection with antibody and radioiodinated protein A', *Analytical biochemistry*. Elsevier, 112(2), pp. 195–203.

Dagert, M. and Ehrlich, S. D. (1979) 'Prolonged incubation in calcium chloride improves the competence of Escherichia coli cells', *Gene*. Elsevier, 6(1), pp. 23–28.

Edwards, M. J., White, G. F., Norman, M., Tome-Fernandez, A., Ainsworth, E., Shi, L., Fredrickson, J. K., Zachara, J. M., Butt, J. N., Richardson, D. J. and Clarke, T. a. (2015) 'Redox Linked Flavin Sites in Extracellular Decaheme Proteins Involved in Microbe-Mineral Electron Transfer.', *Scientific Reports*. Nature Publishing Group, 5(July), p. 11677. doi: 10.1038/srep11677.

Evans, P. R. (2011) 'An introduction to data reduction: space-group determination, scaling and intensity statistics', *Acta Crystallographica Section D: Biological Crystallography*. International Union of Crystallography, 67(4), pp. 282–292.

Gilbert, T. W., Behymer, T. D. and Castaneda, H. B. (1982) 'Determination of dissolved-oxygen in natural and wastewaters', *American Laboratory*. INT SCIENTIFIC COMMUN INC PO BOX 870, 30 CONTROLS DRIVE, SHELTON, CT 06484-0870, 14(3), p. 119.

Guzman, L.-M., Belin, D., Carson, M. J. and Beckwith, J. O. N. (1995) 'Tight regulation, modulation, and high-level expression by vectors containing the arabinose PBAD promoter.', *Journal of bacteriology*. Am Soc Microbiol, 177(14), pp. 4121–4130.

Laemmli, U. K. (1970) 'Cleavage of structural proteins during the assembly of the head of bacteriophage T4', *nature*. Springer, 227(5259), pp. 680–685.

Leslie, A. G. W. and Powell, H. R. (2007) 'Processing diffraction data with MOSFLM', *Evolving methods for macromolecular crystallography*. Springer, 245, pp. 41–51.

McCoy, A. J. (2007) 'Solving structures of protein complexes by molecular replacement with Phaser', *Acta Crystallographica Section D: Biological Crystallography*. International Union of Crystallography, 63(1), pp. 32–41.

Shi, L., Lin, J. T., Markillie, L. M., Squier, T. C. and Hooker, B. S. (2005) 'Overexpression of multi-heme C-type cytochromes', *BioTechniques*, 38(2), pp. 297–299. doi: 10.2144/05382PT01.

Viollier, E., Inglett, P. W., Hunter, K., Roychoudhury, A. N. and Van Cappellen, P. (2000) 'The ferrozine method revisited: Fe (II)/Fe (III) determination in natural waters', *Applied geochemistry*. Elsevier, 15(6), pp. 785–790.

Chapter 3

Effect of Disulphide Bond in MtrC on *S. oneidensis* Growth

3.1 Introduction

An interesting structural feature of MtrC is the conserved disulphide bond found in domain 3 of the protein (Edwards *et al.*, 2015). Although MtrC sequence homology varies between species of *Shewanella* there are a number of features that remain highly conserved throughout the genus. The ten CXXCH heme binding motifs remain conserved as well as a disulphide bond in domain III of the protein. There is another disulphide bond found in domain I, however, this is less conserved (Figure 3.1). Such high levels of conservation imply an evolutionary pressure to maintain this disulphide bond within domain III. It is worth noting MtrC itself is only conserved within the *Shewanella* genus. Other mineral reducing bacteria have evolved separate systems, as described earlier, some of which also function via cytochromes. Further investigation into these other extracellular electron transport pathways may highlight similar structural features as the disulphide bonds in MtrC.

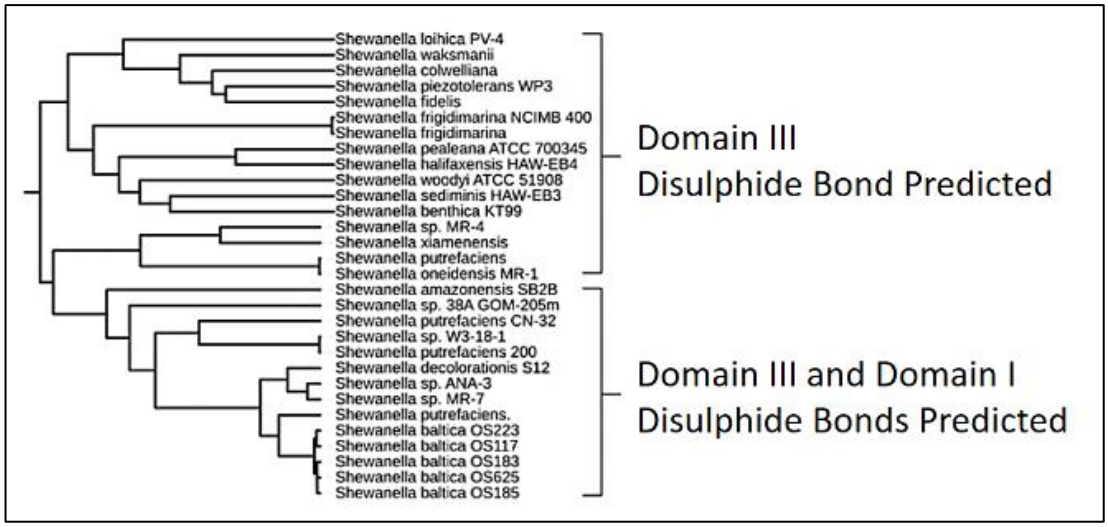

Figure 3.1 – Phylogenetic alignment of MtrC amino acid sequences from different *Shewanella* species. When comparing sequence homology between species, two groups can be observed. One group shows only a single predicted disulphide bond in domain III of MtrC, the other shows this same disulphide in domain III but also an additional disulphide bond in domain I of MtrC. Figure adapted from (Edwards *et al.*, 2015).

This chapter seeks to investigate this relationship between the oxidation state of the disulphide bond in domain III of the MtrC protein and electron transfer mechanisms linking respiration to extracellular terminal electron acceptors. In this chapter we compare three mutant forms of MtrC to native MtrC, all expressed in *S. oneidensis ΔmtrC* (LS661) - generated and supplied by Dr Liang Shi, PNNL. This strain has had the genomic copy of *mtrC* knocked out allowing for clear attribution of growth effects to the pBAD expressed *mtrC* constructs. Two of the mutants were single cysteine substitutions; one having the cysteine at position 444 substituted to alanine (*S. oneidensis ΔmtrC* pC444A), the other having the cysteine at position 453 substituted to alanine (*S. oneidensis ΔmtrC* pC453A). The third mutant is a double cysteine substitution, with both cysteine residues, at positions 444 and 453, mutated to alanine residues (*S. oneidensis ΔmtrC* pC444A,C453A). These and wild type *mtrC* (*S. oneidensis ΔmtrC* pMtrC) were made in a pBAD vector allowing for controlled expression via induction with arabinose.

By generating these mutant constructs on arabinose inducible plasmids, it enabled controlled investigation into the effect of removing the disulphide bond on the bacteria's ability to survive and grow in a range of growth conditions. Comparisons could be drawn between the native MtrC and the mutant forms, with expression in all situations controlled via arabinose inducible plasmids. This analysis was impossible using chemical reduction of the disulphide without limiting the growth conditions or introducing chemicals possibly affecting bacterial growth themselves. The directed mutagenesis approach here should allow a greater understanding of the role the 'switch like' disulphide plays in extracellular electron transfer.

3.2 Results

3.2.1 Strain Generation

Arabinose inducible plasmids containing genes for the expression of MtrC and MtrC mutant constructs were generated as described in Materials and Methods section 2.2 and confirmed via nucleotide sequencing (Figure 3.2). These were pMtrC (containing the wild type *mtrC* gene), pC444A (containing *mtrC* mutated to result in the substitution of the cysteine at amino acid position 444 to alanine), pC453A (containing *mtrC* mutated to result in the substitution of the cysteine at amino acid position 453 to alanine), and pC444A,C453A (containing *mtrC* mutated to result in the substitution of the cysteines at amino acid positions 444 and 453 to alanine residues).

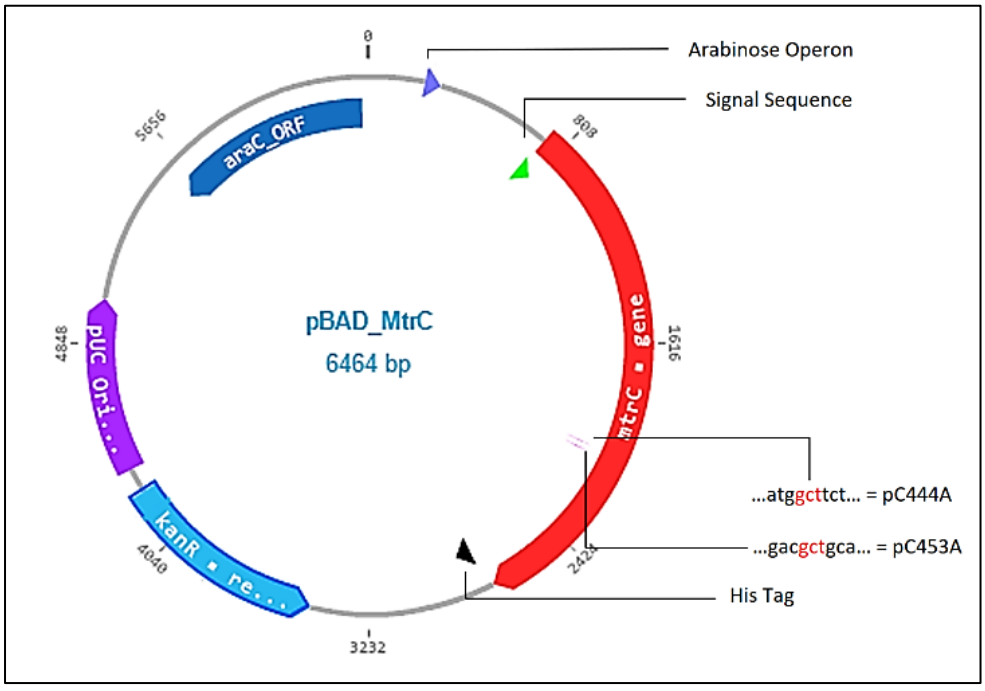

Figure 3.2 – Plasmid map of pBAD_MtrC. Point mutation highlighted for generation of pC444A and pC453A, bases modified from wild type sequence shown in red. Both point mutations were made for generation of pC444A,C453A. Other elements of importance highlighted including arabinose control operon and MtrC C-terminal His tag.

These plasmids, containing *mtrC*, or cysteine substituted mutant variants, were then transformed into *E. coli* 803 before being conjugated into the chosen expression strain, *S. oneidensis ΔmtrC* (LS661), as per Materials and Methods section 2.2.5. Resultant strains: *S. oneidensis ΔmtrC* pMtrC, *S. oneidensis ΔmtrC* pC444A, *S. oneidensis ΔmtrC* pC453A, and *S. oneidensis ΔmtrC* pC444A,C453A were grown under aerobic and anaerobic conditions with results described below.

3.2.2 Growth Profiling

S. oneidensis ΔmtrC pMtrC, *S. oneidensis ΔmtrC* pC444A, *S. oneidensis ΔmtrC* pC453A, and *S. oneidensis ΔmtrC* pC444A,C453A were grown anaerobically in LB media supplemented with 50 mM sodium fumarate as an electron acceptor (Chapter 2.3.1). Each strain was grown either in the absence of arabinose (leading to no expression of plasmid *mtrC* or mutant variants), in the presence of 5 mM arabinose or in the presence of 10 mM arabinose. The last two conditions induced expression of the *mtrC* or mutant variant genes with the higher concentration of arabinose leading to higher levels of expression. Cell optical density was recorded by measuring OD_{600} allowing growth rates of each strain to be measured. The growth profiles showed little difference between the strains or between different arabinose concentrations suggesting expression of *mtrC* or mutant variants did not impair growth, under anaerobic conditions with fumarate as an electron acceptor (Figure 3.3).

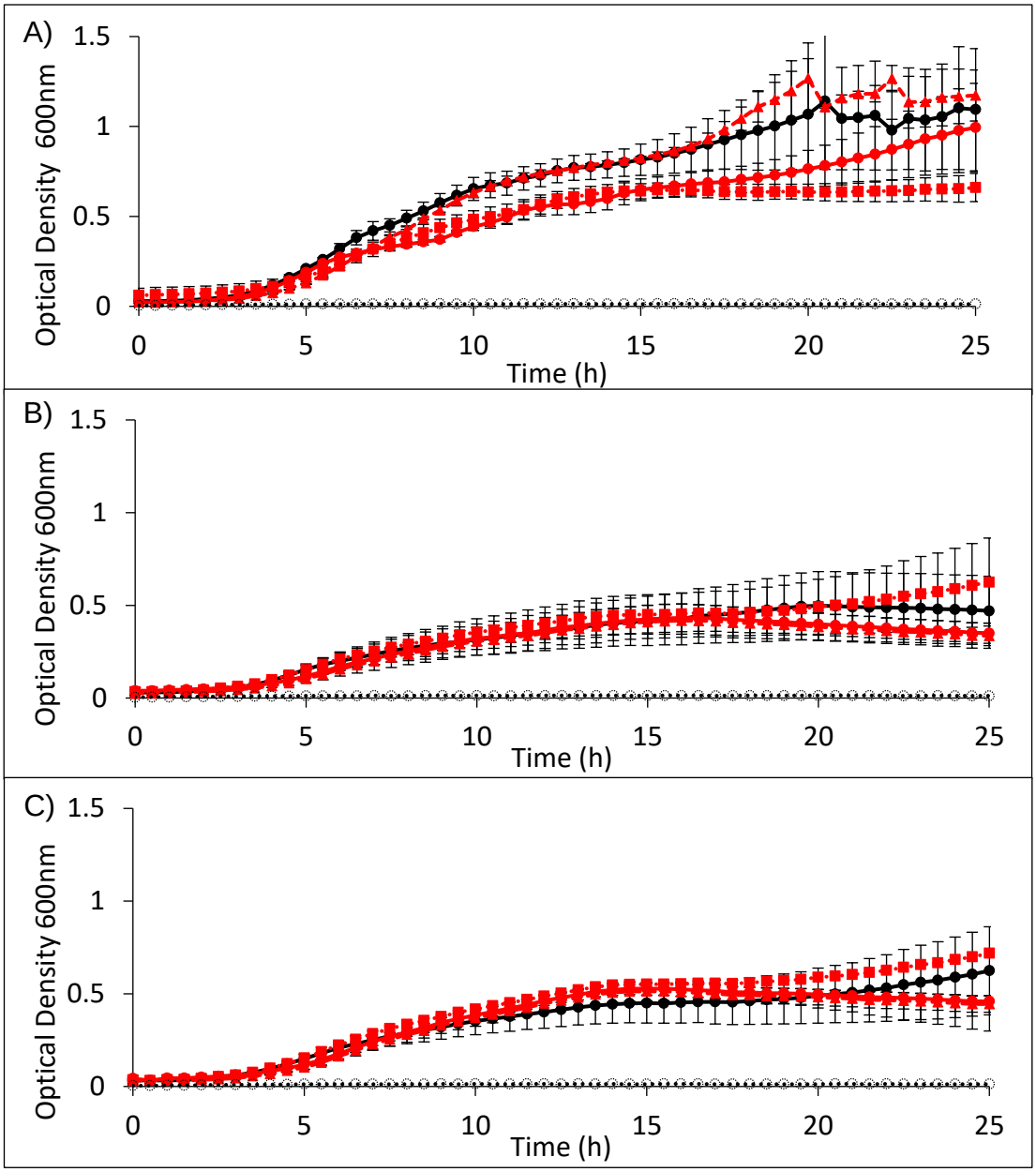

Figure 3.3 – Anaerobic growth profiles derived from optical density at 600 nm of *S. oneidensis ΔmtrC* pMtrC (black solid, circle), *S. oneidensis ΔmtrC* pC444A (red dashed, triangle), *S. oneidensis ΔmtrC* p453A (red solid, circle), *S. oneidensis ΔmtrC* pC444A,C453A (red dotted, square) and anaerobic control lacking fumarate (black dotted, open circle) cells expressing *mtrC* mutant constructs. Cultures induced at time point 0 h with A) 0 mM arabinose, B) 5 mM arabinose, C) 10 mM arabinose. All strains grown in LB supplemented with 50 µg/ml of kanamycin and 50 mM sodium fumarate at 30 ^{O}C.

Growth was again compared between *S. oneidensis ΔmtrC* pMtrC, *S. oneidensis ΔmtrC* pC444A, *S. oneidensis ΔmtrC* pC453A, and *S. oneidensis ΔmtrC* pC444A,C453A, this time under aerobic conditions (Chapter 2.3.1). Under these conditions, when expression was induced with arabinose, growth was seen to be impaired in *S. oneidensis ΔmtrC* pC444A, *S. oneidensis ΔmtrC* pC453A, and *S. oneidensis ΔmtrC* pC444A,C453A (compared to *S. oneidensis ΔmtrC* pMtrC). The mutant *mtrC* expressing cells appeared to display an extended lag phase taking more time to achieve exponential growth, with a greater effect seen in the presence of higher arabinose concentrations (Figure 3.4). Approximately a 15 h delay was observed between *S. oneidensis ΔmtrC* pMtrC and *S. oneidensis ΔmtrC* pC453A reaching similar OD_{600} values when 10 mM arabinose was present in the growth media (Figure 3.4 Panel C). *S. oneidensis ΔmtrC* pMtrC exhibited a wild type growth profile (data not shown) under all conditions whereas there was differences in the extent of extension of lag phase between the different mutant *mtrC* variant expressing cultures.

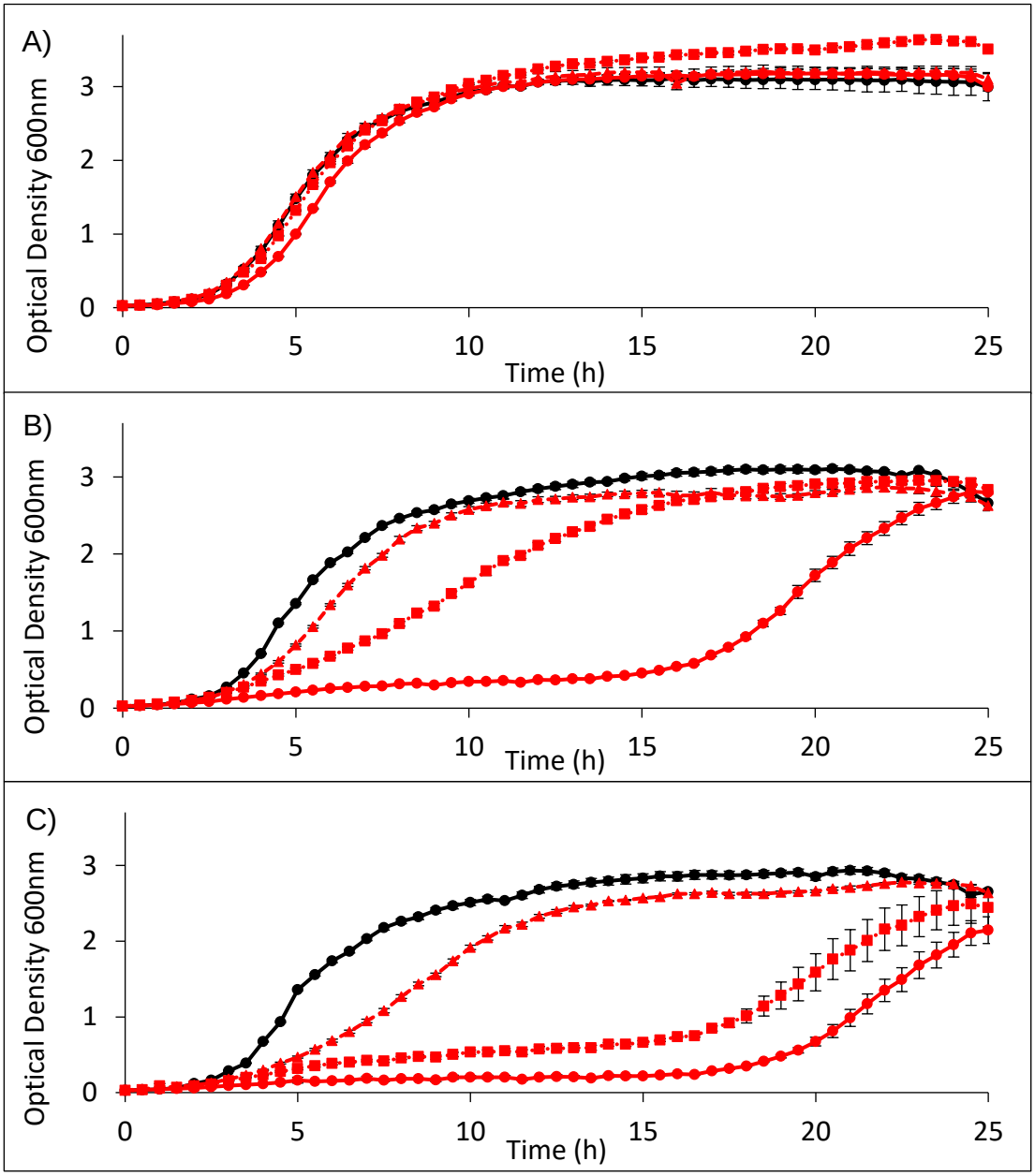

Figure 3.4 – Aerobic growth profiles derived from optical density at 600 nm of *S. oneidensis ΔmtrC* pMtrC (black, circle), *S. oneidensis ΔmtrC* pC444A (red dashed, triangle), *S. oneidensis ΔmtrC* p453A (red solid, circle), and *S. oneidensis ΔmtrC* pC444A,C453A (red dotted, square) cells expressing *mtrC* mutant constructs. Cultures induced at time point 0 h with A) 0 mM arabinose, B) 5 mM arabinose, C) 10 mM arabinose. All strains grown in LB supplemented with 50 µg/ml of kanamycin at 30 ^{O}C, shaking at 400 rpm. Standard error bars obtained from three repeats.

To further analyse the growth profiles of *S. oneidensis ΔmtrC* pMtrC, *S. oneidensis ΔmtrC* pC444A, *S. oneidensis ΔmtrC* pC453A, and *S. oneidensis ΔmtrC* pC444A,C453A, the data was plotted on a semi log plot. This allowed features of data to be highlighted with small differences being emphasised. The OD_{600} values at each time point were logged and plotted against time for both the anaerobic growth profiles (Figure 3.3) and the aerobic growth profiles (Figure 3.4). Again, little difference between the strains could be seen when growing anaerobically (Figure 3.5). The extended lag phase was again observed in S*. oneidensis ΔmtrC* pC444A, *S. oneidensis ΔmtrC* pC453A, and *S. oneidensis ΔmtrC* pC444A,C453A strains growing aerobically with arabinose inducer present. Further to this, the growth of the affected strains appeared to be similar to *S. oneidensis ΔmtrC* pMtrC at the start of growth until around the 5 h time point (Figure 3.6). This potentially suggests an accumulation of a growth inhibiting substance by this time. After this point growth was slowed for approximately 12 h at which time cultures were seen to resume exponential growth.

To confirm the extended lag phase was caused by expression of mutant *mtrC* variants from the pBAD vector, *S. oneidensis ΔmtrC* pMtrC and *S. oneidensis ΔmtrC* pC453A were grown aerobically in LB at 30 ^{O}C with growth at OD_{600} measured and induced with 5 mM arabinose when OD_{600} reached ~0.4. In this experiment, 2 % glucose (weight/volume) was also added to the cultures, either at the point of induction or 2 h after induction, to repress the expression of the proteins on the pBAD vector (Chapter 2.3.3) (Guzman *et al.*, 1995). When glucose was added at the same point as arabinose the extended lag phase previously seen in *S. oneidensis ΔmtrC* pC453A was not observed (Figure 3.7 Panel A). When glucose was added 2 h after induction, the extended lag phase was initially observed after induction but again growth was restored to that of *S. oneidensis ΔmtrC* pMtrC upon glucose addition (Figure 3.7 Panel B).

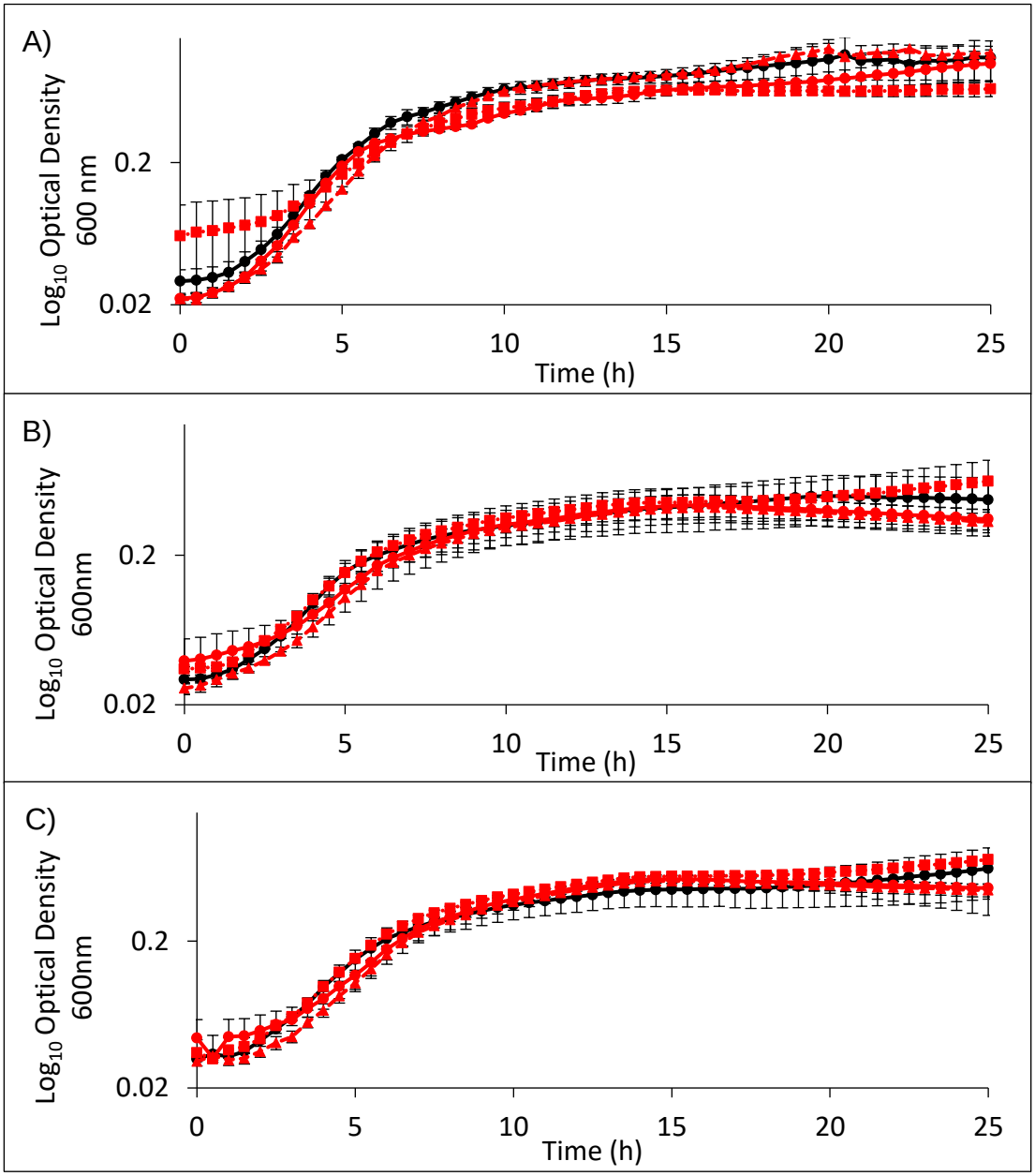

Figure 3.5 – Semi log_{10} plots generated from anaerobic growth profiles of *S. oneidensis ΔmtrC* pMtrC (black, circle), *S. oneidensis ΔmtrC* pC444A (red dashed, trianlge), *S. oneidensis ΔmtrC* p453A (red solid, circle), and *S. oneidensis ΔmtrC* pC444A,C453A (red dotted, square) cells expressing *mtrC* mutant constructs. Cultures induced at time point 0 h with A) 0 mM arabinose, B) 5 mM arabinose, C) 10 mM arabinose. All strains grown in LB supplemented with 50 µg/ml of kanamycin and 50 mM sodium fumarate at 30 ^{O}C. Standard error bars obtained from three repeats.

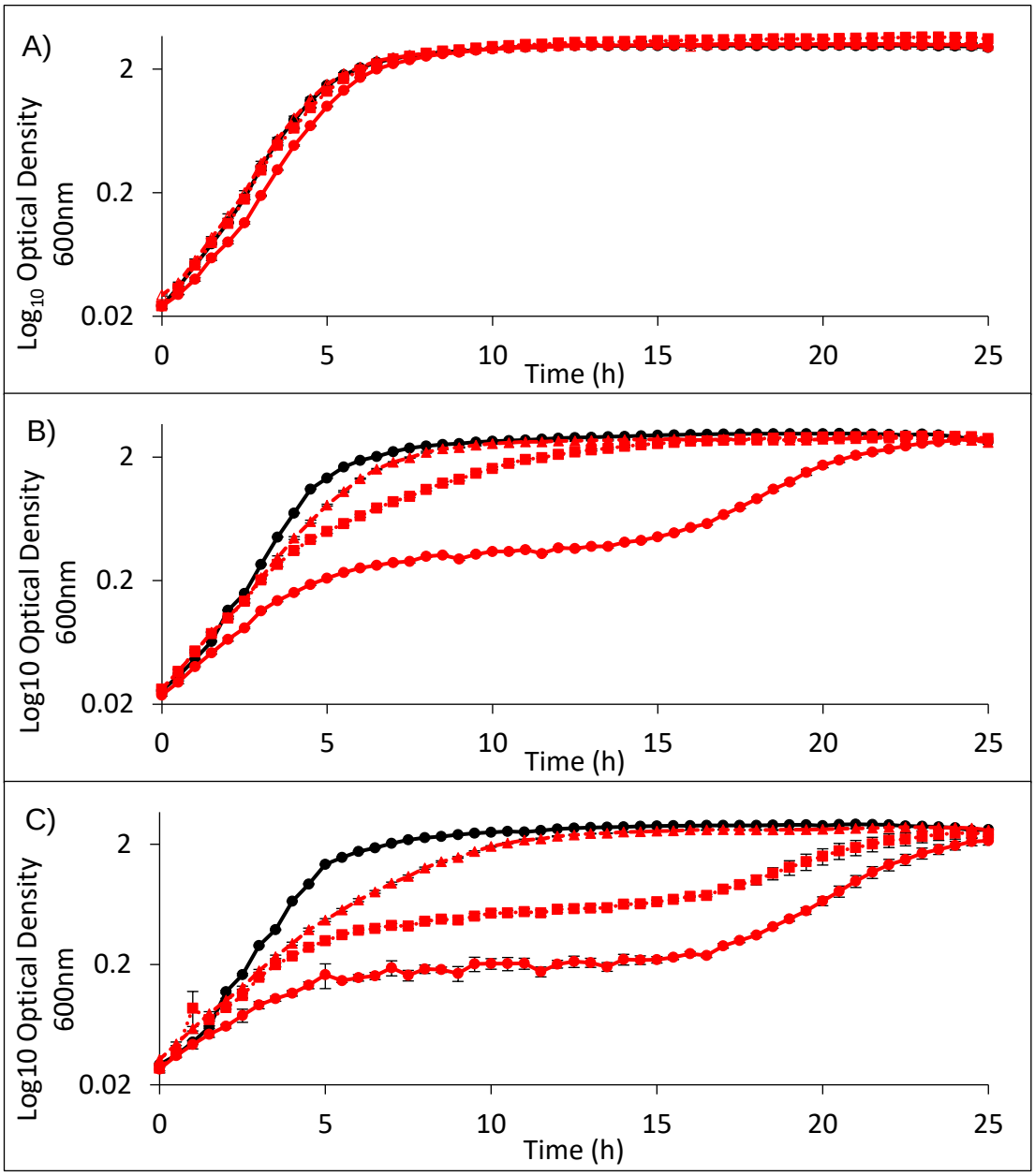

Figure 3.6 – Semi log_{10} plots generated from aerobic growth profiles of *S. oneidensis ΔmtrC* pMtrC (black, circle), *S. oneidensis ΔmtrC* pC444A (red dashed, triangle), *S. oneidensis ΔmtrC* p453A (red solid, circle), and *S. oneidensis ΔmtrC* pC444A,C453A (red dotted, square) cells expressing *mtrC* mutant constructs. Cultures induced at time point 0 h with A) 0 mM arabinose, B) 5 mM arabinose, C) 10 mM arabinose. All strains grown in LB supplemented with 50 µg/ml of kanamycin at 30 ^{O}C, shaking at 400 rpm.

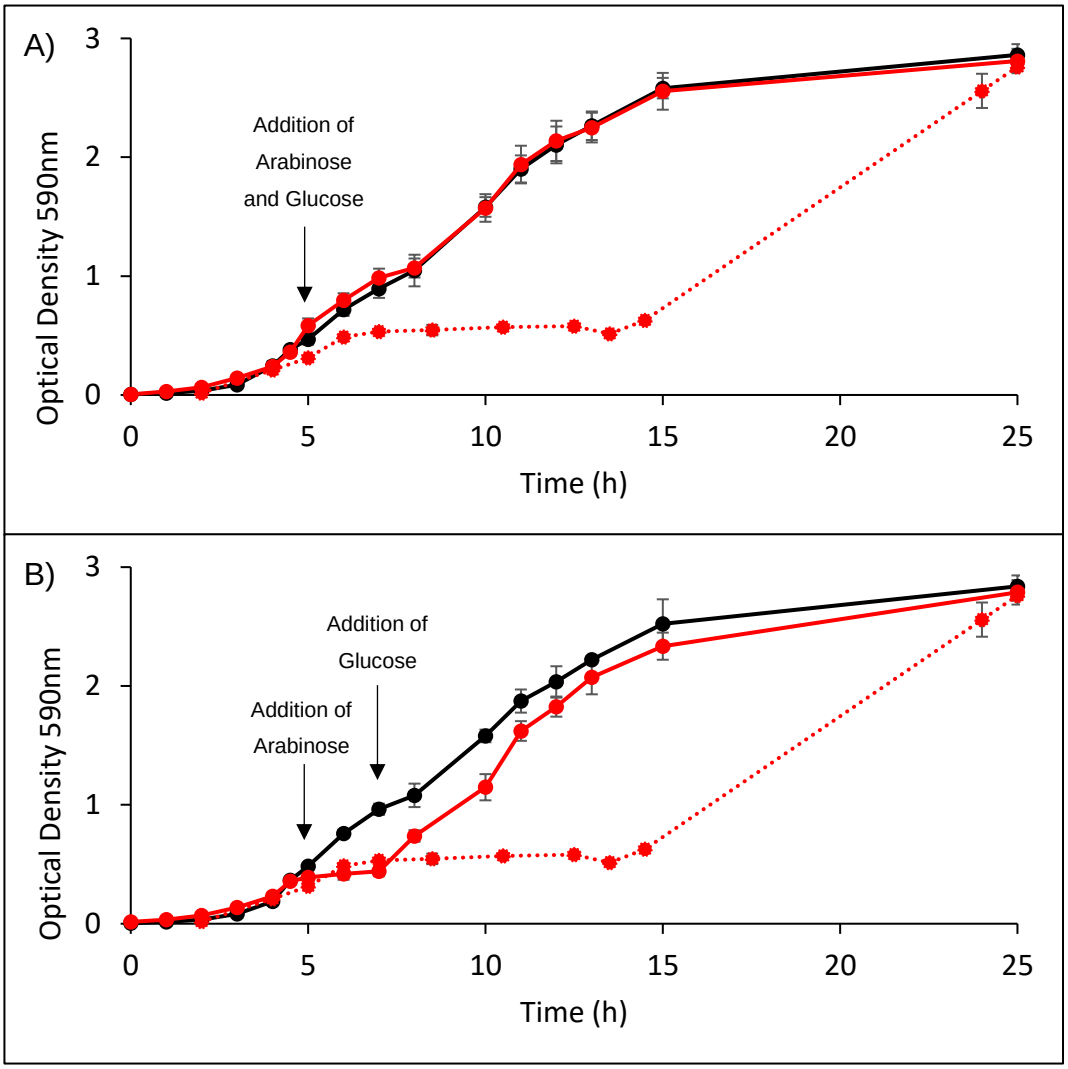

Figure 3.7 - Aerobic growth profiles derived from optical density at 600 nm of *S. oneidensis ΔmtrC* pMtrC (black) and *S. oneidensis ΔmtrC* pC453A (red) when induced with 5 mM arabinose and subsequent repression of expression via addition of 2 % glucose. *S. oneidensis ΔmtrC* pC453A when induced but no glucose added control (red dotted). A) Expression induced via addition of 5mM arabinose at time point 5 h with addition of 2 % glucose occurring simultaneously. B) Expression induced via addition of 5mM arabinose at time point 5 h with addition of 2 % glucose occurring 2 h later at time point 7 h. Additions to cultures indicated on growth profiles. All strains grown in LB supplemented with 50 µg/ml of kanamycin at 30 ^{O}C, shaking at 220 rpm. Standard error bars obtained from three repeats.

3.2.3 Arabinose Induced Expression of *mtrC* and *mtrC* Mutant Variants

To investigate the variations in the extended lag phase observed between *S. oneidensis ΔmtrC* pC444A, *S. oneidensis ΔmtrC* pC453A, and *S. oneidensis ΔmtrC* pC444A,C453A, protein expression levels were measured and compared to expression of native MtrC. Western blotting was used to measure expression of the MtrC protein in anaerobically grown LB cultures induced with 5 mM arabinose and supplemented with 20 mM sodium fumarate as an electron acceptor (Chapter 2.4).Cell fractionation allowed for the localisation of the protein to be ascertained with results indicating MtrC was expressed in all strains with the majority of the protein localising to the membrane fraction of the cell (Figure 3.8 Panel A).

Further study looked at MtrC expression in cultures grown anaerobically to an OD_{600} of ~0.4, expression was then induced using 5 mM arabinose and the culture was made aerobic by removing airtight seals and shaking at 220 rpm for a further 5 h. Of these strains only samples of *S. oneidensis* MR-1, *S. oneidensis ΔmtrC* pMtrC and *S. oneidensis ΔmtrC* pC453A displayed MtrC expression (Figure 3.8 Panel B). Both *S. oneidensis ΔmtrC* pC444A and *S. oneidensis ΔmtrC* pC444A,C453A showed a loss of MtrC expression, although this is difficult to observe due to background coloration in image. This loss of expression is likely due to protein degradation, repression of plasmid expression or a combination of both.

To further investigate the loss of protein expression observed in *S. oneidensis ΔmtrC* pC444A and *S. oneidensis ΔmtrC* pC444A,C453A, cultures were again grown anaerobically, using 20 mM arabinose as an electron acceptor, until an OD_{600} of ~0.4 was achieved. At this point cultures were induced with 5 mM arabinose and again turned aerobic however in this study aerobic conditions were only maintained for 1 h prior to cell harvesting (shorter than the previous 5 h aerobic incubation). Samples of *S. oneidensis ΔmtrC* pMtrC, *S. oneidensis ΔmtrC* pC444A, *S. oneidensis ΔmtrC* pC453A and *S. oneidensis ΔmtrC* pC444A,C453A were run on an SDS polyacrylamide gel and heme stained (Chapter 2.1.4). The resulting MtrC protein bands were compared and quantified relative to pMtrC expression (Figure 3.9).

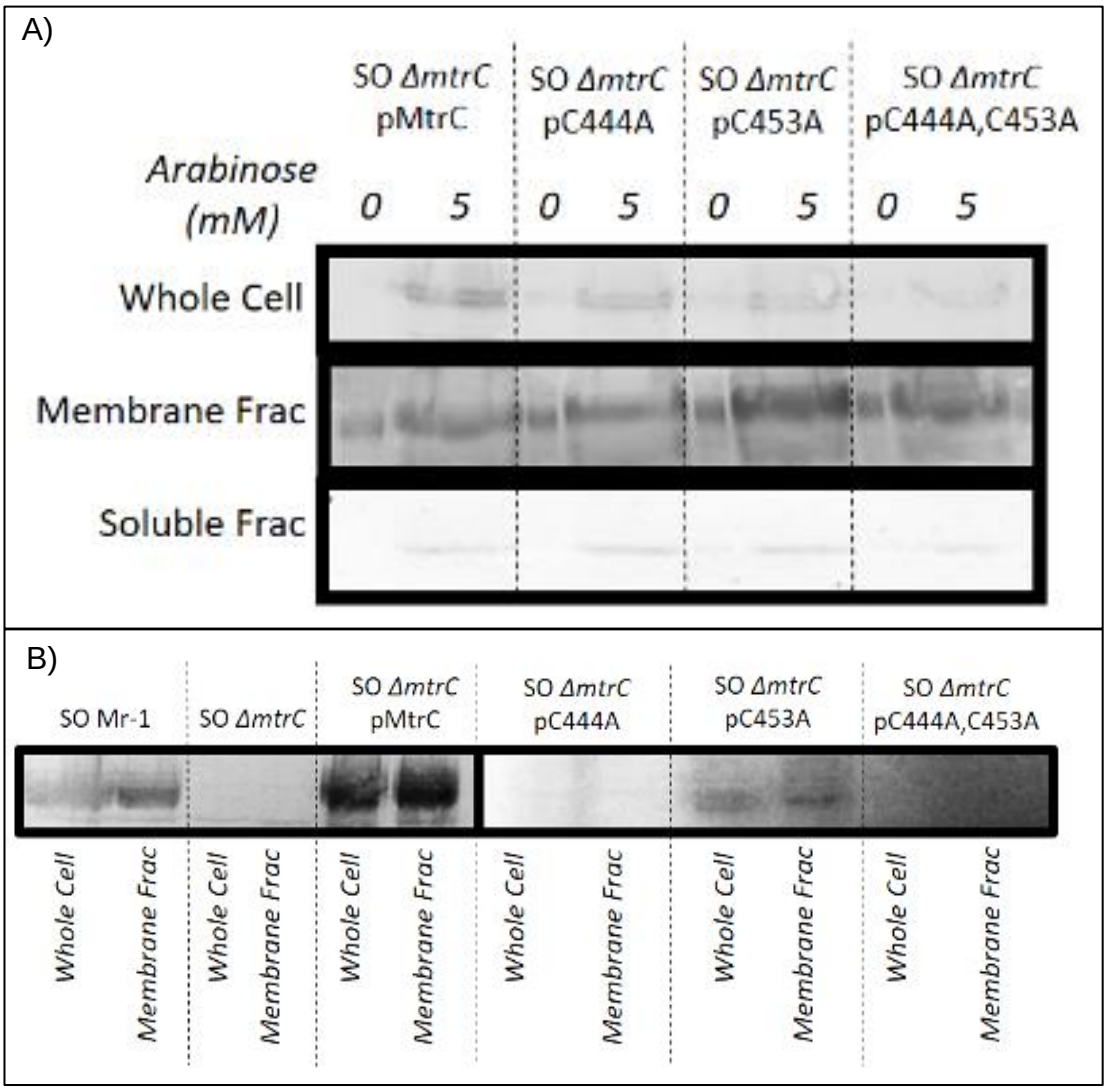

Figure 3.8 – Western blot images showing expression of MtrC in cell fractions (whole cell, membrane fraction, soluble fraction) from anaerobically and aerobically grown cells. A) Anaerobically grown cells (using LB medium supplemented with 50 mM sodium fumarate) either uninduced (0 mM arabinose) or induced with 5 mM arabinose prior to cell fractionation. B) Cells grown anaerobically (in LB supplemented with 20 mM sodium fumarate) until OD_{600} of ~0.4 reached, at which point cells were induced with 5 mM arabinose before 5 h aerobic growth (shaking at 220 rpm). All MtrC bands were observed at 75 kDa. All growth incubations were at 30 ^{O}C.

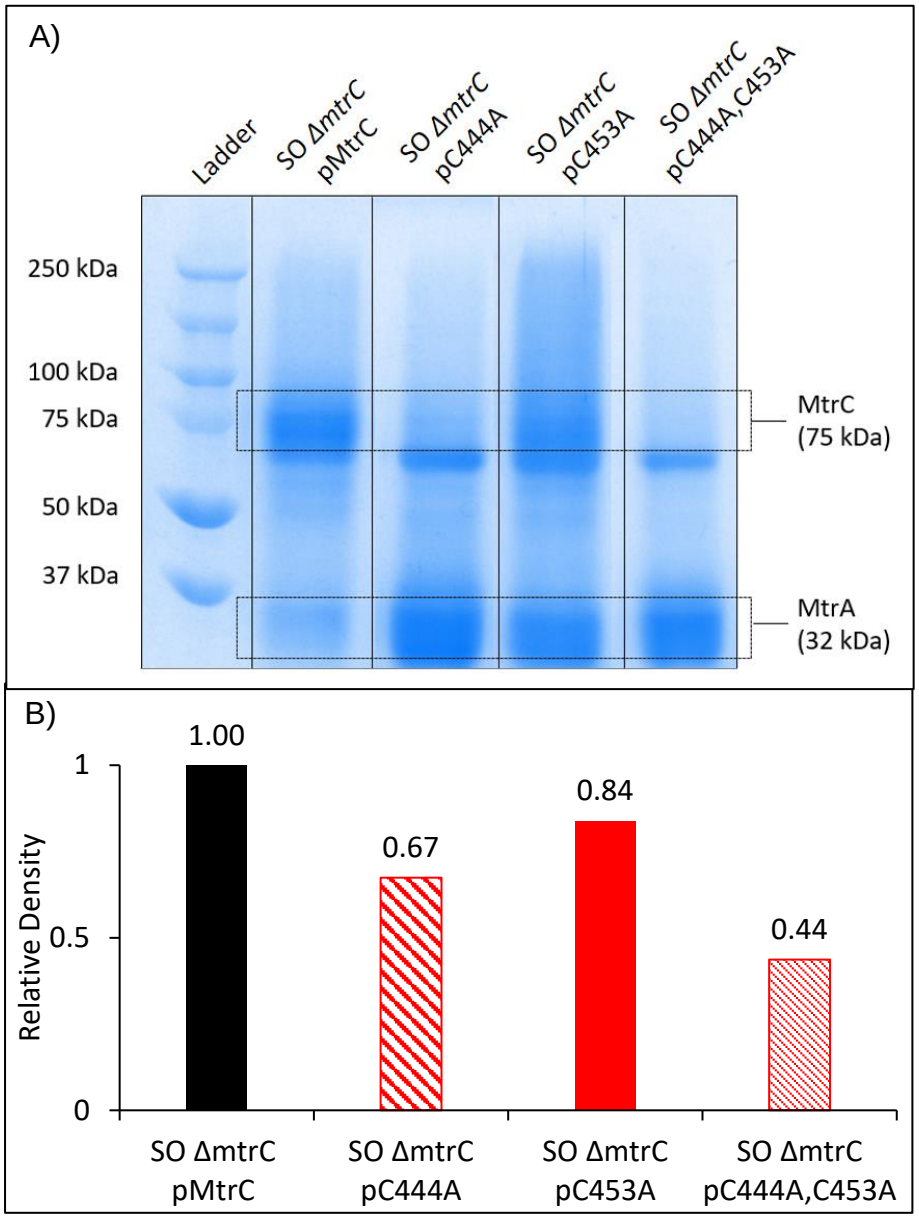

Figure 3.9 – A) Heme stained SDS polyacrylamide gel showing expression of *mtrC* constructs in cultures anaerobically grown to OD_{600} of ~0.4 prior to induction with 5 mM arabinose and 1 h aerobic growth. Cultures grown anaerobically in LB supplemented with 50 µg/ml of kanamycin and 20 mM sodium fumarate at 30 ^{O}C, when under aerobic growth conditions the cultures were put under 220 rpm shaking. B) MtrC Expression levels quantified by calculating the relative band intensities of the mutant MtrC proteins, as a percentage of the native MtrC band intensity (imageJ software used to ascertain pixel density of bands relative to background pixilation).

3.2.4 Physiological Functionality of Expressed MtrC

The ability of *S. oneidensis ΔmtrC* pMtrC, *S. oneidensis ΔmtrC* pC444A, *S. oneidensis ΔmtrC* pC453A, and *S. oneidensis ΔmtrC* pC444A,C453A to reduce ferric iron species was checked to ensure mutant MtrC variants were physiologically functional. The colorimetric ferrozine assay was used to observe the reduction of ferric iron (as a terminal electron acceptor) to soluble ferrous iron by bacterial cells expressing the different MtrC variants (as described in Chapter 2.5).

Initially iron(III) citrate was used as the ferric iron compound, however the negative control of *S. oneidensis* Δ*mtrC* was also able to reduce the ferric iron (Figure 3.10). This suggested iron(III) citrate was not a suitable source of ferric iron to be used as an extracellular terminal electron acceptor in this experiment. The observed iron(III) reduction was likely due to speciation of iron(III) citrate increasing the solubility and making it available to other cellular systems, effectively bypassing the need for MtrC and other OMCs, such as OmcA, capable of linking to the MtrAB pathway (Silva *et al.*, 2009).

Due to this observation, the experiment was repeated substituting iron(III) citrate with goethite as the ferric terminal electron acceptor. As before, cell cultures were grown anaerobically overnight in LB supplemented with 50 mM sodium fumarate and induced with 5 mM arabinose. These cultures were then pelleted and resuspended in 20 mM HEPES, normalising all samples to an OD_{600} of 1. After sparging with nitrogen, cells were added to anaerobic LB supplemented with 20 mM goethite and 5 mM arabinose. The ferrozine assay was then used to monitor iron reduction over time. *S. oneidensis* Δ*mtrC* was seen unable to reduce goethite whereas *S. oneidensis* MR-1 was able to. This suggested that MtrC was required for goethite reduction. *S. oneidensis ΔmtrC* pMtrC, *S. oneidensis ΔmtrC* pC444A, *S. oneidensis ΔmtrC* pC453A, and *S. oneidensis ΔmtrC* pC444A,C453A were also seen to reduce goethite (Figure 3.11). This showed native MtrC and the mutant variants expressed from the pBAD vector were functional and capable of reducing ferric iron.

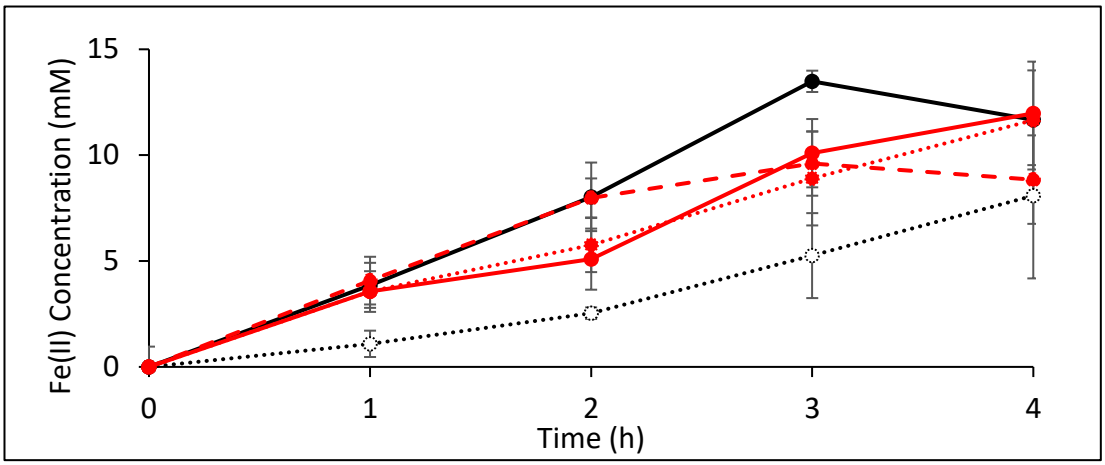

Figure 3.10 – Fe(III) citrate reduction to Fe(II) over time by cultures of *S. oneidensis ΔmtrC* (black dotted), *S. oneidensis ΔmtrC* pMtrC (black solid), *S. oneidensis ΔmtrC* pC444A (red dashed), *S. oneidensis ΔmtrC* pC453A (red solid), and *S. oneidensis ΔmtrC* pC444A,C453A (red dotted). 1.5 ml of resuspended anaerobically grown cultures, normalised to OD_{600} of 1 in 20 mM HEPES, were added to 20 ml LB supplemented with 20 mM Fe(III) citrate and 5 mM arabinose, incubated at 30 ^{O}C. Standard error bars obtained from three repeats.

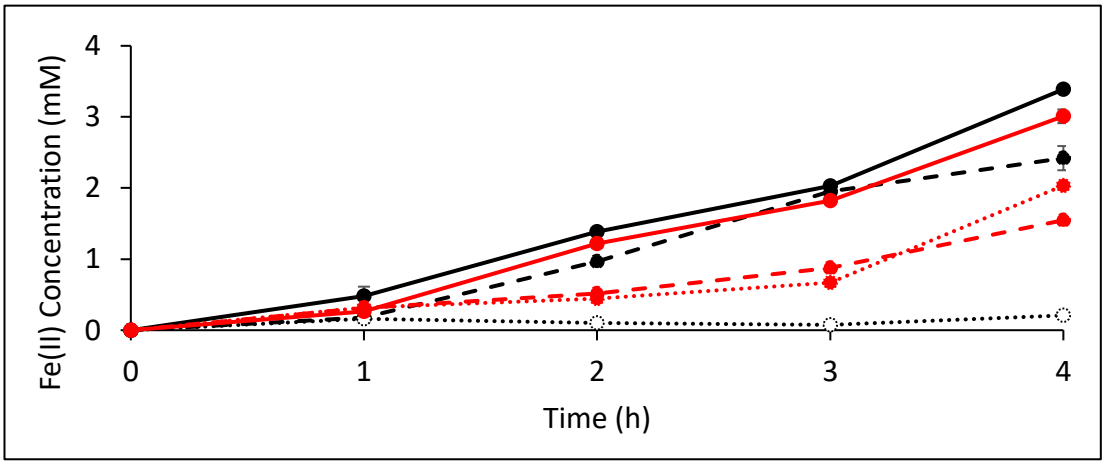

Figure 3.11 – Goethite reduction to Fe(II) over time by cultures of *S. oneidensis* MR-1 (black dashed), *S. oneidensis ΔmtrC* (black dotted), *S. oneidensis ΔmtrC* pMtrC (black solid), *S. oneidensis ΔmtrC* pC444A (red dashed), *S. oneidensis ΔmtrC* pC453A (red solid), and *S. oneidensis ΔmtrC* pC444A,C453A (red dotted). 1.5 ml of resuspended anaerobically grown cultures, normalised to OD_{600} of 1 in 20 mM HEPES, were added to 20 ml LB supplemented with 20 mM goethite and 5 mM arabinose, incubated at 30 ^{O}C shaking at 220 rpm in sealed containers. Standard error bars obtained from three repeats.

To confirm that the observed extracellular iron reduction was maintained over prolonged periods of time (supporting growth) ferrozine reagent was again used to monitor goethite reduction over time (Chapter 2.5.2). *S. oneidensis* MR-1, *S. oneidensis ΔmtrC*, *S. oneidensis ΔmtrC* pMtrC, *S. oneidensis ΔmtrC* pC444A, *S. oneidensis ΔmtrC* pC453A, and *S. oneidensis ΔmtrC* pC444A,C453A were used to inoculate LB supplemented with 20 mM goethite suspension and 5 mM arabinose to induce *mtrC* expression. Samples were taken regularly and underwent the ferrozine assay to monitor ferric iron reduction over time. *S. oneidensis ΔmtrC* was the only strain that did not display iron reduction. *S. oneidensis* MR-1, *S. oneidensis ΔmtrC* pMtrC, *S. oneidensis ΔmtrC* pC444A, *S. oneidensis ΔmtrC* pC453A, and *S. oneidensis ΔmtrC* pC444A,C453A all showed iron reduction after approximately 15 h with ferric iron reduction rising (Figure 3.12).

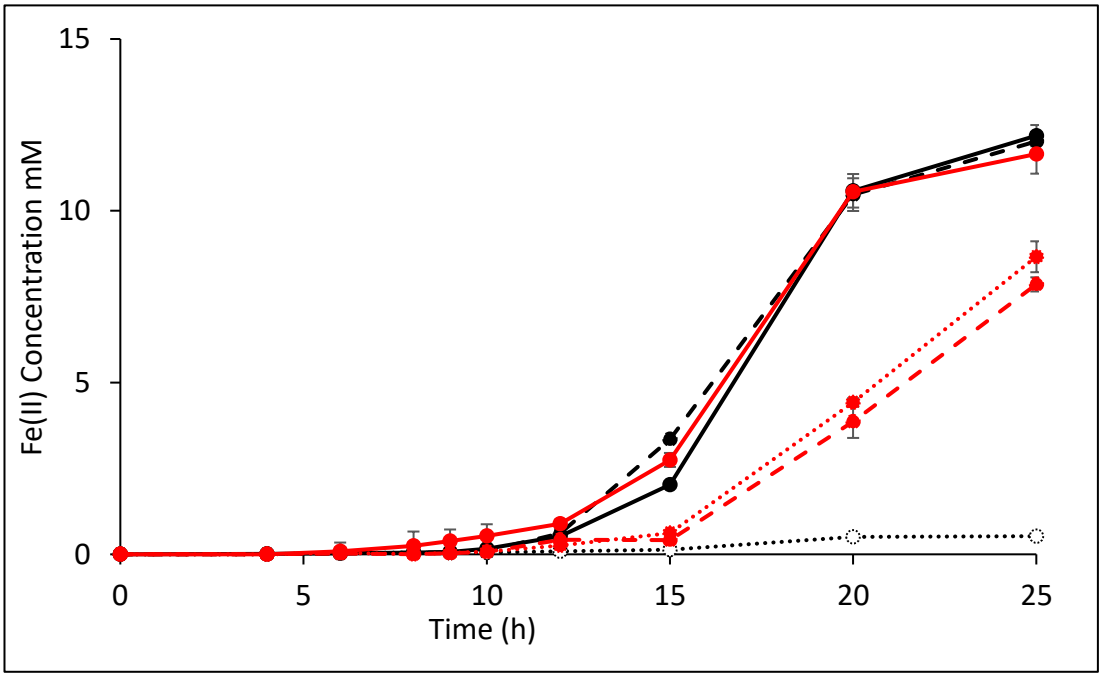

Figure 3.12 – Goethite reduction to Fe(II) over time in LB cultures supplemented with 20 mM goethite suspension and 5 mM arabinose inoculated with *S. oneidensis* MR-1 (black dashed), *S. oneidensis ΔmtrC* (black dotted), *S. oneidensis ΔmtrC* pMtrC (black solid), *S. oneidensis ΔmtrC* pC444A (red dashed), *S. oneidensis ΔmtrC* pC453A (red solid), and *S. oneidensis ΔmtrC* pC444A,C453A (red dotted). Cultures incubated at 30 ^{O}C shaking at 220 rpm. Standard error bars obtained from three repeats.

3.3 Discussion

3.3.1 Generation and Expression of *mtrC* Mutant Variants

Site directed mutations were made to pMtrC to introduce changes into the *mtrC* gene resulting in a substitution of the cysteine residues forming the disulphide bond in domain III of MtrC to alanine residues (Figure 3.2). The decision to substitute the cysteine residues with alanine residues was made in an attempt to minimise alterations in hydrophobicity of the residue. Serine is often used as a substitute for cysteine instead, owing to its similar size. However, as the disulphide bond (and by extension the cysteine residues) has previously linked with flavin binding, changes to hydrophobicity were deemed more likely to impair physiologically relevant flavin binding in this region of the protein due to potential conformational changes to binding pockets (Nelson, Lehninger and Cox, 2008). The study in question has shown that chemical reduction of the disulphide in domain III of native MtrC leads to FMN associating with MtrC. This binding is only observed whilst the disulphide bond remains reduced, when reoxidised the FMN is seen to disassociate from the protein. The implication from this is that breaking the disulphide bond potentially leads to conformational changes in the structure of MtrC and leads to increased accessibility to specific binding pockets (Edwards *et al.*, 2015).

These altered plasmids were then transformed into *S. oneidensis ΔmtrC* (LS661) and nucleotide sequencing was carried out to confirm *S. oneidensis ΔmtrC* pMtrC, *S. oneidensis ΔmtrC* pC444A, *S. oneidensis ΔmtrC* pC453A, and *S. oneidensis ΔmtrC* pC444A,C453A strains had been produced. All strains were seen to express *mtrC* variants when induced with 5 mM arabinose under anaerobic growth conditions (3.8 Panel A). However only *S. oneidensis ΔmtrC* pMtrC and *S. oneidensis ΔmtrC* pC453A were seen to express *mtrC* variants when induced with 5 mM arabinose under aerobic conditions (Figure 3.8 Panel B). Further investigation showed expression of *mtrC* variants in *S. oneidensis ΔmtrC* pC444A and *S. oneidensis ΔmtrC* pC444A,C453A was greatly diminished within 1 h when exposed to oxygen (Figure 3.9). Relative to *S. oneidensis ΔmtrC* pMtrC expression levels, MtrC variant expression was seen to

be 67 %, 88 % and 44 % (pC444A, pC453A and pC444A,C453A respectively). These findings suggested $MtrC_{C444A}$ and $MtrC_{C444A,C453A}$ was removed from bacterial cells through protein degradation or repression of plasmid expression. This difference in expression levels between *S. oneidensis ΔmtrC* pC444A, *S. oneidensis ΔmtrC* pC453A, and *S. oneidensis ΔmtrC* pC444A,C453A strains provided explanation for variations in observed phenotype. The differences in expression could be attributed to the cells recognising the conformation the protein takes when substitution of the cysteine residue at position 444, upon exposure to oxygen, more readily and degrading the mutated protein. This difference in cell recognition of the proteins would explain why the longer the aerobic incubation phase the greater the reduction in protein expression seen on the gel images. It is important to note that expression of native MtrC can be seen in *S. oneidensis* Mr-1 (the wild type control) where expression was not plasmid linked. This emphasises the relevance of the experiments carried out here as it shows expression is seen naturally under these conditions.

3.3.2 Ferric Iron Reduction in MtrC Variant Expressing Cells

Ferrozine assays were used to confirm expressed MtrC variants were physiologically functional and able to reduce ferric iron, as native MtrC has been reported to do (Hartshorne *et al.*, 2009). Cultures of *S. oneidensis ΔmtrC* pMtrC, *S. oneidensis ΔmtrC* pC444A, *S. oneidensis ΔmtrC* pC453A, and *S. oneidensis ΔmtrC* pC444A,C453A were grown (with expression induced) and pelleted before being resuspended and exposed to ferric iron. All strains were seen able to reduce iron(III) citrate, although *S. oneidensis ΔmtrC* was also seen able to reduce iron(III) citrate to some extent (Figure 3.10). This result suggested that MtrC was not essential for iron(III) citrate reduction and so was not an appropriate source of ferric iron for this experiment. The result is worth note as it suggests iron(III) citrate is able to interact with MtrAB and become reduced without the presence of MtrC or by diffusing into the cells in this soluble form where it is then reduced. Previous studies have shown replacing MtrB with its paralogues disrupts the cells ability to reduce iron(III) citrate unless replaced with MtrE (Coursolle and J. a. Gralnick, 2012). Taken with these findings it could be suggested that MtrB has some specificity for ferric compounds in

aspects of mineral reduction. The differences in iron reduction between the strains could be linked to the levels of protein expression. The rate of iron reduction is comparable to the extent of the growth phenotype described. The extent of this appears linked to the levels of protein seen in expression gels.

Due to the observation that *S. oneidensis ΔmtrC* was able to reduce iron(III) citrate, the experiment was repeated with goethite (FeO(OH)) as the ferric extracellular terminal electron acceptor. In this case, *S. oneidensis ΔmtrC* was unable to reduce the goethite whilst *S. oneidensis* MR-1, *S. oneidensis ΔmtrC* pMtrC, *S. oneidensis ΔmtrC* pC444A, *S. oneidensis ΔmtrC* pC453A, and *S. oneidensis ΔmtrC* pC444A,C453A were all seen able to reduce the goethite to ferrous iron (Figure 3.11). This result suggested the expressed MtrC variants were physiologically functional in regard to linking the respiratory pathway of *S. oneidensis* to an extracellular terminal electron acceptor even with the MtrAB proteins under natively controlled expression. Sustained ferric reduction was also shown through inoculation of LB supplemented with 20 mM goethite and 5 mM arabinose with *S. oneidensis ΔmtrC* pMtrC, *S. oneidensis ΔmtrC* pC444A, *S. oneidensis ΔmtrC* pC453A, and *S. oneidensis ΔmtrC* pC444A,C453A rather than resuspending relatively dense cell masses in ferric reducing conditions. Again all strains were seen capable of reducing goethite to ferrous iron with reduction rising exponentially possibly as a result of bacterial cell growth however this was not confirmed.

3.3.3 Growth Profiling

Cultures of *S. oneidensis ΔmtrC* pMtrC, *S. oneidensis ΔmtrC* pC444A, *S. oneidensis ΔmtrC* pC453A, and *S. oneidensis ΔmtrC* pC444A,C453A were under inducing conditions to investigate the effect of *mtrC* variants on bacterial growth. Growth curves were recorded under anaerobic conditions (Figure 3.3) and these showed that the strains expressing any one of the *mtrC* variants grew very similarly to wild type *mtrC* expressing *S. oneidensis ΔmtrC* pMtrC. Final OD_{600} values were lowered in cultures induced with arabinose likely due to the energy cost of protein expression.

However, when this growth study was repeated under aerobic conditions (Figure 3.3), an extended lag phase was be observed in the strains expressing the mutant variants of *mtrC*, compared to growth of *S. oneidensis ΔmtrC* pMtrC. As the phenotype was not present when the strains were grown under anaerobic conditions, it was unlikely due to the proteins themselves being toxic to the cells perhaps from the formation of inclusion bodies within the cells (Ramón, Señorale-Pose and Marín, 2014). Instead, as the phenotype was present only under aerobic conditions, a toxic effect of oxygen reacting with the mutant MtrC variants was implied. One potential explanation of this observation is reactive oxygen species (ROS) forming due to the proteins catalysing electrons reacting with oxygen. Formation of damaging ROS in the presence of iron is well characterised with Fenton chemistry being responsible for the generation of hydroxyl radicals from much less damaging peroxide molecule (Repine, Fox and Berger, 1981; Grossman and Kahan, 2016).

Cultures induced with higher concentrations of arabinose (10 mM compared to 5 mM) displayed a more persistent extended lag phase. This observation highlighted a link between the amount of MtrC variants present in the cultures and the severity of the growth defect. This proportionality between concentration of inducer and levels of expression had long been known and is the result of subpopulations within cultures not being induced due to a lack of inducer. Increasing the amount of arabinose leads to a greater availability and so a greater proportion of cells in the culture are induced and express the protein (Siegele and Hu, 1997). Part of this effect is due to the binding between inducer and operon being weaker than in other expression operons. This leads to a higher concentration of arabinose being needed to ensure binding and expression occurs more often. There were also differences in the extent of the extended lag phase when comparing *S. oneidensis ΔmtrC* pC444A, *S. oneidensis ΔmtrC* pC453A and *S. oneidensis ΔmtrC* pC444A,C453A. *S. oneidensis ΔmtrC* pC453A displayed the most extreme growth defect and this appears linked to the previously described variation in protein expression between the strains when growing aerobically (Figure 3.9).

Further analysis of growth profile data via semi log plots highlighted an interesting feature of the growth defect reported. Anaerobically grown cultures were still seen to grow with little variation between *S. oneidensis ΔmtrC* pMtrC, *S. oneidensis ΔmtrC* pC444A, *S. oneidensis ΔmtrC* pC453A, and *S. oneidensis ΔmtrC* pC444A,C453A cultures whether induced or not (Figure 3.5). However, analysis of aerobically grown cultures in this way allowed investigation into the onset of the extended lag phase phenotype. When comparing the growth (under inducing conditions) of between *S. oneidensis ΔmtrC* pMtrC, *S. oneidensis ΔmtrC* pC444A, *S. oneidensis ΔmtrC* pC453A, and *S. oneidensis ΔmtrC* pC444A,C453A bacterial growth appeared to be very similar between strains for the first few hours of growth (Figure 3.6). It was only later when OD_{600} had reached ~0.15 when growth of *S. oneidensis ΔmtrC* pC444A, *S. oneidensis ΔmtrC* pC453A, and *S. oneidensis ΔmtrC* pC444A,C453A was seen to slow. This delay in growth defect onset is likely due to cytochrome maturation pathways beginning to function at these OD_{600} values when oxygen starts to become more limited. Under these conditions, components of the Ccm system in *S. oneidensis* become upregulated leading to c-type cytochrome maturation (Jin *et al.*, 2013; Brockman, 2014).

The relevance of *mtrC* variant expression as the cause of the extended lag phase was confirmed by growing *S. oneidensis ΔmtrC* pMtrC and *S. oneidensis ΔmtrC* pC453A aerobically with 5 mM arabinose inducer added to cultures when OD_{600} reached ~0.4. In this experiment, glucose was also added to the growth cultures either simultaneously with the inducer (Figure 3.7 Panel A) or after 2 h aerobic growth following induction (Figure 3.7 Panel B). Glucose is known to repress pBAD expression and thus when added to the cultures, expression of pMtrC or pC453Awould halt (Guzman *et al.*, 1995). In both experiments, the addition of glucose was seen to remove the extended lag phase and allow growth of *S. oneidensis ΔmtrC* pC453A to be comparable to that of *S. oneidensis ΔmtrC* pMtrC. This confirmed the presence of MtrC variants was the cause for the extended lag phase observed in aerobically growing cultures.

It is worth noting that the extended lag phase does end in even the most affected cultures without the addition of glucose to repress expression. By time point 20 h exponential growth had resumed in *S. oneidensis ΔmtrC* pC453A suggesting the bacteria had adapted to overcome the cause of the growth defect (Figure 3. 4). Protein expression studies have shown that this is likely due to reduced levels of protein in the bacterial cells. As mentioned previously this may be the result of downregulation of the expression or protein degradation. In either case, the bacteria do not lose their kanamycin resistance that is encoded for on the pBAD plasmid. This suggests that the bacteria are not experiencing plasmid loss as a way to prevent expression of *mtrC* variants (Smith and Bidochka, 1998). Bacterial genomes have the potential for instability and genes are often incorporated into chromosomal DNA when a strong selective pressure, such as antibiotic resistance, is applied (Darmon and Leach, 2014). This could suggest that the kanamycin resistance gene is being incorporated allowing the removal of the plasmid without loss of resistance. However, it is also worth noting bacteria recultured from growth experiments appear to display similar growth defects when expression is again induced under aerobic conditions although thorough investigation of this observation was not undertaken.

3.4 Conclusion

Making site directed mutations to the *mtrC* gene resulting in the substitution of cysteine residues at amino acid positions 444 and 453 generated *mtrC* variants in which the disulphide bond in domain III was disrupted. The MtrC variants continue to be localised to the membrane in *S. oneidensis ΔmtrC* (LS661) when expressed on a pBAD arabinose inducible vector. Here we see that such alterations to the protein do not impair its function in ferric iron reduction when goethite is used as an extracellular terminal electron acceptor.

When growth of *S. oneidensis ΔmtrC* pMtrC, *S. oneidensis ΔmtrC* pC444A, *S. oneidensis ΔmtrC* pC453A, and *S. oneidensis ΔmtrC* pC444A,C453A was investigated, anaerobic growth using sodium fumarate as an electron acceptor was similar to that of wild type. However when the mutant variant strains were grown

aerobically, an extended lag phase was seen in induced cultures. This growth impairment was seen to be caused by the expression of the *mtrC* variants with the extent of the impairment linked to levels of protein expression. Quantiative PCR and micro arrays could be utilised to examine whether the differences in expressed protein observed is the result of cells degrading the proteins, or repressing expression from the plasmids. These would highlight any differences in mRNA levels which would indicate the level of expression of the genes. Further investigation will aim to ascertain the cause of this extended lag phase. As it is limited to cultures grown under aerobic conditions, a toxic effect of oxygen perhaps in the form of reactive oxygen species should first be examined.

3.5 References

Brockman, K. L. (2014) 'Enzyme Activity, Maturation and Regulation of Anaerobic Reductases in Shewanella Oneidensis MR-1', *Theses and Dissertations. Paper 669*. Coursolle, D. and Gralnick, J. a. (2012) 'Reconstruction of extracellular respiratory pathways for iron(III) reduction in Shewanella oneidensis strain MR-1', *Frontiers in Microbiology*, 3(FEB), pp. 1–11. doi: 10.3389/fmicb.2012.00056.

Darmon, E. and Leach, D. R. F. (2014) 'Bacterial Genome Instability', *Microbiology and Molecular Biology Reviews*, 78(1), pp. 1–39. doi: 10.1128/MMBR.00035-13.

Edwards, M. J., White, G. F., Norman, M., Tome-Fernandez, A., Ainsworth, E., Shi, L., Fredrickson, J. K., Zachara, J. M., Butt, J. N., Richardson, D. J. and Clarke, T. a. (2015) 'Redox Linked Flavin Sites in Extracellular Decaheme Proteins Involved in Microbe-Mineral Electron Transfer.', *Scientific Reports*. Nature Publishing Group, 5(July), p. 11677. doi: 10.1038/srep11677.

Grossman, J. N. and Kahan, T. F. (2016) 'Hydroxyl radical formation from bacteria-assisted Fenton chemistry at neutral pH under environmentally relevant conditions', *Environmental Chemistry*. doi: 10.1071/EN15256.

Guzman, L.-M., Belin, D., Carson, M. J. and Beckwith, J. O. N. (1995) 'Tight regulation, modulation, and high-level expression by vectors containing the arabinose PBAD promoter.', *Journal of bacteriology*. Am Soc Microbiol, 177(14), pp. 4121–4130.

Hartshorne, R. S., Reardon, C. L., Ross, D., Nuester, J., Clarke, T. a, Gates, A. J., Mills, P. C., Fredrickson, J. K., Zachara, J. M., Shi, L., Beliaev, A. S., Marshall, M. J., Tien, M., Brantley, S., Butt, J. N. and Richardson, D. J. (2009) 'Characterization of an electron conduit between bacteria and the extracellular environment.', *Proceedings of the National Academy of Sciences of the United States of America*, 106(52), pp. 22169–74. doi: 10.1073/pnas.0900086106.

Jin, M., Jiang, Y., Sun, L., Yin, J., Fu, H., Wu, G. and Gao, H. (2013) 'Unique organizational and functional features of the cytochrome c maturation system in Shewanella oneidensis.', *PloS one*. United States, 8(9), p. e75610. doi: 10.1371/journal.pone.0075610.

Nelson, D. L., Lehninger, A. L. and Cox, M. M. (2008) *Lehninger principles of biochemistry*. Macmillan.

Ramón, A., Señorale-Pose, M. and Marín, M. (2014) 'Inclusion bodies: not that bad…', *Frontiers in Microbiology*. Frontiers Media S.A., 5, p. 56. doi: 10.3389/fmicb.2014.00056.

Repine, J. E., Fox, R. B. and Berger, E. M. (1981) 'Hydrogen peroxide kills Staphylococcus aureus by reacting with staphylococcal iron to form hydroxyl radical', *Journal of Biological Chemistry*, 256(14), pp. 7094–7096.

Siegele, D. A. and Hu, J. C. (1997) 'Gene expression from plasmids containing the araBAD promoter at subsaturating inducer concentrations represents mixed populations.', *Proceedings of the National Academy of Sciences of the United States of America*. United States, 94(15), pp. 8168–8172.

Silva, A. M. N., Kong, X., Parkin, M. C., Cammack, R. and Hider, R. C. (2009) 'Iron(III) citrate speciation in aqueous solution.', *Dalton transactions (Cambridge, England : 2003)*. England, (40), pp. 8616–8625. doi: 10.1039/b910970f.

Smith, M. A. and Bidochka, M. J. (1998) 'Bacterial fitness and plasmid loss: the importance of culture conditions and plasmid size.', *Canadian journal of microbiology*, 44(4), pp. 351–355. doi: 10.1139/w98-020.

Chapter 4:

Oxygen Tolerance of *Shewanella oneidensis*

4.1 Introduction

Prior investigations had highlighted the conserved disulphide bond in domain III of MtrC to be a potential redox sensitive switch. In chapter 3 mutant forms of MtrC were generated where the cysteine residues forming the disulphide bond were substituted to alanine residues. This gave a form of MtrC that could not form the disulphide bond regardless of the environmental redox conditions. Aerobic growth studies showed that removal of this disulphide bond led to an extended lag phase in cultures of *S. oneidensis ΔmtrC* expressing any of the disulphide deficient mutants (pC444A, pC453A or pC444A,C453A). Further studies suggested the proteins were functional and allowed the bacterial cells to reduce solid ferric minerals (in the form of goethite).

This chapter aims to investigate the link between the cysteine residues at amino acid positions 444 and 453 to aerobic growth inhibition by ascertaining the effect expression of $MtrC_{C444A}$, $MtrC_{C453A}$ or $MtrC_{C444A,C453A}$ is having on the bacterial cell cultures. To clarify the cause of the extended lag phase, studies were undertaken looking at oxygen tolerance as the extended lag phase growth defect was only seen under aerobic growth conditions. Much of the investigation here focused on *S. oneidensis ΔmtrC* pC453A as this strain proved to be most comparable to the native expressing MtrC strain (*S. oneidensis ΔmtrC* pMtrC) due to the similar levels of expression constantly observed between the two.

4.2 Results

4.2.1 Nature of Extended Lag Phase

From the growth curve data it was impossible to tell if the reduced optical density was due to bacterial cell death or growth attenuation. To investigate the cell viability, viable cell counts from anaerobically grown bacterial cultures of *S. oneidensis ΔmtrC* pMtrC and *S. oneidensis ΔmtrC* pC453A were compared to cell counts from the same cultures after exposure to aerobic conditions. This allowed for the effect of oxygen on cell viability to be assessed (Chapter 2.3.4).

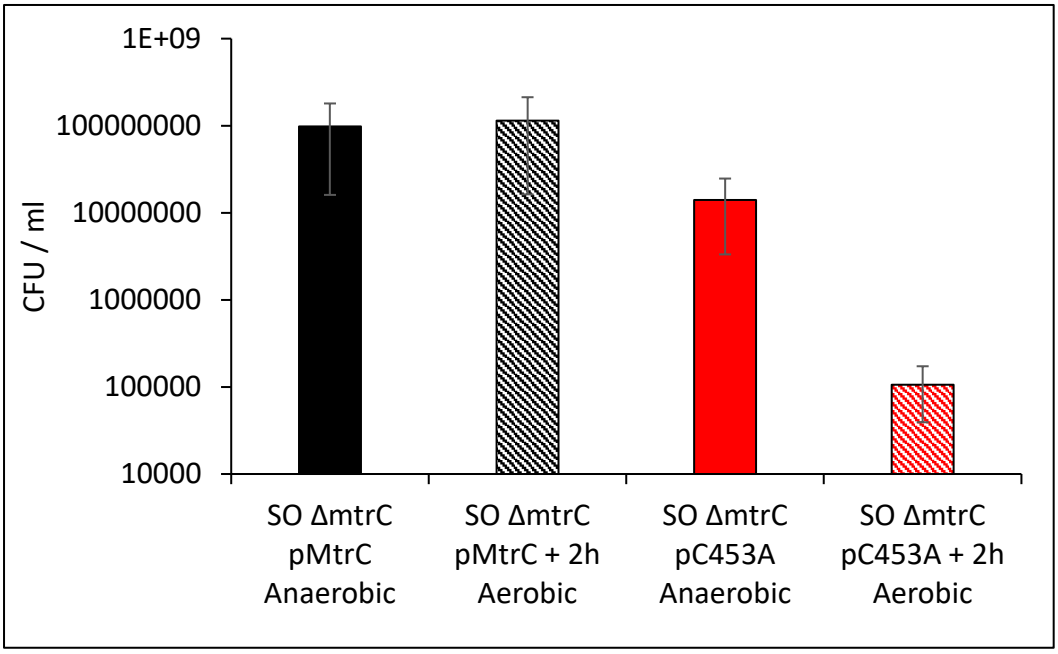

Figure 4.1 – Colony forming unit (CFU) measurements per ml of *S. oneidensis ΔmtrC* pMtrC cultures (Black) and *S. oneidensis ΔmtrC* pC453A cultures (Red). Comparison between anaerobically grown cultures (Solid Bars) and cultures undergoing 2 h aerobic conditions after anaerobic growth (Dashed Bars). Grown on LB agar plates at 30 ^{O}C, standard error bars obtained from three repeats.

When *S. oneidensis ΔmtrC* pC453A induced cultures underwent 2 h aerobic treatment, after anaerobic growth, before plating on a non-inducing medium, there was a large reduction in cell viability after 2 h. Only 0.76 % viability was maintained

(Figure 4.1), compared to cell viability when cells did not undergo aerobic treatment. There was no such decrease in cells expressing native MtrC (*S. oneidensis ΔmtrC* pMtrC). This result suggests that the extended lag phase in cultures expressing the mutant MtrC was due to bacterial cell death caused by exposure to oxygen rather than growth attenuation or stress induced changes to cell morphology.

4.1.2 Reactive Oxygen Species Detection

It is likely that the bacterial cell death in cultures expressing mutant MtrC under aerobic conditions was caused by the formation of a toxic product forming from oxygen. Reactive oxygen species (ROS) are known to form readily during the reduction of oxygen. One of the most stable ROS is hydrogen peroxide (H_2O_2) and so its presence was measured using an indigo carmine assay (Chapter 2.6.1) as an indication of ROS levels in cultures.

In this assay samples from *S. oneidensis ΔmtrC* pMtrC and *S. oneidensis ΔmtrC* pC453A cultures were reacted with the redox indicator indigo carmine. This is oxidised by peroxide or oxygen leading to an absorbance signal at 610 nm (Gilbert, Behymer and Castaneda, 1982). Samples taken from cultures, grown anaerobically, were tested for oxygen and hydrogen peroxide (Figure 4.2). The cultures were then grown aerobically, through the use of shaking incubators, for 3 h prior to again testing samples using indigo carmine. The high concentrations of oxygen in the samples lead to an intense increase in absorbance at 610 nm due to the oxidation of the indigo carmine. Cultures were then sparged with argon to remove dissolved oxygen before being treated with catalase and purged again. This last step allowed the removal of the hydrogen peroxide contribution specifically from the assay. As such, the decrease in absorbance seen after catalase treatment, compared to the result after sparging with argon, is proportional to the amount of hydrogen peroxide (and thus the amount generated during aerobic growth). Taking this decrease in absorbance, and comparing it to a standard curve generated from indigo carmine reacted with known hydrogen peroxide amounts, allowed for measurement of hydrogen peroxide concentration in the culture samples.

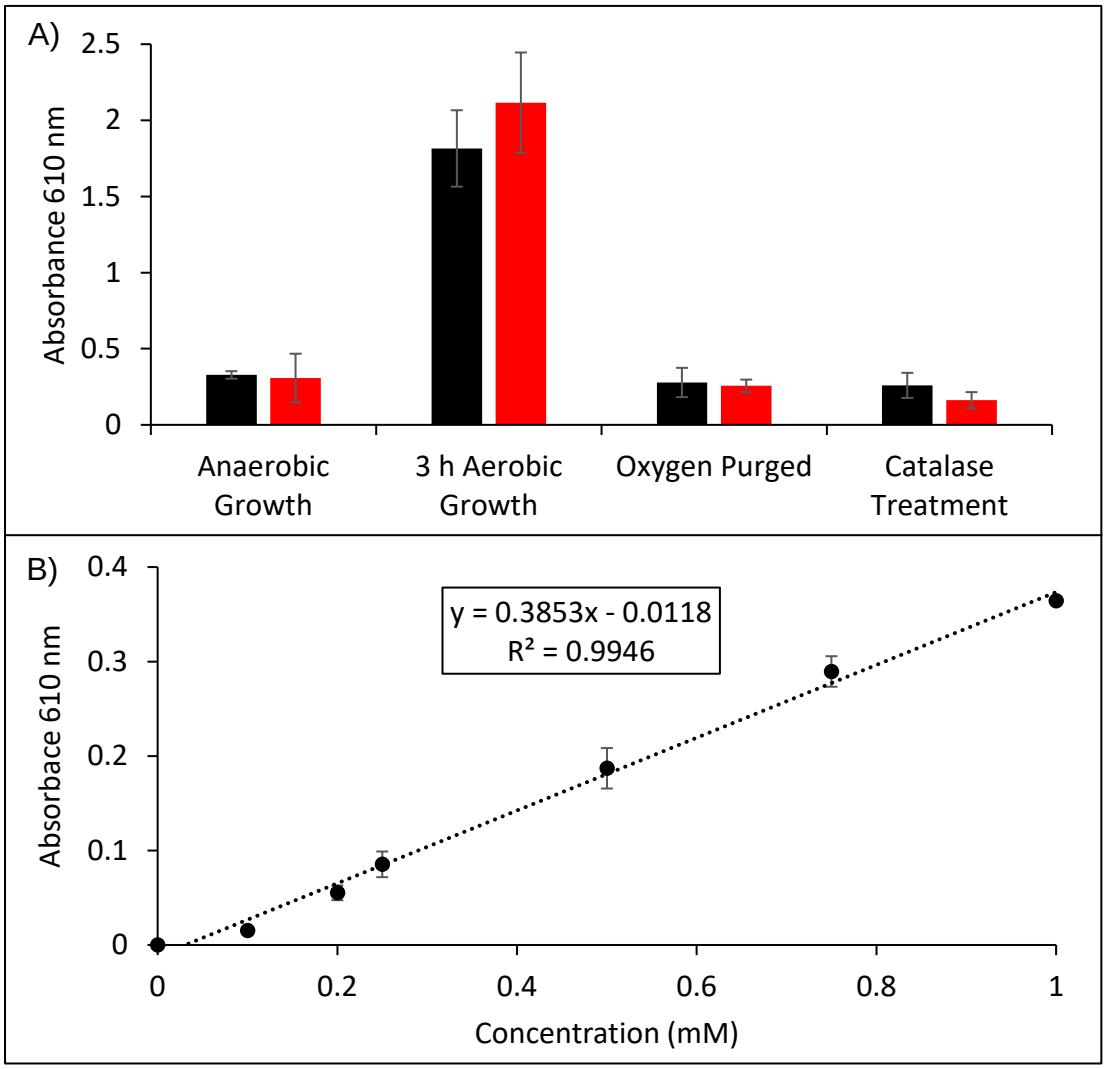

Figure 4.2 – Indigo Carmine assay results representing H_2O_2 concentration in *S. oneidensis ΔmtrC* pMtrC and *S. oneidensis ΔmtrC* pC453A samples under different conditions. A) Absorbance 610 nm for *S. oneidensis ΔmtrC* pMtrC (Black) and *S. oneidensis ΔmtrC* pC453A (Red) samples at each stage of indigo carmine assay. After anaerobic O/N growth, after 3 h aerobic growth phase, once oxygen is purged from the samples and finally after 0.3 U catalase treatment specifically removing H_2O_2 contribution. B) Indigo carmine assay standard curve generated from known H_2O_2 concentration samples. Cultures grown on LB medium supplemented with 5 mM arabinose, incubated at 30 ^{O}C. H_2O_2 standards made from 30 % hydrogen peroxide solution diluted in LB medium. Standard error bars obtained from three repeats.

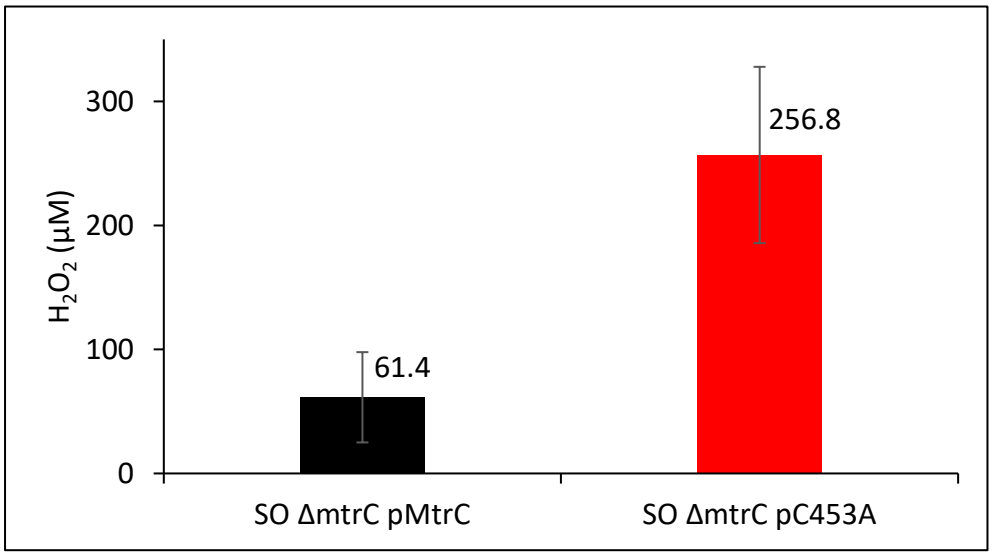

Figure 4.3 – H_2O_2 concentrations detected in bacterial cultures after 3 h exposure to aerobic conditions. *S. oneidensis ΔmtrC* pMtrC sample (Black) and *S. oneidensis ΔmtrC* pC453A sample (Red) after 3 h aerobic growth phase. Concentrations calculated from standard curve – Figure 4.2 B). Standard error bars obtained from three repeats.

The concentration of H_2O_2 in the *S. oneidensis ΔmtrC* pMtrC samples was seen to be 61.4 µM, approximately a quarter of the 256.8 µM detected in the *S. oneidensis ΔmtrC* pC453A samples (Figure 4.3). These results suggest *S. oneidensis ΔmtrC* pC453A cultures have increased levels of reactive oxygen species (specifically H_2O_2).

It is also worth noting that the nature of the *S. oneidensis ΔmtrC* pC453A phenotype means that the cell mass in the mutant samples is much lower than in the *S. oneidensis ΔmtrC* pMtrC samples. When the optical density of the samples was measured (Figure 4.4) it was seen that cell mass was around half in the *S. oneidensis ΔmtrC* pC453A samples compared to the *S. oneidensis ΔmtrC* pMtrC samples (optical density of 0.32 compared to 0.7 respectively). Thus, the rate of H_2O_2 production per cell was greater in *S. oneidensis ΔmtrC* pC453A than *S. oneidensis ΔmtrC* pMtrC.

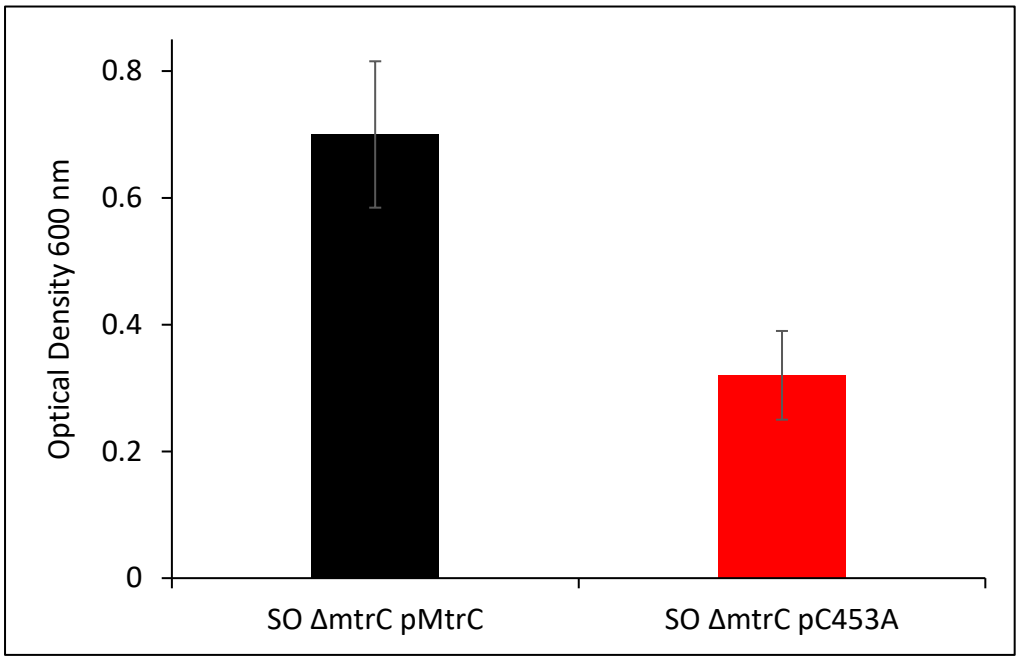

Figure 4.4 – Optical density (absorbance 600 nm) measurement for *S. oneidensis ΔmtrC* pMtrC (Black) and *S. oneidensis ΔmtrC* pC453A (Red) culture samples after aerobic growth phase of indigo carmine assay. Highlighting difference in cell mass between samples (0.7 compared to 0.32, *S. oneidensis ΔmtrC* pMtrC and *S. oneidensis ΔmtrC* pC453A respectively).

4.2.3 Most Dominant ROS

Increased levels of H_2O_2 was detected in *S. oneidensis ΔmtrC* pC453A cultures implicating reactive oxygen species as the main cause of the observed extended lag phase. To confirm this was the case, attempts were made to restore wild type growth to *S. oneidensis ΔmtrC* pC453A cultures. To this end, superoxide dismutase and catalase, capable of catalysing the breakdown of superoxide and H_2O_2, were added to cultures and growth was recorded (Chapter 2.3.2).

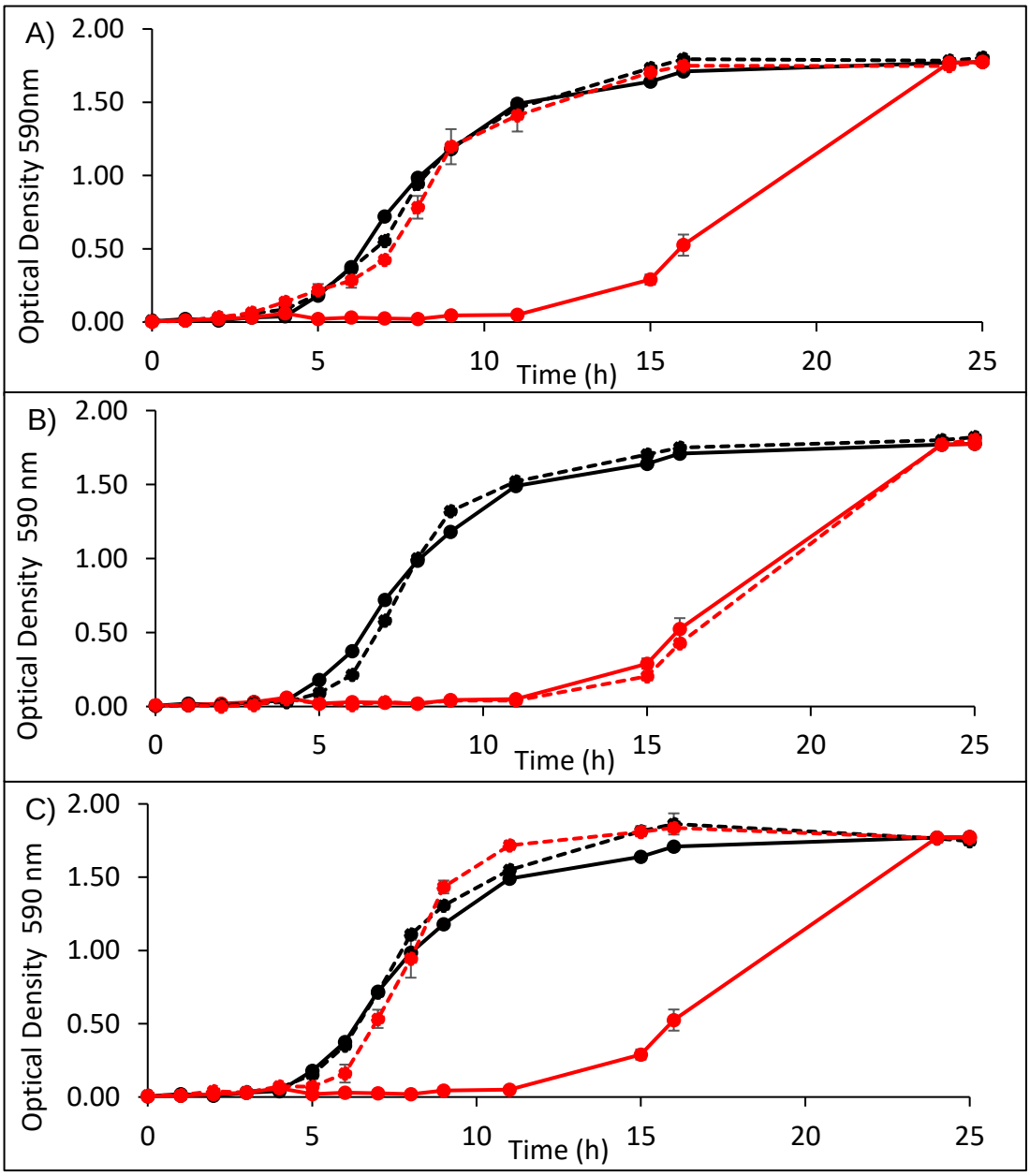

Figure 4.5 – Aerobic growth profiles derived from of *S. oneidensis ΔmtrC* pMtrC (Black) and *S. oneidensis ΔmtrC* pC453A (Red) when LB growth medium supplemented with A) 0.3 U/ml catalase, B) 0.3 U/ml superoxide dismutase or C) both 0.3 U/ml catalase and 0.3 U/ml superoxide dismutase. Comparison of culture growth on media not supplemented with ROS scavengers (Solid) and growth on media supplemented with ROS scavengers (Dashed). Cultures incubated at 30 ^{O}C shaking at 220 rpm, standard error bars obtained from three repeats.

The addition of 0.3 U/ml catalase was seen to fully restore the growth phenotype of *S. oneidensis ΔmtrC* pC453A to that of *S. oneidensis ΔmtrC* pMtrC (Figure 4.5 Panel A). This suggests that H_2O_2 is the dominant ROS responsible for the extended lag phase seen in *S. oneidensis ΔmtrC* pC453A cultures, under aerobic conditions. The addition of 0.3 U/ml superoxide dismutase (SOD) did not restore the growth phenotype. In fact it appeared to slightly extend the lag phase of *S. oneidensis ΔmtrC* pC453A further (Figure 4.5 Panel B). Supplementing the growth medium with 0.3 U/ml catalase and 0.3 U/ml SOD also restored the growth phenotype of *S. oneidensis ΔmtrC* pC453A to that of *S. oneidensis ΔmtrC* pMtrC (Figure 4.5 Panel C).

The same pattern was seen in the other strains of LS661 expressing the other mutant forms of MtrC previously described (*S. oneidensis ΔmtrC* pC444A and *S. oneidensis ΔmtrC* pC444A,C453A). The extended lag phase seen in these cultures, when grown under aerobic conditions, was also shortened to that of wild type *S. oneidensis* when media was supplemented with 0.3 U/ml catalase or 0.3 U/ml catalase and 0.3 U/ml SOD. These strains also showed a slight extension of lag phase when media was supplemented with 0.3 U/ml SOD only (Figure 4.6 Panel A and B)

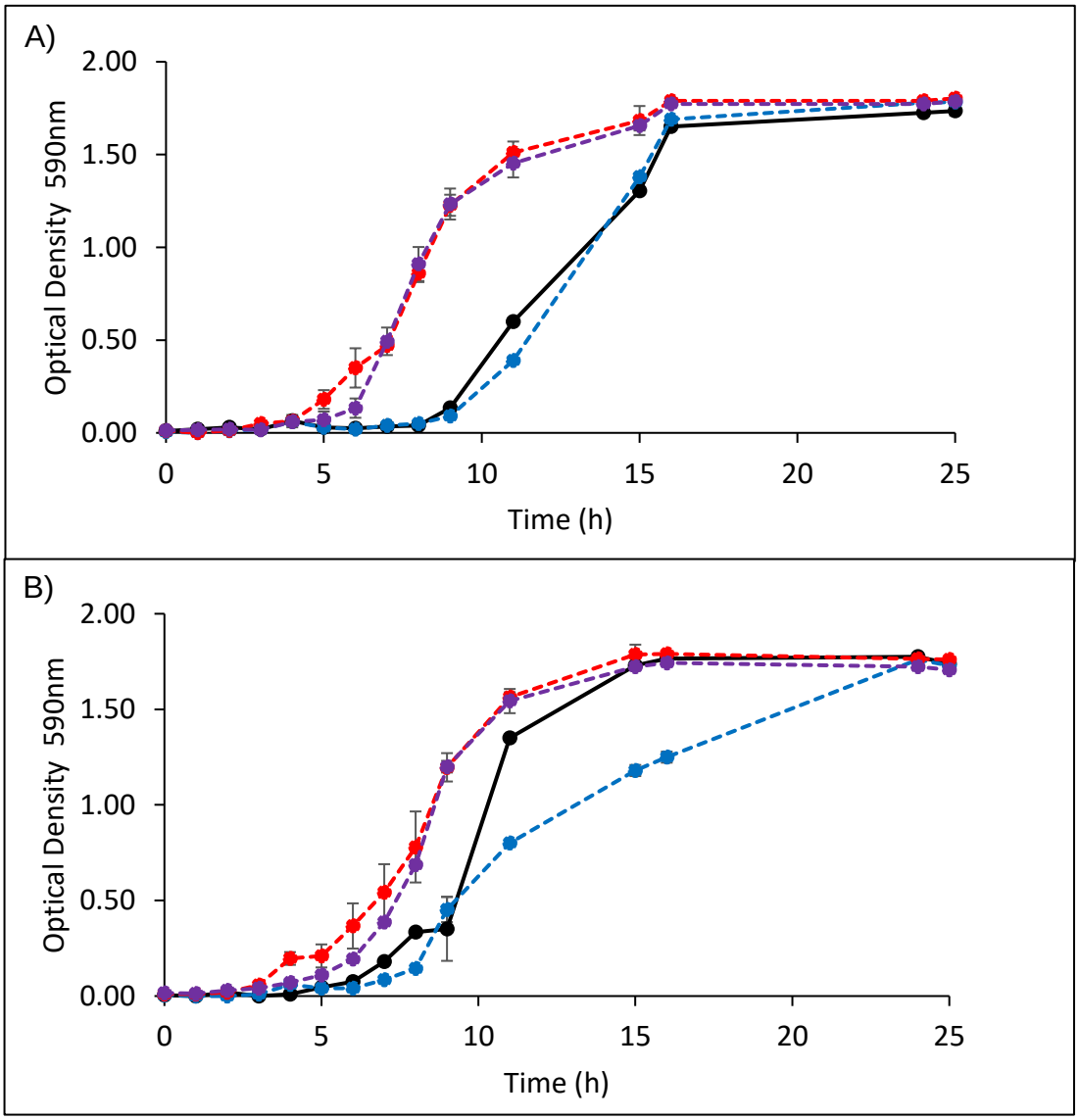

Figure 4.6 – Aerobic growth profiles for A) *S. oneidensis ΔmtrC* pC444A and B) *S. oneidensis ΔmtrC* pC444A,C453A Comparison of effect when LB growth media supplemented no ROS scavenger enzyme (Black Solid), 0.3 U/ml SOD (Blue Dashed), 0.3 U/ml catalase (Red Dashed) or 0.3 U/ml SOD + 0.3 U/ml cat addition (Purple Dashed). Cultures incubated at 30 ^{O}C shaking at 220 rpm, standard error bars obtained from three repeats.

4.2.4 Physiological Relevance of H_2O_2 Detected

As previously shown, H_2O_2 concentration measurements in culture samples of *S. oneidensis ΔmtrC* pC453A and *S. oneidensis ΔmtrC* pMtrC showed differences between the strains. The concentration of H_2O_2 in *S. oneidensis ΔmtrC* pMtrC cultures was measured to be 61.4 µM, lower than the 256.8 µM measured in samples of *S. oneidensis ΔmtrC* pC453A. These measurements highlight the potential amount of H_2O_2 produced by the cultures, however the results thus far mentioned gave no indication if these amounts were sufficient to cause the extended lag phase as seen in Chapter 3. To investigate the physiological relevance of the measured concentrations of H_2O_2 in the samples, *S. oneidensis* cultures were grown with varying levels of H_2O_2 applied to areas of the growth plate. Growth inhibition was measured and compared to that of *E. coli*, grown under the same conditions (Chapter 2.3.6).

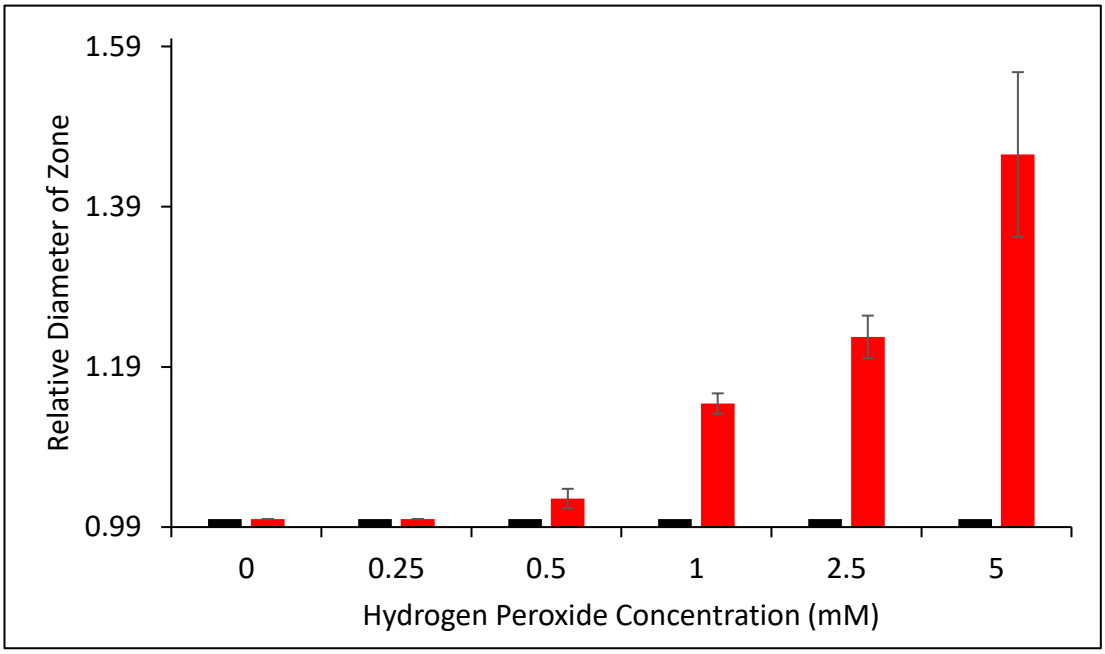

Figure 4.7 – Diameter of zone of inhibition caused by H_2O_2 concentrations (0 – 5 mM) when applied to growing lawn of *E. coli* 803 (Black) and *S. oneidensis* MR-1 (Red). Results shown as diameter of ZOI relative to diameter of application disc highlighting differences in susceptibility to H_2O_2 between bacterial species. Grown on LB agar plates *E. coli* incubated at 37 ^{O}C, *S. oneidensis* incubated at 30 ^{O}C, standard error bars obtained from three repeats.

S. oneidensis growth was seen to be inhibited by much lower levels of H_2O_2 compared to *E. coli*, with levels as low as 0.5 mM H_2O_2 having an inhibitory effect on cultures (Figure 4.7). *E. coli* cultures did not show evidence of growth inhibition even when exposed to concentrations of H_2O_2 as high as 5 mM whereas at these concentrations *S. oneidensis* MR-1 growth was severely affected. These results suggest *S. oneidensis* MR-1 is especially sensitive to reactive oxygen species. This difference is further discussed later.

To evaluate the physiological relevance of the increased H_2O_2 concentrations detected in *S. oneidensis ΔmtrC* pC453A, a more definitive technique was used where cultures of *S. oneidensis* MR-1 and *S. oneidensis ΔmtrC* were incubated with 0, 0.1 or 0.25 mM concentrations of H_2O_2 and cell viability was recorded over time (Chapter 2.3.5). It was seen that H_2O_2 as low as 0.1 mM had an effect of cell viability after 5 min incubation. Even more striking was the effect of incubating cultures with 0.25 mM H_2O_2 (levels detected in *S. oneidensis ΔmtrC* pC453A samples). Cell viability fell by 99.98 and 99.84 % over the course of 15 min (*S. oneidensis* MR-1 and *S. oneidensis ΔmtrC* respectively), compared to cultures incubated without H_2O_2 addition (Figure 4.8). From this result it can be concluded that the 256.8 µM H_2O_2 produced by *S. oneidensis ΔmtrC* pC453A cultures (Figure 4.3) is sufficient to cause bacterial cell death.

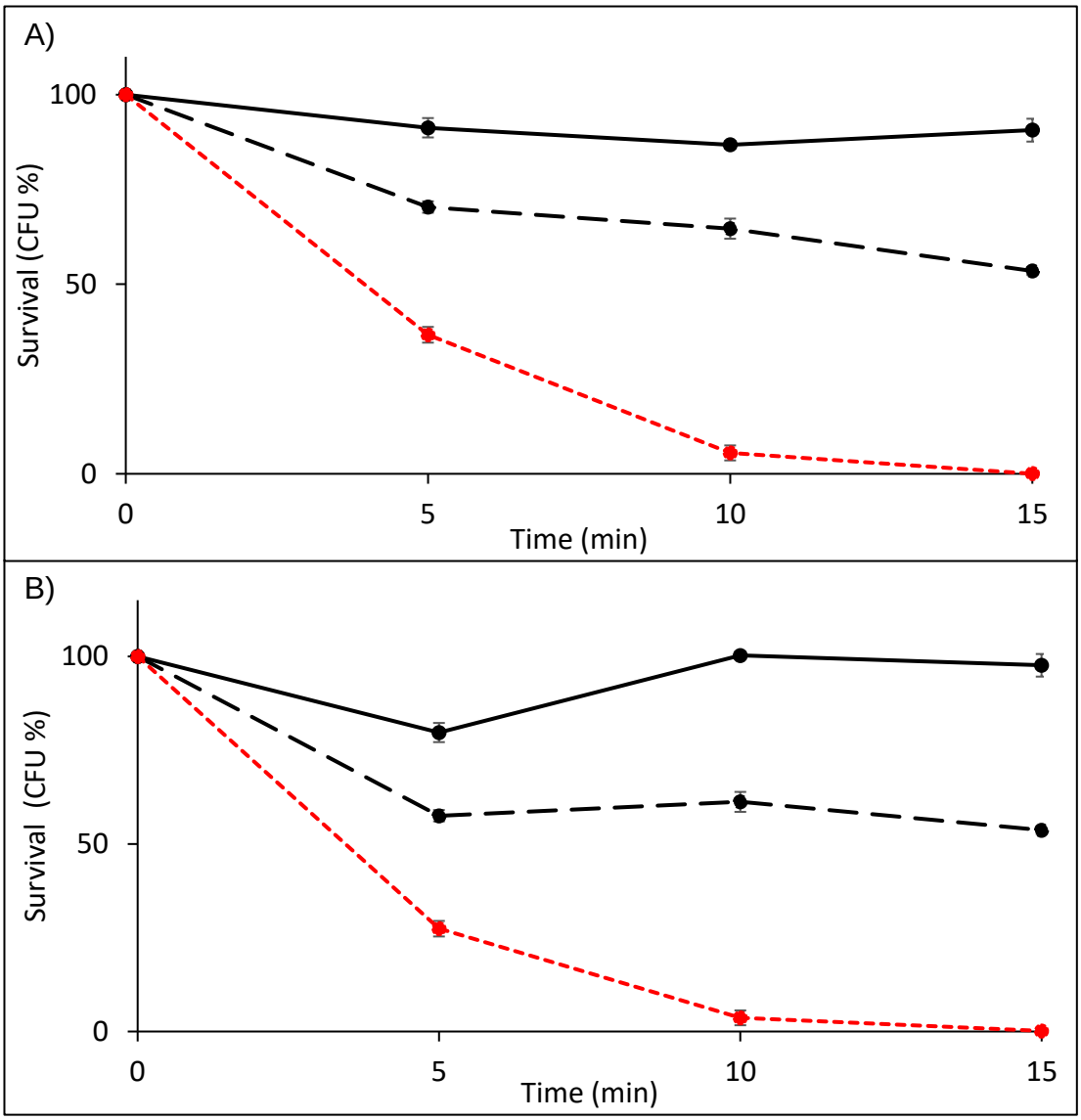

Figure 4.8 – Kill curves showing survival of A) *S. oneidensis* MR-1 and B) *S. oneidensis ΔmtrC* culture samples, incubated with 0-0.25 mM H_2O_2, over time. Survival shown as % of colony forming units, as compared to 0 min point. Control of 0 mM H_2O_2 (Solid Black) showed no reduction in CFU, 0.1 mM H_2O_2 (Dashed Black) showed 53.5 % and 53.69 % survival after 15 min (*S. oneidensis* MR-1 and *S. oneidensis ΔmtrC* respectively). 0.25 mM H_2O_2 (Red Dashed) showed only 0.02 % and 0.16 % survival after 15 min (*S. oneidensis* MR-1 and *S. oneidensis ΔmtrC* respectively). Incubations with H_2O_2 carried out aerobically at room temperature prior to plating on LB agar plates then incubated at 30 ^{O}C.

4.3 Discussion

4.3.1 Nature of Extended Lag Phase

An extended lag phase was described in aerobically grown cultures of LS661 (*ΔmtrC*) expressing MtrC where the cysteine residues forming a disulphide bridge in domain 3 had been substituted. Taking *S. oneidensis ΔmtrC* pC453A as an example, cultures were seen to grow after approximately 15 h of lag phase (Figure 3.4) and investigation showed this growth coincided with the reduction in $MtrC_{C453A}$ expression in the cells (Figure 3.9). However, the investigation did not show if the bacterial cells were dying, keeping the optical density of the cultures low, until further generations had adapted to reduce the $MtrC_{C453A}$ expression, allowing growth to be seen. An alternative explanation for the phenotype seen in *S. oneidensis ΔmtrC* pC453A could be that cell division had been delayed by the expression of the MtrC mutants. This would have again kept the optical density of the cultures low and it would only been when the cells had altered expression of $MtrC_{C453A}$ that division was able to resume. As it is not possible to distinguish between these explanations from optical density data in growth curves, cell viability of *S. oneidensis ΔmtrC* pC453A was instead chosen as a measure. This technique would also remove the problem of cell stress affecting size and shape of cells, which is also known to affect optical density readings (Madigan *et al.*, 2008).

Cell viability of *S. oneidensis ΔmtrC* pC453A cultures, which underwent 2 h of aerobic treatment, dropped by 99.24 % compared to controls where no aerobic growth phase was introduced (Figure 4.1). This drop in cell viability was not seen in the same experiment carried out on *S. oneidensis ΔmtrC* pMtrC. These results show that the cells were indeed dying when oxygen was introduced to the cultures, whilst expressing $MtrC_{C453A}$. If their growth had simply been slowed, cell viability would not be expected to drop as once plated, under non-inducing conditions, the cells would have resumed growth.

4.3.2 Reactive Oxygen Species Detection

As the extended lag phase was only seen in cultures expressing the mutant forms of MtrC under aerobic conditions (Figure 3.4), it suggested a toxic effect of oxygen to the cells. One well known cause of oxygen toxicity are reactive oxygen species (ROS). These molecules are generated under aerobic conditions by natural enzymes in the electron transport chain (ETC) of cells (Nelson, Lehninger and Cox, 2008). These enzymes catalyse the partial reduction of oxygen, by electrons provided by NADH, to superoxide ($O2^{-}$•). A chain reaction (Figure 4.9) then occurs leading to the generation of hydrogen peroxide (H_2O_2) followed by hydroxyl radicals (OH•).

1.	$O_2 + e^- \rightarrow O_2^-$•
2.	$2H^+ + 2O_2^-$• $\rightarrow H_2O_2 + O_2$
3.	$H_2O_2 + e^- \rightarrow OH^- + OH$•

Figure 4.9 – Chemical equations showing the typical path of reactive oxygen species formation inside cells with the product from each reaction acting as substrate for the next. Equation 1: formation of superoxide from oxygen molecules reduction by free electrons. Equation 2: Formation of H_2O_2 from protons reacting with superoxide. Equation 3: Hydroxyl radical formation generated by reduction of H_2O_2.

Due to the prevalence of these damaging molecules, it was hypothesised that *S. oneidensis ΔmtrC* pC453A (and the other MtrC mutants in this study) were generating increased levels of ROS and this was leading to the reduction in cell viability seen. Of the strains expressing mutant forms of MtrC, *S. oneidensis ΔmtrC* pC453A was selected to undergo comparative experiments with *S. oneidensis ΔmtrC* pMtrC. The decision to move this one strain forward into testing was made owing to time constraints and also because it was deemed a more relevant comparison as the $MtrC_{C453A}$ protein had previously been identified as expressing most comparatively to the native MtrC expressing strain. To test this, levels of H_2O_2 were measured in cultures. H_2O_2 was chosen as an indicator due to it being one of the most stable

reactive oxygen species and so one of the more reliable to measure (Reth, 2002). There are a number of established methods for measuring H_2O_2 concentration. One such method is to use dihydrofluorescein acetate (DHF). This compound reacts with H_2O_2 in the presence of peroxidase resulting in the liberation of fluorescein. This chemical fluoresces and can thus be measured using a fluorimeter, the more H_2O_2 in a sample the more fluorescein (and so fluorescence) detected. This method is often used to measure very low levels of H_2O_2 in eukaryotic cell samples and is very precise (Rhee *et al.*, 2010). Another method is to use indigo carmine. This redox indicator is widely used to monitor levels of H_2O_2 generated by bacteria in wastewater and turns blue upon oxidation (Gilbert, Behymer and Castaneda, 1982). This colour change can be followed by recording absorbance 562 nm which is proportional to the level of oxidation of the indicator.

It was decided to use the indigo carmine assay to measure levels of H_2O_2 in the *S. oneidensis ΔmtrC* pC453A cultures and the results were compared to the levels detected in *S. oneidensis ΔmtrC* pMtrC cultures. The indigo carmine assay was chosen as a pre-prepared kit (K-7503, CHEMetrics) could detect an optimal range of H_2O_2 concentrations from 0.2 to 2 ppm. The assay also worked on culture samples without the need to first remove the bacterial cells, allowing for measurements to be taken quickly and accurately. The DHF assay, on the other hand, required cells to be removed before the assay was carried out to avoid cells affecting the florescence of the sample. Initial trials using the DHF assay also showed high levels of background reaction when peroxidase was added (data not shown). This appeared to be the result of interactions between the peroxidase used and the DMSO solubilised DHF. For these reasons the DHF assay was deemed unsuitable for this study.

Indigo carmine can also be oxidised by oxygen, seen in Figure 4.2 Panel A, and is affected by pH (Gilbert, Behymer and Castaneda, 1982). To make the assay specific to the levels of H_2O_2 in the sample, a reading was taken after the cultures had undergone an aerobic growth phase of 3 h, this showed the oxidising power of everything that was in the sample. The cultures were then treated with catalase, an enzyme that catalyses the conversion of H_2O_2 to oxygen and water, and sparged of

all oxygen produced in the reaction using argon. This allowed duplicate samples, with and without catalase sparged with argon to be taken and recorded using the assay. This second result now showed the background level indigo carmine oxidised by the sample but now with the contribution of H_2O_2 removed. By comparing the two recordings (with and without catalase treatment), it can be inferred that the reduction in oxidised indigo carmine (after catalase treatment) is proportional to the amount of H_2O_2 in the sample. It is perhaps of note that the sample taken from cultures after 3 h aerobic growth showed differing levels of absorbance at 562 nm. The *S. oneidensis ΔmtrC* pC453A sample showed higher levels than the *S. oneidensis ΔmtrC* pMtrC sample. This could be the result of less respiration occurring in the *S. oneidensis ΔmtrC* pC453A sample due to bacterial cell death under these aerobic conditions.

Using a standard curve (Figure 4.2 Panel B). The amount of H_2O_2 in cultures of *S. oneidensis ΔmtrC* pC453A was measured to be 256.8 µM. This approximately four times as high as the 61.4 µM measured in *S. oneidensis ΔmtrC* pMtrC cultures (Figure 4.3). However, there are a number of considerations to take into account with these results. The first is the difference in cell number between the cultures of *S. oneidensis ΔmtrC* pMtrC and *S. oneidensis ΔmtrC* pC453A. Due to the toxic effect of oxygen to *S. oneidensis ΔmtrC* pC453A, the number of live cells in the cultures is reduced during the experimental 3 h aerobic phase. The cultures of *S. oneidensis ΔmtrC* pMtrC were not affected in these conditions and continued to grow. The optical density of the cultures confirmed that there was a difference in cell mass with *S. oneidensis ΔmtrC* pMtrC measurements of 0.7 compared to 0.32 in *S. oneidensis ΔmtrC* pC453A cultures (Figure 4.4). If this difference in cell number is taken into account, it can be estimated that 802.5 µM H_2O_2 would be produced by *S. oneidensis ΔmtrC* pC453A and 87.7 µM H_2O_2 by *S. oneidensis ΔmtrC* pMtrC, per 1 OD unit. This would be a much more significant difference in H_2O_2 levels between the cultures. Another consideration is that amount of H_2O_2 measured is not the amount generated by the cultures in a given time frame, but rather a measurement of the equilibrium level of H_2O_2 in the cultures. Normalising to protein amount rather than cell mass would have been a better comparison between the samples however it was decided

the toxicity to oxygen may be increasing the expression levels of response pathways and as such could artificially inflate total protein measurements.

Almost all microorganisms capable of aerobic respiration also have genes coding for enzymes capable of removing endogenous and exogenous reactive oxygen species. One group of these enzymes are peroxidases that preferentially catalyse the degradation of H_2O_2 before further reactive oxygen species can be generated (Vatansever *et al.*, 2013). *S. oneidensis* has a number of peroxidase enzymes, with one of the main H_2O_2 responses being the derepression of catalase (*katB*) and *dps* genes via the OxyR regulatory pathway (Jiang *et al.*, 2014). Other's implicated in ROS detoxification include; catalase/peroxidase (*katG1* and *katG2*), organic hydroperoxide resistance protein (*ohr*), and alkyl hydroperoxide reductase (*ahpC* and *ahpF*) encoded in its genome to scavenge reactive oxygen species (Qiu *et al.*, 2005). Such enzymes appear to vary in protective power and inducing conditions. Another peroxidase in *Shewanella,* cytoplasmic glutathione peroxidase (CgpD), is constitutively expressed, seemingly to deal with background levels of peroxide. In contrast, periplasmic glutathione peroxidase (PgpD) is up regulated by the sigma factor RpoE2 under oxidative stress conditions. This peroxidase is seen to play a greater role in the removal of peroxide than CgpD, as when knocked out cell mass is seen to significantly drop (Dai *et al.*, 2015). The ability to measure increased levels of H_2O_2 in *S. oneidensis ΔmtrC* pC453A samples even with these homeostatic systems suggests the actual amounts being generated were such that the oxidative stress response could not remove the ROS fast enough to keep up.

4.3.3 Most Dominant ROS

H_2O_2 concentration was measured in cultures due to its stability and was only an indicator of reactive oxygen species level. To investigate if H_2O_2 was indeed the dominant ROS causing the extended lag phase in aerobically grown *S. oneidensis ΔmtrC* pC453A, enzymes were added to the culture media in an attempt to neutralise the toxic affect on the cells. When growth media was supplemented with 0.3 U catalase, wild type growth was restored to *S. oneidensis ΔmtrC* pC453A. This

restoration was not seen when 0.3 U superoxide dismutase was added to the growth media suggesting that H_2O_2 was indeed the dominate ROS affecting bacterial growth in cultures of *S. oneidensis ΔmtrC* pC453A (Figure 4.5 Panel A and B). This assumption can be made as catalase specifically catalyses the conversion of H_2O_2 to water and oxygen whereas superoxide dismutase specifically removes superoxide from the system (Figure 4.10) and so restoration of wild type growth would be expected, in cultures supplemented with superoxide dismutase, if superoxide was the dominant cause of the extended lag phase.

Catalase	$2H_2O_2 \rightarrow 2H_2O + O_2$
Superoxide Dismutase	$2O_2^- \bullet + 2H^+ \rightarrow H_2O_2 + O_2$

Figure 4.10 – Chemical equations of reactions catalysed by catalase and superoxide dismutase. Both are common ROS scavenging enzymes.

In fact, when cultures were supplemented with superoxide dismutase, the extended lag phase persisted for longer than when no enzyme was added to cultures (Figure 4.5 Panel B). This was likely due to the added superoxide dismutase converting superoxide to H_2O_2 at an enhanced rate (compared to the native SodB activity) which lead to more stress on the cells (Qiu *et al.*, 2015). This would also explain why when media was supplemented with both catalase and SOD the lag phase was reduced to wild type length and a slight increase in maximum cell density was observed. In this case the SOD was converting any superoxide to H_2O_2 but the supplemented catalase was enough to compensate for this (Figure 4.5 Panel C). These results were also seen when the experiment was repeated on the other mutant strains previous described *S. oneidensis ΔmtrC* pC444A and *S. oneidensis ΔmtrC* pC444A,C453A (Figure 4.6 Panel A and B). This shows that the extended lag phase in all strains had the same cause (increased levels of H_2O_2) and that differences in phenotypes were due to variations in expression levels of the MtrC (Chapter 3.9). Taken together, these results suggest that H_2O_2 is more toxic to the *S. oneidensis* cells than other reactive oxygen species (such as superoxide) and is the cause of the extended lag phase seen in *S. oneidensis* expressing MtrC with mutated disulphide bonds.

4.3.4 Physiological Relevance of H_2O_2 Detected

We were unable to measure the rate of H_2O_2 generated by *S. oneidensis ΔmtrC* pC453A cells, leading to the extended lag phase, due to the equilibrium nature of H_2O_2 in samples. Rather, the resulting concentration of H_2O_2 was measured. The levels detected were investigated further to ascertain if they themselves were enough to cause a growth defect or if a much higher amount (likely hidden by the bacterial peroxidase activity) was needed. There is already a precedent in the literature for *S. oneidensis* to be especially susceptible to oxidative stress when compared to other bacteria such as *E. coli* (Jiang *et al.*, 2014a). This was demonstrated again here when zone of inhibition (ZOI) studies were used to compare the effect of H_2O_2 concentration on cell viability in *S. oneidensis* and *E. coli*. Even at 5 mM H_2O_2 concentrations there was no measureable inhibition of *E. coli* growth. Whereas *S. oneidensis* growth was seen to be inhibited at concentrations of 0.5 mM - 10 fold lower (Figure 4.7). These levels were still higher than the 256.8 μM H_2O_2 detected in *S. oneidensis ΔmtrC* pC453A aerobically growing cultures (Figure 4.3). A more sensitive method was employed to ascertain if these lower levels were still enough to inhibit growth of *S. oneidensis*.

S. oneidensis cells not expressing the mutant MtrC (linked with the generation of H_2O_2) were incubated with varying concentrations of H_2O_2 and samples were taken over time to monitor viable cells within the cultures. It was seen that just 0.1 mM H_2O_2 was enough to affect cell viability after just 5 min incubation. When cultures were incubated with 0.25 mM H_2O_2 (levels similar to that measured in aerobically growing *S. oneidensis ΔmtrC* pC453A) cell viability dropped by 99.84 % within 15 min (Figure 4.8). This result showed the level of H_2O_2, generated by aerobically growing *S. oneidensis ΔmtrC* pC453A, was capable of causing significant bacterial cell death wild type *S. oneidensis* and physiologically relevant.

Bacterial susceptibility to oxidative stress has been linked to the abundancy of cytochromes in the genome. This alongside intracellular manganese : iron ratio

seems to be a good indicator of sensitivity to oxidative stress (Daly, 2004). When oxidative stress was induced by irradiating cultures of; *S. oneidensis, E. coli*, and *Deinococcus radiodurans*, *S. oneidensis* was seen to have survive far less well than the other species examined. *E. coli* only has 6 expression inducible c-type cytochromes in comparison to *S. oneidensis* having 39, often constituently expressed, c-type cytochromes. This appears to give *E.coli* more resistance to ROS and *D. radiodurans* was even more resistant seemingly due to it having a 0.24:1 ratio of intracellular manganese to iron, compared to <0.001:1 ratio in *S. oneidensis* (Ghosal *et al.*, 2005). These interesting observations highlight a link between iron and the toxicity of ROS to cultures, possibly the result of Fenton chemistry.

It has long been known that increasing concentrations of iron in growth media leads to an increased sensitivity to H_2O_2 in a wide range of bacteria, including *Staphylococcus aureus*, through the Fenton reaction (Repine, Fox and Berger, 1981). The Fenton reaction is the conversion of H_2O_2 to the hydroxyl radical catalysed by reduced iron (Figure 4.11).

$$Fe^{2+} + H_2O_2 \rightarrow Fe^{3+} + OH^- + OH\bullet$$

Figure 4.11 – Fenton reaction chemical equation. Showing the reduction of H_2O_2 by ferrous iron (often contained within intracellular cytochromes) to the more damaging hydroxyl radical.

The generation of the hydroxyl radical makes the oxidative stress much higher in the cell as this ROS is far more reactive than H_2O_2 and is capable of reacting with a huge range of cellular macromolecules (Sharma *et al.*, 2012). *S. oneidensis* has very high levels of intracellular iron due to the large number of c-type cytochromes in the cell, many of which contain multiple heme groups (Meyer *et al.*, 2004). During the biosynthesis of these c-type cytochromes, the heme iron is in a reduced state and under these conditions the iron can generate ROS through Fenton reactions (Kranz *et al.*, 2009; Hamza and Dailey, 2012) . It would seem likely that this high risk of toxicity is why diheme cytochrome *c* peroxidase (C*c*pA) is expressed in *S. oneidensis* even under anaerobic and micro aerobic conditions. The expression of this gene is

seen to give a growth advantage to the bacteria, when compared to *ΔccpA* - knockout strains of *S. oneidensis* (Schütz *et al.*, 2011). Perhaps because without CcpA even small amounts of H_2O_2 generated anaerobically generate damaging hydroxyl radicals through the Fenton reaction. Further investigation will be needed to link any specific peroxidase systems in *S. oneidensis* to the increased levels of H_2O_2 reported here. This could be done via the use of qPCR and microarrays to highlight changes of expression in ROS response pathways.

4.4 Conclusion

Substituting the cysteine residues that from the disulphide bridge in domain 3 of MtrC leads to an extended lag phase seen in cells under aerobic growth conditions. Here we have shown this is the result of bacterial cell death caused by an increase in H_2O_2 concentration in the samples. *S. oneidensis* is highly sensitive to oxidative stress largely due to the high number of heme multi-heme cytochromes acting as catalysts for the generation of the highly damaging hydroxyl radical from H_2O_2 via the Fenton reaction.

Importantly this phenomenon was not seen in *S. oneidensis ΔmtrC* pMtrC or wild type *S. oneidensis* Mr1. This suggests the disruption of the disulphide bond in MtrC impacts on generation of H_2O_2 and, either directly through increased reactivity or indirectly simply by providing more H_2O_2 to be catalysed, generation of hydroxyl radicals. Taken with the knowledge that CcpA (a native peroxidase) is downregulated under fully aerobic conditions, it is suggested that a previously unreported mechanism preventing the generation of reactive oxygen species in these bacteria, with highly reactive cytochrome complexes, could exist.

4.5 References

Dai, J., Wei, H., Tian, C., Damron, F. H., Zhou, J. and Qiu, D. (2015) 'An extracytoplasmic function sigma factor-dependent periplasmic glutathione peroxidase is involved in oxidative stress response of Shewanella oneidensis', *BMC Microbiology*, 15(1), pp. 1–12. doi: 10.1186/s12866-015-0357-0.

Daly, M. J. (2004) 'Accumulation of Mn(II) in Deinococcus radiodurans Facilitates Gamma-Radiation Resistance', *Science*, 306(5698), pp. 1025–1028. doi: 10.1126/science.1103185.

Ghosal, D., Omelchenko, M. V., Gaidamakova, E. K., Matrosova, V. Y., Vasilenko, A., Venkateswaran, A., Zhai, M., Kostandarithes, H. M., Brim, H., Makarova, K. S., Wackett, L. P., Fredrickson, J. K. and Daly, M. J. (2005) 'How radiation kills cells: Survival of Deinococcus radiodurans and Shewanella oneidensis under oxidative stress', *FEMS Microbiology Reviews*, 29(2), pp. 361–375. doi: 10.1016/j.femsre.2004.12.007.

Gilbert, T. W., Behymer, T. D. and Castaneda, H. B. (1982) 'Determination of dissolved-oxygen in natural and wastewaters', *American Laboratory*. INT SCIENTIFIC COMMUN INC PO BOX 870, 30 CONTROLS DRIVE, SHELTON, CT 06484-0870, 14(3), p. 119.

Hamza, I. and Dailey, H. A. (2012) 'One ring to rule them all: trafficking of heme and heme synthesis intermediates in the metazoans', *Biochimica Et Biophysica Acta (BBA)-Molecular Cell Research*. Elsevier, 1823(9), pp. 1617–1632.

Jiang, Y., Dong, Y., Luo, Q., Li, N., Wu, G. and Gao, H. (2014a) 'Protection from oxidative stress relies mainly on derepression of OxyR-dependent KatB and Dps in Shewanella oneidensis', *Journal of Bacteriology*, 196(2), pp. 445–458. doi: 10.1128/JB.01077-13.

Jiang, Y., Dong, Y., Luo, Q., Li, N., Wu, G. and Gao, H. (2014b) 'Protection from oxidative stress relies mainly on derepression of OxyR-dependent KatB and Dps in Shewanella oneidensis.', *Journal of bacteriology*, 196(2), pp. 445–58. doi: 10.1128/JB.01077-13.

Kranz, R. G., Richard-Fogal, C., Taylor, J.-S. and Frawley, E. R. (2009) 'Cytochrome c Biogenesis: Mechanisms for Covalent Modifications and Trafficking of Heme and for Heme-Iron Redox Control', *Microbiology and Molecular Biology Reviews : MMBR*. American Society for Microbiology (ASM), 73(3), pp. 510–528. doi: 10.1128/MMBR.00001-09.

Madigan, M. T., Martinko, J. M., Dunlap, P. V and Clark, D. P. (2008) 'Brock biology of microorganisms 12th edn', *Int. Microbiol*, 11, pp. 65–73.

Meyer, T. E., Tsapin, A. I., Vandenberghe, I., de Smet, L., Frishman, D., Nealson, K. H., Cusanovich, M. A. and van Beeumen, J. J. (2004) 'Identification of 42 possible cytochrome C genes in the Shewanella oneidensis genome and characterization of six soluble cytochromes.', *Omics : a journal of integrative biology*. United States, 8(1), pp. 57–77. doi: 10.1089/153623104773547499.

Nelson, D. L., Lehninger, A. L. and Cox, M. M. (2008) *Lehninger principles of biochemistry*. Macmillan.

Qiu, T. A., Bozich, J. S., Lohse, S. E., Vartanian, A. M., Jacob, L. M., Meyer, B. M., Gunsolus, I. L., Niemuth, N. J., Murphy, C. J., Haynes, C. L. and Klaper, R. D. (2015) 'Gene expression as an indicator of the molecular response and toxicity in the bacterium Shewanella oneidensis and the water flea Daphnia magna exposed to functionalized gold nanoparticles', *Environ. Sci.: Nano*. Royal Society of Chemistry, 2(6), pp. 615–629. doi: 10.1039/C5EN00037H.

Qiu, X., Sundin, G., Wu, L., Zhou, J. and Tiedje, J. (2005) 'for article: Comparative Analysis of Differentially Expressed Genes in Shewanella oneidensis MR-1 Following Exposure to UVC, UVB and UVA Radiation', *Am Soc Microbiol*, 187(10), p. 3556. doi: 10.1128/JB.187.10.3556.

Repine, J. E., Fox, R. B. and Berger, E. M. (1981) 'Hydrogen peroxide kills Staphylococcus aureus by reacting with staphylococcal iron to form hydroxyl radical', *Journal of Biological Chemistry*, 256(14), pp. 7094–7096.

Reth, M. (2002) 'Hydrogen peroxide as second messenger in lymphocyte activation', *Nature immunology*. Nature Publishing Group, 3(12), pp. 1129–1134.

Rhee, S. G., Chang, T.-S., Jeong, W. and Kang, D. (2010) 'Methods for detection and measurement of hydrogen peroxide inside and outside of cells', *Molecules and Cells*, 29(6), pp. 539–549. doi: 10.1007/s10059-010-0082-3.

Schütz, B., Seidel, J., Sturm, G., Einsle, O. and Gescher, J. (2011) 'Investigation of the electron transport chain to and the catalytic activity of the diheme cytochrome c peroxidase CcpA of Shewanella oneidensis', *Applied and Environmental Microbiology*, 77(17), pp. 6172–6180. doi: 10.1128/AEM.00606-11.

Sharma, P., Jha, A. B., Dubey, R. S. and Pessarakli, M. (2012) 'Reactive oxygen species, oxidative damage, and antioxidative defense mechanism in plants under stressful conditions', *Journal of botany*. Hindawi Publishing Corporation, 2012.

Vatansever, F., de Melo, W. C. M. A., Avci, P., Vecchio, D., Sadasivam, M., Gupta, A., Chandran, R., Karimi, M., Parizotto, N. A. and Yin, R. (2013) 'Antimicrobial strategies centered around reactive oxygen species–bactericidal antibiotics, photodynamic therapy, and beyond', *FEMS microbiology reviews*. Blackwell Publishing Ltd Oxford, UK, 37(6), pp. 955–989.

Chapter 5

Generation of a Reactive Flavocytochrome

5.1 Introduction

The results in chapter 3 showed an extended lag phase growth phenotype in *S. oneidensis*, growing aerobically, expressing mutant MtrC. This form of MtrC had the disulphide bond in domain III of the protein disrupted via substitution of the cysteine residues to alanine residues. The protein's functionality in mineral respiration was maintained as goethite reduction was observed with similar rates to that of wild type *S. oneidensis*. This result, together with the fact the extended lag phase was not observed under aerobic conditions, suggested a reaction in the presence of oxygen leading to the observed growth defect. The results of chapter 4 showed that this extension of the lag phase was the result of cell death caused by generation of the reactive oxygen species H_2O_2. This stress was the result of the reduction of molecular oxygen to H_2O_2 which in turn can be converted to even more damaging chemicals via Fenton chemistry. Investigation turned to characterising the protein itself. By further understanding the implications of removing the disulphide bond on the protein itself, the cause of the aforementioned observations could be elucidated. It is clear that the disulphide bind in domain III of MtrC has a role in controlling the rate of oxygen reduction, and thus the rate of reactive oxygen species formation. It is however unclear what that role is.

This chapter aims to carry out a biochemical analysis of purified $MtrC_{C453A}$. A large focus will be put on the ability of flavin molecules to bind to the purified protein as the formation of the flavocytochrome complex has previously been suggested to be much more reactive than the protein alone. This increase in reactivity could explain the generation of H_2O_2 observed in cultures. Other potential mechanisms will also be investigated here, such as the effect of the mutation on the overall structure of the protein. Conformational changes or changes in heme environments could also be leading to the increased reactivity previously described.

5.2 Results

5.2.1 Interaction of Flavin with $MtrC_{C453AA}$-MtrAB

Purification of $MtrC_{C453A}$ from *S. oneidensis ΔmtrC* pC453A revealed that MtrC had formed a complex with MtrAB ($MtrC_{C453A}$-MtrAB). Purification described in methods (Chapter 2.7.1).

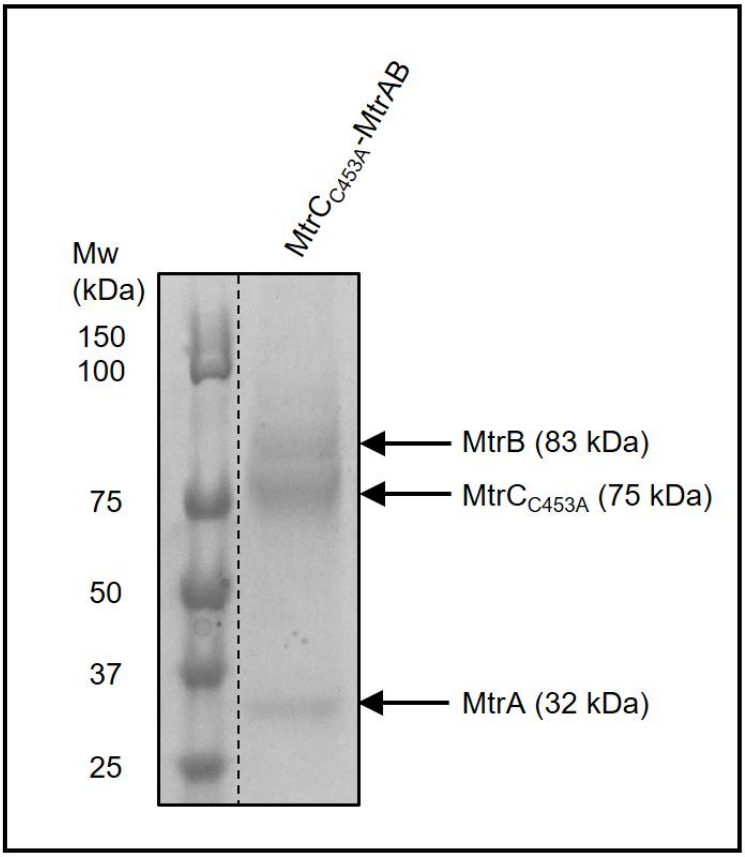

Figure 5.1 – SDS-PAGE gel coomassie stained to show all proteins present after purification. $MtrC_{C453A}$-MtrAB present with bands representative of MtrB (83 kDa), $MtrC_{C453A}$ (75 kDa) and MtrA (32 kDa) highlighted. No other clear bands shown, indicating pure $MtrC_{C453A}$-MtrAB complex obtained.

Coomassie stained SDS-PAGE gel images showed pure MtrC$_{C453A}$-MtrAB had been obtained. The MtrA band is clear at 32 kDa, MtrC can be seen at 75 kDa and MtrB appears at approximates 83 kDa (Figure 5.1). These weights are consistent with those previous attributed to the MtrCAB complex when purified (Ross *et al.*, 2007). This result indicates that MtrC$_{C453A}$ is able to form a complex with MtrAB in a similar way to that of native MtrC. This supports goethite iron reduction experiments that show electron transfer through MtrC$_{C453A}$-MtrAB was maintained.

MtrC$_{C453A}$-MtrAB samples underwent flavin interaction studies first via fluorescence quenching studies. In this FMN was added to samples and its fluorescence measured at time intervals (Chapter 2.9.2). Here if FMN was interacting with MtrC$_{C453A}$-MtrAB, a decrease in fluorescence at 510 nm (indicative of FMN) was expected due to previously reported quenching effects resulting from the interaction between FMN with MtrC$_{C453A}$-MtrAB (Edwards *et al.*, 2015). Such quenching interactions reduce the fluorescence as the excitation and emission energy of the molecule is altered.

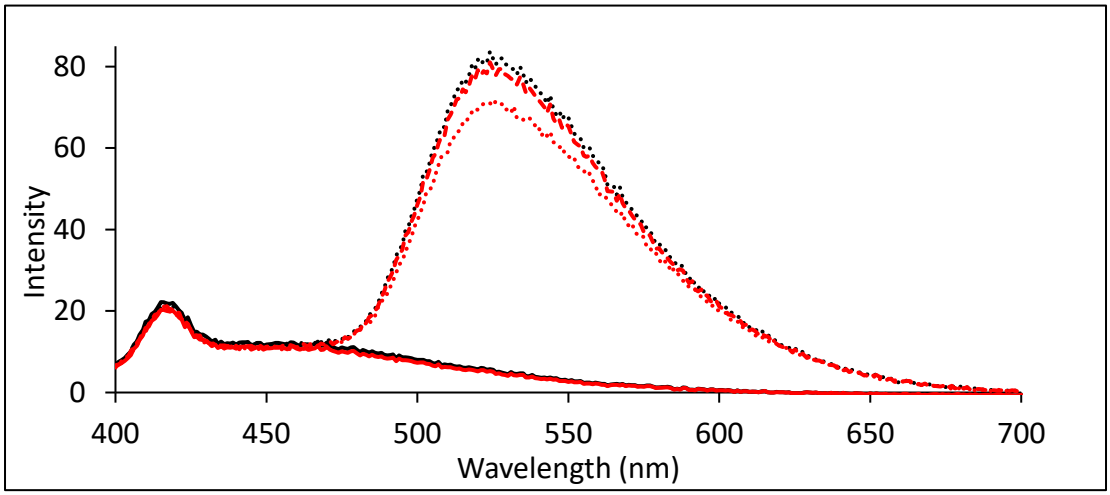

Figure 5.2 – Fluorescence spectra of 0.5 µM MtrC (black) and MtrC$_{C453A}$-MtrAB (red) samples before and after FMN addition resulting in 0.5 µM final concentration. Excitation held at 365 nm, emission wavelength scanned 400 – 700 nm. In samples where FMN was added, spectra was taken at time points (0 min and 10 min) to test for quenching indicative of FMN interacting with the protein. MtrC and MtrC$_{C453A}$-MtrAB without addition of FMN shown as black and red solid lines respectively. Dashed lines represent spectra upon addition of FMN

(0.5 µM final concentration). Dotted lines represent spectra of protein mixed with FMN after 10 min elapsed. 20 mM HEPES pH 7.5 with 5 mM LDAO buffer used throughout.

When 0.5 µM $MtrC_{C453A}$-MtrAB was incubated with 0.5 µM final concentration FMN for 10 min there was a noticeable drop in fluorescence around 510 nm, compared to when the FMN was first added to the solution (Figure 5.2). This decrease was not seen in samples of native MtrC under the same conditions. This showed evidence of quenching of the fluorescence and therefore flavin interaction with $MtrC_{C453A}$-MtrAB.

To gain further evidence of FMN interacting with $MtrC_{C453A}$-MtrAB to support the fluorescence's quenching studies, samples of $MtrC_{C453A}$-MtrAB were incubated with FMN prior to elution through PD10 size exclusion column (Chapter 2.9.3). Here the smaller FMN molecules were able to pass through the column quicker than the much larger protein molecules. Free flavin would pass through before fractions were collected, whilst flavin bound to MtrC would elute in the protein containing fractions. FMN seen bound to MtrC would be binding as a result of the disruption of the disulphide bond. Fractions containing the protein were recovered and fluorescence spectra was analysed for a peak at 510 nm, indicative of FMN. No peak was observed at 510 nm, suggesting that all FMN had remained unbound and was eluted from the column in later fractions (Figure 5.3).

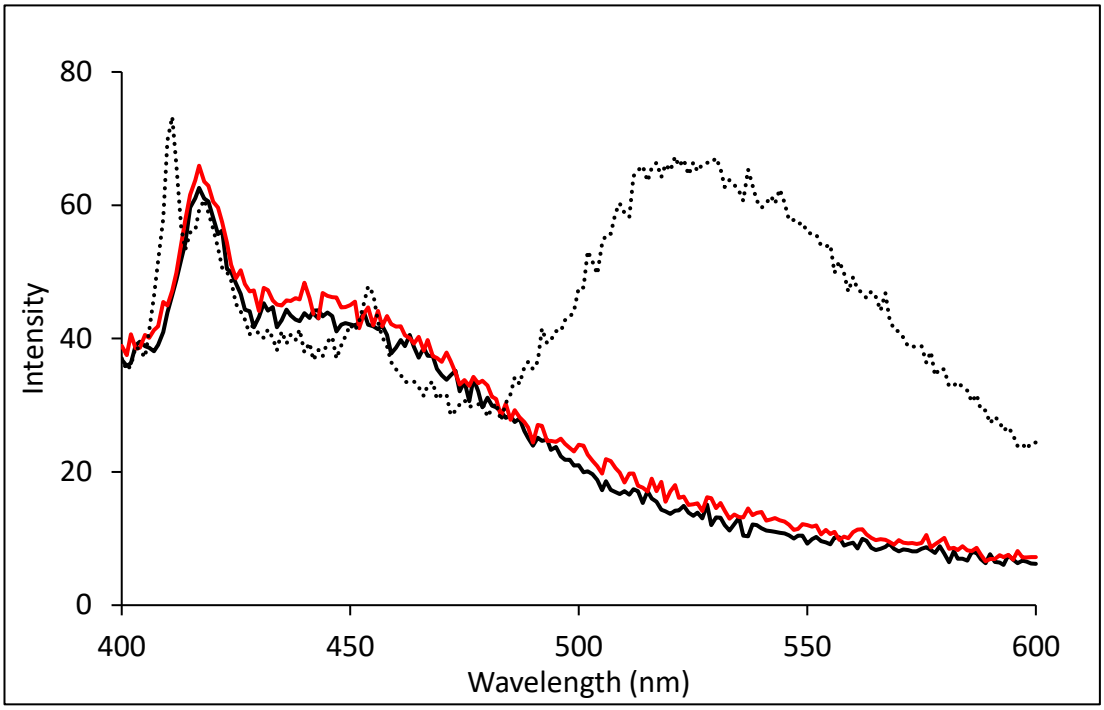

Figure 5.3 – Fluorescence spectra of samples after elution through PD10 size exclusion column under aerobic conditions. Excitation held at 365 nm, emission wavelength scanned 400 – 700 nm. Prior to elution 0.5 µM protein incubated with 0.5 µM FMN for 30 min. FMN control (black dotted line) shows peak at 510 nm indicative of FMN presence. Neither MtrC (black solid line) or $MtrC_{C453A}$-MtrAB (red solid line) samples show signs of 510 nm peak and as such no FMN presence after elution.

5.2.2 Soluble $MtrC_{C453A}$ Generation and Purification

To carry out a detailed study of $MtrC_{C453A,}$ and further investigate possible interactions between FMN and $MtrC_{C453A}$, higher yields of pure $MtrC_{C453A}$ was needed. Purification yield of $MtrC_{C453A}$ was increased via generation of a soluble form of the *mtrC* gene (pLS146 plasmid purified from *S. oneidensis* LS329 supplied by Dr Liang Shi, PNNL and modified by Dr Jessica Van Wonderen, UEA). Mutations were made to the *mtrC* gene, following the previously described protocol (Chapter 2.2), to produce pC453A soluble form with the lipid anchor removed and a strep tag added to the c-terminus (Figure 5.4). This was then transformed into *S. oneidensis ΔmtrC* (LS661) to be expressed using 5 mM arabinose to induce.

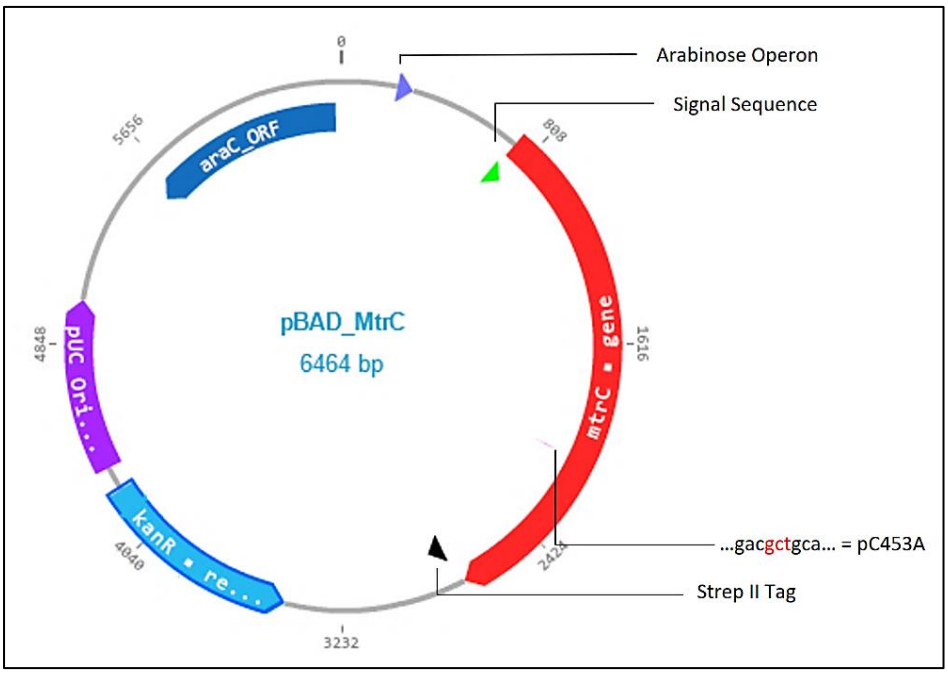

Figure 5.4 – Plasmid map of pBAD_MtrC. Point mutation highlighted for generation of pC453A, bases modified from wild type sequence shown in red. Other elements of use highlighted including arabinose control operon and MtrC C-terminal strep II purification tag.

$MtrC_{C453A}$ was purified from culture media (Chapter 2.7.2). Purity was confirmed through SDS-PAGE gel showing the initial total protein content and the increase in purity of MtrC after strep II tagged purification (Figure 5.5, Panel A) A single band at molecular weight of 75 kDa was seen on Coomassie stained gels (Figure 5.5, Panel B). This indicates pure $MtrC_{C453A}$ was obtained. Dimerization of $MtrC_{C453A}$ could also be checked through the use of non-reducing SDS-PAGE gel technique to run purified protein. The formation of such dimers could have been the result of the free cysteine in the protein's structure (at amino acid position 444). As the gel showed a single band at the expected 75 kDa suggesting no formation of dimers.

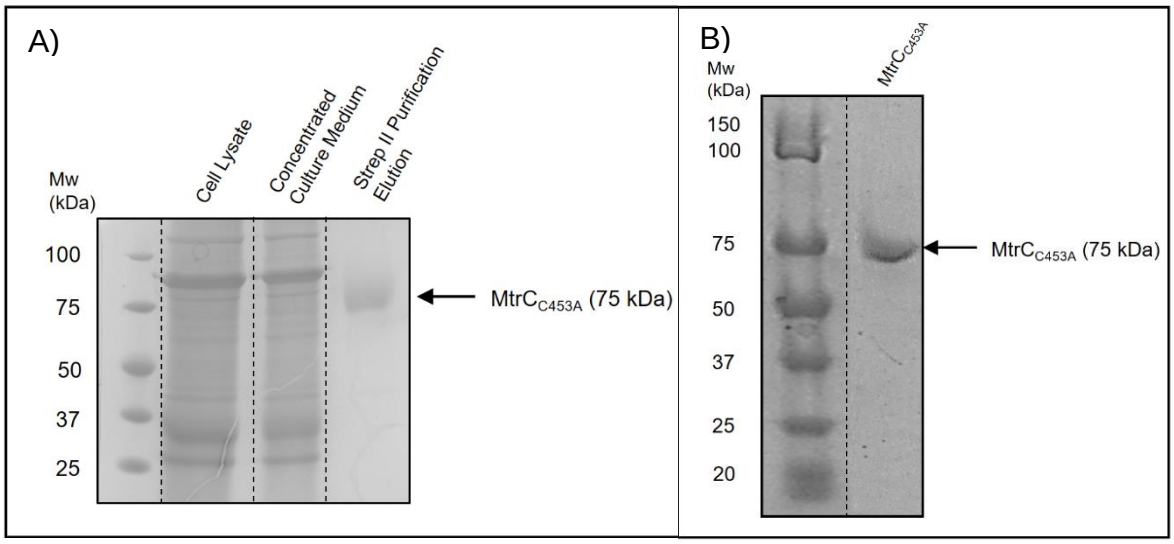

Figure 5.5 – Purification of Soluble MtrC. A) Coomassie stained SDS polyacrylamide gel showing proteins present in cell lysate, concentrated culture medium and elution after strep II purification process. B) Non-reducing Coomassie stained SDS polyacrylamide gel showing concentrated sample after purification process. MtrC$_{C453A}$ present with representative band at 75 kDa highlighted. No other protein bands shown, indicating pure yield of MtrC$_{C453A}$ soluble form obtained.

These results were confirmed via intact mass spectrometry carried out by Dr Gerhard Saalbach at the John Innes Centre proteomics facility. The MALDI-TOF mass spectra of the sample was obtained and run against a mass spectra database to ascertain the peptide chains of the fragments (Figure 5.6). The results from the sample sent showed a full length peptide molecular weight of 75.46 kDa consistent with that of reported monomeric MtrC (75 kDa). It was also consistent with the calculated expected Mw of MtrC: 75.53 kDa (calculated from molecular weight of protein sequence, accounting for cysteine to alanine substitution). These results again suggest pure MtrC$_{C453A}$ was obtained with no contaminants bound to the free thiol residue to the remaining cysteine at amino acid position 444.

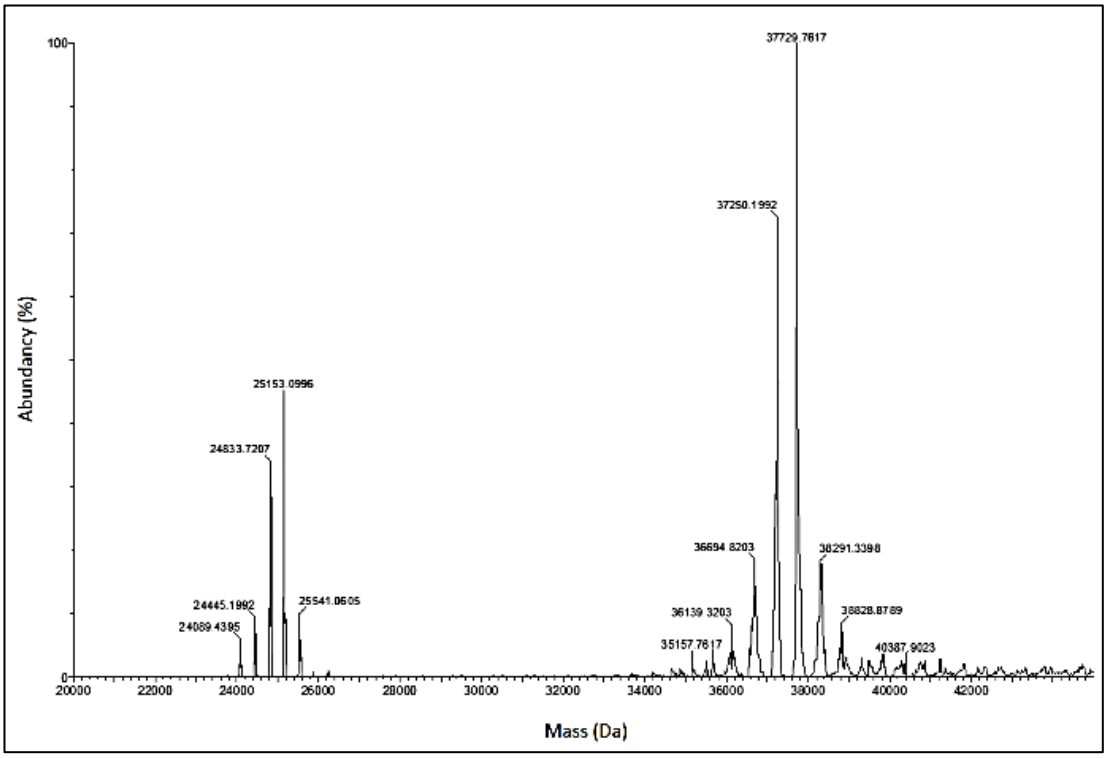

Figure 5.6 – MALDI-TOF mass spectra of $MtrC_{C453A}$ protein sample after purification. Abundance of peptide sequence shown. Clear +2 and +3 charged populations resulting in molecular weight calculation of 75.459 kDa ±0.1. Analysis carried out by the John Innes Centre Proteomics Facility on 20 µl of 1 µg/ml sample in 20 mM HEPES pH 7.6, checked for purity via SDS-PAGE.

5.2.3 Biochemical Characterisation of $MtrC_{C453A}$

UV-visible spectrometry was used to compare the native MtrC to the mutant $MtrC_{C453A}$. The results of this was used to look for bound flavin, remaining through the purification process, as well as investigating the potential presence of a high spin heme, generated by the mutation. Samples of each protein were fully oxidised before sodium dithionite was added causing the proteins to become reduced.

When the oxidised spectra of the native MtrC is overlaid with the oxidised spectra of $MtrC_{C453A}$ and normalised to 1 µM protein concentration, there is no difference in absorbance at 470 nm (Figure 5.7). This suggests that there is no flavin bound to the $MtrC_{C453A}$ sample. Sodium dithionite was then added into samples of MtrC and

$MtrC_{C453A}$ to observe reduced spectra of the proteins (Figure 5.8). Both MtrC and $MtrC_{C453A}$ samples behaved similarly in this experiment with both showing spectra associated with heme reduction. These spectra were used to investigate the potential presence of high spin hemes in the $MtrC_{C453A}$ sample, however there was no discernible peak at ~630 nm (indicative of high spin heme) upon reduction suggesting no evidence of high spin hemes (Saraiva *et al.*, 1990).

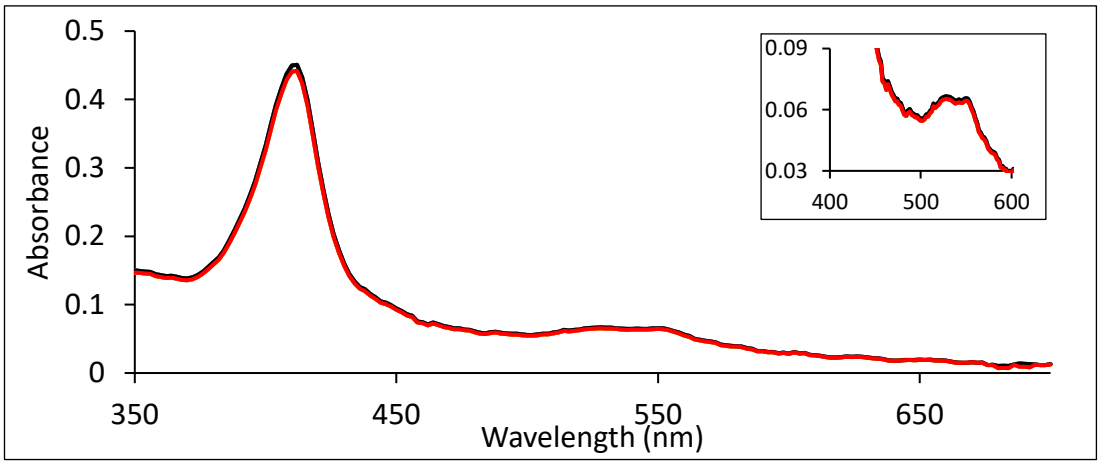

Figure 5.7 – Comparison of normalised UV-vis spectra, 350 nm to 700 nm, for 1 μM oxidised samples of MtrC (black line) and $MtrC_{C453A}$ (red line). *Inset:* area around 470 nm (indicative of flavin binding) highlighted to show no noticeable difference between the traces. 20 mM HEPES pH 7.5 buffer used throughout.

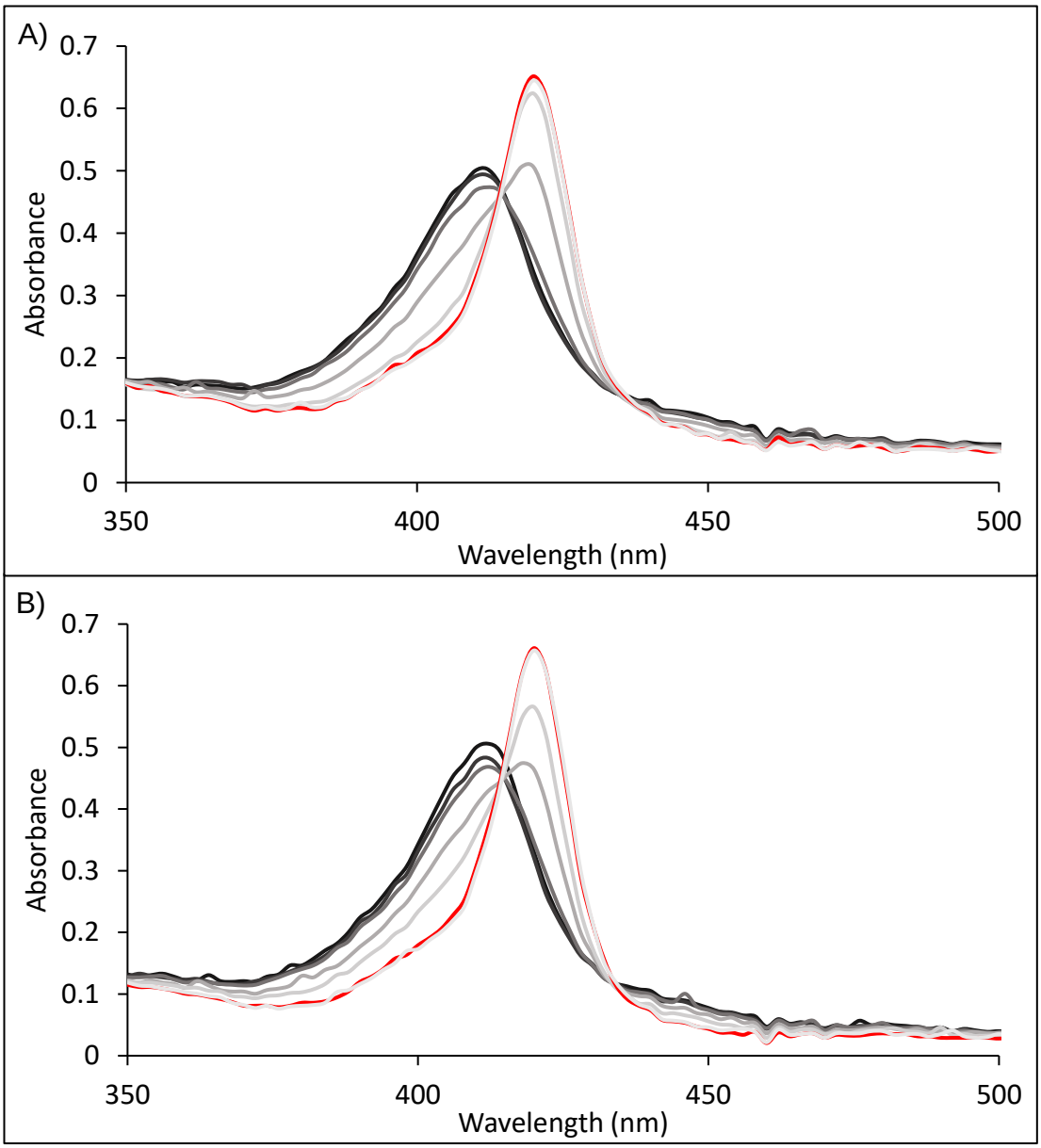

Figure 5.8 – Oxidised (black) to reduced (red) UV-vis spectra, 350 nm to 500 nm, of A) MtrC and B) $_{MtrCC453A}$ protein upon sequential addition of 0.5 µM sodium dithionite. Both A) MtrC and B) MtrC$_{C453A}$ both show distinctive heme reduction trace with soret peak at 410 nm transitioning to 420 nm as reduction of heme residues occurs. Progression of reduction shown in grey with complete reduction occurring when no change in absorbance detected upon 0.5 µM addition of sodium dithionite. 20 mM HEPES pH 7.5 buffer used throughout.

Due to the decaheme nature of MtrC, a single high spin heme in $MtrC_{C453A}$ would only account for 10 % of the heme signal detected. This high spin heme may not appear across the whole population of $MtrC_{C453A}$ and so the signal could be further lowered. This means a high spin heme signature in the UV-vis spectrum could be obscured and so samples of $MtrC_{C453A}$ were sent to a collaborator (Ricardo Louro, ITQB) to undergo NMR analysis. This analysis again showed no indication of a high spin heme being present in $MtrC_{C453A}$ (data not shown).

To further analyse the effect disrupting the disulphide bond in domain III of MtrC had on the structure of the protein, samples underwent crystallisation trials (Chapter 2.8). All experiments and analysis in this section were carried out under the supervision and guidance of Dr Marcus Edwards, UEA. Mtr_{C453A} samples were concentrated to 10 $mg.ml^{-1}$ (final concentration) and quantified via spectroscopy. Sitting drop vapour diffusion crystallisation was then carried out using a range of conditions. After approximately 72 h incubation at 16 ^{o}C crystal formation was observed. Crystals were harvested using 0.1-0.2 mm LithoLoops from conditions containing 30 % PEG 6000, 0.2 M sodium acetate pH 5 and 0.1 M calcium chloride (Figure 5.9). These were then cryoprotected in solution containing 12 % glycerol as a cryoprotectant prior to vitrifying in liquid nitrogen.

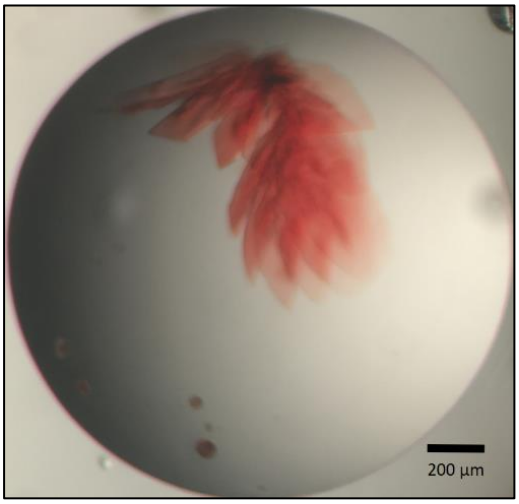

Figure 5.9 – Crystals of strep II tagged $MtrC_{C453A}$ grown at 16 ^{o}C in optimised conditions containing 0.2 M sodium acetate pH 5, 0.1 M calcium chloride and 21 % PEG 6000. All crystals grown using sitting drop vapour diffusion method.

X-ray diffraction of $MtrC_{C453A}$ crystals was carried out using beamline i04 (Diamond Light Source). Wavelength of 0.97 Å was used to collect 360° of data using 0.2° Ω oscillations with 0.1 s exposures to the unattenuated 20 x 20 µm beam. This produced 900 images of data that were integrated using Mosflm (Leslie and Powell, 2007) and scaled using Aimless from the CCP4 suite, which allowed a maximum resolution of 1.86 Å to be determined from the Bragg spots reported by the detector (Figure 5.10). A space group of $P2_12_12_1$ was determined using POINTLESS form the CCP4 suite (Evans, 2011). Average unit cell dimensions were calculated to be a = 53.06, b = 90.33 and c =154.81 Å. The half dataset correlation coefficient ($CC_{1/2}$) was found to be 0.974, suggesting a high level of internal consistency within the scaled and averaged data. Full statistics for the data were also calculated and outputted form Aimless (Table 5.1).

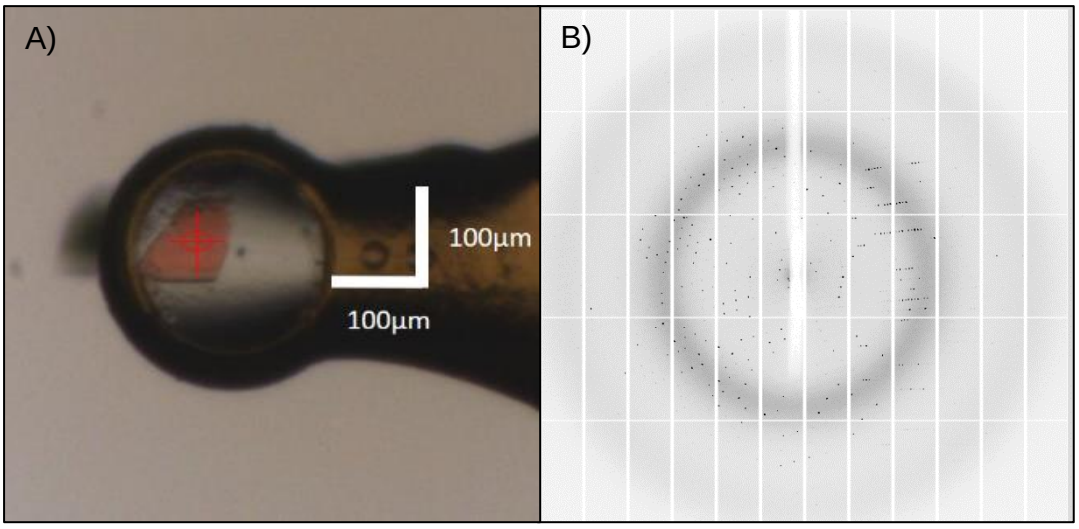

Figure 5.10 – $MtrC_{C453A}$ crystal used for x-ray diffraction data collection. A) X-ray diffraction (λ = 0.97 Å) to a resolution of 1.86 Å on $MtrC_{C453A}$ crystal grown in 21 % PEG 6000, 0.2 M sodium acetate and 0.1 M calcium chloride prior to cryoprotection in 12 % glycerol. B) Bragg spots observed at a maximum resolution of 1.86 Å on detector.

Table 5.1 – Data collection and refinement statistics associated with the crystallographic solution of $MtrC_{C453A}$. Data collection parameters and statistics obtained using XIA2 with final model refinement statistics obtained using PHENIX

Data Collection	**$MtrC_{C453A}$**
Space Group	$P2_12_12_1$
Cell Dimensions	
a, b, c (Å)	53.06, 90.33, 154.81
A, β, ϒ (º)	90, 90, 90
Wavelength (Å)	0.97 Å
Resolution (Å)	1.86 – 90.33
$CC_{1/2}$	0.974
R_{pim} (%)	5.4 (23.7)
I/σI	10.9 (3.3)
Completeness (%)	100
Redundancy	5.9 (5)
Refinement	
Resolution (Å)	1.86
No. Reflections Used	62969
Rwork/Rfree	0.1555/0.1905
No. Atoms	
Protein	9266
Ligand	785
Water	952
RMSD	
Bond Lengths (Å)	0.024
Bond Angles (º)	2.231

Collected datasets were used to solve the structure of $MtrC_{C453A}$ via molecular replacement using Phaser from the CCP4 suite. This was then refined using Phenix.refine from the Phenix suite (McCoy, 2007) giving a final R_{work} of 0.1555 and R_{free} of 0.1905. The protein structure returned was highly similar to that of native MtrC showing no evidence of conformational change resulting from the substitution of the cysteine residue to alanine at amino acid position 453 (Figure 5.11). The dataset showed loss of electron density in a region of domain III of the structure compared to the native MtrC structure (Edwards *et al.*, 2015). This was seen to correlate with the location of the disulphide bond in the native MtrC structure and so confirmed the disruption of the bond in the $MtrC_{C453A}$ structure (Figure 5.12).

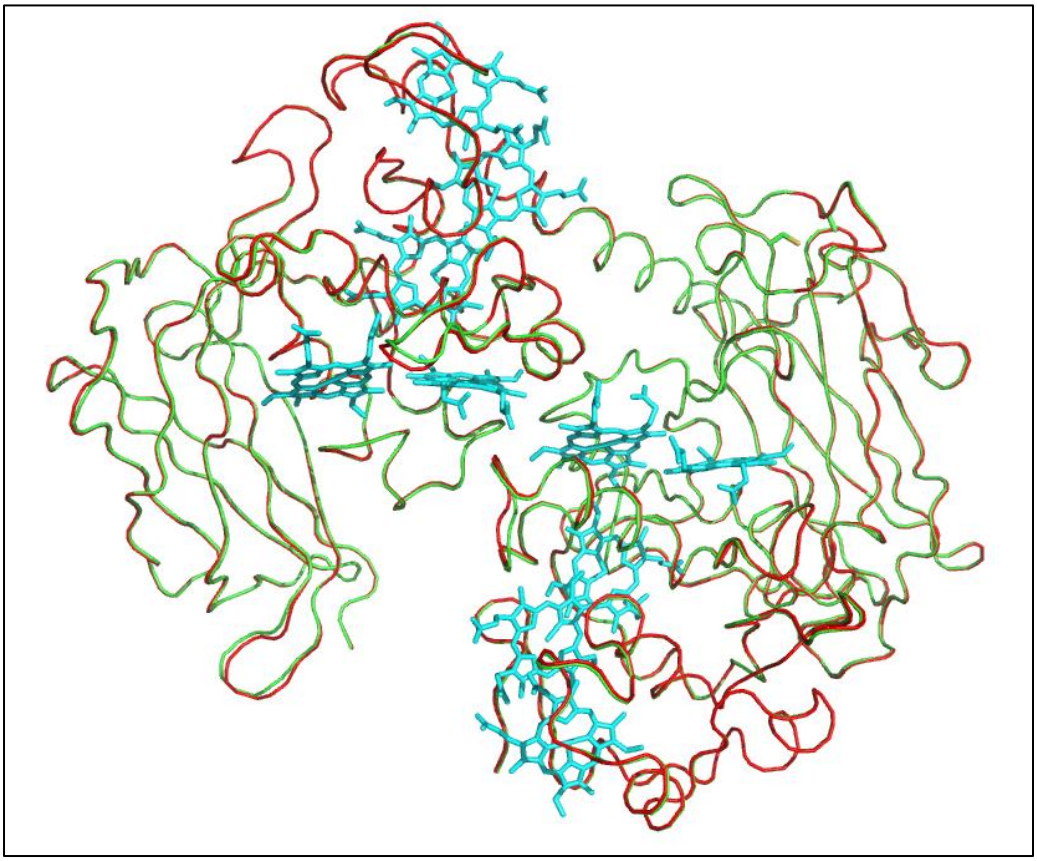

Figure 5.11 – Overlay of MtrC structure (red) with $MtrC_{C453A}$ structure (green). Ribbon representation of amino acid chains with heme residues shown in blue. Cys444 and Ala453 residues shown as sticks. Image produced using PyMOL software.

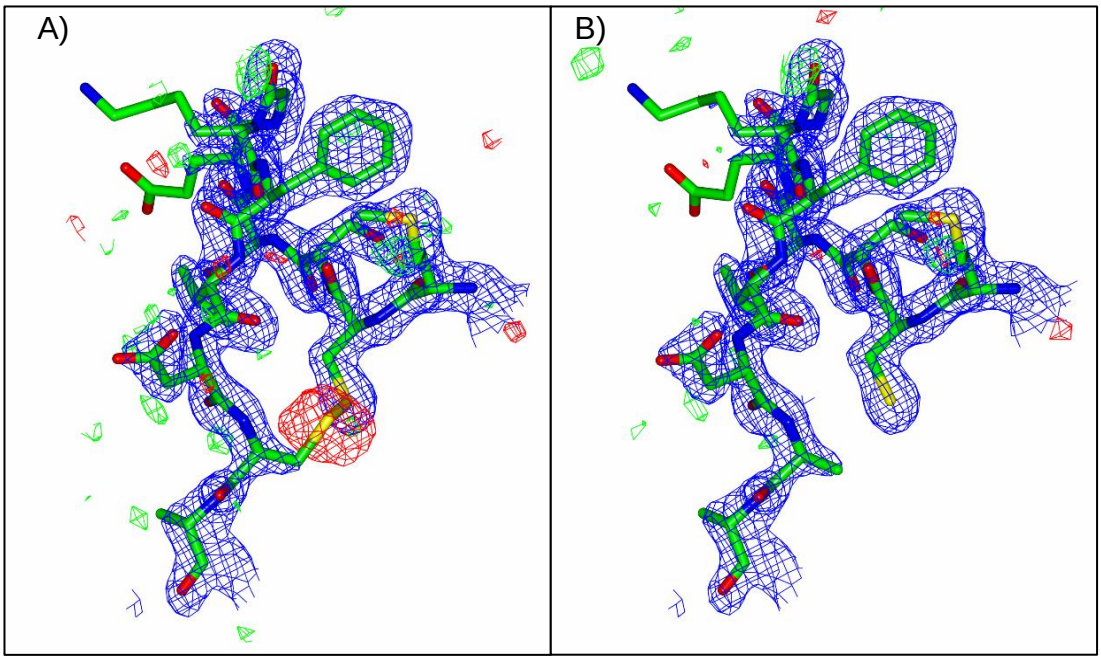

Figure 5.12 – Electron density map with solved amino acid protein structure overlaid. A) Electron density generated form dataset showed high similarity to known structure of Native MtrC (4LM8). Area of low electron density, not matching with overlaid structure highlighted in red. B) Disulphide bond in structure removed by replacing cysteine at amino acid position 453 with alanine residue, showing loss of electron density consistent with mutation introduced into the $MtrC_{C453A}$ structure. Amino acid substituted and image generated using COOT (Emsley *et al.*, 2010).

5.2.4 Flavin Binding to MtrC under Aerobic, Thiol Reducing, and Sodium Dithionite Reducing Conditions

After seeing no evidence of flavin remaining bound to $MtrC_{C453A}$ through the purification process, FMN was added into samples under aerobic conditions. This was done to ascertain if $MtrC_{C453A}$ could indeed bind flavin molecules (which were then stripped during the purification process) or if interactions could not occur under aerobic conditions (Chapter2.9.2).

The results showed no indication of flavin interacting with $MtrC_{C453A}$ (Figure 5.13). Fluorescence intensity, being measured at 510 nm, continued to rise linearly throughout the experiment, consistent with no interaction between the FMN and the protein, counter to similar experiments carried out on $MtrC_{C453A}$-MtrAB.

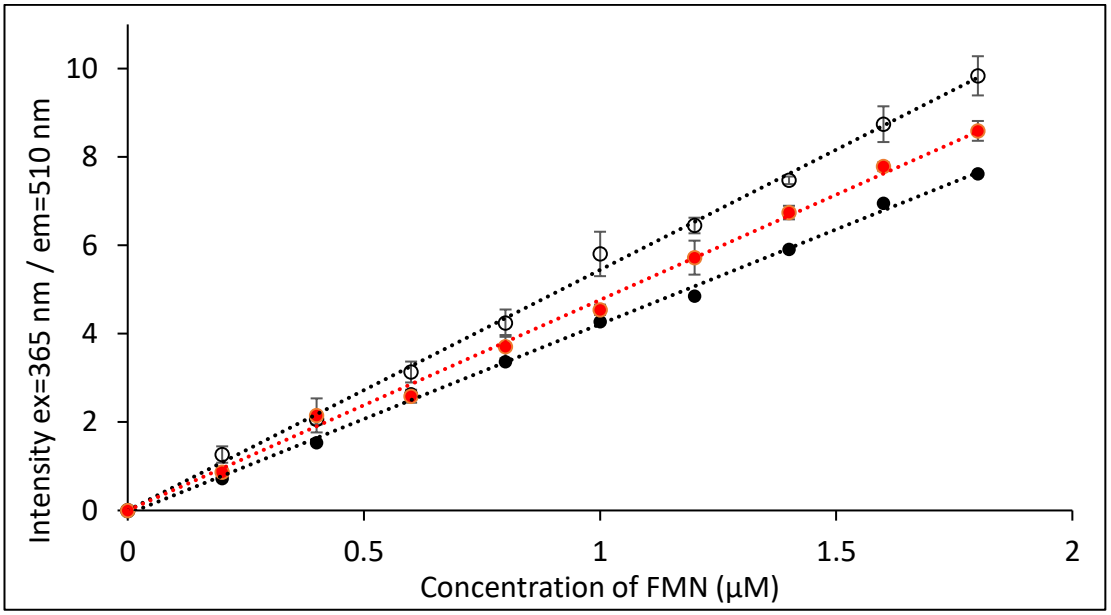

Figure 5.13 – Fluorescence intensity during addition of FMN into 0.5 µM MtrC protein samples. Excitation held at 365 nm and emission readings taken at 510 nm. Readings taken every 0.2 µM addition of FMN (final concentration). 20 mM HEPES pH 7.5 buffer control (open black circles) showed a linear rise in fluorescence intensity as FMN concentration increased. This was mirrored by MtrC (solid black circles) and $MtrC_{C453A}$ (solid red circles) samples suggesting no interaction was occurring between FMN and the protein.

Further investigation was carried out to ascertain if flavin molecules could bind $MtrC_{C453A}$ under thiol reducing conditions. Anaerobic conditions were applied to remove the potential interference of oxygen. Experiments were carried out where FMN was incubated with protein samples prior to elution through a PD10 column. This process separated small molecules such as free FMN from protein (and thus FMN bound protein if present). Fluorescence spectra of the fractions containing protein were then taken to look for presence of bound flavin (Chapter 2.9.3). Again, no peak was observed at 510 nm suggesting FMN had not bound in samples of $MtrC_{C453A}$, just as binding was not seen in native MtrC under these conditions (Figure 5.14).

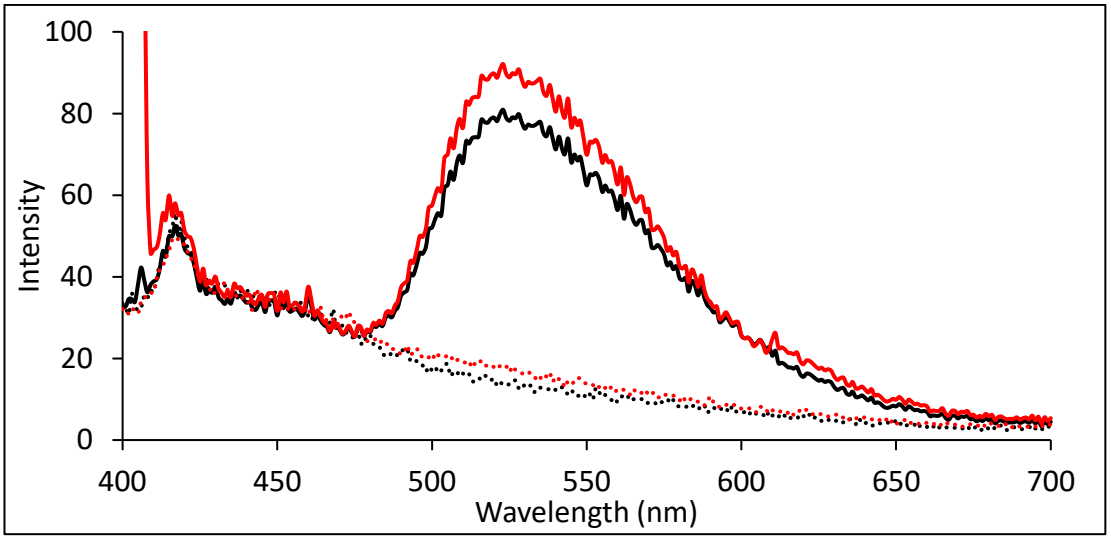

Figure 5.14 – Fluorescence spectra of MtrC (black) and $MtrC_{C453A}$ (red) samples incubated with 1 mM DTT (solid lines) after elution through anaerobic PD10 size exclusion column under anaerobic conditions. Excitation held at 365 nm, emission wavelength scanned 400 – 700 nm. Prior to elution 0.5 µM protein samples were incubated with 0.5 µM FMN for 30 min either in the presence (solid) or absence (dotted) of 1 mM DTT. Carried out in 20 mM HEPES pH 7.5 buffer, normalised to protein concentration.

Replication of previously published results, showing FMN can bind to MtrC when a reducing agent such as DTT is present, was used a positive control for the experiment. DTT was added to separate samples of protein prior to incubation with FMN. Under these conditions MtrC did elute with bound FMN. Interestingly, with DTT present $MtrC_{C453A}$ also eluted with FMN bound (Figure 5.14).

The DTT reducing agent was substituted for another, this time sodium dithionite, before the experiment was repeated. There was again no observed binding of FMN to MtrC or $MtrC_{C453A}$ in the absence of the reducing agent. However, in the presence of 50 µM dithionite, a peak at 510 nm was seen in the fluorescence spectra for $MtrC_{C453A}$ samples (Figure 5.15). This peak was not observed in the MtrC sample suggesting that, under these conditions, only $MtrC_{C453A}$ was capable of binding flavin. With sodium dithionite present in the experiment, FMN and the heme groups of MtrC / $MtrC_{C453A}$ were reduced. The result here implies that the reduction of one or both of these elements allowed for the formation of the flavocytochrome

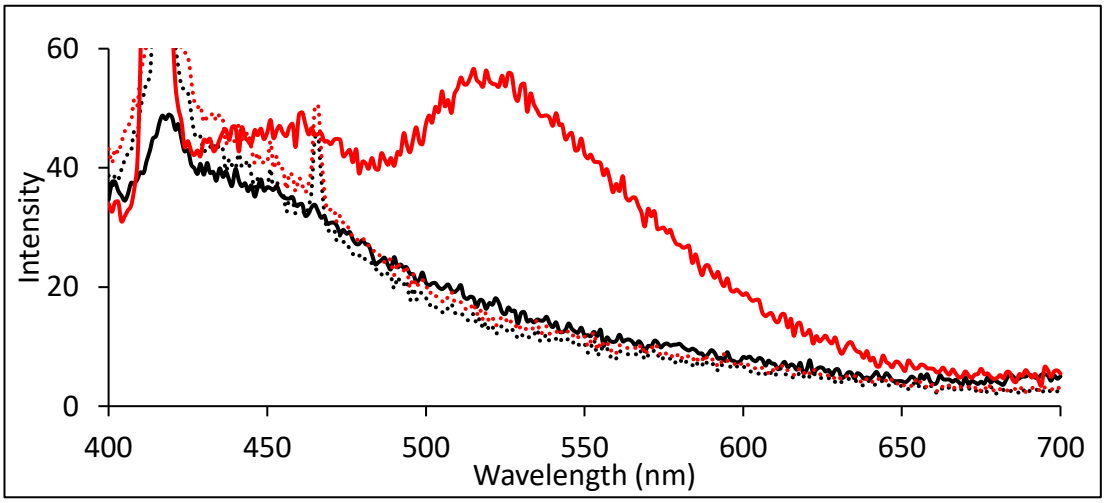

Figure 5.15 – Fluorescence spectra of MtrC (black) and $MtrC_{C453A}$ (red) samples incubated with 50 µM sodium dithionite (solid lines) after elution through anaerobic PD10 size exclusion column under anaerobic conditions. Excitation held at 365 nm, emission wavelength scanned 400 – 700 nm. Prior to elution 0.5 µM protein samples were incubated with 0.5 µM FMN for 30 min either in the presence (solid) or absence (dotted) of 50 µM sodium dithionite. Carried out in 20 mM HEPES pH 7.5 buffer, normalised to protein concentration.

Samples of FMN complexed MtrC and MtrC$_{C453A}$ were exposed to oxygen before being eluted through a further PD10 column. Fluorescence indicative of FMN was measured to compare the protein's ability to retain FMN after exposure to oxidising conditions (Chapter 2.9.3). Native MtrC containing fractions were seen to have no evidence of FMN remaining bound to the protein. Fractions containing MtrC$_{C453A}$ however retained some bound FMN. This could be seen by the rise in intensity at 510 nm above the control of pure MtrC$_{C453A}$ not incubated with FMN (Figure 5.16).

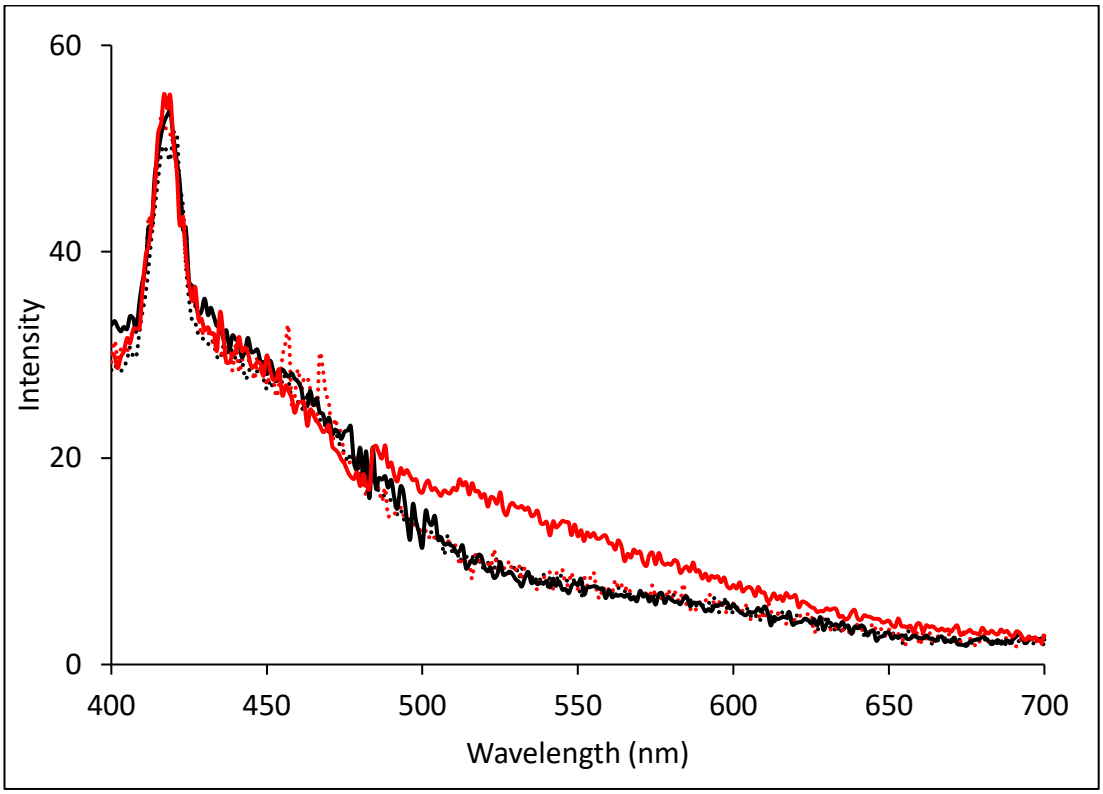

Figure 5.16 – Fluorescence spectra of samples after elution of 0.5 µM protein samples through PD10 size exclusion column under aerobic conditions. Excitation held at 365 nm, emission wavelength scanned 400 – 700 nm. MtrC-FMN flavocytochrome (black solid line) seen to disassociate resulting in loss of 510 nm peak in protein containing fraction, indicating FMN no long bound. MtrC$_{C453A}$-FMN flavocytochrome sample (red solid line) retained partial peak at around 510 nm, indicating some FMN binding remained. Results were confirmed by comparison against protein samples not exposed to DTT, previously shown to be unable to bind FMN (black dotted line MtrC and red dotted line MtrC$_{C453A}$ respective).

5.2.5 H_2O_2 Production by $MtrC_{C453A}$

To investigate the reactivity of $MtrC_{C453A}$ compared to native MtrC, a H_2O_2 fluorescence based assay was employed. This assay allowed for concentration measurements in the nanomolar to micromolar ranges. Protein samples were reduced, under anaerobic conditions, prior to exposure to oxygen. The amount of H_2O_2 formed in the solution was then measured via a fluorescence assay (Chapter 2.6.2). This assay was used to compare the reactivity of the each of the forms of MtrC (native and $MtrC_{C453A}$) as well as comparing the reactivity when FMN was added to the reduced protein prior to exposing to oxygen.

There was no noticeable difference in the amount of H_2O_2 produced by reduced $MtrC_{C453A,}$ compared to native MtrC (+/- 1 nM difference). However, when oxidised FMN was added to protein samples prior to exposure to oxygen, an increased level of H_2O_2 could be seen in both. MtrC + FMN samples generated 8.94 nM H_2O_2 compared to 3.57 nM generated by MtrC alone. The difference was even more pronounced in the $MtrC_{C453A}$ samples. $MtrC_{C453A}$ + FMN generated 23.79 nM H_2O_2 compared to 4.43 nM detected in $MtrC_{C453A}$ samples (Figure 5.17 Panel A). All concentrations were calculated from standard curve of known H_2O_2 standards (Figure 5.17 Panel B). These results suggest that interactions between FMN and the protein did increase reactivity of MtrC. This reactivity was especially increased in $MtrC_{C453A}$ + FMN samples which generated 266 % more H_2O_2 than the native MtrC + FMN flavocytochrome.

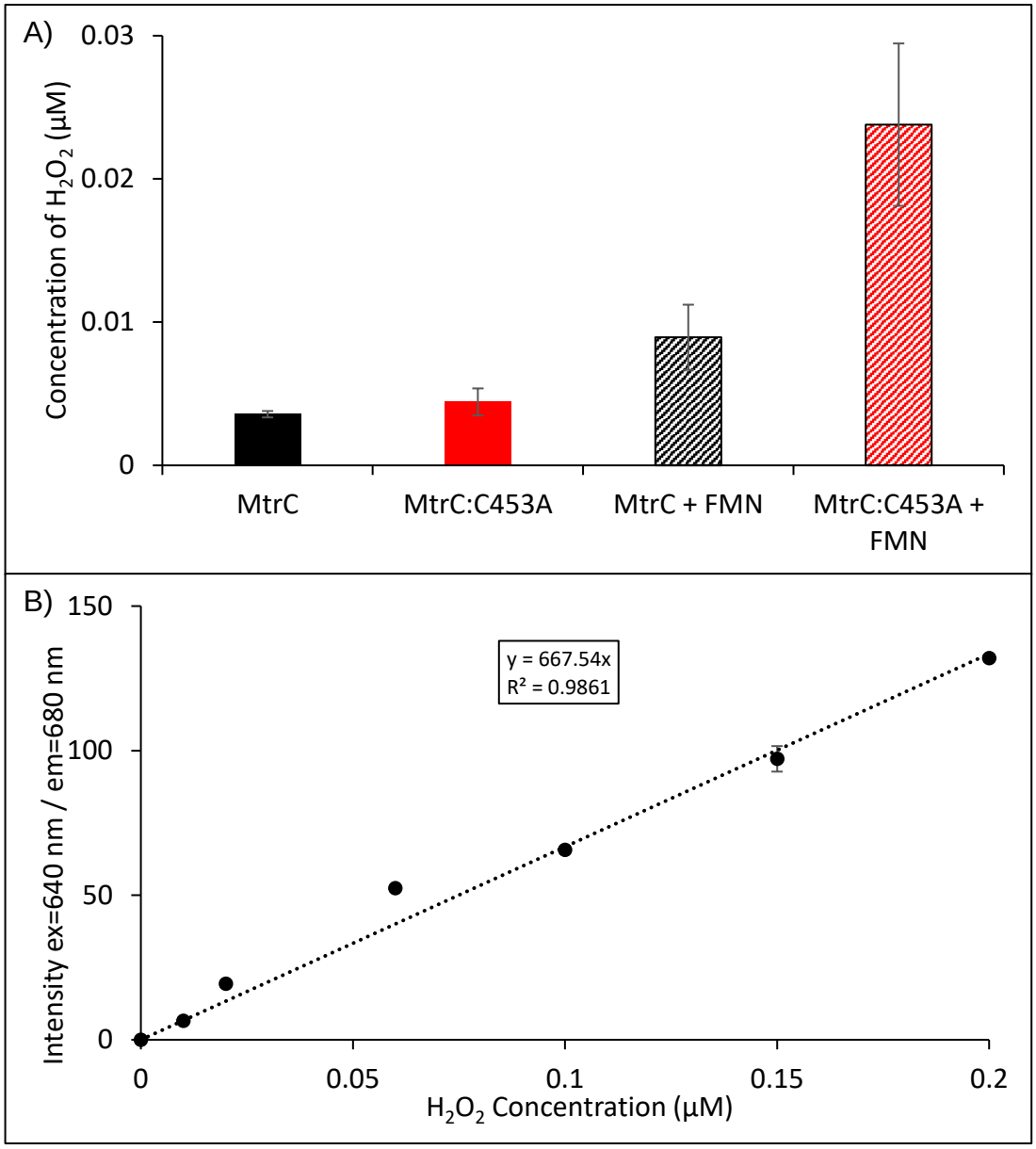

Figure 5.17 – H_2O_2 concentration generated by 0.5 μM reduced cytochrome when exposed to oxygen, with and without the addition of 0.1 μM oxidised FMN. A) concentration of H_2O_2 detected in samples of: MtrC (solid black bar) = 3.57×10^{-3} μM, $MtrC_{C453A}$ (solid red bar) = 4.43×10^{-3} μM, MtrC + FMN (dashed black bar) = 8.94×10^{-3} μM, and $MtrC_{C453A}$ + FMN flavocytochrome (dashed red bar) = 2.38×10^{-2} μM. B) Standard curve generated from known H_2O_2 standards for calculation of concentrations in samples; $y=667.54x$, $R^2=0.9861$. Experiment carried out in 20 mM HEPES pH 7.5 buffer.

5.3 Discussion

5.3.2 Soluble MtrC Generation and Purification

A more detailed investigation into FMN-$MtrC_{C453A}$ complex formation required the separation of $MtrC_{C453A}$ from the complex with MtrAB. This would remove any potential interaction or disruption of MtrAB on FMN-$MtrC_{C453A}$ association. Binding of FMN has largely been investigated and shown in MtrC (un-complexed from MtrAB), and as such, this study may have shown blocking of this FMN binding pocket upon MtrCAB complexation. Current molecular dynamic simulations suggest an optimal FMN binding site close to heme 7 of MtrC (Breuer, Rosso and Blumberger, 2015). Although agreement in the field has MtrC displayed with heme 10 at the interface between MtrC and MtrA, there is little experimental evidence for this. Much of the evidence for this orientation comes from the heme potential estimations from molecular dynamic simulations. However, some studies have suggested alternative orientations for MtrC on the surface of the membrane. As such, it was important to ascertain if removing $MtrC_{C453A}$ from complex with MtrAB was the determining factor in observing FMN binding.

A soluble form of the *mtrC* gene (generated by Dr Marcus Edwards, The University of East Anglia) was used as a template to again substitute the disulphide forming cysteine residues to alanine residues. The decision to move away from the membrane-anchored form was taken to allow higher yields of $MtrC_{C453A}$ to be obtained more quickly. Removing the membrane anchor also allowed for the removal of detergents from buffers, thus removing contributions from said detergents from results. The soluble form *mtrC:C453A* gene was the same as the previously described pBAD_C453A construct (membrane bound form) with two distinct differences. The sequence coding for the lipid anchor that holds MtrC in the outer membrane was deleted. This lead to secretion of the $MtrC_{C453A}$ protein into the growth medium upon exportation to the outer membrane, via the Sec pathway in the *S. oneidensis ΔmtrC* expression strain (Shi *et al.*, 2006). Once in the growth medium, the solution could be concentrated rapidly prior to purification. The second difference between this soluble

form $MtrC_{C453A,}$ compared to the membrane bound form used in previous studies, was the replacement of the His-tag with a strep II-tag. When purifying the membrane bound form, only low efficiency binding was observed between the his-tag and the nickel charged column. This lead to the purification method utilising anion exchange and gel filtration in a two-step process (Chapter 2.7.1). Further investigation, via western blotting with his-tag targeted antibodies, suggested that the his-tag was being cleaved from the protein (data not shown). Due to the membrane bound form requiring the presence of detergent in the purification process, the change to a strep II-tag was not feasible prior to the generation of the soluble form. This was because detergents are known to disrupt the strep-tactin binding to the column resin which can lead to premature elution and sample contamination (Ivanov *et al.*, 2014). Due to the purification protocol for the soluble form $MtrC_{C453A}$ not requiring detergent to be present, the strep II-tag was used and this allowed for one-step purification (Kimple, Brill and Pasker, 2013). The purification process assessed via coomassie stained gel images. Samples of cell lysate and concentrated culture medium were run on a gel and both showed similar protein profiles. The similarity between the samples was likely the result of proteins, released into the culture medium via cell lysis during culturing, being concentrated to similar levels of that seen in the cell lysate samples. A further sample was run of the fraction eluted from the strep II column which showed the majority of proteins had been removed, with a band matching the weight of MtrC (75 kDa) visible. Purity was confirmed via Coomassie protein staining of SDS-polyacrylamide gels containing concentrated samples of the eluted fraction from the strep II purification process. These showed a clear distinct band at approximately 75 kDa, indicating $MtrC_{C453A}$ was present. No other bands were observed suggesting a high purity had been obtained (Figure 5.5, Panel B).

Having obtained purified $MtrC_{C453A,}$ further checks were carried out to ensure physiologically relevant characteristics had been maintained through the purification process. Having a free cysteine remaining in the $MtrC_{C453A}$ structure could have led to unspecific cross-linking. This and the possibility of dimer formation between $MtrC_{C453A}$ molecules could have caused aggregation and other features capable of causing the observed phenotype (Murphy, Ivanenkov and Kirley, 2002). Up until this

point, the ferric iron reduction assays (Chapter 3) were the only evidence of the mutant protein maintaining a functional structure.

Samples of $MtrC_{C453A}$ were run on non-reducing SDS-polyacrylamide gels prior to coomassie protein staining. These showed a single distinct band indicating that monomers had been maintained (Figure 5.5). The exclusion of beta-mercaptoethanol from the SDS-polyacrylamide gel sample buffer removed all reducing agents. If non-specific disulphide bonding was present in the sample, it would not have been disrupted by the gel electrophoresis. If this was the case then the protein band would be expected at a higher molecular weight relative to the polymeric weight (Rao and Murthy, 1991).

Intact mass spectrometry was also carried out on the sample by Dr Gerhard Saalbach at the John Innes Centre proteomics facility. In this technique, proteins are ionised using Matrix-assisted laser ionisation (MALDI) before here being introduced to a time of flight (TOF) mass spectrometer (Chait, 2011). The matrix contained compounds that readily absorb energy from a 266 nm laser. Once ionised, these molecule go onto ionise the sample, causing less fragmentation than direct ionisation of the sample (Hillenkamp *et al.*, 1991). The charged molecules are then subjected to an electric field causing movement based on charge and weight through space to a detector. The resultant signals are allow identification of molecular weight from the mass : charge ratio (Nelson and Cox, 2005). This top-down approach allows for the molecular weight of the whole protein to be measured. The resulting mass spectra shows abundancy of the differently charged fragments. Through charge attribution, molecular weight can be assigned to peptides (Tipton *et al.*, 2011). This allowed full length peptide molecular weight to be calculated as 75.459 kDa ±0.1 from the +3 and +2 charge populations detected in spectra (Figure 5.6). This result again indicates pure $MtrC_{C453A}$ was obtained as the calculated weight fits with the reported 75 kDa and calculated weight of 75.53 kDa (calculated from molecular weight of protein sequence, accounting for cysteine to alanine substitution).

5.3.3 Biochemical Characterisation of $MtrC_{C453A}$

Once pure $MtrC_{C453A}$ obtained; UV-vis spectra, redox titrations and crystallography were employed to evaluate the biochemical characteristics of the protein. Throughout, native MtrC was used as a comparison to ascertain if the disruption of the disulphide bind in domain III of the protein had effected the overall protein structure, as well as any heme environments and cofactor binding.

UV-vis spectra was taken of 1 µM oxidised MtrC and $MtrC_{C453A}$ before overlaying for comparison (Figure 5.7). No significant variation in spectra was observed between the two protein samples. Notably the traces did not vary around 470 nm (see inset). This region has previously been shown to be affected by flavin binding to the MtrC protein and can be used to calculate amounts of bound flavin (Edwards *et al.*, 2015). This result indicates that no flavin molecules were bound to either the MtrC or $MtrC_{C453A}$ samples immediately after purification. As previously discussed, MtrC is known to not bind flavin under the oxidising conditions of the purification process due to the presence of the disulphide bond in domain III of the protein. As $MtrC_{C453A}$ also shows no evidence of flavin binding it could be surmised that disruption of the disulphide was not adequate to allow for said binding. However, it is also feasible that the binding affinity of flavin to the protein would not be sufficient to allow sustained binding throughout the purification process. This lowered level of binding affinity is expected in a flavoprotein where the flavin cofactor is not covalently bound to the protein (Hefti, Vervoort and Van Berkel, 2003).

Samples of MtrC and $MtrC_{C453A}$ underwent a redox titration to obtain fully reduced samples. To achieve this sodium dithionite was added in 0.5 µM (final concentration) increments and UV-vis spectra was taken (Figure 5.8). Both protein samples became fully reduced after 2.5 µM sodium dithionite had been reached. After this point, further additions of sodium dithionite did not alter the characteristic reduced heme spectra. As heme proteins become reduced, the soret peak at 410 nm shifts to give maxima at 420 nm and two more peaks appear at 530 nm and 557 nm in accordance to the formation of ferrous heme. This allows reduction of the protein to be tracked and reduced MtrC and $MtrC_{C453A}$ to be obtained without excess reductant being present

in the sample. Again, spectra for MtrC and $MtrC_{C453A}$ showed no distinct variation indicating that the heme states of the protein had not been altered by the mutation of cysteine to alanine at amino acid position 453. The heme groups of native MtrC are known to be in the low spin state (Hartshorne *et al.*, 2007). It is these low spin heme groups that give rise to the distinctive soret peak at 415 - 417 nm. High spin heme groups display a soret peak at ~630 nm (Saraiva *et al.*, 1990). In the spectra of $MtrC_{C453A}$ described in this section, no evidence of high spin heme can be observed. If a high spin heme was present in the $MtrC_{C453A}$ structure, it could cause the apparent increase in reactivity leading to the production of H_2O_2 seen in whole cell investigations (Chapter 4).

Although no evidence of high spin heme groups was seen in UV-vis spectra of MtrC-C453A samples, the nature of the decaheme protein could be obscuring the data. The heme groups of MtrC all contribute to the spectral trace and as such variation in the signal provided by a single heme in the protein may not be apparent when comparing UV-vis spectra (Ross, Brantley and Tien, 2009). To confirm the result, samples of $MtrC_{C453A}$ underwent NMR analysis (carried out by Ricardo Louro, ITQB) where heme resonance can be attributed to high spin heme (Shokhireva *et al.*, 2007). This experiment confirmed that no high spin heme groups were present in the $MtrC_{C453A}$ structure (data not shown). The presence of a high spin heme could have accounted for the increased H_2O_2 generation owing to changes in the reduction potential of the residue (Saraiva *et al.*, 1990). The absence of such a high spin heme implies that the H_2O_2 production is instead being caused via another mechanism involving $MtrC_{C453A}$.

The crystal structure of $MtrC_{C453A}$ was solved to allow investigation into possible changes in the protein's conformation following the disruption of the disulphide bond in domain III of the protein. Such conformational change could be the mechanism that allows flavin binding to the protein when the disulphide bond is reduced. $MtrC_{C453A}$ Crystals were grown in conditions known to allow native MtrC crystal formation and harvested before undergoing experimentation at Diamond Light Source. Data was collected and processed to allow elucidation of the protein's structure. All experiments

and data processing was carried out under the guidance of Dr Marcus Edwards (The University of East Anglia). The space group $P2_12_12_1$ was determined by POINTLESS with dimensions of a = 53.06, b = 90.33 and c = 154.81 Å (Table 5.1). This was comparable to the cell dimensions previously reported for native MtrC of a = 53.12, b = 90.44 and c = 154.34 Å (Edwards *et al.*, 2015). After processing the $CC_{1/2}$ statistical test showed high level of internal consistency for the scaled and averaged data with a value of 0.974, well within the recommended $CC_{1/2}$ of 0.5 (Diederichs and Karplus, 2013). The electron density map generated from the data was overlaid with the structure of native MtrC to highlight changes between the two structures. A notable loss in electron density was observed in domain III where the disulphide bond appears in the native structure but no other significant variations were seen. Molecular replacement was used to solve the structure of the $MtrC_{C453A}$ and this confirmed that the loss in electron density noted was the result of the disulphide bond now being absent from the structure (Figure 5.12). Some residue side chains assigned to the $MtrC_{C453A}$ structure did not fit well into the electron density map, however in all cases this was the result of the residues having flexible sidechains and being located in looping regions resulting in disorder that affects the electron density map (Papaleo *et al.*, 2016). As noted the overall structure of $MtrC_{C453A}$ was unchanged to that of native MtrC suggesting the disruption of the disulphide bond had not lead to the opening of a flavin binding pocket on the surface of the protein. However it should be noted that the $MtrC_{C453A}$ protein was crystallised without FMN being bound. Crystal trials with FMN added were unsuccessful (data not shown) and as such it is unknown if binding of FMN would be needed to stabilise any conformational change through the crystallising process.

5.3.4 Binding of Flavin to $MtrC_{C453A}$

To undertake a biochemical characterisation of the $MtrC_{C453A}$ protein, purified samples were first needed. Initially, outer membranes were extracted from cultures of pBAD_C453A before solubilising, allowing for purification of $MtrC_{C453A}$ in complex with MtrAB ($MtrC_{C453A}$-MtrAB). Samples were run on SDS-PAGE gels prior to coomassie staining, allowing visualisation of all proteins present. Distinct bands were

observed at molecular weights expected for MtrA (32 kDa), MtrB (83 kDa) and MtrC-$_{C453A}$ (75 kDA). No other clear bands were observed indicating high purity (Figure 5.1). The ability to purify MtrC$_{C453A}$ in complex with MtrAB again shows that the substitution of the cysteine residue to an alanine residue does not impact on the proteins physiological function. This finding also supports the previously described finding that *S. oneidensis ΔmtrC* expressing pC453A was capable of ferric iron reduction through the MtrCAB pathway.

The isolation of the protein complex allowed for experiments to be carried out without contribution from other cellular proteins or processes. Investigations into FMN binding to the purified complex aimed to ascertain if the removal of the disulphide bond in domain III of the protein allowed for FMN-MtrC$_{C453A}$ complexes to form as previously hypothesised in studies (Edwards *et al.*, 2015). Fluorescence quenching studies were first carried out. In which 0.5 µM FMN was added to 0.5 µM MtrC and MtrC$_{C453A}$-MtrAB. Fluorescence spectra was taken just after addition as well as 10 min after addition. The presence of FMN gave rise to the distinctive flavin signal at approximately 510 nm in all samples. After 10 min the intensity of the peak had decreased in samples of MtrC$_{C453A}$-MtrAB whilst remaining unchanged in MtrC samples (Figure 5.2). This result shows evidence of fluorescence quenching, contrary to result from soluble form MtrC$_{C453A}$. However, it is worth noting that previously described fluorescence quenching upon FMN-MtrC interactions was much greater than reported in this study with MtrC$_{C453A}$-MtrAB. A 5-fold reduction in fluorescence intensity was previously reported when FMN was incubated with MtrC using glutathione to reduce the disulphide bond in domain III of the protein (Edwards *et al.*, 2015). This compared to only a small reduction in this study, which implies that the interactions observed here are fewer than in the previous study with much of the FMN remaining in free solution. In these experiments, we observe a case of static quenching. This is when complex formation occurs between a fluorophore and another non-fluorescent molecule (in this case the MtrC protein) resulting in a change in the ground state of the new complex. When the fluorophore is then excited, the resulting fluorescence is emitted at a lower intensity allowing identification of interactions between the fluorophore and the protein (Weber, 1948).

Previous studies have shown FMN-MtrC complex formation through the use of a size exclusion column to separate protein from free FMN in solution (Edwards *et al.*, 2015). These experiments were replicated to further test the observed association between $MtrC_{C453A}$-MtrAB and FMN. As seen in the aforementioned studies, FMN-MtrC complexes did not form when protein was incubated with FMN prior to elution through a PD10 size exclusion column (Figure 5.3). Interestingly there was also no peak observed at approximately 510 nm in the fluorescence spectra of $MtrC_{C453A}$-MtrAB samples. The lack of the indicative flavin peak shows $MtrC_{C453A}$ also failed to associate tightly with FMN in this experiment. Although the evidence might suggest no FMN-$MtrC_{C453A}$ complex was formed (and thus the $MtrC_{C453A}$-MtrAB protein eluted without the FMN), it could also imply a weak interaction between the $MtrC_{C453A}$ and FMN. In this case, FMN-$MtrC_{C453A}$-MtrAB complexes did form, however, the association was not tight enough to be maintained when eluted through the column (Hu *et al.*, 2012). In either case, the results suggested removal of the disulphide bond via mutation (as in $MtrC_{C453A}$) did not allow for tight association between $MtrC_{C453A}$-MtrAB and FMN as seen when the disulphide bond in isolated native MtrC is chemically disrupted.

The presence of the MtrAB in complex with $MtrC_{C453A}$ made it difficult to probe the system further. Further flavin binding experiments were carried out on isolated $MtrC_{C453A}$ purified from *S. oneidensis ΔmtrC* expressing the previously described soluble form of MtrC. First the protein's ability to bind FMN under aerobic conditions was assessed. When FMN was added into samples of purified $MtrC_{C453A}$, fluorescence intensity was seen to rise linearly as more FMN was added to the sample (Figure 5.13). This results suggests that there was no binding interaction between the FMN and $MtrC_{C453A}$. Similar experiments carried out on known flavin binding proteins have shown that if flavin molecules bind to proteins, there is a quenching of fluorescence. Results in this case would show a slow increase in intensity until the protein had become saturated with flavin molecule, at which point the fluorescence would increase dramatically as the full flavin signal would be detected (Duurkens *et al.*, 2007). In our experiment it is known that excess FMN has been titrated into protein samples as previous studies have shown an approximate

1:1 binding ratio or FMN to MtrC (Edwards *et al.*, 2015). This means that an increase in fluorescence intensity would have been expected after 0.5 µM FMN had been titrated into the 0.5 µM $MtrC_{C453A}$ sample if binding was occurring.

Further investigation into FMN interaction with $MtrC_{C453A}$ looked to establish if binding could occur under previously reported conditions that demonstrated reduction of the disulphide bond in domain III allowed binding between FMN and MtrC (Edwards *et al.*, 2015). MtrC and $MtrC_{C453A}$ samples were incubated with FMN for 30 min prior to elution through PD10 size exclusion columns. Other protein samples were first treated with DTT to reduce any bonds forming between cysteine residues in the proteins before undergoing FMN incubation and elution through columns. Fluorescence spectra for samples that underwent the experiment without exposure to DTT showed no FMN signal in protein containing fractions. This result showed no binding of FMN to purified $MtrC_{C453A}$. However, the spectra for the samples that were treated with DTT prior to FMN incubation did show the presence of the distinctive FMN signal at 510 nm (Figure 5.14). This result reinforced the published results of FMN-MtrC complexes forming when the disulphide in domain III of the protein had been chemically reduced (Edwards *et al.*, 2015). It also raised the question of what effect the DTT was having on $MtrC_{C453A}$ which lacks the disulphide bond thus cannot be being reduced allowing for FMN to bind to the protein. Non-reducing gels and intact NMR had also shown no evidence of higher order complexes forming in the protein samples - a potential result of the remaining free cysteine in the $MtrC_{C453A}$ structure (Figure 5.5 and Figure 5.6).

Samples of MtrC and $MtrC_{C453A}$ was again incubated with FMN prior to elution through size exclusion columns, however, this experiment included the reducing agent sodium dithionite rather than DTT. When $MtrC_{C453A}$ was treated with sodium dithionite before incubation with FMN, the protein was seen to elute with FMN in complex. This can be seen by the presence of the distinctive flavin signal in the fluorescence spectra at 510 nm (Figure 5.15). In this experiment, no FMN-MtrC complex was seen to form in samples of native protein. This shows distinct difference in the FMN binding mechanism between MtrC and $MtrC_{C453A}$. Unlike DTT, Sodium dithionite appears unable to reducing the disulphide bond in this experiment, perhaps due to the pH of

the system not allowing for sufficient protonation of the thiol groups during disulphide reduction (Hoffman and Hayon, 1972). Although dithionite is a stronger reducing agent than DTT they reduce disulphide bonds via different mechanisms. DTT reduces disulphide bonds through two sequential thio-disulphide exchange reactions in which the thiolate of DTT first reacts with one of the cysteine residues forming the disulphide bond. The second thiol of DTT then becomes oxidised leading to full reduction of the disulphide bond (Cleland, 1964). Sodium dithionite instead reduces the disulphide bond via formation of the SO_2^- ion (Bradic and Wilkins, 1984). This difference in mechanism may also lead to differences in disulphide reduction. Further investigation will be needed to confirm the underlying difference. However whatever the case, this data suggests that in both experiments the reducing agents were having a greater effect than simply reducing the disulphide bond. It suggests that the flavin molecules must become reduced before they are able to bind to the MtrC protein where the disulphide bond in domain III is reduced or removed via mutation.

Flavin molecules are known to readily reduce in light as an organic photosensitiser. In this process light energy is absorbed electrons in the molecule become excited to a higher energy state. This is known to happen under both aerobic and anaerobic conditions when FMN is exposed to light. However, the amount of photoreduction of FMN in aqueous solution is usually low. When a reducing agent such as DTT or sodium dithionite is present in the solution, the amount of photoreduction of FMN is increased. Under these conditions the re-oxidation rate of FMN is also slowed, allowing the reduced state to persist in solution longer (Song, Dick and Penzkofer, 2007). Generally, the excited electron losses energy via vibrational transitions before returning to its ground state. This process can see energy emitted as heat and / or fluorescence. However, it is also possible for energy to be transferred from the photo-excited molecule to another molecule in close proximity, termed molecular quenching. This process has been observed between FMN and MtrC in studies showing sufficient molecular quenching occurs to drive electrons through MtrC and across a liposome membrane with no other electron driving source (Ainsworth *et al.*, 2016). With this in mind, it can be postulated that once FMN becomes bound to MtrC, photoreduction could lead to excitation within the MtrC protein. This could in turn affect the driving

force of electrons through the staggered heme cross motif and the heme potentials themselves (again making electron transfer through MtrC more favourable). If remained bound, with no other source of electrons, this photoreduction could itself provide a source of electrons to transfer through MtrC.

FMN dissociation from the MtrC complex upon exposure to oxygen has previously been attributed to the oxidation of the disulphide bond (Edwards *et al.*, 2015). In this study, when exposed to aerobic conditions (prior to further elution through size exclusion columns) partial dissociation of FMN from $MtrC_{C453A}$ was observed. This indicative peak at 510 nm was seen to decrease in intensity, however it did not deplete entirely as seen in MtrC native samples (Figure 5.16). It can be inferred from this result that there is stringer interactions between $MtrC_{C453A}$ and FMN than there for MtrC. This would be consistent with the hypothesis that the redox state of the disulphide bind does play a role in controlling interactions between FMN and MtrC. The experiment does not address the effect of the FMN becoming oxidised under these conditions. This could also be a contributing factor leading to dissociation of the complex, as its reduction has here been shown to be crucial for stronger interactions to occur.

5.3.5 H_2O_2 Production by $MtrC_{C453A}$

Having established conditions where $MtrC_{C453A}$-FMN complexes form, studies were carried out to ascertain the effect of such binding on reactivity of the protein. Previous experiments have implicated $MtrC_{C453A}$ in increased H_2O_2 generation under aerobic conditions (Chapter 4). Anaerobic protein samples were reduced prior to exposure to oxygen and levels of H_2O_2 generated were measured as a measure of reactivity. This experiment showed no significant difference in H_2O_2 generation between purified 0.5 µM MtrC and 0.5 µM $MtrC_{C453A}$ samples. However, when reduced MtrC and $MtrC_{C453A}$ were incubated with 0.1 µM FMN prior to exposure to oxygen, increased levels of H_2O_2 were observed. Samples of MtrC were seen to produce 250 % more H_2O_2 than samples without FMN addition. $MtrC_{C453A}$ samples were seen to make 537 % more H_2O_2 than $MtrC_{C453A}$ without FMN addition (Figure 5.14). It should be noted that the

absolute H_2O_2 values measured may not have been accurate due to the range of standards used not being ideal. However, even though the amounts may vary upon more detailed study, the proportional differences still show that more H_2O_2 was produced in the $MtrC_{C453A}$ samples when FMN was present.

The increase in H_2O_2 concentration detected in MtrC with addition of FMN could be down to reduction of the FMN by the MtrC protein. It has previously been proposed that OMCs of *S. oneidensis* could reduce FMN in a 2-electron transfer reaction (Brutinel and Gralnick, 2012). In this scenario, the FMN could likely then reduce the molecular oxygen leading to the generation of H_2O_2. However, further studies into FMN reduction by MtrC have suggested the reaction to be thermodynamically unfavourable with an E_m of free FMN being -220 mM versus SHE, far lower than that of MtrC (Okamoto *et al.*, 2013). An alternative mechanism could involve the MtrC protein reducing molecular oxygen itself with photoreduction in the presence of FMN helping to drive the electron transfer, though whether the FMN is bound during this interaction is unknown. As previously described, FMN can readily be photoreduced with and without addition of an exogenous reducing agent (Song, Dick and Penzkofer, 2007). This has been seen able to drive the reduction of MtrC through electron transfer between the FMN and MtrC protein with the HEPES buffer potentially functioning as a sacrificial electron donor (Ainsworth *et al.*, 2016). The increase in H_2O_2 was much higher in the $MtrC_{C453A}$ samples (with addition of FMN) suggesting an additional mechanism, beyond background photoreduction of MtrC via FMN, contributing to H_2O_2 generation. These results would suggest an increase in reactivity of $MtrC_{C453A}$ over that of native MtrC and perhaps suggests $MtrC_{C453A}$ more readily interacts with FMN than MtrC.

Further experiments would be needed to fully explore this. It can be hypothesised that the reduced $MtrC_{C453A}$ reduces the FMN in solution allowing it to form a complex with the protein. The native MtrC would likely also be reducing the FMN, however, the presence of the disulphide bond inhibits interactions between FMN and the protein. This would suggest that reactivity is increased upon formation of the $MtrC_{C453A}$-FMN flavocytochrome. In this study, it is not currently clear if this is the result of the complex

increasing the frequency of photoreduciton, leading to effectively higher concentrations of reducing agents for the oxygen. Alternatively, the interaction of FMN could lead to changes in the heme potentials of MtrC. This could make the reduction potential of the protein more favourable for oxygen reduction and facilitate faster electron transfer through the protein. This model of increased reactivity upon binding of flavin to outer membrane cytochromes has previously been supported with molecular dynamic simulations. These indicated an up shift in oxidised FMN and semi-quinone (FMNH) transfer redox potentials and a down shift in semi-quinone and hydro-quinone ($FMNH_2$) potentials when flavin is bound, resulting in a stronger driving force of electrons through the protein (Hong and Pachter, 2016).

5.4 Conclusion

Disruption of the disulphide bond in domain III of MtrC via substitution of the cysteine residue at amino acid position 453 to an alanine residue alone does not lead to formation of flavocytochrome. There was quenching evidence that, when $MtrC_{C453A}$ was in complex with native MtrAB, FMN interacted with the protein. However, further investigations showed any potential association to be far weaker than previously expected. Further investigation into $MtrC_{C453A}$ flavin binding also showed no evidence of FMN binding to protein under the conditions and environment it was purified in.

Due to challenges faced when working with $MtrC_{C453A}$-MtrAB solubilised in detergent, a soluble form of $MtrC_{C453A}$ was generated. The removal of the membrane anchor and the replacement of the His purification tag with a strep-II tag allowed for relatively large amounts to be purified. Binding of FMN to soluble $MtrC_{C453A}$ could be seen upon the introduction of reducing agents (previously seen capable of chemically disrupting the disulphide bond in native MtrC). This was not due to the reducing agent resolving interference caused by a free cysteine residue as studies showed no structural or topological effects of said cysteine. Further studies using reducing agents unable to affect disulphide bridges highlighted binding to be only be possible in the presence of reduced . This interaction was seen to persist upon exposure to oxidising conditions,

suggesting requirements for initial interaction to be reduction of the disulphide bond in domain III of MtrC and reduction of the flavin. Whereas, once bound the oxidation of FMN is not the singular cause of disassociation.

When native MtrC is incubated with DTT the disulphide bond in domain III of MtrC becomes reduced. The FMN present in solution also becomes reduced and interacts with the protein. Upon exposure to oxygen, the disulphide bond and the FMN becomes oxidised and no longer interact in the same manner (Figure 5.18 Panel A). When sodium dithionite is instead used as the reducing agent, the FMN becomes reduced but the disulphide bond does not. The disulphide bond prevents the interaction of FMN with MtrC by maintaining structural rigidity of the protein (Figure 5.18 Panel). In the case of $MtrC_{C453A}$, whether DTT or sodium dithionite is incubated with the protein, FMN becomes reduced. In both cases the disulphide bond is already disrupted due to the substitution of the cysteine residue with alanine. This allows interactions between FMN and $MtrC_{C453A}$ to occur and this association is maintained to some degree upon exposure to oxygen (Figure 5.18 Panel C).

This flavocytochrome form of MtrC appears to be more reactive than the protein alone. Studies showed that reduced $MtrC_{C453A}$ was able to reduce oxygen more easily than native MtrC when FMN was present in solution. In this case, the reduction of FMN appears to be allowing for interactions with the protein leading to increased electron transfer and the possibility of photoreduced FMN providing electrons for the reduction of oxygen through the cytochrome.

This chapter has shown conditions under which FMN can be seen interacting to MtrC and results have implicated this flavocytochrome as a more reactive form of the protein. This work provides the biochemical basis to explain the whole cell phenotype characterised in previous chapters caused by increased H_2O_2 in cell cultures.

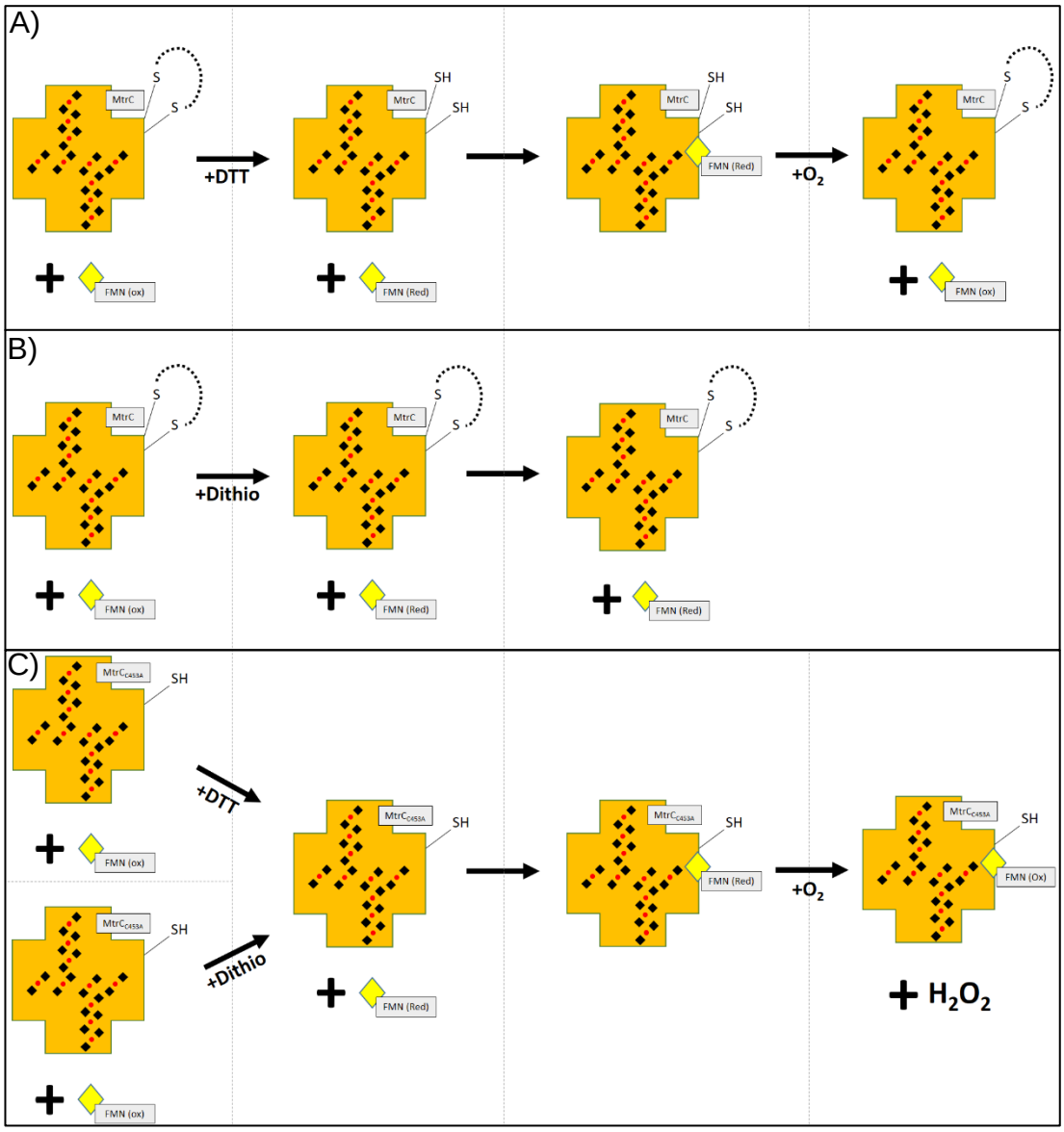

Figure 5.18 – Diagrammatical representation of FMN interaction with MtrC and MtrC$_{C453A}$ upon addition of reducing agents and subsequent exposure to oxygen. A) Native MtrC with addition of DTT leading to reduction of disulphide bond and FMN, this leads to formation of flavocytochrome which disassociates upon exposure to oxygen. B) Native MtrC with addition of sodium dithionite (dithio) leading to the reduction of FMN but no change to disulphide meaning flavocytochrome does not form. C) MtrC$_{C453A}$ with addition of DTT or sodium dithionite (dithio) leading to reduction of FMN and, as disulphide is already disrutpted, formation of flavocytochrome. Upon exposure to oxygen FMN becomes oxidised but does not disassociate as quickly due to disulphide bond not forming, leading to generation of H_2O_2.

5.5 References

Ainsworth, E. V, Lockwood, C. W. J., White, G. F., Hwang, E. T., Sakai, T., Gross, M. A., Richardson, D. J., Clarke, T. A., Jeuken, L. J. C., Reisner, E. and Butt, J. N. (2016) 'Photoreduction of Shewanella oneidensis Extracellular Cytochromes by Organic Chromophores and Dye-Sensitized TiO(2) ', *Chembiochem*. Hoboken: John Wiley and Sons Inc., 17(24), pp. 2324–2333. doi: 10.1002/cbic.201600339.

Bradic, Z. and Wilkins, R. G. (1984) 'Comparative behavior in the kinetics of reduction by superoxide and dithionite ions', *Journal of the American Chemical Society*. American Chemical Society, 106(8), pp. 2236–2239. doi: 10.1021/ja00320a002.

Breuer, M., Rosso, K. M. and Blumberger, J. (2015) 'Flavin Binding to the Deca-heme Cytochrome MtrC: Insights from Computational Molecular Simulation', *Biophysj*. The Authors, 109(12), pp. 2614–2624. doi: 10.1016/j.bpj.2015.10.038.

Brutinel, E. D. and Gralnick, J. A. (2012) 'Shuttling happens: soluble flavin mediators of extracellular electron transfer in Shewanella', *Applied microbiology and biotechnology*. Springer, 93(1), pp. 41–48.

Chait, B. T. (2011) 'Mass Spectrometry in the Postgenomic Era', *Annual Review of Biochemistry*, 80(1), pp. 239–246. doi: 10.1146/annurev-biochem-110810-095744.
Cleland, W. W. (1964) 'Dithiothreitol, a new protective reagent for SH groups', *Biochemistry*. ACS Publications, 3(4), pp. 480–482.

Diederichs, K. and Karplus, P. A. (2013) 'Better models by discarding data?', *Acta Crystallographica Section D: Biological Crystallography*. International Union of Crystallography, 69(7), pp. 1215–1222.

Duurkens, R. H., Tol, M. B., Geertsma, E. R., Permentier, H. P. and Slotboom, D. J. (2007) 'Flavin Binding to the High Affinity Riboflavin Transporter RibU *', 282(14), pp. 10380–10386. doi: 10.1074/jbc.M608583200.

Edwards, M. J., White, G. F., Norman, M., Tome-Fernandez, A., Ainsworth, E., Shi, L., Fredrickson, J. K., Zachara, J. M., Butt, J. N., Richardson, D. J. and Clarke, T. a. (2015) 'Redox Linked Flavin Sites in Extracellular Decaheme Proteins Involved in Microbe-Mineral Electron Transfer.', *Scientific Reports*. Nature Publishing Group, 5(July), p. 11677. doi: 10.1038/srep11677.

Emsley, P., Lohkamp, B., Scott, W. G. and Cowtan, K. (2010) 'Features and development of Coot', *Acta Crystallographica Section D: Biological Crystallography*. International Union of Crystallography, 66(4), pp. 486–501.

Evans, P. R. (2011) 'An introduction to data reduction: space-group determination, scaling and intensity statistics', *Acta Crystallographica Section D: Biological Crystallography*. International Union of Crystallography, 67(4), pp. 282–292.

Hartshorne, R. S., Jepson, B. N., Clarke, T. A., Field, S. J., Fredrickson, J., Zachara, J., Shi, L., Butt, J. N. and Richardson, D. J. (2007) 'Characterization of Shewanella oneidensis MtrC: A cell-surface decaheme cytochrome involved in respiratory electron transport to extracellular electron acceptors', *Journal of Biological Inorganic Chemistry*, 12(7), pp. 1083–1094. doi: 10.1007/s00775-007-0278-y.

Hefti, M. H., Vervoort, J. and Van Berkel, W. J. H. (2003) 'Deflavination and reconstitution of flavoproteins', *European Journal of Biochemistry*. Blackwell Science Ltd, 270(21), pp. 4227–4242. doi: 10.1046/j.1432-1033.2003.03802.x.

Hillenkamp, F., Karas, M., Beavis, R. C. and Chait, B. T. (1991) 'Matrix-Assisted Laser Desorption/Ionization Mass Spectrometry of Biopolymers', *Analytical Chemistry*. American Chemical Society, 63(24), p. 1193A–1203A. doi: 10.1021/ac00024a716.

Hoffman, M. Z. and Hayon, E. (1972) 'One-electron reduction of the disulfide linkage in aqueous solution. Formation, protonation, and decay kinetics of the RSSR- radical', *Journal of the American Chemical Society*. American Chemical Society, 94(23), pp. 7950–7957. doi: 10.1021/ja00778a002.

Hong, G. and Pachter, R. (2016) 'Bound Flavin–Cytochrome Model of Extracellular Electron Transfer in Shewanella oneidensis: Analysis by Free Energy Molecular Dynamics Simulations', *The Journal of Physical Chemistry B*. American Chemical Society, 120(25), pp. 5617–5624. doi: 10.1021/acs.jpcb.6b03851.

Hu, S., Whitten, A. E., King, G. J., Jones, A., Rowland, A. F., James, D. E. and Martin, J. L. (2012) 'The Weak Complex between RhoGAP Protein ARHGAP22 and Signal Regulatory Protein 14-3-3 Has 1 : 2 Stoichiometry and a Single Peptide Binding Mode', 7(8). doi: 10.1371/journal.pone.0041731.

Ivanov, K. I., Bašić, M., Varjosalo, M. and Mäkinen, K. (2014) 'One-step Purification of Twin-Strep-tagged Proteins and Their Complexes on Strep-Tactin Resin Cross-linked With Bis(sulfosuccinimidyl) Suberate (BS3)', *Journal of Visualized Experiments : JoVE*. MyJove Corporation, (86), p. 51536. doi: 10.3791/51536.

Kimple, M. E., Brill, A. L. and Pasker, R. L. (2013) 'Overview of Affinity Tags for Protein Purification', *Current protocols in protein science / editorial board, John E. Coligan ... [et al.]*, 73, p. Unit-9.9. doi: 10.1002/0471140864.ps0909s73.

Leslie, A. G. W. and Powell, H. R. (2007) 'Processing diffraction data with MOSFLM', *Evolving methods for macromolecular crystallography*. Springer, 245, pp. 41–51.

McCoy, A. J. (2007) 'Solving structures of protein complexes by molecular replacement with Phaser', *Acta Crystallographica Section D: Biological Crystallography*. International Union of Crystallography, 63(1), pp. 32–41.

Murphy, D. M., Ivanenkov, V. V and Kirley, T. L. (2002) 'Identification of Cysteine Residues Responsible for Oxidative Cross- linking and Chemical Inhibition of Human Nucleoside-triphosphate Diphosphohydrolase 3 *', 277(8), pp. 6162–6169. doi: 10.1074/jbc.M110105200.

Nelson, D. and Cox, M. (2005) 'Lehninger principles of biochemistry (4th ed.)', *Biochemistry and Molecular Biology Education*, 33(1), pp. 74–75. doi: 10.1002/bmb.2005.494033010419.

Okamoto, A., Hashimoto, K., Nealson, K. H. and Nakamura, R. (2013) 'Rate enhancement of bacterial extracellular electron transport involves bound flavin semiquinones', *Proceedings of the National Academy of Sciences*, 110(19), pp. 7856–7861.

Papaleo, E., Saladino, G., Lambrughi, M., Lindorff-Larsen, K., Gervasio, F. L. and Nussinov, R. (2016) 'The Role of Protein Loops and Linkers in Conformational Dynamics and Allostery', *Chemical Reviews*. American Chemical Society, 116(11), pp. 6391–6423. doi: 10.1021/acs.chemrev.5b00623.

Rao, U. S. and Murthy, S. K. (1991) 'The effects of beta-mercaptoethanol and sodium dodecyl sulfate on the Humicola insolens beta-glucosidase.', *Biochemistry international*. Australia, 23(2), pp. 343–348.

Ross, D. E., Brantley, S. L. and Tien, M. (2009) 'Kinetic characterization of OmcA and MtrC, terminal reductases involved in respiratory electron transfer for dissimilatory iron reduction in Shewanella oneidensis MR-1', *Applied and Environmental Microbiology*, 75(16), pp. 5218–5226. doi: 10.1128/AEM.00544-09.

Ross, D. E., Ruebush, S. S., Brantley, S. L., Hartshorne, R. S., Clarke, T. a, Richardson, D. J. and Tien, M. (2007) 'Characterization of protein-protein interactions involved in iron reduction by Shewanella oneidensis MR-1.', *Applied and environmental microbiology*, 73(18), pp. 5797–808. doi: 10.1128/AEM.00146-07.

Saraiva, L. M., Liu, M. Y., Payne, W. J., Legall, J., Moura, J. J. and Moura, I. (1990) 'Spin-equilibrium and heme-ligand alteration in a high-potential monoheme cytochrome (cytochrome c554) from Achromobacter cycloclastes, a denitrifying organism.', *European journal of biochemistry*. England, 189(2), pp. 333–341.

Shi, L., Chen, B., Wang, Z., Elias, D. A., Mayer, M. U., Gorby, Y. A., Ni, S., Lower, B. H., Kennedy, D. W. and Wunschel, D. S. (2006) 'Isolation of a high-affinity functional protein complex between OmcA and MtrC: two outer membrane decaheme c-type cytochromes of Shewanella oneidensis MR-1', *J Bacteriol*, 188. doi: 10.1128/JB.01966-05.

Shokhireva, T. K., Smith, K. M., Berry, R. E., Shokhirev, N. V, Balfour, C. A., Zhang, H. and Walker, F. A. (2007) 'Assignment of the Ferriheme Resonances of the High-Spin Forms of Nitrophorins 1 and 4 by (1)H NMR Spectroscopy: Comparison to Structural Data Obtained from X-ray Crystallography', *Inorganic chemistry*, 46(1), pp. 170–178. doi: 10.1021/ic061407t.

Song, S. H., Dick, B. and Penzkofer, A. (2007) 'Photo-induced reduction of flavin mononucleotide in aqueous solutions', *Chemical Physics*, 332(1), pp. 55–65. doi: 10.1016/j.chemphys.2006.11.023.

Tipton, J. D., Tran, J. C., Catherman, A. D., Ahlf, D. R., Durbin, K. R. and Kelleher, N. L. (2011) 'Analysis of intact protein isoforms by mass spectrometry', *Journal of Biological Chemistry*, 286(29), pp. 25451–25458. doi: 10.1074/jbc.R111.239442.

Weber, G. (1948) 'The quenching of fluorescence in liquids by complex formation. Determination of the mean life of the complex', *Transactions of the Faraday Society*. The Royal Society of Chemistry, 44(0), pp. 185–189. doi: 10.1039/TF9484400185.

Chapter 6

General Discussion

6.1 Significance of Thesis

Microbial mineral respiration is known to play a key role in many environmental inorganic metal cycles (Gadd, 2010). The act of respiring on metal containing minerals causes changes in the redox state which in turn can affect the solubility and overall chemical composition of minerals (Gadd, 2010). This affects the bioavailability of many metals crucial for life. An example of such metals often in limited supply to organisms is iron. Without these processes cycling iron in the environment growth of many organisms, including microbes, would be limited (Hibbing *et al.*, 2010).

Since its isolation in Lake Oneida (NY), *S. oneidensis* has been known to utilise extracellular electron transfer to facilitate anaerobic growth. This bacteria is known to use a wide variety of terminal electron acceptors including many insoluble extracellular acceptors with iron and manganese being two of the best documented (Myers and Nealson, 1988). Many studies have investigated extracellular electron transfer in this organism leading to the identification of an outer membrane spanning complex, termed the MtrCAB complex, as the primary electron transfer conduit linking the respiratory electron pool to the extracellular environment (Hartshorne *et al.*, 2009). Electrons are transferred through this complex, first across the periplasmic decaheme MtrA before electrons are transferred to the extracellular facing, outer membrane anchored, MtrC decaheme cytochrome. The MtrB porin aids the association of the complex, bringing the Mtr proteins together. This facilitates the association and the transfer of electrons between MtrA and MtrC, functioning much like an isolating sheaf to the conductive cytochromes (White *et al.*, 2013)

Although the system is well studied, there remains questions as to the mechanism of electron transfer from MtrC to the terminal electron acceptor. The most widely accepted theories are that of direct electron transfer and that of electron transfer via soluble electron shuttles (Fredrickson *et al.*, 2008). Advances in the field have implicated naturally secreted flavin molecules as having a major importance in facilitating electron transfer in both models (Marsili *et al.*, 2008). FMN and FAD are known to be the predominant flavin secreted by *Shewanella* via the Bfe exporter, with

low micromolar concentrations detected in cultures, though their physiological function remains unclear (von Canstein *et al.*, 2008).

There is evidence that these flavin molecules can act as electron shuttles to facilitate the transfer of electrons from MtrC to extracellular terminal electron acceptors (N J Kotloski and Gralnick, 2013). OMCs have been seen capable of reducing FMN with interactions between the two seemingly transient based on the 29 µM dissociation constant recorded between MtrC and FMN (Paquete *et al.*, 2014). However, electrochemical studies have shown semi reduced flavin formation at the biofilm / flavin interface. This work suggests a tighter, cofactor like association between the flavin and MtrC (Okamoto *et al.*, 2014). The formation of this flavocytochrome allows direct electron transfer from the FMN-MtrC complex to the terminal electron acceptor to achieve much high rates than reported for electron transfer through MtrC alone (Okamoto *et al.*, 2013). Molecular dynamic simulations have also suggested potential FMN binding sites within the structure of MtrC that could impact on electron transfer through the protein upon flavin association (Babanova *et al.*, 2017)

This seeming disparity in results could perhaps be explained by the switching of electron transfer systems dependant on if *S. oneidensis* is growing under aerobic or anaerobic conditions. The chemical reduction of the conserved disulphide bond in domain III of MtrC has been seen to allow for tighter associations between FMN and the protein to form (Edwards *et al.*, 2015). This disulphide bond is in relative close proximity to a potential flavin binding pocket within the protein structure as highlighted by molecular dynamic simulations (Breuer, Rosso and Blumberger, 2015). As such further investigation documented in this thesis into the physiological relevance of the conserved disulphide bond, and its effect on flavocytochrome formation, could implicate protein level control over FMN-MtrC interactions.

6.2 Results Summary

6.2.1 Chapter 3

The work in Chapter 3 focused on the generation of mutant *mtrC* where the disulphide bond in domain III of MtrC had been disrupted. This mutated gene was then transformed into *S. oneidensis ΔmtrC* to investigate its effect on the bacteria and to ascertain if it functioned physiologically like the wild type *mtrC.* Three forms of the mutant *mtrC* were generated: pC444A, pC453A and pC444A,C453A. In two of the forms each of the single cysteine residues (at amino acid position 444 and 453) forming the disulphide were substituted to an alanine residue, allowing expression of the $MtrC_{C453A}$ and $MtrC_{C444A}$ variants of MtrC. The third form was a double cysteine substitution where both cysteine at position 444 and 453 were substituted for alanine residues, allowing expression of the $MtrC_{C444A,C453A}$ variant. Growth studies showed that when *S. oneidensis ΔmtrC* expressed any of these mutants ($MtrC_{C444A}$, $MtrC_{C453A}$, or $MtrC_{C444A,C453A}$) under aerobic conditions, the lag phase of the cultures was extended compared to growth observed in *S. oneidensis ΔmtrC* expressing native MtrC (*S. oneidensis ΔmtrC* pMtrC strain). *S. oneidensis ΔmtrC* pC453A showed the most extreme growth defect with variations between the strains linked to the expression levels of the mutant *mtrC* forms (the higher the expression the more severe the growth defect). Under anaerobic conditions the growth of all strains was seen to be similar to that of wild type *S. oneidensis* MR-1 suggesting expression of MtrC lacking the disulphide bond in domain III led to oxygen toxicity. The ability of the bacteria to reduce ferric iron in the form of goethite was maintained in all strains, suggesting the mutant forms of MtrC were still forming physiologically functional complexes with MtrAB and the growth defects observed were not the result of non-specific protein folding.

6.2.2 Chapter 4

The aim of Chapter 4 was to ascertain the cause of the growth defect observed in cultures of *S. oneidensis ΔmtrC* when grown aerobically expressing pC444A, pC453A

or pC444A,C453A. Reactive oxygen species formation was implicated due to the apparent oxygen toxicity. Measurements indeed showed increased levels of H_2O_2 in cultures of *S. oneidensis ΔmtrC* pC453A, compared to levels detect in *S. oneidensis ΔmtrC* pMtrC cultures. This was shown to be the predominant toxic species as removal of H_2O_2 through the use of catalase restored growth to that comparable to wild type *mtrC* expressing cultures. The H_2O_2 levels measured in these studies were likely an equilibrium measurement between the increased amount of H_2O_2 produced in the samples and the amount removed via increased peroxidase activity. investigation showed the levels measured as sufficient to greatly reduce cell viability. This is in line with the known sensitivity of *S. oneidensis* to oxidative stress not seen in other species such as *E. coli*. The effect of ROS on *S. oneidensis* growth is exacerbated by Fenton reactions due to the high cytochrome (and thus iron) content of the cells (Repine, Fox and Berger, 1981; Grossman and Kahan, 2016).

6.2.3 Chapter 5

Having established that *S. oneidensis ΔmtrC* pC453A displays an extended lag phase when grown aerobically due to the generation of the reactive oxygen species H_2O_2, biochemical analysis of the protein itself was carried. Chapter 5 focused on investigating $MtrC_{C453A}$ and comparing it to native MtrC to ascertain what difference the removal of the disulphide bond was having on the protein. A large focus of this investigation was looking at the ability of FMN to form a tight association with MtrC / $MtrC_{C453A}$. This was due to previously reported work highlighting the disulphide bond as controlling cofactor-like binding between the two (Edwards *et al.*, 2015). Crystallography showed the structure of $MtrC_{C453A}$ to be largely similar to that of native MtrC (presented in the aforementioned study), suggesting that the increased reactivity of the protein seen in the whole cell experiments was not the result of large scale changes of conformation or heme environment caused by the disruption of the disulphide bond. This does not rule out the possibility for large scale changes to occur once FMN has bound to the protein. The conditions $MtrC_{C453A}$ was crystallised under were based on conditions native MtrC crystallises in and did not include FMN This would have added a bias for similar structural conformations to crystallise more easily.

Once this had been ascertained, conditions where FMN could tightly associated with MtrC and $MtrC_{C453A}$ were highlighted through binding studies. It was found that chemical reducing agents, such as DTT, were still needed to allow tight binding of FMN to $MtrC_{C453A}$ (this had been previously reported in FMN-MtrC binding studies). However, sodium dithionite was seen to also allow binding of FMN to $MTrC_{C453A}$ whereas it had no affect on FMN binding in native MtrC. It was hypothesised that this lack of effect on binding to native MtrC was the result of sodium dithionite being unable to reduce the disulphide bond of MtrC. In $MtrC_{C453A}$ the disulphide was disrupted by the amino acid substitution and implicated sodium dithionite reduction of FMN as the factor allowing the binding of FMN to the protein. Together this data highlighted both the reduction of the disulphide bond in domain III of MtrC and the reduction of FMN as critical to allow tight association between the two. The reduction of the disulphide bond likely affects the structural rigidity of MtrC perhaps leading to conformational change (Thangudu *et al.*, 2008). This combined with molecular shape changes in reduced FMN, resulting from changes to the atomic bond angles, could allow for access to previously inaccessible binding sites within the structure of MtrC (Breuer, Rosso and Blumberger, 2015). The formation of this flavocytochrome was seen to result in an increase of reactivity leading to increased generation of H_2O_2 when the $MtrC_{C453A}$ was exposed to oxygen with FMN present, compared to levels detected in samples of native MtrC under the same conditions.

6.3 Physiological Overview of System

6.3.1 Disulphide Bonds as Switches

Disulphide bridges are often structural features shaping the tertiary structure of many proteins. They also play a large role in stabilising quaternary structures. This feature often allows them to act as redox switches. The ability of thiols to become readily oxidised and reduced lends them to effective intracellular oxygen sensors. Often oxidising conditions lead to disulphide bridges forming between monomeric proteins.

This oligomerisation raises the affinity of many proteins for DNA which in turn allows for regulation of gene transcription (Wouters, Fan and Haworth, 2010). Disulphide bonds also function very effectively as sensors of oxidative stress. Upon exposure to reactive oxygen species, such as H_2O_2, sulfenic acid (RSOH) forms as an unstable intermediate. This readily reacts with cysteine residues localised in close proximity allowing the formation of the disulphide bond (Rehder and Borges, 2010). This in turn allows rapid regulation of oxidative stress response pathways.

As well as causing structural changes to proteins, the oxidation and reduction of disulphide bonds has been seen to affect enzymatic activity of enzymes. Often the formation of disulphide bonds leads to an increase in rigidity which prevents catalytic function (Klomsiri, Karplus and Poole, 2011). This has been seen in the cold activated amylase in *Pseudoalteromonas haloplanktis where the redox state of disulphide bonds impact on localised conformational changes in the protein rather than global stability. This has been seen to affect the strength of interactions between the active site and binding partners (Siddiqui et al., 2005).* This is very similar to what is observed in the MtrCAB system, with the formation of the disulphide bond in domain III of MtrC preventing the transfer of electrons to terminal electron acceptors.

Although this study highlights the redox sensitive disulphide of MtrC as a novel control mechanism for extracellular electron transfer, the precedent for such protein level control is well known. Often redox sensitive disulphides responding to oxidative stress are observed in the periplasm responding to reactive oxygen species formed during oxidative phosphorylation. As mineral respiration involves electrons at the bacterial cell surface, a similar control mechanism was to be expected localised accordingly. This protein level of control allows for the rapid regulation of electron transfer, far faster than genetic regulation alone could (Linke and Jakob, 2003).

6.3.2 Hypothesised Overview of the System

In the natural environment, wild type *S. oneidensis* expresses native MtrC which associates to MtrAB and forms a complex capable of carrying out electron transfer to extracellular terminal electron acceptors (Hartshorne *et al.*, 2009). Under anaerobic conditions the disulphide bond in domain III of the protein may become reduced and this allows naturally secreted FMN to interact with MtrC. The exact mechanism for reduction of the disulphide on outer membrane proteins is unknown with a previously undescribed outer membrane associated oxidoreductases or naturally occurring environmental reducing agents both capable of such reactions. It is also worth noting that current understanding of how disulphide bond machinery interplays with periplasmic chaperone pathways to ensure correct folding of OMCs is relatively unclear (Denoncin and Collet, 2013). This provides scope for post-translational modifications, such as disulphide bond reduction, to have dedicated pathways.

Under these anaerobic conditions, FMN has been seen to become reduced by OMCs with evidence in this thesis suggesting this leads to relatively strong binding of FMN to MtrC (Clarke *et al.*, 2011). Evidence for this was shown in Chapter 5 when FMN was seen to bind to MtrC when both the disulphide bond and FMN was reduced. When the flavocytochrome has formed, it becomes more favourable for electrons to be conducted through the heme residues and through the protein. In the presence of insoluble terminal electron acceptors such as ferric iron, these electrons can then pass to the extracellular electron acceptor oxidising MtrC (Figure 6.1). This allows for the cell's metabolism to continue and electrons originating at the electron transport chain to be removed from the system (Fredrickson *et al.*, 2008). If the environment becomes aerobic (perhaps due to sediment disruption by marine life) the disulphide bond becomes oxidised leading to the dissociation of bound FMN and prevents further FMN binding to the protein regardless of oxidation state of the FMN. In this unbound form of MtrC, it is less favourable for electrons to pass through the protein and so they remain within the cell to be removed via terminal oxidases (Okamoto *et al.*, 2013).

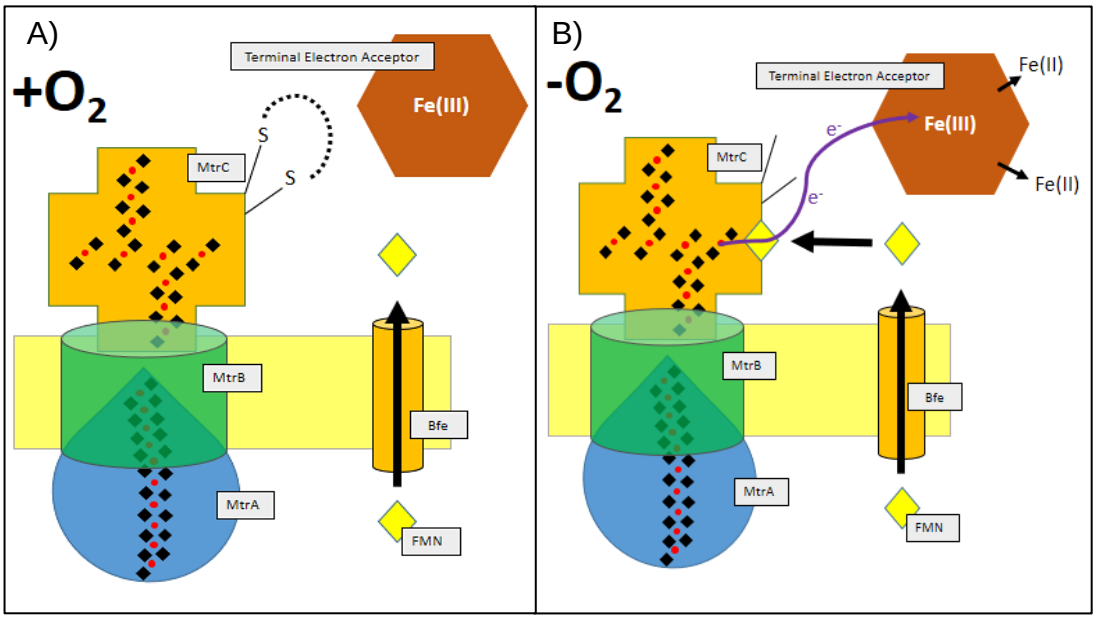

Figure 6.1 – Diagrammatical representation of wild type MtrCAB system in extracellular electron transfer under A) aerobic and B) anaerobic conditions. Reduction state of disulphide highlighted under aerobic ($+O_2$) and anaerobic ($-O_2$) conditions. Electron movement from MtrC to insoluble terminal electron acceptor (shown as Fe(III)) indicated by purple arrow.

In the case of *S. oneidensis ΔmtrC* pC453A, the bacteria is expressing a mutant form of MtrC where the disulphide bond in domain III is not present and cannot form (due to the removal of the cysteine residue). It can be assumed that under anaerobic conditions this form of MtrC behaves in a similar manner to that of the native form. With the disulphide bond broken reduced FMN can form a relatively tight bond to the protein. This flavocytochrome is more reactive than the protein alone and this leads to an increase in favourability for electrons to conduct through the MtrC protein and away from the cell. This is supported by work in Chapter 3 showing that *S. oneidensis ΔmtrC* expressing either native MtrC or $MtrC_{C453A}$ can reduce goethite equally well during mineral respiration. However, under aerobic conditions $MtrC_{C453A}$ remains in the flavocytochrome state due to the substitution of the cysteine residues preventing the formation of the disulphide bond. As previously explained, the

disulphide of native MtrC would instead become oxidised leading to electron conduction through MtrC becoming unfavourable. As $MtrC_{C453A}$ remains in the flavocytochrome state, it is still favourable for electrons to pass through the protein and out to the extracellular environment.

Although the oxygen present under these conditions becomes the terminal electron acceptor via reduction by terminal oxidases, the quinone pool, and downstream cytochromes, of *S. oneidensis* may still become partially reduced during replicative growth. Of the three oxidases found in the *S. oneidensis* genome, the cbb_3-type oxidase is the predominantly expressed oxidase. However, the level of expression is low under anaerobic conditions and rises as environments become aerobic (Le Laz *et al.*, 2016). This will remove electrons from the reduced ubiquinone pool of *S. oneidensis* however, the menaquinone pool is less readily oxidised by Cbb_3. This distinct electron pool is more readily oxidised by CymA leading to both pathways remaining active during aerobic respiration (Ross *et al.*, 2011). Although the levels of ubiquinol increase under aerobic conditions, whilst the levels of menaquinol falls by as much as fivefold, there is still sufficient amounts to result in cytochrome reduction (Søballe and Poole, 1999; Myers and Myers, 2000). Electrons could still be transferred to the $MtrC_{C453A}$-MtrAB complex whilst the oxidase expression is upregulated. This pathway does not lead to the full reduction of oxygen to H_2O but instead leads to the formation of reactive oxygen species, which in turn, damage and kill the bacterial cells. This was further discussed in Chapter 4 where increased levels of H_2O_2 were detected in *S. oneidensis* ***ΔmtrC*** pC453A cultures leading to Fenton reactions and the formation of more damaging oxygen species (Figure 6.2).

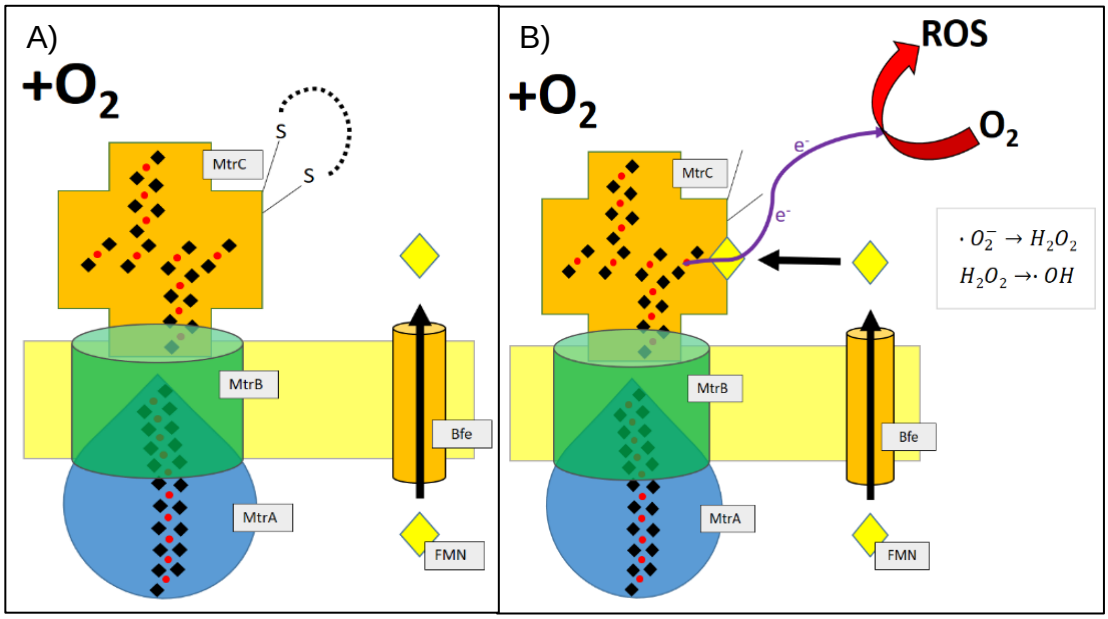

Figure 6.2 – Diagrammatical representation of MtrCAB system in A) wild type and B) cysteine substituted (mutant) forms under aerobic (+O_2) conditions. Reduction state of disulphide highlighted in both forms with it being present (oxidised) in wild type but absent in mutant form owing to the removal of cysteine residues to from disulphide bond. Electron movement from MtrC indicated by purple line, with proposed reaction with molecular oxygen indicated. Downstream reactive oxygen species formation also shown.

6.4 Perspective Future Studies

6.4.1 MtrC

The work presented in this thesis has expanded our knowledge of extracellular electron transport in the model organism *S. oneidensis*. More focus is given to the role of FMN in the system and how it might facilitate electron transfer from MtrC to terminal electron acceptors. This thesis has built on previous experiments, published alongside work here (Edwards *et al.*, 2015), that highlighted the reduction and oxidation of the disulphide bind in domain III of MtrC as a control mechanism for the formation of a flavocytochrome. Here we suggest an increase in reactivity of MtrC upon formation of the flavocytochrome adding weight to the hypothesised flavin cofactor system (Okamoto *et al.*, 2013). In turn, the disulphide bond has been implicated as a physiologically relevant oxidative stress response. When this protein level control is removed, changes in the bacterial environment that lead to the introduction of oxygen cause a reduction in cell viability. This extra level of control, beyond gene regulation, appears to have evolved as a defence against reactive oxygen species undergoing Fenton reactions and causing further cellular damage. Thus facilitating anaerobic to aerobic respiratory switching to sustain growth in the ecological niche of *S. oneidensis*.

Although more is now known about the disulphide bond in domain III of MtrC and the role FMN plays in electron transport through MtrC, this study has also highlighted avenues of further investigation. Work here showed the flavocytochrome to be more reactive than the protein alone, however it is still unclear where this reactivity is coming from. There is the potential for photoreduction of the FMN to be driving electron transfer through MtrC and thus leading to further reduction of oxygen to H_2O_2. However equally the

binding of FMN may be affecting the reduction potentials of the heme residues in MtrC. Further molecular dynamic simulation investigations would be a good way to investigate the impact of FMN binding in this way. For this work to be successful, it would be greatly beneficial to know where the site of FMN binding is on MtrC. Previous studies have highlighted a potential binding pocket near heme 7 (Hong and Pachter, 2016). To experimentally study this, crystallising MtrC in the presence of FMN may allow the structure of the flavocytochrome to be solved and thus the binding site to be identified. This experiment was attempted in this study however no crystals were recovered. Further attempts should be carried out with the now known conditions for flavocytochrome generation incorporated into the crystallising conditions. Building on from this line of investigation, NMR studies could be employed to more accurately measure binding affinity between FMN and MtrC. In this study the association between FMN and $MtrC_{C453A}$ appears strong as it is maintained during elution through a size exclusion column and some binding temporarily remains bound after the protein is exposed to oxygen. However, quantitative measurements would allow a better understanding of the association. It would provide more evidence as to whether or not the flavocytochrome complex is long lasting, with the FMN potentially functioning in a cofactor like manner, as suggested here. These studies could also provide information as to the path electrons through the flavocytochrome complex. Current models have electrons exiting the protein at heme 10 however it is also possible that electrons could pass from heme 7 to a bound flavin molecule (if predicted binding sites are correct). With electrons then passing to the terminal electron acceptor from here (Shi *et al.*, 2012).

Another question that remains unanswered is that of how the disulphide bond is naturally reduced. It is possible that a reducing agent is present in the natural environment leading to the initial reduction of the disulphide bond. Once activated, the extracellular transfer of electrons through the MtrCAB pathway

may produce further reducing agents that go on to reduce the disulphide bonds of other MtrCAB units, leading to a cascade like activation. In many studies the readiness of FMN to photo-reduce has been highlighted (Song, Dick and Penzkofer, 2007) and this has been shown to be capable of in turn reducing MtrC (Ainsworth *et al.*, 2016). This study itself suggests reduction, possibly photo-induced, as a required condition for flavocytochrome formation. It is therefore also possible that reduced flavin molecules could play a role in the initial reduction of the disulphide on allowing for the formation of the more reactive flavocytochrome. Future studies could look to test these theories by incubating MtrC with FMN under photo-inducing conditions and specifically looking for the generation of the flavocytochrome. Liposome models or inside out vesicles with MtrC embedded into them could be a useful tool in these experiments, as they could allow imitation of the bacterial outer membrane and have been used in other outer membrane cytochrome studies (White *et al.*, 2012).

6.4.2 Other Outer Membrane Cytochromes

Although the work in this thesis focused on MtrC, the results may be applicable to other outer membrane cytochromes and help to understand other extracellular electron transport systems. OmcA is another well studied outer membrane cytochrome that share many structural features to that of MtrC. Notably both MtrC and OmcA display the staggered heme cross motif and a disulphide bond in domain III of the protein (Edwards *et al.*, 2014). OmcA is known to facilitate extracellular electron transport even in the absence of MtrC under manganese reducing conditions (Bücking *et al.*, 2010). This similarity in function and structure indicates a conserved mechanism between the OmcA and MtrC systems. As such, similar investigations as documented in this thesis could indicate if oxygen sensitive redox switching is also conserved across systems. Combining studies could also provide a clearer view on electron

transport through these systems. NMR and stop flow studies have begun looking at electron driving force through OmcA when mutations are introduced on the distal axial legend of heme 7. In these studies, alterations to the heme ligand are seen to increase the driving force towards electron shuttles such as FMN. This suggests that changes to the environment around the heme residue can indeed affect reactivity of the outer membrane cytochrome to certain electron acceptors (Neto *et al.*, 2017). This heme is located nearby to a proposed FMN binding site on the cytochrome. Investigations should begin to look at disrupting the disulphide bind in domain III of the protein to see if FMN binding can be observed. If binding is seen and can be localised to this region nearby heme 7, similar NMR and stop flow studies could be used to analyse the effect of flavocytochrome formation on heme 7 and thus on the driving force through OmcA. Studies such as these would also help to elucidate the effect FMN binding is having in MtrC.

It is important to note significant differences between the MtrC studied here and other outer membrane cytochromes. OmcA and UndA both have an additional disulphide bond in their structures. The disulphide in domain III is conserved however, there is also a disulphide in domain I of the proteins. Investigations into this additional disulphide could not only shed light on further redox sensitive control mechanisms, but also on how flavin function varies between outer membrane cytochromes. Studies have already indicated that reduction of the disulphide in domain III leads to formation of a flavocytochrome, much like that observed in MtrC (Edwards *et al.*, 2015). However, in those studies there was no specificity over which disulphide bond was reduced. There is another proposed flavin binding site in domain I of the outer membrane cytochromes (Clarke *et al.*, 2011). Under the proposed binding conditions evidenced in this thesis, it is reasonable to assume this binding site is controlled by the nearby additional disulphide bond. Implementing a site directed mutagenesis approach, as used here, could

provide evidence for this and allow for detailed investigation of the function of the additional disulphide in these cytochromes. It is worth noting that the MtrC protein structure in some species of *S. oneidensis* also contain this additional disulphide bond and so these other forms of MtrC would also be ideal candidates for further investigation (Edwards *et al.*, 2015).

6.5 References

Ainsworth, E. V, Lockwood, C. W. J., White, G. F., Hwang, E. T., Sakai, T., Gross, M. A., Richardson, D. J., Clarke, T. A., Jeuken, L. J. C., Reisner, E. and Butt, J. N. (2016) 'Photoreduction of Shewanella oneidensis Extracellular Cytochromes by Organic Chromophores and Dye-Sensitized TiO(2) ', *Chembiochem*. Hoboken: John Wiley and Sons Inc., 17(24), pp. 2324–2333. doi: 10.1002/cbic.201600339.

Babanova, S., Matanovic, I., Cornejo, J., Bretschger, O., Nealson, K. and Atanassov, P. (2017) 'Outer membrane cytochromes/flavin interactions in Shewanella spp.—A molecular perspective', *Biointerphases*. AVS, 12(2), p. 21004.

Breuer, M., Rosso, K. M. and Blumberger, J. (2015) 'Flavin Binding to the Deca-heme Cytochrome MtrC: Insights from Computational Molecular Simulation', *Biophysj*. The Authors, 109(12), pp. 2614–2624. doi: 10.1016/j.bpj.2015.10.038.

Bücking, C., Popp, F., Kerzenmacher, S. and Gescher, J. (2010) 'Involvement and specificity of Shewanella oneidensis outer membrane cytochromes in the reduction of soluble and solid-phase terminal electron acceptors', *FEMS Microbiology Letters*, 306(2), pp. 144–151. doi: 10.1111/j.1574-6968.2010.01949.x.

von Canstein, H., Ogawa, J., Shimizu, S. and Lloyd, J. R. (2008) 'Secretion of flavins by Shewanella species and their role in extracellular electron transfer.', *Applied and environmental microbiology*, 74(3), pp. 615–23. doi: 10.1128/AEM.01387-07.

Clarke, T. A., Edwards, M. J., Gates, A. J., Hall, A., White, G. F., Bradley, J., Reardon, C. L., Shi, L., Beliaev, A. S., Marshall, M. J., Wang, Z., Watmough, N. J., Fredrickson, J. K., Zachara, J. M., Butt, J. N. and Richardson, D. J. (2011) 'Structure of a bacterial cell surface decaheme electron conduit'. doi: 10.1073/pnas.1017200108/-/DCSupplemental.www.pnas.org/cgi/doi/10.1073/pnas.1017200108.

Denoncin, K. and Collet, J.-F. (2013) 'Disulfide Bond Formation in the Bacterial Periplasm: Major Achievements and Challenges Ahead', *Antioxidants & Redox Signaling*. 140 Huguenot Street, 3rd FloorNew Rochelle, NY 10801USA: Mary Ann Liebert, Inc., 19(1), pp. 63–71. doi: 10.1089/ars.2012.4864.

Edwards, M. J., Baiden, N., Johs, A., Tomanicek, S. J., Liang, L., Shi, L., Fredrickson, J. K., Zachara, J. M., Gates, A. J., Butt, J. N., Richardson, D. J. and Clarke, T. A. (2014) 'The X-ray crystal structure of Shewanella oneidensis OmcA reveals new insight at the microbe-mineral interface.', *FEBS letters*.

Edwards, M. J., White, G. F., Norman, M., Tome-Fernandez, A., Ainsworth, E., Shi, L., Fredrickson, J. K., Zachara, J. M., Butt, J. N., Richardson, D. J. and Clarke, T. a. (2015) 'Redox Linked Flavin Sites in Extracellular Decaheme Proteins Involved in Microbe-Mineral Electron Transfer.', *Scientific Reports*. Nature Publishing Group, 5(July), p. 11677. doi: 10.1038/srep11677.

Fredrickson, J. K., Romine, M. F., Beliaev, A. S., Auchtung, J. M., Driscoll, M. E., Gardner, T. S., Nealson, K. H., Osterman, A. L., Pinchuk, G., Reed, J. L., Rodionov, D. a, Rodrigues, J. L. M., Saffarini, D. a, Serres, M. H., Spormann, A. M., Zhulin, I. B. and Tiedje, J. M. (2008) 'Towards environmental systems biology of Shewanella.', *Nature reviews. Microbiology*, 6(8), pp. 592–603. doi: 10.1038/nrmicro1947.

Gadd, G. M. (2010) 'Metals, minerals and microbes: Geomicrobiology and bioremediation', *Microbiology*, 156(3), pp. 609–643. doi: 10.1099/mic.0.037143-0.

Grossman, J. N. and Kahan, T. F. (2016) 'Hydroxyl radical formation from bacteria-assisted Fenton chemistry at neutral pH under environmentally relevant conditions', *Environmental Chemistry*. doi: 10.1071/EN15256.

Hartshorne, R. S., Reardon, C. L., Ross, D., Nuester, J., Clarke, T. a, Gates, A. J., Mills, P. C., Fredrickson, J. K., Zachara, J. M., Shi, L., Beliaev, A. S., Marshall, M. J., Tien, M., Brantley, S., Butt, J. N. and Richardson, D. J. (2009) 'Characterization of an electron conduit between bacteria and the extracellular environment.', *Proceedings of the National Academy of Sciences of the United States of America*, 106(52), pp. 22169–74. doi: 10.1073/pnas.0900086106.

Hibbing, M. E., Fuqua, C., Parsek, M. R. and Peterson, S. B. (2010) 'Bacterial competition: surviving and thriving in the microbial jungle', *Nature reviews. Microbiology*, 8(1), pp. 15–25. doi: 10.1038/nrmicro2259.

Hong, G. and Pachter, R. (2016) 'Bound Flavin–Cytochrome Model of Extracellular Electron Transfer in Shewanella oneidensis: Analysis by Free Energy Molecular Dynamics Simulations', *The Journal of Physical Chemistry B*. American Chemical Society, 120(25), pp. 5617–5624. doi: 10.1021/acs.jpcb.6b03851.

Klomsiri, C., Karplus, P. A. and Poole, L. B. (2011) 'Cysteine-based redox switches in enzymes.', *Antioxidants & redox signaling*, 14(6), pp. 1065–77. doi: 10.1089/ars.2010.3376.

Kotloski, N. J. and Gralnick, J. A. (2013) 'Flavin electron shuttles dominate extracellular electron transfer by Shewanella oneidensis', *MBio*, 4(1). doi: 10.1128/mBio.00553-12.

Le Laz, S., kpebe, A., Bauzan, M., Lignon, S., Rousset, M. and Brugna, M. (2016) 'Expression of terminal oxidases under nutrient-starved conditions in Shewanella oneidensis: detection of the A-type cytochrome c oxidase'. The Author(s), 6, p. 19726. Available at: http://dx.doi.org/10.1038/srep19726.

Linke, K. and Jakob, U. (2003) 'Not every disulfide lasts forever: disulfide bond formation as a redox switch.', *Antioxidants & redox signaling*, 5(4), pp. 425–434. doi: 10.1089/152308603768295168.

Marsili, E., Baron, D. B., Shikhare, I. D., Coursolle, D., Gralnick, J. a and Bond, D. R. (2008) 'Shewanella secretes flavins that mediate extracellular electron transfer.', *Proceedings of the National Academy of Sciences of the United States of America*, 105(10), pp. 3968–3973. doi: 10.1073/pnas.0710525105.

Myers, C. and Nealson, K. H. (1988) 'Bacterial manganese reduction and growth with manganese oxide as the sole electron acceptor', *Science*, 240. doi: 10.1126/science.240.4857.1319.

Myers, J. M. and Myers, C. R. (2000) 'Role of the tetraheme cytochrome CymA in anaerobic electron transport in cells of Shewanella putrefaciens MR-1 with normal levels of menaquinone', *Journal of bacteriology*. Am Soc Microbiol, 182(1), pp. 67–75.

Neto, S. E., de Melo-Diogo, D., Correia, I. J., Paquete, C. M. and Louro, R. O. (2017) 'Characterization of OmcA Mutants from *Shewanella oneidensis* MR-1 to Investigate the Molecular Mechanisms Underpinning Electron Transfer Across the Microbe-Electrode Interface', *Fuel Cells*. doi: 10.1002/fuce.201700023.

Okamoto, A., Hashimoto, K., Nealson, K. H. and Nakamura, R. (2013) 'Rate enhancement of bacterial extracellular electron transport involves bound flavin semiquinones', *Proceedings of the National Academy of Sciences*, 110(19), pp. 7856–7861.

Okamoto, A., Kalathil, S., Deng, X., Hashimoto, K., Nakamura, R. and Nealson, K. H. (2014) 'Cell-secreted Flavins Bound to Membrane Cytochromes Dictate Electron Transfer Reactions to Surfaces with Diverse Charge and pH.', *Scientific reports*, 4, p. 5628. doi: 10.1038/srep05628.

Paquete, C. M., Fonseca, B. M., Cruz, D. R., Pereira, T. M., Pacheco, I., Soares, C. M. and Louro, R. O. (2014) 'Exploring the molecular mechanisms of electron shuttling across the microbe/metal space', *Frontiers in Microbiology*, 5(JUN), pp. 1–12. doi: 10.3389/fmicb.2014.00318.

Rehder, D. S. and Borges, C. R. (2010) 'Cysteine sulfenic Acid as an Intermediate in Disulfide Bond Formation and Nonenzymatic Protein Folding', *Biochemistry*. American Chemical Society, 49(35), pp. 7748–7755. doi: 10.1021/bi1008694.

Repine, J. E., Fox, R. B. and Berger, E. M. (1981) 'Hydrogen peroxide kills Staphylococcus aureus by reacting with staphylococcal iron to form hydroxyl radical', *Journal of Biological Chemistry*, 256(14), pp. 7094–7096.

Ross, D. E., Flynn, J. M., Baron, D. B., Gralnick, J. A. and Bond, D. R. (2011) 'Towards electrosynthesis in Shewanella: Energetics of reversing the Mtr pathway for reductive metabolism', *PLoS ONE*, 6(2). doi: 10.1371/journal.pone.0016649.

Shi, L., Rosso, K. M., Clarke, T. a, Richardson, D. J., Zachara, J. M. and Fredrickson, J. K. (2012) 'Molecular Underpinnings of Fe(III) Oxide Reduction by Shewanella Oneidensis MR-1.', *Frontiers in microbiology*, 3(February), p. 50. doi: 10.3389/fmicb.2012.00050.

Siddiqui, K. S., Poljak, A., Guilhaus, M., Feller, G., D'Amico, S., Gerday, C. and Cavicchioli, R. (2005) 'Role of Disulfide Bridges in the Activity and Stability of a Cold-Active α-Amylase', *Journal of Bacteriology*. American Society for Microbiology, 187(17), pp. 6206–6212. doi: 10.1128/JB.187.17.6206-6212.2005.

Søballe, B. and Poole, R. K. (1999) 'Microbial ubiquinones: multiple roles in respiration, gene regulation and oxidative stress management', *Microbiology*. Microbiology Society, 145(8), pp. 1817–1830.

Song, S. H., Dick, B. and Penzkofer, A. (2007) 'Photo-induced reduction of flavin mononucleotide in aqueous solutions', *Chemical Physics*, 332(1), pp. 55–65. doi: 10.1016/j.chemphys.2006.11.023.

Thangudu, R. R., Manoharan, M., Srinivasan, N., Cadet, F., Sowdhamini, R. and Offmann, B. (2008) 'Analysis on conservation of disulphide bonds and their structural features in homologous protein domain families', *BMC Structural Biology*, 8(1), p. 55. doi: 10.1186/1472-6807-8-55.

White, G. F., Shi, Z., Shi, L., Dohnalkova, A. C., Fredrickson, J. K., Zachara, J. M., Butt, J. N., Richardson, D. J. and Clarke, T. a (2012) 'Development of a proteoliposome model to probe transmembrane electron-transfer reactions.', *Biochemical Society transactions*, 40(6), pp. 1257–60. doi: 10.1042/BST20120116.

White, G. F., Shi, Z., Shi, L., Wang, Z., Dohnalkova, A. C., Marshall, M. J., Fredrickson, J. K., Zachara, J. M., Butt, J. N., Richardson, D. J. and Clarke, T. a (2013) 'Rapid electron exchange between surface-exposed bacterial cytochromes and Fe(III) minerals.', *Proceedings of the National Academy of Sciences of the United States of America*, 110(16), pp. 6346–51. doi: 10.1073/pnas.1220074110.

Wouters, M. A., Fan, S. W. and Haworth, N. L. (2010) 'Disulfides as redox switches: from molecular mechanisms to functional significance.', *Antioxidants & redox signaling*. United States, 12(1), pp. 53–91. doi: 10.1089/ars.2009.2510.